


Power functional theory for many-body dynamics

Matthias Schmidt^{*}

*Theoretische Physik II, Physikalisches Institut, Universität Bayreuth,
D-95447 Bayreuth, Germany*

 (published 28 March 2022)

The rich and diverse dynamics of particle-based systems ultimately originates from the coupling of their degrees of freedom via internal interactions. To arrive at a tractable approximation of such many-body problems, coarse graining is often an essential step. Power functional theory provides a unique and microscopically sharp formulation of this concept. The approach is based on an exact one-body variational principle to describe the dynamics of both overdamped and inertial classical and quantum many-body systems. In equilibrium, density-functional theory is recovered, and hence spatially inhomogeneous systems are described correctly. The dynamical theory operates on the level of time-dependent one-body correlation functions. Two- and higher-body correlation functions are accessible via the dynamical test-particle limit and the nonequilibrium Ornstein-Zernike route. The structure of this functional approach to many-body dynamics is described, including much background as well as applications to a broad range of dynamical situations, such as the van Hove function in liquids, flow in nonequilibrium steady states, motility-induced phase separation of active Brownian particles, lane formation in binary colloidal mixtures, and both steady and transient shear phenomena.

DOI: [10.1103/RevModPhys.94.015007](https://doi.org/10.1103/RevModPhys.94.015007)

CONTENTS

I. Introduction	1	I. Superdemixing and laning	46
A. Soft matter dynamics	1	J. Active Brownian particles	47
B. Forces as the basis	4	V. Conclusions and Outlook	49
II. Many-Body Description	10	Acknowledgments	51
A. Internal and external forces	10	Appendix: Functional Calculus	51
B. Hamiltonian dynamics	10	1. Variations and Hamilton's principle	51
1. Distribution functions as averages	11	2. Spatiotemporal and time-slice functional derivatives	52
2. One-body equation of motion	11	3. Gibbs-Appell-Gaussian classical mechanics	53
C. Brownian dynamics	11	References	53
D. Quantum dynamics	13		
III. The Adiabatic State	16		
A. The adiabatic construction	16		
B. Timeline of density-functional theory	19		
C. Sketch of classical DFT	20		
D. Statistical mechanics and variations	21		
E. Levy's constrained search	23		
F. Static two-body correlation functions	25		
G. Static Ornstein-Zernike relation	26		
H. Approximate free energy functionals	27		
I. Dynamical density-functional theory	28		
IV. Power Functional Theory	30		
A. Dynamic minimization principle	30		
B. Microscopic foundation	34		
1. Power functional for molecular dynamics	34		
2. Power functional for Brownian dynamics	35		
3. Quantum power functional theory	35		
C. Superadiabatic free power approximations	37		
D. Nonequilibrium Ornstein-Zernike relation	39		
E. Dynamical test-particle limit and mixtures	41		
F. Custom flow algorithm	43		
G. Viscous and structural forces	45		
H. Viscoelasticity and memory	46		
		I. INTRODUCTION	
		A. Soft matter dynamics	
		Soft matter science covers a broad range of diverse systems and their phenomena. Nagel (2017) and Evans, Frenkel, and Dijkstra (2019) described the gamut from colloids to polymers, from granulates to active systems, from liquid crystals to biomolecular systems, and beyond those. Although the systems are typically out of true equilibrium, in many instances the concepts of equilibrium statistical physics can be fruitfully exploited in order to understand and predict the behavior observed in the lab. However, the genuine dynamical behavior of soft matter is varied and rich, and it often constitutes the central focus of research. Balucani and Zoppi (1994), Dhont (1996), Zwanzig (2001), Götze (2008), and not least Hansen and McDonald (2013) provided accessible and thorough treatments of soft matter and dynamical liquid state theory. Schilling (2021) gave a recent comprehensive review of dynamical coarse-graining strategies.	
		Specific recent studies were aimed at the dynamical structure of the hard sphere liquid (Stopper <i>et al.</i> , 2018) as well as of complex ordered states (Bier <i>et al.</i> , 2008), microfluidics (Squires and Quake, 2005), slow dynamics and the glass transition (Dyre, 2006), gelation, and the topical field of	

^{*}Matthias.Schmidt@uni-bayreuth.de; <http://www.mschmidt.uni-bayreuth.de>

active systems, as reviewed by Marchetti *et al.* (2013) and Bechinger *et al.* (2016). Starting from a microscopic point of view, one would expect phenomena such as these to ultimately originate from the large number of degrees of freedom in the system, which are coupled via the interparticle interactions.¹ On the many-body level of description, computer simulation techniques offer in principle direct access to the physical behavior of a given system. To rationalize the bare data that are output from simulations, however, a theoretical framework is required, which (i) condenses the many-body information into digestible and intelligible form, and (ii) formulates interrelations between the simulated quantities. Furthermore, (iii) both strong conceptual and practical reasons (such as computational efficiency) speak for having a reliable and predictive stand-alone theory.

For equilibrium properties classical density-functional theory (DFT), as established by Evans (1979), satisfies the previously mentioned needs. Its basic (variational) variable is the density profile, i.e., the position-resolved microscopic probability to find a particle at the given space point. The density profile determines all physical properties of the system, at given thermodynamic state point, and in the presence of a fixed external one-body potential. Hence, the equation of state, the phase diagram, correlation functions, solvation forces, interfacial tension, etc., are all accessible. The DFT framework was originally conceived for quantum systems at zero temperature (i.e., for the ground state) by Hohenberg and Kohn (1964).² Only one year later, Mermin (1965) accomplished the generalization to finite temperatures. Evans (1979) formulated the classical version of DFT, and his approach has become textbook material (Hansen and McDonald, 2013). The quantum and classical theories are similar in their formal structure, although the approximative functional forms that are used in either field differ substantially from each other.³

To give a sense of the breadth of classical DFT subject matters, we enlist recent pivotal DFT studies. These have addressed atomically resolved three-dimensional structures of electrolytes near a solid surface (Martin-Jimenez *et al.*, 2016; Hernández-Muñoz, Chacón, and Tarazona, 2019), solvation phenomena in water (Jeanmairet *et al.*, 2013), and water-graphene capacitors (Jeanmairet *et al.*, 2019). Much work addressing hydrophobicity has been carried out, where liquid water (or a more general liquid) avoids contact with a substrate or solute. Here the density fluctuations near the substrate were quantified (Evans and Wilding, 2015) and a unified description was obtained for hydrophilic and superhydrophobic surfaces in terms of wetting and drying transitions of liquids

(Evans, Stewart, and Wilding, 2019; Remsing, 2019). Furthermore, critical drying of liquids (Evans, Stewart, and Wilding, 2016) and superhydrophobicity (Giacomello *et al.*, 2016, 2019) were investigated. There has been much progress on the conceptual level, as exemplified by the recent systematic incorporation of two-body correlation functions (Tschopp *et al.*, 2020; Tschopp and Brader, 2021) and fluctuation profiles (Eckert *et al.*, 2020) into the one-body DFT framework.

A time-dependent version of classical DFT, or “dynamical DFT,” was proposed by Evans (1979) and later much advocated for by Marconi and Tarazona (1999) and Archer and Evans (2004). Selected examples of insightful dynamical DFT studies include the uptake kinetics of molecular cargo into hollow hydrogels (Moncho-Jordá *et al.*, 2019), the particle-scale-resolved nonequilibrium sedimentation of colloids (Royall *et al.*, 2007), the bulk dynamics of colloidal Brownian hard disks (Stopper *et al.*, 2018), the pair dynamics in inhomogeneous liquids and glasses (Archer, Hopkins, and Schmidt, 2007; Hopkins *et al.*, 2010), and the growth of monolayers of hard rods on planar substrates (Klopotek *et al.*, 2017). The dynamical DFT can be viewed as being based on the approximation that the nonequilibrium dynamics are represented as a sequence of “adiabatic states” that each are taken to be in equilibrium. While the adiabatic approximation for dynamical processes can be valid in certain cases, important physical effects are absent (Fortini *et al.*, 2014), such as drag forces (Krininger, Schmidt, and Brader, 2016), viscosity (de las Heras and Schmidt, 2018a), and structural nonequilibrium forces (Stuhlmüller *et al.*, 2018; de las Heras and Schmidt, 2020; Geigenfeind, de las Heras, and Schmidt, 2020; Treffenstädt and Schmidt, 2021).

Going beyond the somewhat *ad hoc* equation of motion of dynamical DFT is facilitated by the formally exact power functional variational framework of Schmidt and Brader (2013). Power functional theory provides a minimization principle for the description of the dynamics. The internal force field, as arising from the interparticle interactions of particles that undergo Brownian dynamics, consists of both adiabatic and superadiabatic (above adiabatic) contributions. The former are accounted for in dynamical DFT; the latter possess genuine nonequilibrium character, as they are generated from a *kinematic* functional of the density profile and of the microscopically resolved flow. The variational fields are dynamical one-body objects, i.e., they depend on the position coordinate and the time. In particular, the superadiabatic force field is a functional of these kinematic fields, while the adiabatic force field is a functional of the instantaneous density profile alone. The power functional theory has been formulated for different types of underlying many-body dynamics, such as overdamped Brownian motion (Schmidt and Brader, 2013), including active systems (Krininger, Schmidt, and Brader, 2016; Hermann *et al.*, 2019; Hermann, de las Heras, and Schmidt, 2019; Krininger and Schmidt, 2019), classical Hamiltonian dynamics as relevant for molecular dynamics (Schmidt, 2018), and nonrelativistic quantum dynamics (Schmidt, 2015). The last case promises to help overcome the limitations of adiabatic time-dependent electronic DFT, and furthermore to act as a conceptual bridge between the classical and quantum worlds, due to the strong

¹There are interesting counterexamples, where the dynamics of a single particle already are exceedingly rich, such as in magnetically driven topological transport (Loehr *et al.*, 2016, 2018) and in active (Maes, 2020) and viscoelastic (Berner *et al.*, 2018) solvents.

²Accessible and compact descriptions of electronic DFT were given by Kohn (1999), Jones and Gunnarsson (1989), and Jones (2015).

³See the excellent reviews by Tarazona, Cuesta, and Martínez-Ratón (2008), Lutsko (2010), and Roth (2010), for descriptions of the state of the art of classical DFT; the foreword by Evans *et al.* (2016) of a special issue on classical DFT described recent progress.

formal similarities between the classical Hamiltonian and quantum versions of the power functional. Developing time-dependent quantum DFT (Runge and Gross, 1984) [see Chan and Finken (2005) for a classical analog] constitutes an active field of research (Onida, Reining, and Rubio, 2002; Nakatsukasa *et al.*, 2016). There is much current interest in bringing the quantum and classical DFT communities closer together (Dufty *et al.*, 2019), and power functional theory provides a concrete theoretical structure for making the corresponding progress.

The review is organized as follows. Section I.B gives an overview of the central power functional concept of working on the level of locally resolved forces and exploiting functional dependencies. Section II begins with a specification of the splitting of the forces that act in typical many-body systems into internal and external contributions (Sec. II.A). The splitting applies to a generic and broad class of systems and it forms the primary motivation for the specific choice of one-body kinematic fields as fundamental dynamical variables. We then turn to the level of one-body fields and derive corresponding equations of motion, starting with underlying classical (Newtonian) dynamics of the many-body system. This includes the equations of motion for the one-body operators, i.e., for phase space functions that represent the density and current. The form of these equations is that of a force balance relationship, or Newton's second law, including transport effects (Sec. II.B). While transport effects are familiar from a hydrodynamic standpoint, the present treatment is entirely microscopic and does not involve coarse graining in the sense of averaging out microscopic length scales. The description is microscopically "sharp." One-body distribution functions are obtained by averaging over the many-body phase space probability distribution function (of which the time evolution is governed by the Liouville equation).

The one-body equations of motion for overdamped Brownian classical motion (Sec. II.C) and for nonrelativistic quantum dynamics (Sec. II.D) are similar to the previously mentioned Newtonian case. Although the respective derivations are elementary (to a certain degree) and the underlying dynamics are apparently different from each other, it is surprising that the one-body description possesses universal status. There are clear differences though. The quantum one-body dynamics feature additional genuine quantum contributions (dependent on \hbar), the appearance of the quantum kinetic stress tensor distribution as well as of different types of force densities. For overdamped classical dynamics, the local force directly translates into an instantaneous particle current, and not into its time derivative, as is the case for quantum and Newtonian dynamics, which instead feature inertia. As we demonstrate, in all considered cases of many-body time evolution, the nontrivial coupling arises directly in the force density distribution (along with the kinetic stress in the inertial cases). The details of the definition of the internal force density differ among the three types of dynamics, as do the different types of averages (phase space average, quantum expectation value, and positional configuration space integral). Nevertheless, one can view these differences as merely technical and the internal force density as a universal and fundamental physical object. At this stage, however, the internal force density is defined only as a many-body average. Hence, the one-body theory is not closed and does not yet

form a stand-alone framework. The one-body quantities merely constitute observables, which, although characteristic of the full dynamics, lack a mechanism to restore the full information and evolve the system in time.

In equilibrium, a closed theory on the one-body level is available through the well-established framework of density-functional theory, which ascertains that the reduction of information that is inherent to relying on one-body fields is perfectly compensated for, without any principle loss, by the recognition and use of functional dependencies. Section III hence describes the adiabatic state and its treatment via the classical version of density-functional theory, which is prominently used in the description of bulk and inhomogeneous fluids, solids, liquid crystals, and further self-organized states of matter (Hansen and McDonald, 2013; Evans *et al.*, 2016). The reasons for laying out the framework are twofold. The first reason is that DFT forms a blueprint, or prototype, for the subsequent construction of the power functional framework. Both approaches share on an abstract, formal level many similarities, such as a truly microscopic foundation, the existence of a central functional object, which is minimized at the physical solution, and the generation of meaningful averages (correlators) via functional differentiation. Physically, however, the frameworks are distinct as to whether equilibrium (DFT) or nonequilibrium (power functional theory) situations are addressed. The second, and possibly more important, reason for covering DFT is its relevance in genuine nonequilibrium for the description of the adiabatic state (Sec. III.A). Any dynamical theory on the one-body level that can account for spatial inhomogeneity needs to reduce to DFT in the equilibrium limit. In power functional theory, this reduction is generic. The adiabatic contribution to the dynamics is unique and forms the part that is independent of the flow.

After an overview of the history of DFT (Sec. III.B) and its general structure (Sec. III.C), we start from the partition sum (Sec. III.D) and show how its functional derivative(s) with respect to the external potential are meaningful response functions; these are equivalent to correlation functions in the classical case. We cover several recent developments that are crucial for the dynamical material to follow and that are not covered in the previously mentioned standard introductory DFT literature. This includes the derivation of the Mermin-Evans variational principle via the Levy constrained search method (Sec. III.E). The intrinsic elegance and prowess of this method are not only a boon for the equilibrium framework, as a delicate *reductio ad absurdum* argument is circumvented, but also vital for the construction of the power functional. We describe two-body correlation functions (Sec. III.F) and derive the Ornstein-Zernike relation directly from the DFT minimization principle (Sec. III.G). This derivation cleanly separates the fundamental concept from the technicalities of defining and manipulating the various response and correlation functions that are involved. It is this type of derivation that is later generalized to the dynamical functional calculus in order to obtain the nonequilibrium version of the Ornstein-Zernike relation. An overview of approximate free energy functionals is presented (Sec. III.H). We conclude the section with an account of dynamical density-functional theory (Sec. III.I).

Section IV describes power functional theory, starting with an overview of the concept (Sec. IV.A). We cover the

formulations for classical inertial dynamics and for diffusive overdamped Brownian dynamics, as well as for nonrelativistic many-body quantum dynamics. In all these cases the power functional not only plays the role of a Gibbs-Appell Gaussian that determines the dynamics via a minimization principle but also constitutes a functional generator for time correlation functions. The reduction to the one-body level is performed using a dynamic generalization of the Levy search method, where, in particular, the constraint of fixed one-body current creates a one-body extremal principle with respect to the current (or the time derivative of the current in the inertial cases). This concept allows to formulate closed one-body equations of motion in all three cases of microscopic dynamics considered (Sec. IV.B), i.e., for molecular dynamics, overdamped Brownian motion, and quantum mechanics. It is shown that the natural splitting into intrinsic and external (and additional transport effects, in the inertial cases) translates into an analogous splitting of the functional generator. In all cases, the internal force density plays a central role in coupling the microscopic degrees of freedom. The interrelated kinematic one-body fields, i.e., the density profile, the local current or velocity, and the local acceleration, play the role of order parameters.

The superadiabatic force contributions act on top of the adiabatic force field. Although there is no exact solution for the superadiabatic functional contribution available (similar to the corresponding situation in equilibrium DFT, where the excess free energy functional is unknown in general), the framework shows existence and uniqueness. In contrast to the deterministic Gibbs-Appell-Gaussian formulation in classical mechanics, the constraint is a statistical one, as has been used in the Levy method of classical DFT construction. The framework implies a fundamental functional map from the density and current (and the current time derivative, in the inertial cases) to the external force field that generates these dynamics. A discussion is given of simple approximate forms of the superadiabatic free power functional (Sec. IV.C). We show how local and semilocal gradient functionals describe important classes of physically distinct effects, such as drag, viscous, and structural nonequilibrium forces. Based on the concept of functional differentiation of the Euler-Lagrange equation, we describe the derivation of nonequilibrium Ornstein-Zernike relations (Sec. IV.D). This includes the introduction of time direct correlation functions, which are identified as functional derivatives of the superadiabatic free power functional.

We then turn to several recent applications. The dynamical test-particle limit (Sec. IV.E) constitutes an alternative, formally exact route to the time-dependent two-body structure. A practical and simple explicit computational simulation scheme that implements kinematic functional dependencies is provided by the custom flow method, which we lay out for overdamped Brownian dynamics (Sec. IV.F). This method is vital in the study of viscous and structural forces (Sec. IV.G), which is based on splitting the Brownian dynamics into flow and structural contributions. Viscoelasticity, as originating from memory dependence of the superadiabatic free power functional, is demonstrated to occur for hard spheres under time-dependent step shear (Sec. IV.H). Lane formation in counterdriven mixtures is shown to originate from a

superadiabatic demixing force contribution (Sec. IV.I). An overview of power functional theory for active Brownian particles, including the treatment of motility-induced phase separation, is described (Sec. IV.J). We draw conclusions and provide an outlook on future work in Sec. V.

The Appendix contains an overview of Hamilton's action principle (Appendix A.1), from which both the Lagrangian and Hamiltonian formulations of classical mechanics are derived. This familiar material serves to review the essentials of functional calculus, which we spell out explicitly in spatiotemporal and time-slice forms (Appendix A.2). As Hamilton's principle requires only stationarity and not necessarily an extremum of the functional, this case also constitutes a counterexample to dynamical minimization, as performed in the Gibbs-Appell-Gaussian formulation of classical mechanics (Appendix A.3). Despite the considerable fame of its originators and its wide use both in the nonequilibrium liquids computer simulation community (Evans and Morriss, 2013) and in mechanical applications of classical dynamics with constraints, the method seems to be crucially undervalued and little known in the wider statistical physics community. As the power functional performs a similar variation, we lay out the deterministic Gibbs-Appell-Gaussian theory.

B. Forces as the basis

The forces that govern the behavior of typical many-body systems naturally split into internal forces, which act between the constituent particles, whether they be atoms, molecules, or colloids, and forces that are of an external nature. Typically the external forces depend on a single space coordinate only, i.e., the external force that acts on a given particle i depends only on its position \mathbf{r}_i , and possibly explicitly on time. If the particles possess additional degrees of freedom, such as the orientations of anisotropic particles, then the external force field can also depend on these, as it might on the type of particle in the case of multicomponent systems. Thus, in general the external force will depend on the same degrees of freedom that characterize a single particle (such as position, orientation, and species). Hence, one refers to such forces as *one-body* forces (of external nature in the present case). Even in cases where no explicit external forces are present, such as in a bulk fluid, one might regard one of the particles being fixed, say, at the origin and consider the forces that this "test" particle exerts on the remaining system as external. This is Percus's test-particle limit (Percus, 1962), which relates inhomogeneous one-body distribution functions to bulk two-body correlation functions.

The external forces can be of various physical origins and hence model a broad range of real-world experimental situations, such as gravity, container walls, light, and electric and magnetic fields. The mathematical description of forces via one-body fields allows for systematic classification into conservative contributions, as derived by the negative gradient of an external potential, and nonconservative contributions, where such a potential does not exist. Both types of forces might be simultaneously present, and they might, or might not, be time dependent. A mesoscopic example of the time-dependent conservative case is the switching of a laser tweezer in strength and/or position. Nonconservative forces can represent the influence of shear flow in overdamped systems,

such as sheared hard spheres at a hard wall (Brader and Krüger, 2011).

Restricting ourselves to the simple case of a one-component system of spheres, the external force field is

$$\mathbf{f}_{\text{ext}}(\mathbf{r}, t) = -\nabla V_{\text{ext}}(\mathbf{r}, t) + \mathbf{f}_{\text{nc}}(\mathbf{r}, t), \quad (1)$$

where $V_{\text{ext}}(\mathbf{r}, t)$ is the external potential and $\mathbf{f}_{\text{nc}}(\mathbf{r}, t)$ is the nonconservative contribution to the force field; here \mathbf{r} indicates position, t indicates time, and ∇ denotes the derivative with respect to \mathbf{r} .

In cases where the nonconservative forces vanish [$\mathbf{f}_{\text{nc}}(\mathbf{r}, t) \equiv 0$] and the external potential is time independent [$V_{\text{ext}}(\mathbf{r}, t) \equiv V_{\text{ext}}(\mathbf{r})$], a well-defined equilibrium state typically exists. Averaging over the equilibrium time evolution of the system then provides a method to calculate the quantities of interest. On physical grounds one would be interested in the response of the preferred particle positions to the action of $V_{\text{ext}}(\mathbf{r})$. Valleys in the external potential should be populated more likely by particles than peaks of the external potential. As the external potential acts on single particles individually, a meaningful corresponding observable is the one-body density distribution (or “density profile”)

$$\rho(\mathbf{r}, t) = \left\langle \sum_i \delta(\mathbf{r} - \mathbf{r}_i) \right\rangle, \quad (2)$$

where the sum is over all particles $i = 1, \dots, N$, with N the total number of particles, $\delta(\cdot)$ the Dirac function, and the angles representing a statistical average (specified in detail later) over microstates. For an equilibrium system, the one-body density distribution will be time independent, but in general be “inhomogeneous” in space, i.e., $\rho(\mathbf{r}) \neq \text{const}$. In practice, Eq. (2) amounts to “counting” the number of occurrences of any particle (hence the sum) at a given position \mathbf{r} ; see Rotenberg (2020) for an account of modern and more efficient “force-sampling” simulation methods. Hence, Eq. (2) can be viewed as an idealized, infinitely sharply resolved histogram of particle positions. Its normalization is $\int d\mathbf{r} \rho(\mathbf{r}, t) = N$ due to the property of the Dirac distribution $\int d\mathbf{r} \delta(\mathbf{r}) = 1$ (for a suitable integration domain).

Summarizing, in an equilibrium many-body system, it is natural to consider the influence of a position-dependent external potential $V_{\text{ext}}(\mathbf{r})$ on the system. As a result it is plausible to consider $\rho(\mathbf{r})$ a meaningful response function to assess the physical behavior. One would view the relationship between the two fields to be a causal one; i.e., $V_{\text{ext}}(\mathbf{r})$ provides the physical reason for the form of $\rho(\mathbf{r})$. A primary example is the barometric law of the isothermal atmosphere with an exponentially (in height) decreasing density profile in response to gravity. A diffusive force field emerges in such an inhomogeneous system $-k_B T \nabla \ln \rho(\mathbf{r})$, where k_B is the Boltzmann constant and T indicates temperature. The diffusive force can counteract the external force, such as the gravitational pull in the previous example. This effect is already present in the ideal gas. In an interacting system, however, the relationship between external potential and the density profile is a much more subtle, and by far richer, one.

In equilibrium the system will on average not move. Hence, the external forces need to be balanced by an average intrinsic force field, which consists of the previously mentioned ideal diffusive contribution and an interparticle interaction contribution $\mathbf{f}_{\text{int}}(\mathbf{r})$. Hence, in equilibrium the sum of all forces must vanish,

$$-k_B T \nabla \ln \rho(\mathbf{r}) + \mathbf{f}_{\text{int}}(\mathbf{r}) + \mathbf{f}_{\text{ext}}(\mathbf{r}) = 0. \quad (3)$$

As a result of the force cancellation, no temporal changes occur in the averaged quantities. Here the intrinsic force field $-k_B T \nabla \ln \rho(\mathbf{r}) + \mathbf{f}_{\text{int}}(\mathbf{r})$ consists of a sum of ideal and excess (above ideal) contributions, and hence it contains all effects that are not of an external nature. The excess contribution $\mathbf{f}_{\text{int}}(\mathbf{r})$ arises from the internal interactions and is given by

$$\mathbf{f}_{\text{int}}(\mathbf{r}) = - \left\langle \sum_i \delta(\mathbf{r} - \mathbf{r}_i) \nabla_i u(\mathbf{r}^N) \right\rangle / \rho(\mathbf{r}), \quad (4)$$

where $u(\mathbf{r}^N)$ is the interparticle interaction potential; the set of all particle position coordinates is denoted by $\mathbf{r}^N \equiv \mathbf{r}_1, \dots, \mathbf{r}_N$, and ∇_i is the derivative with respect to \mathbf{r}_i . Here $u(\mathbf{r}^N)$ can be, but need not be, due to only pairwise contributions.

The average in Eq. (4) can again be viewed as a histogram, but in contrast to the one-body density (2) the entries are not simply events that are being counted but rather (vectorial) values ($-\nabla_i u$). Hence the “bin” corresponding to \mathbf{r} can attain large values due to both a large number of events and large values of the local force. The normalizing factor $1/\rho(\mathbf{r})$ scales out the first of these effects (number of events). While the force density “operator” in Eq. (4) is entirely deterministic, the statistical nature of the problem is prominently present in the average over microstates.

It could be argued that the dependence of the positions on the forces is a concept that dates back to Newton, with Gibbs’s extension to a statistical description. However, the precise nature of the relationship between density and external potential is an equally important and arguably more fundamental one, as established in the 1960s (and described in Sec. III). In fact, for a given system (as specified by its internal interactions), knowledge of the one-body distribution function alone is sufficient to reconstruct the corresponding external potential. This mathematical map is at the heart of both quantum and classical DFT; see Mermin (1965) and Evans (1979), respectively.

Within classical DFT one expresses the equilibrium force field (4) that arises due to the internal interactions as the gradient of a functional derivative as follows:

$$\mathbf{f}_{\text{int}}(\mathbf{r}) = -\nabla \frac{\delta F_{\text{exc}}[\rho]}{\delta \rho(\mathbf{r})}. \quad (5)$$

In Eq. (5) $F_{\text{exc}}[\rho]$ is a mathematical map from the function $\rho(\mathbf{r})$ to the value of the excess (over ideal gas) intrinsic Helmholtz free energy. As an intrinsic contribution, this value is due solely to the internal interactions $u(\mathbf{r}^N)$, regardless of the external potential. Such a map constitutes a *functional*. The functional derivative $\delta/\delta\rho(\mathbf{r})$ creates the “response” of the value of $F_{\text{exc}}[\rho]$ to changes in density $\rho(\mathbf{r})$ at position \mathbf{r} ;

a pragmatic introduction to functional calculus is given in Appendixes A.1 and A.2.

The result of the functional derivative is hence position dependent, and we have made this position dependence explicit in the notation on the left-hand side of Eq. (5). Recall that the position dependence in the ‘‘probabilistic’’ expression (4) arises due to the presence of the delta function. The functional $F_{\text{exc}}[\rho]$ depends also on T (and on system volume V), and the functional is specific to the choice of interparticle interaction potential $u(\mathbf{r}^N)$. One highly nontrivial feature is that $F_{\text{exc}}[\rho]$ is independent of $V_{\text{ext}}(\mathbf{r})$. Recall that Eq. (4) at face value seems to depend on $V_{\text{ext}}(\mathbf{r})$, as the external potential enters the Boltzmann factor and hence determines the statistical ensemble that defines the average. However, the existence of the unique relationship $\rho(\mathbf{r}) \rightarrow V_{\text{ext}}(\mathbf{r})$ frees $F_{\text{exc}}[\rho]$ of any dependence on $V_{\text{ext}}(\mathbf{r})$, and hence renders it an entirely *intrinsic* quantity.

It is instructive to use Eq. (5) to rewrite the equilibrium force balance condition (3) as

$$-k_B T \nabla \ln \rho(\mathbf{r}) - \nabla \frac{\delta F_{\text{exc}}[\rho]}{\delta \rho(\mathbf{r})} = \nabla V_{\text{ext}}(\mathbf{r}), \quad (6)$$

and we recall that any nonconservative contribution to the external force field (1) needs to be absent and the external potential must be independent of time in order for an equilibrium state to exist.

Equation (6) can be viewed as an overall gradient of a scalar function, and upon spatial integration (and multiplication by -1) one obtains

$$k_B T \ln[\rho(\mathbf{r})\Lambda^d] + \frac{\delta F_{\text{exc}}[\rho]}{\delta \rho(\mathbf{r})} = \mu - V_{\text{ext}}(\mathbf{r}), \quad (7)$$

where μ arises formally as an integration constant, which can be identified with the chemical potential. Furthermore, $\Lambda = \sqrt{2\pi\beta\hbar^2/m}$ is the thermal de Broglie wavelength (Hansen and McDonald, 2013), with particle mass m , inverse temperature $\beta = 1/k_B T$, and spatial dimensionality d of the system; note that $\nabla \ln[\rho(\mathbf{r})\Lambda^d] = \nabla \ln \rho(\mathbf{r})$, as Λ is a constant. In practical applications of equilibrium DFT, one typically solves Eq. (7), or its exponentiated version, numerically for $\rho(\mathbf{r})$ given $V_{\text{ext}}(\mathbf{r})$. This is a nontrivial problem, as Eq. (7) is an implicit equation for $\rho(\mathbf{r})$ due to the complex (in general) dependence of $F_{\text{exc}}[\rho]$ on $\rho(\mathbf{r})$.

Practical applications of DFT require one to make approximations for $F_{\text{exc}}[\rho]$. A famous exception, where the exact solution was obtained by Percus (1976) [see Robledo and Varea (1981)], is the one-dimensional system of hard rods. However, for certain realistic systems, such as three-dimensional hard spheres, powerful approximations are available (Rosenfeld, 1989; Tarazona, 2000; Roth *et al.*, 2002); these can yield highly accurate results relative even to large-scale simulation results.

Even simple, mean-field-like approximations to $F_{\text{exc}}[\rho]$ often yield physically correct qualitative and semiquantitative results. Here the accessibility of physical quantities goes far beyond the one-body density profile, as thermodynamics, phase behavior, two- and higher-body correlation functions,

etc., can be obtained. One of the reasons for both the robust reliability of simple DFT approximations and the width of the range of accessible quantities lies in the fact that Eq. (7) constitutes, within the calculus of variations, an Euler-Lagrange equation corresponding to *minimization* of the grand potential functional $\Omega[\rho]$. At the minimum of the functional

$$\frac{\delta \Omega[\rho]}{\delta \rho(\mathbf{r})} = 0 \quad (\text{min}), \quad (8)$$

where $\Omega[\rho]$ consists of the following sum of intrinsic and external contributions:

$$\Omega[\rho] = F_{\text{id}}[\rho] + F_{\text{exc}}[\rho] + \int d\mathbf{r} \rho(\mathbf{r}) [V_{\text{ext}}(\mathbf{r}) - \mu]. \quad (9)$$

In Eq. (9) the intrinsic free energy functional for the ideal gas is

$$F_{\text{id}}[\rho] = k_B T \int d\mathbf{r} \rho(\mathbf{r}) \{ \ln[\rho(\mathbf{r})\Lambda^d] - 1 \}. \quad (10)$$

The functional derivative with respect to the density profile yields $\delta F_{\text{id}}[\rho]/\delta \rho(\mathbf{r}) = k_B T \ln[\rho(\mathbf{r})\Lambda^d]$, as appears in Eq. (7). In carrying out the derivative, as is typical in functional differentiation, the space integral is canceled by a Dirac delta function that arises from the identity $\delta \rho(\mathbf{r})/\delta \rho(\mathbf{r}') = \delta(\mathbf{r} - \mathbf{r}')$.

Given the many successes of equilibrium DFT, it is natural to use it as a springboard for the formulation of dynamical theories. One way of doing so is to start with a description of the forces that are present in the system. The challenge for such a formulation is to come to grips with the internal force field (4), where the average is now built over the non-equilibrium distribution of microstates at a given time t . Knowing the forces is crucial, as this allows one to progress in time and obtain the complete dynamics of the system, as we demonstrate in Sec. II.

If the system is driven out of equilibrium, either because the external potential changes in time or through the addition of a nonconservative contribution to the external force field, then a nonvanishing average flow will result. The flow is quantified by the average current distribution as follows:

$$\mathbf{J}(\mathbf{r}, t) = \left\langle \sum_i \delta(\mathbf{r} - \mathbf{r}_i) \mathbf{v}_i \right\rangle, \quad (11)$$

where we recall that \mathbf{r}_i is the position of particle i , its velocity is \mathbf{v}_i , and the average is performed at time t . As in the case of the internal force field (4), the average (11) will acquire large values at position \mathbf{r} due to frequent occurrences of particles, but also due to large values of the many-body velocity \mathbf{v}_i . Scaling out the former effect leads to the definition of the local velocity field

$$\mathbf{v}(\mathbf{r}, t) = \mathbf{J}(\mathbf{r}, t)/\rho(\mathbf{r}, t), \quad (12)$$

which is fully microscopically resolved (and hence different from a hydrodynamic field as appearing in, say, the Navier-Stokes equation). In a truly microscopic treatment,

we need to specify the time evolution of the positions \mathbf{r}^N on the many-body level. Several choices exist; for simplicity, but also because of its practical relevance in the description of colloidal systems, we focus first on overdamped Brownian dynamics. Typical implementations in computer simulations are based on the Euler algorithm⁴ to perform the time evolution; here the particle displacements are induced by (i) all deterministic forces that act on particle i at time t , and (ii) an additional random (white noise) displacement that models diffusion at constant T . Hence, the time evolution is based on stochastic trajectories, i.e., on the Langevin picture. An equivalent, and for theoretical purposes often more convenient and arguably more powerful, formulation is based on the many-body probability distribution function $\Psi(\mathbf{r}^N, t)$ for finding microstate \mathbf{r}^N at time t . Access to $\Psi(\mathbf{r}^N, t)$ allows averages [such as the density profile (2), the internal force field (4), and the current distribution (11)] to be explicitly specified, via integration over all microstates, as follows: $\langle \cdot \rangle = \int d\mathbf{r}^N \cdot \Psi(\mathbf{r}^N, t)$. In the overdamped limit considered here, there is no need to keep track of the momentum part of classical phase space; only the position (configuration) part is relevant.

The Smoluchowski equation (Dhont, 1996) is the dynamical equation for $\Psi(\mathbf{r}^N, t)$ for overdamped Brownian motion. This Fokker-Planck equation can be viewed as the following many-body continuity equation that expresses conservation of probability:

$$\frac{\partial \Psi(\mathbf{r}^N, t)}{\partial t} = - \sum_i \nabla_i \cdot \mathbf{v}_i(\mathbf{r}^N, t) \Psi(\mathbf{r}^N, t), \quad (13)$$

where the expression on the right-hand side is the negative divergence of the probability current $\mathbf{v}_i(\mathbf{r}^N, t) \Psi(\mathbf{r}^N, t)$ in configuration space. Here the ‘‘configurational’’ many-body velocity $\mathbf{v}_i(\mathbf{r}^N, t)$ of particle i is given via

$$\gamma \mathbf{v}_i(\mathbf{r}^N, t) = -\nabla_i u(\mathbf{r}^N) + \mathbf{f}_{\text{ext}}(\mathbf{r}_i, t) - k_B T \nabla_i \ln \Psi(\mathbf{r}^N, t), \quad (14)$$

where γ is the friction constant against a static background. The first and second terms on the right-hand side of Eq. (14) are due to the internal and external (deterministic) forces, respectively, and the third term represents the thermal force that arises due to the diffusive Brownian motion. For the present case of overdamped Brownian motion, it is the configurational velocity \mathbf{v}_i , as given by Eq. (14), that enters the averaged one-body current distribution (11). We reiterate the conceptual and practical difference of Eq. (14) from the one-body velocity field $\mathbf{v}(\mathbf{r}, t)$; see Eq. (12). The former is a configuration space function, and hence constitutes an important formal object, whereas the latter is the result of microscopically sharp coarse graining. Therefore, this is a more concrete and intuitively accessible vector field in physical space.

Given an initial state of the system at time t , the time evolution is fully determined by Eqs. (13) and (14). This is a high-dimensional problem, and the feasibility of direct solutions can be assessed with the reasoning used by Kohn

⁴The benefits of using adaptive time stepping in Brownian dynamics were described by Sammüller and Schmidt (2021).

(1999) in equilibrium: If we were to attempt a numerical solution in a one-dimensional problem of, say, ten particles and restrict ourselves to a numerical grid containing ten grid points, with 10 bytes to represent the value at each grid point, we would need 100 GB memory in order to store a single instance of Ψ . (Optimists in the development of computer resources may consider 20 particles.) In the power functional context, for small systems, both analytical (Hermann and Schmidt, 2018) and numerical (Stuhlmüller *et al.*, 2018) solutions were obtained. For conceptual purposes, it is important to have specified a concrete many-body dynamics. In practice trajectory-based Brownian dynamics simulations (see Sammüller and Schmidt, 2021) offer a powerful alternative, based on importance sampling, that is well suited for tackling realistic, large systems.

Developing a stand-alone theoretical dynamical framework both offers practical benefits of computational efficiency and provides a conceptual framework for formulating fundamental physical questions, analyzing simulation data, and identifying physical mechanisms for phenomena that are observed in simulation work and in experiment. As the external forces (1) remain of one-body character even if the system is no longer in equilibrium, we seek a description on the basis of one-body correlation functions.

In a time-dependent situation, the sum of the external and internal forces will not cancel in general, and will hence influence the average motion. Hence, the sum of the terms on the left-hand side of the force balance relation (3) will no longer vanish. Moreover, having a nonconservative contribution to the external force field is no longer forbidden, as was the case in equilibrium. In the overdamped limit considered here, the resulting driving force will be balanced by a friction force $-\gamma \mathbf{v}(\mathbf{r}, t)$. This plausibility argument leads to the correct one-body equation of motion,

$$\begin{aligned} \gamma \mathbf{v}(\mathbf{r}, t) = & -k_B T \nabla \ln \rho(\mathbf{r}, t) - \nabla \frac{\delta F_{\text{exc}}[\rho]}{\delta \rho(\mathbf{r}, t)} \\ & + \mathbf{f}_{\text{sup}}(\mathbf{r}, t) + \mathbf{f}_{\text{ext}}(\mathbf{r}, t), \end{aligned} \quad (15)$$

where the one-body density profile $\rho(\mathbf{r}, t)$ and the velocity field $\mathbf{v}(\mathbf{r}, t)$ are microscopically resolved in space and time. The forces on the right-hand side of Eq. (15) represent (i) ideal diffusion, (ii) an internal ‘‘adiabatic’’ excess force that arises from the excess free energy functional $F_{\text{exc}}[\rho]$, (iii) an additional internal superadiabatic force field $\mathbf{f}_{\text{sup}}(\mathbf{r}, t)$ that is due to the flow and occurs only in nonequilibrium, and (iv) the external driving force field $\mathbf{f}_{\text{ext}}(\mathbf{r}, t)$. Here the superadiabatic force field $\mathbf{f}_{\text{sup}}(\mathbf{r}, t)$ accounts for all contributions, due to internal interactions, that are of a genuine nonequilibrium character and hence are not contained in the adiabatic excess force field.

One might be surprised by the occurrence of a genuine equilibrium object, the excess free energy functional $F_{\text{exc}}[\rho]$, in an out-of-equilibrium situation. As $F_{\text{exc}}[\rho]$ requires an underlying statistical ensemble and Boltzmann distributed microstates, one might question its validity in Eq. (15). However, this situation is well founded due to the *adiabatic construction*. Here one considers a hypothetical adiabatic equilibrium system that possesses the same interparticle interaction potential $u(\mathbf{r}^N)$ as the real system. Furthermore, the adiabatic

system possesses the same one-body density distribution as the nonequilibrium system at a fixed snapshot in time t ,

$$\rho_{\text{ad},t}(\mathbf{r}) = \rho(\mathbf{r}, t), \quad (16)$$

where $\rho_{\text{ad},t}(\mathbf{r})$ is the density profile in the adiabatic system. One can perform the adiabatic construction at each point in time; hence, $\rho_{\text{ad},t}(\mathbf{r})$ inherits an apparent time dependence, although by construction the underlying many-body system is in equilibrium with no explicit time dependence. As the adiabatic system is in equilibrium, we may invoke the Mermin-Evans theorem of DFT and conclude that there is a unique adiabatic external potential $V_{\text{ad},t}(\mathbf{r})$ that stabilizes the given density $\rho_{\text{ad},t}(\mathbf{r})$.

Hence, we can formulate the force balance (3) in the adiabatic system as

$$-k_B T \nabla \ln \rho_{\text{ad},t}(\mathbf{r}) + \mathbf{f}_{\text{ad}}(\mathbf{r}, t) = \nabla V_{\text{ad},t}(\mathbf{r}), \quad (17)$$

where the adiabatic excess force field $\mathbf{f}_{\text{ad}}(\mathbf{r}, t)$ is given either (i) by the microscopic average (4) over the equilibrium ensemble of the adiabatic system or (ii) as the density-functional relationship (5). In the first case, we may sample $\mathbf{f}_{\text{ad}}(\mathbf{r}, t)$ directly with an equilibrium method that offers access to the adiabatic system. This task involves finding $V_{\text{ad},t}(\mathbf{r})$. This constitutes an inverse problem that requires computational effort. A brute force method consists of guessing $V_{\text{ad},t}(\mathbf{r})$ and sampling $\rho_{\text{ad},t}(\mathbf{r})$ and then adjusting $V_{\text{ad},t}(\mathbf{r})$ iteratively, such that the external potential is increased in regions with excessively high density relative to the target density. Once a satisfactorily small error in Eq. (16) is achieved, one can

directly solve Eq. (17) for $\mathbf{f}_{\text{ad}}(\mathbf{r}, t)$. However, more direct methods based on the custom flow method exist (as described in Sec. IV.F).

Within DFT the inverse problem has already been addressed implicitly and, as a result, the adiabatic force field is directly available. We can hence make the second term on the right-hand side of the equation of motion (15) fully explicit as

$$\mathbf{f}_{\text{ad}}(\mathbf{r}, t) = -\nabla \left. \frac{\delta F_{\text{exc}}[\rho]}{\delta \rho(\mathbf{r})} \right|_{\rho(\mathbf{r})=\rho(\mathbf{r},t)}, \quad (18)$$

which shows explicitly how the equilibrium free energy functional enters the dynamical theory (15) in a well-defined and unambiguous way.

In the time evolution equation (15) the genuine nonequilibrium contributions to the internal force field are contained in $\mathbf{f}_{\text{sup}}(\mathbf{r}, t)$. These forces do not occur in equilibrium and cannot be obtained based on a free energy description. Setting $\mathbf{f}_{\text{sup}}(\mathbf{r}, t) = 0$ can in specific cases be a reasonable approximation, and the resulting dynamical theory is commonly referred to as the dynamical density-functional theory (DDFT).

A simple counterexample, where the adiabatic approximation fails, is steady shear of a homogeneous fluid, where $\rho(\mathbf{r}, t) = \text{const}$. As the density is constant, no adiabatic effects occur on the one-body level [the gradient in Eq. (18) vanishes], although the system can be driven arbitrarily far out of equilibrium by increasing the shear rate. [This concept was carried much further by [de las Heras and Schmidt \(2020\)](#); see their Supplemental Material for fully inhomogeneous flow patterns.] Figure 1 shows results from an adiabatic treatment of sedimentation [Fig. 1(a)] and superadiabatic

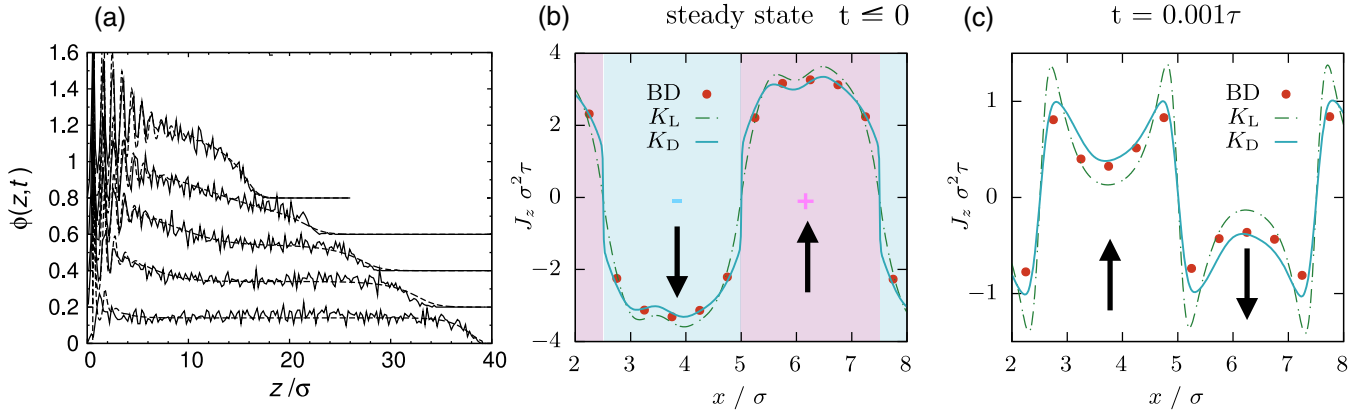


FIG. 1. Dynamics of the density profile of colloidal hard spheres in (a) dynamical sedimentation, as primarily governed by adiabatic forces, and (b),(c) motion reversal under temporal switching of step shear, as a purely superadiabatic effect. (a) Local packing fraction $\phi(z, t) = \rho(z, t)\pi\sigma^3/6$ as a function of the scaled height coordinate z/σ , where σ is the hard sphere diameter. Results at increasing time are shifted upward by 0.2 units. The system is initially almost homogeneous and, over the course of time, develops a strong density gradient, including layering at the bottom of the container. Shown are results from confocal microscopy experiment (solid lines) and from DDFT (dashed lines) using a density-dependent mobility. (b),(c) Current profiles in the flow \mathbf{e}_z direction $J_z \sigma^2 \tau$ as a function of the position x in the gradient \mathbf{e}_x direction of the inhomogeneous shear field. The system is three dimensional and it is homogeneous in the third direction \mathbf{e}_y . Shear is induced by a square wave external force that acts by alternating in the positive (light violet and +) and negative (light cyan and -) \mathbf{e}_z direction with strength $5k_B T/\sigma$ for times $t < 0$. At time $t = 0$ the external force is switched off. Because of the viscoelastic memory of the hard sphere fluid, the current immediately reverses its direction, as can be seen by comparing the down-up sequence of arrows in (b) to the up-down sequence in (c). Results are obtained from event-driven BD simulations (symbols) and from power functional theory with spatially local (K_L) and nonlocal diffusing memory kernel (K_D). (a) Adapted from [Royall *et al.*, 2007](#). (b),(c) Adapted from [Treffenstädt and Schmidt, 2020](#).

effects in time-dependent shear [Figs. 1(b) and 1(c)] of Brownian hard spheres.

Hence, a complete dynamical theory needs to specify the superadiabatic force field $\mathbf{f}_{\text{sup}}(\mathbf{r}, t)$. This task is accomplished within the power functional framework, where the superadiabatic force field is expressed as a functional derivative (Schmidt and Brader, 2013), as follows:

$$\mathbf{f}_{\text{sup}}(\mathbf{r}, t) = -\frac{\delta P_t^{\text{exc}}[\rho, \mathbf{J}]}{\delta \mathbf{J}(\mathbf{r}, t)}. \quad (19)$$

In Eq. (19) the variation is performed at a fixed density distribution and at fixed time t , and the superadiabatic excess power functional $P_t^{\text{exc}}[\rho, \mathbf{J}]$ is a functional of both the density and the current distribution. As $P_t^{\text{exc}}[\rho, \mathbf{J}]$ originates from $u(\mathbf{r}^N)$, it is in general both nonlocal in space and nonlocal in time. The dependence is on the history of both fields, i.e., on their values at times $< t$, where t is the time at which the variation (19) is performed; the continuity equation holds (Schmidt and Brader, 2013). The functional carries units of energy per time, or power, $[P_t^{\text{exc}}] = \text{J/s} = \text{W}$.

Besides the occurrence of memory effects, the mathematical structure is significantly richer than that of the DDFT, due to the fact that the dependence on the current now occurs on both sides of Eq. (15), on the left-hand side via Eq. (12) and on the right-hand side via Eq. (19). Hence, the current is defined by an implicit relationship, which offers far greater flexibility in describing physical effects than an explicit theory such as the DDFT. Recall that the Euler-Lagrange equation (7) of equilibrium DFT is an implicit equation as well, albeit one for the density profile. In equilibrium, it is precisely this structure that allows freezing, capillary behavior, wetting, etc. (Evans *et al.*, 2016), to be described.

For completeness, the temporal changes of the density profile $\rho(\mathbf{r}, t)$ are obtained from the current $\mathbf{J}(\mathbf{r}, t)$ via the continuity equation

$$\frac{\partial \rho(\mathbf{r}, t)}{\partial t} = -\nabla \cdot \mathbf{J}(\mathbf{r}, t). \quad (20)$$

The variational structure of power functional theory is analogous to that of equilibrium DFT. However, the similarity occurs on a deep structural level, as power functional theory is based on a variational (extremal) principle, akin to the equilibrium minimization principle with respect to the density distribution (8). In the dynamical case, the minimization is instead performed with respect to the current, at fixed density distribution, and at fixed time as follows:

$$\frac{\delta R_t[\rho, \mathbf{J}]}{\delta \mathbf{J}(\mathbf{r}, t)} = 0 \quad (\text{min}). \quad (21)$$

In Eq. (21) the total power functional $R_t[\rho, \mathbf{J}]$ consists of a sum

$$R_t[\rho, \mathbf{J}] = \dot{F}[\rho] + P_t[\rho, \mathbf{J}] - X_t[\rho, \mathbf{J}], \quad (22)$$

where $\dot{F}[\rho]$ is the time derivative of the total (ideal and excess) intrinsic free energy functional $F[\rho] = F_{\text{id}}[\rho] + F_{\text{exc}}[\rho]$, the superadiabatic contribution $P_t[\rho, \mathbf{J}]$ accounts for genuine

nonequilibrium effects, and $X_t[\rho, \mathbf{J}]$ is the external power. Both $\dot{F}[\rho]$ and $P_t[\rho, \mathbf{J}]$ are of an intrinsic nature; i.e., they depend on $u(\mathbf{r}^N)$ but not on the external force field.

The genuine nonequilibrium power splits into ideal and excess (superadiabatic) contributions ($P_t[\rho, \mathbf{J}] = P_t^{\text{id}}[\rho, \mathbf{J}] + P_t^{\text{exc}}[\rho, \mathbf{J}]$), where the exact ideal gas dissipation contribution is local in space and time and given by

$$P_t^{\text{id}}[\rho, \mathbf{J}] = \frac{\gamma}{2} \int d\mathbf{r} \frac{\mathbf{J}^2(\mathbf{r}, t)}{\rho(\mathbf{r}, t)}. \quad (23)$$

The external power is the following sum of mechanical and motionless contributions:

$$X_t[\rho, \mathbf{J}] = \int d\mathbf{r} [\mathbf{J}(\mathbf{r}, t) \cdot \mathbf{f}_{\text{ext}}(\mathbf{r}, t) - \rho(\mathbf{r}, t) \dot{V}_{\text{ext}}(\mathbf{r}, t)]. \quad (24)$$

Inserting the decomposition (22) into the dynamical extremal principle (21) and carrying out the functional derivative yield an Euler-Lagrange equation that is identical to the equation of motion (15) with the superadiabatic excess force given by Eq. (19). The proof of this identity requires the derivative $\delta P_t^{\text{id}}[\rho, \mathbf{J}]/\delta \mathbf{J}(\mathbf{r}, t) = \gamma \mathbf{J}(\mathbf{r}, t)/\rho(\mathbf{r}, t)$.

Furthermore, using successively the functional chain rule, the continuity equation, and spatial integration by parts, one finds the total time derivative of the intrinsic free energy functional as

$$\dot{F}[\rho] = \frac{d}{dt} F[\rho] = \int d\mathbf{r} \frac{\delta F[\rho]}{\delta \rho(\mathbf{r}, t)} \dot{\rho}(\mathbf{r}, t) \quad (25)$$

$$= - \int d\mathbf{r} \frac{\delta F[\rho]}{\delta \rho(\mathbf{r}, t)} \nabla \cdot \mathbf{J}(\mathbf{r}, t) \quad (26)$$

$$= \int d\mathbf{r} \mathbf{J}(\mathbf{r}, t) \cdot \nabla \frac{\delta F[\rho]}{\delta \rho(\mathbf{r}, t)}. \quad (27)$$

Because of the linear dependence on $\mathbf{J}(\mathbf{r}, t)$, the form (27) can be differentiated easily with respect to the current with the density profile held fixed. The result is the following total (ideal and excess) adiabatic force field:

$$\begin{aligned} -\frac{\delta \dot{F}[\rho]}{\delta \mathbf{J}(\mathbf{r}, t)} &= -\nabla \frac{\delta F[\rho]}{\delta \rho(\mathbf{r}, t)} \\ &= -k_B T \nabla \ln \rho(\mathbf{r}, t) - \nabla \frac{\delta F_{\text{exc}}[\rho]}{\delta \rho(\mathbf{r}, t)}, \end{aligned} \quad (28)$$

where the last term is $\mathbf{f}_{\text{ad}}(\mathbf{r}, t)$; see Eq. (18). Finally, the derivative of the external power is $\delta X_t[\rho, \mathbf{J}]/\delta \mathbf{J}(\mathbf{r}, t) = \mathbf{f}_{\text{ext}}(\mathbf{r}, t)$. The equation of motion (15) follows straightforwardly upon the collection of all terms.

That the power functional (22) exists is not an assumption. Via a constructive proof it is derived from an underlying many-body extremal principle. We do not reproduce the proof here (see Sec. IV.B.2), but instead state only the starting point, which is a many-body version of the one-body power functional (22) defined as

$$\mathcal{R}_t = \int d\mathbf{r}^N \Psi(\mathbf{r}^N, t) \sum_i \left(\frac{\gamma \tilde{\mathbf{v}}_i^2}{2} - \tilde{\mathbf{v}}_i \cdot \mathbf{f}_i^{\text{tot}} + \dot{V}_{\text{ext}}(\mathbf{r}_i, t) \right). \quad (29)$$

In Eq. (29) $\tilde{\mathbf{v}}_i(\mathbf{r}^N, t)$ are configuration space functions that represent trial velocities and $\mathbf{f}_i^{\text{tot}}$ is the total force acting on particle i . The physical values of the velocities are attained upon minimizing \mathcal{R}_t with respect to $\tilde{\mathbf{v}}_i$ [which can easily be explicitly performed due to the simple quadratic structure of Eq. (29)]. Using a dynamical version of Levy's constrained search method (Levy, 1979; Dwandaru and Schmidt, 2011) yields the one-body power functional $R_t[\rho, \mathbf{J}]$ given in Eq. (22), with the one-body minimization principle (21). In the following we flesh out this material and first turn to the fundamentals.

II. MANY-BODY DESCRIPTION

A. Internal and external forces

We consider particles (colloids, atoms, molecules, macromolecules, or quantum particles) with position coordinates \mathbf{r}_i , where the particle index $i = 1, \dots, N$ and N is the total number of particles. As a shorthand notation $\mathbf{r}^N \equiv \mathbf{r}_1, \dots, \mathbf{r}_N$. Position space is d dimensional with $d = 3$ often being the most relevant case, but important systems, such as particles adsorbed at substrates or confined between plates, have $d = 2$ or even $d = 1$ (confinement in channels). The case $d = 1$ is also important for conceptual purposes, as some exact results are available.

The force on particle i is also a d -dimensional vector, which typically can be split into internal and external parts as follows:

$$\mathbf{f}_i(\mathbf{r}^N, t) = \mathbf{f}_{\text{int},i}(\mathbf{r}^N) + \mathbf{f}_{\text{ext}}(\mathbf{r}_i, t). \quad (30)$$

In Eq. (30) $\mathbf{f}_{\text{int},i}(\mathbf{r}^N)$ is the internal force on particle i that is exerted due to the cumulative effect of all other particles in the system. There are typically no self-interactions, and the internal interactions do not depend explicitly on time. The external force field, however, is in general time dependent and characterized (defined by) the property that it depends only on the position of particle i , not on the positions of all other particles $j \neq i$. Hence, $\mathbf{f}_{\text{ext}}(\mathbf{r}, t)$ can be viewed as a prescribed external force field of a generic position coordinate \mathbf{r} and time t . The external force field hence couples to the degrees of freedom in the system, but there is no ‘‘backaction’’; i.e., $\mathbf{f}_{\text{ext}}(\mathbf{r}, t)$ is externally imposed, independent of the system degrees of freedom.

We consider internal forces that are obtained from an interparticle interaction potential $u(\mathbf{r}^N)$ as the following negative gradient:

$$\mathbf{f}_{\text{int},i}(\mathbf{r}^N) = -\nabla_i u(\mathbf{r}^N), \quad (31)$$

where, as before, ∇_i denotes the derivative with respect to \mathbf{r}_i . The total internal potential energy $u(\mathbf{r}^N)$ can, but need not, come from pairwise interparticle interactions.

B. Hamiltonian dynamics

We consider classical particles first and start by deriving the microscopic continuity equation by building the time derivative of the density operator as follows:

$$\frac{d}{dt} \hat{\rho} = \frac{d}{dt} \sum_i \delta(\mathbf{r} - \mathbf{r}_i) \quad (32)$$

$$= \sum_i \left(\frac{\partial}{\partial \mathbf{r}_i} \delta(\mathbf{r} - \mathbf{r}_i) \right) \cdot \dot{\mathbf{r}}_i \quad (33)$$

$$= \sum_i \left(\frac{\partial}{\partial (\mathbf{r}_i - \mathbf{r})} \delta(\mathbf{r} - \mathbf{r}_i) \right) \cdot \mathbf{v}_i \quad (34)$$

$$= \sum_i \left(-\frac{\partial}{\partial \mathbf{r}} \delta(\mathbf{r} - \mathbf{r}_i) \right) \cdot \mathbf{v}_i \quad (35)$$

$$= -\frac{\partial}{\partial \mathbf{r}} \cdot \sum_i \delta(\mathbf{r} - \mathbf{r}_i) \mathbf{v}_i \quad (36)$$

$$= -\nabla \cdot \hat{\mathbf{J}}, \quad (37)$$

where the spatial derivative is $\nabla = \partial/\partial \mathbf{r}$, the microscopic density operator is defined as $\hat{\rho} = \sum_i \delta(\mathbf{r} - \mathbf{r}_i)$, and the microscopic one-body current operator is given as $\hat{\mathbf{J}} = \sum_i \delta(\mathbf{r} - \mathbf{r}_i) \mathbf{v}_i$. Note the sign change in Eq. (35) from the change to the argument of the derivative. This substitution enables one in Eq. (36) to move the divergence operator outside of what becomes the current operator.

As the Newtonian dynamics are second order in time, we expect to obtain a useful result when differentiating one more in time. Hence, consider

$$\frac{d^2}{dt^2} \hat{\rho} = \frac{d}{dt} (-\nabla \cdot \hat{\mathbf{J}}) = -\nabla \cdot \frac{d}{dt} \hat{\mathbf{J}}, \quad (38)$$

where we have used Eq. (37) in the first step. We can make progress with the following time derivative of the current operator:

$$\frac{d\hat{\mathbf{J}}}{dt} = \frac{d}{dt} \sum_i \delta(\mathbf{r} - \mathbf{r}_i) \mathbf{v}_i \quad (39)$$

$$= \sum_i \left(\frac{d}{dt} \delta(\mathbf{r} - \mathbf{r}_i) \right) \mathbf{v}_i + \sum_i \delta(\mathbf{r} - \mathbf{r}_i) \frac{d\mathbf{v}_i}{dt} \quad (40)$$

$$= \sum_i \frac{\partial \delta(\mathbf{r} - \mathbf{r}_i)}{\partial \mathbf{r}_i} \cdot \dot{\mathbf{r}}_i \mathbf{v}_i + \sum_i \delta(\mathbf{r} - \mathbf{r}_i) \frac{\mathbf{f}_i}{m} \quad (41)$$

$$= -\nabla \cdot \sum_i \delta(\mathbf{r} - \mathbf{r}_i) \mathbf{v}_i \mathbf{v}_i + \frac{\hat{\mathbf{F}}}{m} \quad (42)$$

$$= \frac{\nabla \cdot \hat{\boldsymbol{\tau}}}{m} + \frac{\hat{\mathbf{F}}}{m}, \quad (43)$$

where the kinetic stress operator is defined as $\hat{\boldsymbol{\tau}} = -\sum_i m \mathbf{v}_i \mathbf{v}_i \delta(\mathbf{r} - \mathbf{r}_i)$ and the force density operator is $\hat{\mathbf{F}} = \sum_i \delta(\mathbf{r} - \mathbf{r}_i) \mathbf{f}_i$. Hence, we have obtained the operator equation of motion

$$m \frac{d}{dt} \hat{\mathbf{J}} = \nabla \cdot \hat{\boldsymbol{\tau}} + \hat{\mathbf{F}}, \quad (44)$$

which expresses the total change in current (multiplied by mass) as the sum of the divergence of the stress tensor (as a transport effect) plus the force density. Equation (44) can be viewed as Newton's second law on the classical one-body operator level. Readers with a background in hydrodynamics will immediately be familiar with the kinetic stress being a velocity-velocity dyadic product, as this appears in standard derivations of the Navier-Stokes equation; see Hansen and McDonald (2013). However, in contrast to a continuum mechanical treatment, here $\hat{\boldsymbol{\tau}}$ is resolved on a microscopic scale (via the delta function in position). Note also that the trace $\text{Tr} \hat{\boldsymbol{\tau}}/2$ is the locally resolved kinetic energy density operator.

1. Distribution functions as averages

We obtain *one-body distribution functions* via averaging according to

$$O(\mathbf{r}, t) = \langle \hat{O}(\mathbf{r}, t; \mathbf{r}^N, \mathbf{p}^N) \rangle, \quad (45)$$

where \hat{O} is a phase space function (operator) that additionally depends on a generic position argument \mathbf{r} and explicitly on time, in the most general case. In Eq. (45) the average is over the probability distribution of microstates at time t . (This is now a statistical description; an ensemble of systems is propagated forward in time.) Hence,

$$\langle \cdot \rangle = \int d\mathbf{r}^N d\mathbf{p}^N \cdot \Psi(\mathbf{r}^N, \mathbf{p}^N, t), \quad (46)$$

where Ψ is the many-body probability distribution function to find microstate $\mathbf{r}^N, \mathbf{p}^N$ at time t . The differential phase space volume element (which determines how to integrate over Ψ in order to obtain probabilities) is $d\mathbf{r}^N d\mathbf{p}^N$, and the distribution function is normalized [$\int d\mathbf{r}^N d\mathbf{p}^N \Psi(\mathbf{r}^N, \mathbf{p}^N, t) = 1$] at all times t . For classical inertial dynamics the time evolution of Ψ is governed by the following Liouville equation:

$$\frac{\partial \Psi}{\partial t} = -\sum_i \left(\frac{\mathbf{p}_i}{m} \cdot \frac{\partial}{\partial \mathbf{r}_i} + \mathbf{f}_i \cdot \frac{\partial}{\partial \mathbf{p}_i} \right) \Psi. \quad (47)$$

2. One-body equation of motion

The operator identities for the time derivative of density (37) and current (44) can be averaged over the phase space distribution function according to Eq. (46). This yields the following reduced, yet microscopically sharp, one-body equations of motion:

$$\dot{\rho}(\mathbf{r}, t) = -\nabla \cdot \mathbf{J}(\mathbf{r}, t), \quad (48)$$

$$m \dot{\mathbf{J}}(\mathbf{r}, t) = \nabla \cdot \boldsymbol{\tau}(\mathbf{r}, t) + \mathbf{F}_{\text{int}}(\mathbf{r}, t) + \rho(\mathbf{r}, t) \mathbf{f}_{\text{ext}}(\mathbf{r}, t). \quad (49)$$

In Eq. (49) the one-body distribution functions are averaged according to Eq. (46), i.e., $\rho(\mathbf{r}, t) = \langle \hat{\rho} \rangle$, $\mathbf{J}(\mathbf{r}, t) = \langle \hat{\mathbf{J}} \rangle$, $\boldsymbol{\tau}(\mathbf{r}, t) = \langle \hat{\boldsymbol{\tau}} \rangle$, $\mathbf{F}(\mathbf{r}, t) = \langle \hat{\mathbf{F}} \rangle$, etc.; the internal force density operator is $\hat{\mathbf{F}}_{\text{int}} = -\sum_i \delta(\mathbf{r} - \mathbf{r}_i) \nabla_i u(\mathbf{r}^N)$. The kinematic fields are interrelated by time integration. Let the system initially be in equilibrium and $\rho(\mathbf{r}, t \leq 0) = \rho(\mathbf{r}, 0)$, and let $\mathbf{J}(\mathbf{r}, t \leq 0) = 0$. At times $t > 0$, then

$$\mathbf{J}(\mathbf{r}, t) = \int_0^t dt' \dot{\mathbf{J}}(\mathbf{r}, t'), \quad (50)$$

$$\rho(\mathbf{r}, t) = \rho(\mathbf{r}, 0) - \int_0^t dt' \nabla \cdot \mathbf{J}(\mathbf{r}, t'). \quad (51)$$

(Note that rotational contributions to the current leave the density unchanged.) The one-body equations of motion are not closed as $\rho(\mathbf{r}, t)$, $\mathbf{J}(\mathbf{r}, t)$, $\nabla \cdot \boldsymbol{\tau}(\mathbf{r}, t)$, and $\mathbf{F}_{\text{int}}(\mathbf{r}, t)$ are unknown; only $\mathbf{f}_{\text{ext}}(\mathbf{r}, t)$ is given, and we have only two equations.

The nontrivial contribution due to transport and the inter-particle coupling is

$$\begin{aligned} \nabla \cdot \boldsymbol{\tau}(\mathbf{r}, t) + \mathbf{F}_{\text{int}}(\mathbf{r}, t) \\ \equiv -\nabla \cdot \left\langle \sum_i \delta(\mathbf{r} - \mathbf{r}_i) \frac{\mathbf{p}_i \mathbf{p}_i}{m} \right\rangle - \left\langle \sum_i \delta(\mathbf{r} - \mathbf{r}_i) \nabla_i u(\mathbf{r}^N) \right\rangle. \end{aligned} \quad (52)$$

We treat this force density field in Sec. IV.B using dynamical functional methods.

C. Brownian dynamics

We turn to the case of N classical colloidal particles in d -dimensional space, dispersed in a solvent at temperature T and undergoing overdamped Brownian motion with friction coefficient γ , internal interaction potential $u(\mathbf{r}^N)$, and under the influence of an external force field $\mathbf{f}_{\text{ext}}(\mathbf{r}, t)$. The Langevin equations of motion are

$$\gamma \dot{\mathbf{r}}_i = \mathbf{f}_i^{\text{det}}(\mathbf{r}^N, t) + \boldsymbol{\xi}_i(t), \quad (53)$$

where the deterministic force acting on particle i is a vector field given by

$$\mathbf{f}_i^{\text{det}}(\mathbf{r}^N, t) = -\nabla_i u(\mathbf{r}^N) + \mathbf{f}_{\text{ext}}(\mathbf{r}_i, t). \quad (54)$$

The random contribution on the right-hand side of Eq. (53) is a stochastic white noise term with prescribed moments

$$\overline{\boldsymbol{\xi}_i(t)} = 0, \quad (55)$$

$$\overline{\boldsymbol{\xi}_i(t) \boldsymbol{\xi}_j(t')} = 2k_B T \gamma \delta_{ij} \mathbf{1} \delta(t - t'), \quad (56)$$

where the overline denotes an average over the noise realizations, the left-hand side of Eq. (56) is a dyadic product, δ_{ij} denotes the Kronecker symbol, and $\mathbf{1}$ indicates the $d \times d$ unit matrix.

The Langevin scheme is well suited to carrying out computer simulations via discretizing the equations of motion and using a simple Euler or an adaptive time-stepping algorithm (Sammüller and Schmidt, 2021) to integrate the positions forward in time. The noise can be generated from pseudo-random number algorithms (such as the Box-Muller transform to generate Gaussian distributed random numbers). Building averages then requires one, in principle, to average both over initial states (of which the distribution function needs to be known and is in practice often assumed to be equilibrated) and over different realizations of the noise. In the Langevin framework, the time-dependent probability distribution function of microstates $\Psi(\mathbf{r}^N, t)$ does not appear explicitly. This often makes calculations difficult, as averages of interest have to be reduced to the only known ones for the noise, Eqs. (55) and (56).

Having $\Psi(\mathbf{r}^N, t)$ is a powerful feature, with the microscopic foundation of the concept of entropy resting upon it. The explicit introduction of $\Psi(\mathbf{r}^N, t)$ into the framework is achieved by complementing the Langevin picture by the corresponding Fokker-Planck equation of motion for $\Psi(\mathbf{r}^N, t)$. In the present case of overdamped motion this is the following Smoluchowski equation:

$$\frac{\partial \Psi}{\partial t} = - \sum_i \nabla_i \cdot \mathbf{v}_i \Psi. \quad (57)$$

In Eq. (57) the many-body configurational velocity $\mathbf{v}_i(\mathbf{r}^N, t)$ of particle i is a function (not a differential operator) defined via

$$\gamma \mathbf{v}_i = \mathbf{f}_i^{\text{det}} - k_B T \nabla_i \ln \Psi \quad (58)$$

$$= -\nabla_i u(\mathbf{r}^N) + \mathbf{f}_{\text{ext}}(\mathbf{r}_i, t) - k_B T \nabla_i \ln \Psi, \quad (59)$$

where we have used Eq. (54) to make $\mathbf{f}_i^{\text{det}}(\mathbf{r}^N, t)$ explicit. The last term on the right-hand sides corresponds to the noise contribution in the Langevin equation (53); by differentiating the logarithm, the term can be analogously rewritten as $-(k_B T / \Psi) \nabla_i \Psi$. The position derivative in the Smoluchowski equation (57) acts both on \mathbf{v}_i and on the distribution function; hence, Eq. (57) has the form of a continuity equation for the local conservation of probability, as the right-hand side expresses the negative divergence of a probability current $\mathbf{v}_i \Psi$.

It is instructive to rewrite the Smoluchowski equation in operator form as follows:

$$\frac{\partial \Psi}{\partial t} = - \sum_i \nabla_i \cdot \gamma^{-1} (\mathbf{f}_i^{\text{det}} - k_B T \nabla_i \ln \Psi) \Psi \quad (60)$$

$$= -\gamma^{-1} \sum_i [(\nabla_i \cdot \mathbf{f}_i^{\text{det}}) + \mathbf{f}_i^{\text{det}} \cdot \nabla_i - k_B T \nabla_i^2] \Psi \quad (61)$$

$$\equiv \hat{\Omega} \Psi, \quad (62)$$

where the *Smoluchowski operator* is defined as

$$\hat{\Omega} = -\gamma^{-1} \sum_i [(\nabla_i \cdot \mathbf{f}_i^{\text{det}}) + \mathbf{f}_i^{\text{det}} \cdot \nabla_i - k_B T \nabla_i^2]. \quad (63)$$

The Smoluchowski equation is in compact notation simply

$$\frac{\partial \Psi}{\partial t} = \hat{\Omega} \Psi, \quad (64)$$

which is a partial differential equation of first order in time and second order in position. However, in contrast to the Schrödinger equation, here Ψ is real. Hence, there is no coupling of real and imaginary parts, as occurs in quantum mechanics. The Smoluchowski equation is instead a drift-diffusion equation for the many-body distribution function. In particular, the diffusive effect is generated by the Laplace operator ∇_i^2 .

Again, one central purpose of Ψ is to facilitate building averages O via

$$O = \langle \hat{O} \rangle = \int d\mathbf{r}^N \hat{O} \Psi(\mathbf{r}^N, t), \quad (65)$$

where \hat{O} is an operator that constitutes a physical observable. If \hat{O} is a configuration space function $\hat{O}(\mathbf{r}^N, t)$, then the order of terms in the integrand does not matter ($\langle \hat{O} \rangle = \int d\mathbf{r}^N \hat{O} \Psi = \int d\mathbf{r}^N \Psi \hat{O}$).

For the case of the density operator $\hat{\rho} = \sum_i \delta(\mathbf{r} - \mathbf{r}_i)$ we obtain the one-body density distribution

$$\rho(\mathbf{r}, t) = \langle \hat{\rho} \rangle = \int d\mathbf{r}^N \sum_i \delta(\mathbf{r} - \mathbf{r}_i) \Psi(\mathbf{r}^N, t). \quad (66)$$

We turn to the description of the one-body dynamics and are interested in the time evolution of $\rho(\mathbf{r}, t)$. Hence, we consider the time derivative

$$\frac{\partial}{\partial t} \rho(\mathbf{r}, t) = \frac{\partial}{\partial t} \int d\mathbf{r}^N \sum_i \delta(\mathbf{r} - \mathbf{r}_i) \Psi \quad (67)$$

$$= \int d\mathbf{r}^N \sum_i \delta(\mathbf{r} - \mathbf{r}_i) \frac{\partial \Psi}{\partial t} \quad (68)$$

$$= - \int d\mathbf{r}^N \sum_i \delta(\mathbf{r} - \mathbf{r}_i) \sum_j \nabla_j \cdot \mathbf{v}_j \Psi \quad (69)$$

$$= \int d\mathbf{r}^N \sum_i \sum_j [\nabla_j \delta(\mathbf{r} - \mathbf{r}_i)] \cdot \mathbf{v}_j \Psi \quad (70)$$

$$= -\nabla \cdot \int d\mathbf{r}^N \sum_i \delta(\mathbf{r} - \mathbf{r}_i) \mathbf{v}_i \Psi \quad (71)$$

$$= -\nabla \cdot \mathbf{J}(\mathbf{r}, t), \quad (72)$$

where we have used the Smoluchowski equation (57) for Eq. (69), integration by parts for Eq. (70), and the identity $\nabla_j \delta(\mathbf{r} - \mathbf{r}_i) = -\delta_{ij} \nabla \delta(\mathbf{r} - \mathbf{r}_i)$ for Eq. (71). In the last step [Eq. (72)] we have defined the one-body current distribution as

$$\mathbf{J}(\mathbf{r}, t) = \langle \hat{\mathbf{J}} \rangle, \quad (73)$$

$$\hat{\mathbf{J}} = \sum_i \delta(\mathbf{r} - \mathbf{r}_i) \mathbf{v}_i, \quad (74)$$

where $\hat{\mathbf{J}}$ is the current operator. As an aside, the current operator can alternatively be expressed, using the *velocity differential operator* $\hat{\mathbf{v}}_i$, as

$$\hat{\mathbf{J}} = \sum_i \delta(\mathbf{r} - \mathbf{r}_i) \hat{\mathbf{v}}_i, \quad (75)$$

$$\gamma \hat{\mathbf{v}}_i = \mathbf{f}_i^{\text{det}} - k_B T \nabla_i, \quad (76)$$

where $\mathbf{f}_i^{\text{det}}(\mathbf{r}^N, t)$ is still given via Eq. (54). It is straightforward to show that $\hat{\mathbf{v}}_i \Psi = \mathbf{v}_i \Psi$, and hence that both velocity representations yield the same one-body current distribution. [The many-body velocity should not be confused with the average, microscopically resolved *velocity field* $\mathbf{v}(\mathbf{r}, t) = \mathbf{J}(\mathbf{r}, t) / \rho(\mathbf{r}, t)$.]

It remains to express the current distribution via the forces that act in the system. As the dynamics are overdamped, no further time derivative is required. We instead rewrite the distribution as follows:

$$\gamma \mathbf{J}(\mathbf{r}, t) = \gamma \int d\mathbf{r}^N \sum_i \delta(\mathbf{r} - \mathbf{r}_i) \mathbf{v}_i \Psi \quad (77)$$

$$= \int d\mathbf{r}^N \sum_i \delta(\mathbf{r} - \mathbf{r}_i) (\mathbf{f}_i^{\text{det}} - k_B T \nabla_i \ln \Psi) \Psi \quad (78)$$

$$= \int d\mathbf{r}^N \sum_i \delta(\mathbf{r} - \mathbf{r}_i) \times [-(\nabla_i u) + \mathbf{f}_{\text{ext}}(\mathbf{r}_i, t) - k_B T \nabla_i] \Psi \quad (79)$$

$$= - \int d\mathbf{r}^N \sum_i \delta(\mathbf{r} - \mathbf{r}_i) (\nabla_i u) \Psi + \int d\mathbf{r}^N \sum_i \delta(\mathbf{r} - \mathbf{r}_i) \mathbf{f}_{\text{ext}}(\mathbf{r}_i, t) \Psi - \int d\mathbf{r}^N \sum_i \delta(\mathbf{r} - \mathbf{r}_i) k_B T \nabla_i \Psi \quad (80)$$

$$\equiv \mathbf{F}_{\text{int}}(\mathbf{r}, t) + \rho(\mathbf{r}, t) \mathbf{f}_{\text{ext}}(\mathbf{r}, t) - k_B T \nabla \rho(\mathbf{r}, t). \quad (81)$$

In Eq. (81) we have defined the first integral in Eq. (80) as the internal force density distribution

$$\mathbf{F}_{\text{int}}(\mathbf{r}, t) = - \int d\mathbf{r}^N \sum_i \delta(\mathbf{r} - \mathbf{r}_i) (\nabla_i u) \Psi. \quad (82)$$

In the second integral in Eq. (80) we have replaced $\mathbf{f}_{\text{ext}}(\mathbf{r}_i, t)$ with $\mathbf{f}_{\text{ext}}(\mathbf{r}, t)$ due to the presence of the delta function. In the third integral in Eq. (80) we have integrated by parts and once more used $\nabla_i \delta(\mathbf{r} - \mathbf{r}_i) = -\nabla \delta(\mathbf{r} - \mathbf{r}_i)$.

The equations of motion of motion follow as

$$\gamma \mathbf{J}(\mathbf{r}, t) = \mathbf{F}_{\text{int}}(\mathbf{r}, t) + \rho(\mathbf{r}, t) \mathbf{f}_{\text{ext}}(\mathbf{r}, t) - k_B T \nabla \rho(\mathbf{r}, t), \quad (83)$$

$$\frac{\partial \rho(\mathbf{r}, t)}{\partial t} = -\nabla \cdot \mathbf{J}(\mathbf{r}, t). \quad (84)$$

The current can be eliminated to obtain a single equation for the time evolution of the one-body density

$$\frac{\partial \rho(\mathbf{r}, t)}{\partial t} = -\gamma^{-1} \nabla \cdot \mathbf{F}_{\text{int}}(\mathbf{r}, t) - \gamma^{-1} \nabla \cdot \rho(\mathbf{r}, t) \mathbf{f}_{\text{ext}}(\mathbf{r}, t) + D \nabla^2 \rho(\mathbf{r}, t), \quad (85)$$

where $D = k_B T / \gamma$ is the diffusion constant according to Einstein's relation.

It is instructive to scale Eq. (83) by the density profile. We first define the internal microscopic one-body force field by normalizing as follows:

$$\mathbf{f}_{\text{int}}(\mathbf{r}, t) = \mathbf{F}_{\text{int}}(\mathbf{r}, t) / \rho(\mathbf{r}, t). \quad (86)$$

The microscopic velocity field is obtained as before as the ratio

$$\mathbf{v}(\mathbf{r}, t) = \mathbf{J}(\mathbf{r}, t) / \rho(\mathbf{r}, t). \quad (87)$$

We can now rewrite the force density balance (83) by dividing by the density profile, which yields the following *force balance* relationship:

$$\gamma \mathbf{v}(\mathbf{r}, t) = \mathbf{f}_{\text{int}}(\mathbf{r}, t) + \mathbf{f}_{\text{ext}}(\mathbf{r}, t) - k_B T \nabla \ln \rho(\mathbf{r}, t). \quad (88)$$

Note that there are no transport contributions (kinetic stress is absent), as the motion is overdamped. However, diffusive effects do occur. The equations of motion are not closed on the one-body level, as the internal force density distribution $\mathbf{F}_{\text{int}}(\mathbf{r}, t)$ is unknown at this stage and defined only via the many-body average (82).

There are three possible ways out.

- (i) Solve the many-body dynamics numerically, using either trajectory-based Brownian dynamics (BD) or, for a small number of degrees of freedom, the Smoluchowski equation.
- (ii) Relate $\mathbf{F}_{\text{int}}(\mathbf{r}, t)$ to higher-body (two-body, three-body, etc.) correlation functions and formulate closure relations. This is both technically and conceptually difficult.
- (iii) Express $\mathbf{F}_{\text{int}}(\mathbf{r}, t)$ in a variational way via a generator (generating functional). This is also technically and conceptually difficult, but it is complementary to (i) and (ii). [Hybrid forms of (i) and (iii) could be imagined.] We describe the power functional for overdamped BD in Sec. IV.B.

D. Quantum dynamics

Besides its relevance in a broad variety of systems, the importance of quantum dynamics in this context lies not least

in its formal similarities with the classical Hamiltonian dynamics (Sec. II.B). As we demonstrate in the following, a case can be made for the universality of the dynamical one-body point of view.⁵ Readers who are interested primarily in classical systems may proceed directly to Sec. III, where we cover classical density-functional theory. Besides the significant importance in its own right, this approach also acts as both a blueprint and an integral component for the dynamical theory. The connection is via the adiabatic construction, as described in Sec. III.A.

We consider N spinless nonrelativistic quantum particles that are coupled using an internal interaction potential $u(\mathbf{r}^N)$. The particles have an electrical charge q and mass m . The particles are exposed to a magnetic vector potential $\mathbf{A}(\mathbf{r}, t)$ and an external potential energy $V_{\text{ext}}(\mathbf{r}, t)$. The form of $u(\mathbf{r}^N)$ is general, possibly including a Coulombic contribution. We use the position representation of the Schrödinger equation

$$i\hbar \frac{\partial}{\partial t} \Psi(\mathbf{r}^N, t) = \hat{H} \Psi(\mathbf{r}^N, t), \quad (89)$$

with $\Psi(\mathbf{r}^N, t)$ the quantum mechanical wave function and \hat{H} the Hamiltonian. The wave function is normalized at all times as $\int d\mathbf{r}^N \Psi^* \Psi = \int d\mathbf{r}^N |\Psi|^2 = 1$; the asterisk denotes the complex conjugate. The Hamiltonian has the following form of kinetic energy plus potential energy:

$$\hat{H} = \sum_i \frac{\hat{\mathbf{p}}_i^2}{2m} + u(\mathbf{r}^N) + \sum_i V_{\text{ext}}(\mathbf{r}_i, t), \quad (90)$$

where the kinematic momentum operator is

$$\hat{\mathbf{p}}_i = -i\hbar \nabla_i - q\mathbf{A}(\mathbf{r}_i, t), \quad (91)$$

with the first term acting via differentiation and the second term acting via multiplication (on the wave function in position representation).

Our goal is to obtain the reduced one-body dynamics. Consider the following general Heisenberg equation of motion for an operator \hat{O} :

$$\frac{d\hat{O}}{dt} = \frac{i}{\hbar} [\hat{H}, \hat{O}] + \frac{\partial \hat{O}}{\partial t}, \quad (92)$$

where the brackets denote the commutator of two operators. Quantum mechanical averages O are built using the following bra-ket sandwich:

$$O = \langle \hat{O} \rangle = \langle \Psi | \hat{O} | \Psi \rangle = \int d\mathbf{r}^N \Psi^* \hat{O} \Psi, \quad (93)$$

where, depending on the form of the operator \hat{O} , its expectation value can have both explicit and implicit time dependence.

⁵See Tchenkoue *et al.* (2019) and Tarantino and Ullrich (2021) for recent work addressing the force balance in the context of time-dependent density-functional theory.

Applying Eq. (92) to the position operator yields

$$\frac{d\mathbf{r}_i}{dt} = \frac{\hat{\mathbf{p}}_i}{m}, \quad (94)$$

which shows that calling Eq. (91) the kinematic momentum is justified.

We next differentiate $\hat{\mathbf{p}}_i$ in time. The calculation (which is omitted) is lengthier but straightforward. We define the force operator for particle i as

$$\hat{\mathbf{f}}_i = -[\nabla_i u(\mathbf{r}^N)] - [\nabla_i V_{\text{ext}}(\mathbf{r}_i, t)] - q\dot{\mathbf{A}}(\mathbf{r}_i, t) + \frac{q}{2m} [\hat{\mathbf{p}}_i \times \mathbf{B}(\mathbf{r}_i, t) - \mathbf{B}(\mathbf{r}_i, t) \times \hat{\mathbf{p}}_i], \quad (95)$$

where the magnetic field is $\mathbf{B}(\mathbf{r}, t) = \nabla \times \mathbf{A}(\mathbf{r}, t)$.

The equation of motion (92) for $\hat{\mathbf{p}}_i$ then attains the compact form

$$\frac{d\hat{\mathbf{p}}_i}{dt} = \hat{\mathbf{f}}_i, \quad (96)$$

which is Newton's second law on the operator level.

We next summarize the relevant one-body operators, for density \hat{n} , current $\hat{\mathbf{J}}$, kinetic stress $\hat{\boldsymbol{\tau}}$, and internal force density $\hat{\mathbf{F}}_{\text{int}}$. These are defined, respectively, by

$$\hat{n} = \sum_i \delta(\mathbf{r} - \mathbf{r}_i), \quad (97)$$

$$\hat{\mathbf{J}} = \frac{1}{2m} \sum_i [\hat{\mathbf{p}}_i \delta(\mathbf{r} - \mathbf{r}_i) + \delta(\mathbf{r} - \mathbf{r}_i) \hat{\mathbf{p}}_i], \quad (98)$$

$$\hat{\boldsymbol{\tau}} = -\frac{1}{2m} \sum_i (\hat{\mathbf{p}}_i \delta_i \hat{\mathbf{p}}_i + \hat{\mathbf{p}}_i \delta_i \hat{\mathbf{p}}_i^{\text{T}}), \quad (99)$$

$$\hat{\mathbf{F}}_{\text{int}} = -\sum_i [\nabla_i u(\mathbf{r}^N)] \delta(\mathbf{r} - \mathbf{r}_i), \quad (100)$$

where we have used the shorthand notation $\delta_i = \delta(\mathbf{r} - \mathbf{r}_i)$ in Eq. (99) and the superscript T indicates the transpose of a $d \times d$ matrix (here a dyadic product). Both the density and internal force density are multiplication operators. All occurring kinematic momentum operators act on all arguments to their right.

We now derive the corresponding equations of motion, beginning with the density operator. (The change of notation from $\hat{\rho}$ to \hat{n} is cosmetic, done in order to conform to quantum convention.) We consider the density operator for particle i and apply the Heisenberg equation of motion (92), which yields

$$\frac{d}{dt} \delta(\mathbf{r} - \mathbf{r}_i) = \frac{i}{\hbar} [\hat{H}, \delta(\mathbf{r} - \mathbf{r}_i)] + \frac{\partial}{\partial t} \delta(\mathbf{r} - \mathbf{r}_i) \quad (101)$$

$$= \frac{i}{2m\hbar} \sum_j [\hat{\mathbf{p}}_j^2, \delta(\mathbf{r} - \mathbf{r}_i)], \quad (102)$$

where the commutator of the potential energy contributions and the density operator (delta function) vanishes, as does the partial time derivative of the delta function.

To address Eq. (102), we consider the following general form of the commutator of $\hat{\mathbf{p}}_i^2 \equiv p^2$ with a function $g(\mathbf{r}^N)$:

$$[p^2, g(\mathbf{r}^N)] = p^2g - pgp + pgp - gp^2 \quad (103)$$

$$= p(pg - gp) + (pg - gp)p \quad (104)$$

$$= p[p, g] + [p, g]p \quad (105)$$

$$= p(-i\hbar\nabla_i g) - i\hbar(\nabla_i g)p, \quad (106)$$

where we have used $[p, g] = -i\hbar(\nabla_i g)$. Returning to the full notation, hence, we have

$$[\hat{\mathbf{p}}_i^2, g(\mathbf{r}^N)] = -i\hbar[\hat{\mathbf{p}}_i \cdot (\nabla_i g) + (\nabla_i g) \cdot \hat{\mathbf{p}}_i]. \quad (107)$$

The application to Eq. (102) yields zero for the case $i \neq j$. For $i = j$ we obtain

$$\frac{i}{2m\hbar} [\hat{\mathbf{p}}_i^2, \delta(\mathbf{r} - \mathbf{r}_i)] \quad (108)$$

$$= \frac{-i^2\hbar}{2m\hbar} \{ \hat{\mathbf{p}}_i \cdot [\nabla_i \delta(\mathbf{r} - \mathbf{r}_i)] + [\nabla_i \delta(\mathbf{r} - \mathbf{r}_i)] \cdot \hat{\mathbf{p}}_i \} \quad (109)$$

$$= -\nabla \cdot \frac{1}{2m} [\hat{\mathbf{p}}_i \delta(\mathbf{r} - \mathbf{r}_i) + \delta(\mathbf{r} - \mathbf{r}_i) \hat{\mathbf{p}}_i], \quad (110)$$

where we have used $\nabla_i \delta(\mathbf{r} - \mathbf{r}_i) = -\nabla \delta(\mathbf{r} - \mathbf{r}_i)$. Recalling that the left-hand side of Eq. (101) is the time derivative of $\delta(\mathbf{r} - \mathbf{r}_i)$ and summing over all particles yields

$$\frac{d}{dt} \hat{n} = -\nabla \cdot \hat{\mathbf{J}}, \quad (111)$$

which can rightfully be called the operator continuity equation. Here the anticipated form (98) of the current operator $\hat{\mathbf{J}}$ applies. Building quantum mechanical expectation values yields the one-body density distribution and the one-body current distribution, which are defined, respectively, by

$$n(\mathbf{r}, t) = \langle \hat{n} \rangle = \int d\mathbf{r}^N \Psi^* \hat{n} \Psi, \quad (112)$$

$$\mathbf{J}(\mathbf{r}, t) = \langle \hat{\mathbf{J}} \rangle = \int d\mathbf{r}^N \Psi^* \hat{\mathbf{J}} \Psi. \quad (113)$$

Building the quantum average over the operator continuity equation (111) yields the continuity equation

$$\frac{\partial}{\partial t} n(\mathbf{r}, t) = -\nabla \cdot \mathbf{J}(\mathbf{r}, t), \quad (114)$$

where we have changed the notation from total to partial time derivative. This is purely cosmetic; the character of the time derivative has not changed. In both cases the time derivative is with respect to the real dynamics and at fixed position \mathbf{r} . The form of Eq. (114) is identical to that of the classical result [Eq. (48)].

Current operator dynamics.—We turn to the time evolution of the current operator (98). Our hope, if not our expectation, is to be able to identify a relationship to the transport contribution represented by the kinetic stress tensor (99) and to the internal force density operator (100). Hence, we are seeking an analog of the classical MD force density relationship [Eq. (44)]. This can indeed be established, albeit not without a certain level of engagement in the quantum formalism; however, all manipulations are straightforward in principle. We start by considering the time evolution of the current operator of particle i , defined as $\mathbf{J}_i = (\delta_i \hat{\mathbf{p}}_i + \hat{\mathbf{p}}_i \delta_i)/2m$, where $\delta_i = \delta(\mathbf{r} - \mathbf{r}_i)$, such that the total current operator is $\hat{\mathbf{J}} = \sum_i \hat{\mathbf{J}}_i$. Hence,

$$\frac{d}{dt} \hat{\mathbf{J}}_i = \frac{i}{\hbar} [\hat{H}, \hat{\mathbf{J}}_i] + \frac{\partial}{\partial t} \hat{\mathbf{J}}_i. \quad (115)$$

The last term in Eq. (115) can be simplified as

$$\frac{\partial}{\partial t} \hat{\mathbf{J}}_i = \frac{1}{2m} \frac{\partial}{\partial t} (\delta_i \hat{\mathbf{p}}_i + \hat{\mathbf{p}}_i \delta_i) \quad (116)$$

$$= \frac{1}{2m} \{ \delta_i [-q\dot{\mathbf{A}}(\mathbf{r}_i, t)] + [-q\dot{\mathbf{A}}(\mathbf{r}_i, t)] \delta_i \} \quad (117)$$

$$= -\frac{q}{m} \delta_i \dot{\mathbf{A}}(\mathbf{r}_i, t), \quad (118)$$

which is a multiplication operator and an expected part of the force density balance. We hence still need to consider the first (commutator) term in Eq. (115). We first address the following kinetic energy contribution to the Hamiltonian:

$$\begin{aligned} & \frac{i}{\hbar} \left[\sum_j \frac{\hat{\mathbf{p}}_j^2}{2m}, \frac{\hat{\mathbf{p}}_i \delta_i + \delta_i \hat{\mathbf{p}}_i}{2} \right] \\ &= \frac{i[\hat{\mathbf{p}}_i^2, \hat{\mathbf{p}}_i \delta_i + \delta_i \hat{\mathbf{p}}_i]}{4m\hbar} \\ &= \frac{i}{4m\hbar} (\hat{p}_i^\alpha [\hat{p}_i^\alpha, \hat{\mathbf{p}}_i \delta_i + \delta_i \hat{\mathbf{p}}_i] + [\hat{p}_i^\alpha, \hat{\mathbf{p}}_i \delta_i + \delta_i \hat{\mathbf{p}}_i] \hat{p}_i^\alpha), \end{aligned} \quad (119)$$

where \hat{p}_i^α is the α th Cartesian component of $\hat{\mathbf{p}}_i$ and the Einstein summation convention over α is implied. Contributions with $i \neq j$ vanish as there is no coupling between ∇_j and \mathbf{r}_i . Hence, we need the following commutator identity (which can be explicitly proven):

$$\begin{aligned} & \frac{i}{4m\hbar} \sum_i [\hat{\mathbf{p}}_i^2, \hat{\mathbf{p}}_i \delta_i + \delta_i \hat{\mathbf{p}}_i] \\ &= \nabla \cdot \hat{\boldsymbol{\tau}} + \frac{q}{2m} \sum_i [\delta_i (\hat{\mathbf{p}}_i \times \mathbf{B}_i - \mathbf{B}_i \times \hat{\mathbf{p}}_i) \\ & \quad + (\hat{\mathbf{p}}_i \times \mathbf{B}_i - \mathbf{B}_i \times \hat{\mathbf{p}}_i) \delta_i] + \frac{\hbar^2}{4m} \nabla \nabla^2 \hat{n}, \end{aligned} \quad (120)$$

where the kinetic one-body stress operator is a second-rank tensor given by

$$\hat{\boldsymbol{\tau}} = -\frac{1}{2m} \sum_i (\hat{\mathbf{p}}_i \delta_i \hat{\mathbf{p}}_i + \hat{\mathbf{p}}_i \delta_i \hat{\mathbf{p}}_i^T). \quad (121)$$

It remains to consider the potential energy contribution to the commutator in Eq. (115). Defining the total potential energy as $V(\mathbf{r}^N) = u(\mathbf{r}^N) + \sum_i V_{\text{ext}}(\mathbf{r}_i, t)$, we have

$$\frac{i}{\hbar} \left[V, \frac{\hat{\mathbf{p}}_i \delta_i + \delta_i \hat{\mathbf{p}}_i}{2m} \right] = -\frac{i}{2m\hbar} [\hat{\mathbf{p}}_i \delta_i + \delta_i \hat{\mathbf{p}}_i, V] \quad (122)$$

$$= -\frac{i}{2m\hbar} (-i\hbar) [\nabla_i \delta_i + \delta_i \nabla_i, V], \quad (123)$$

as the magnetic contribution $-2q\mathbf{A}_i \delta_i$ commutes with the potential energy. Hence, we can rewrite Eq. (123) as

$$-\frac{1}{2m} ([\nabla_i \delta_i, V] + [\delta_i \nabla_i, V]) \quad (124)$$

$$= -\frac{1}{2m} (\nabla_i \delta_i V - V \nabla_i \delta_i + \delta_i \nabla_i V - V \delta_i \nabla_i) \quad (125)$$

$$= -\frac{1}{2m} [(\nabla_i \delta_i) V + \delta_i (\nabla_i V) + \delta_i V \nabla_i - V (\nabla_i \delta_i) - V \delta_i \nabla_i + \delta_i (\nabla_i V) + \delta_i V \nabla_i - V \delta_i \nabla_i] \quad (126)$$

$$= \frac{1}{m} \delta_i (-\nabla_i V) \quad (127)$$

$$= \frac{1}{m} \delta(\mathbf{r} - \mathbf{r}_i) (-\nabla_i V) \quad (128)$$

$$= \frac{1}{m} \{ \delta_i [-\nabla_i u(\mathbf{r}^N)] + \delta_i [-\nabla_i V_{\text{ext}}(\mathbf{r}_i, t)] \}, \quad (129)$$

where in the last step we have split the total potential energy into internal and external contributions. Equation (129) is the (perhaps expected) contribution to the force density due to potential forces.

Collecting all terms, i.e., Eqs. (118), (120), and (129), yields

$$m \frac{d}{dt} \hat{\mathbf{J}} = \nabla \cdot \hat{\boldsymbol{\tau}} + \frac{\hbar^2}{4m} \nabla \nabla^2 \hat{n} + \hat{\mathbf{F}}, \quad (130)$$

where the total force density operator is defined as

$$\hat{\mathbf{F}} = \frac{1}{2} \sum_i (\hat{\mathbf{f}}_i \delta_i + \delta_i \hat{\mathbf{f}}_i), \quad (131)$$

with the force operator of particle i given by

$$\hat{\mathbf{f}}_i = -[\nabla_i u(\mathbf{r}^N)] - [\nabla_i V_{\text{ext}}(\mathbf{r}_i, t)] - q \dot{\mathbf{A}}(\mathbf{r}_i, t) + \frac{q}{2m} (\hat{\mathbf{p}}_i \times \mathbf{B}_i - \mathbf{B}_i \times \hat{\mathbf{p}}_i). \quad (132)$$

Building the quantum average $\langle \cdot \rangle = \int d\mathbf{r}^N \Psi^* \cdot \Psi$ of Eq. (130) yields the following force density balance in the form of Newton's second law for one-body current and force density distributions:

$$m \frac{d}{dt} \mathbf{J}(\mathbf{r}, t) = \frac{\hbar^2}{4m} \nabla \nabla^2 n(\mathbf{r}, t) + \nabla \cdot \boldsymbol{\tau}(\mathbf{r}, t) + \mathbf{F}(\mathbf{r}, t). \quad (133)$$

Here the total one-body force density is given by

$$\mathbf{F}(\mathbf{r}, t) = \mathbf{F}_{\text{int}}(\mathbf{r}, t) - n(\mathbf{r}, t) [\nabla V_{\text{ext}}(\mathbf{r}, t) + q \dot{\mathbf{A}}(\mathbf{r}, t)] + q \mathbf{J}(\mathbf{r}, t) \times \mathbf{B}(\mathbf{r}, t), \quad (134)$$

and the internal force density is given by the quantum average $\mathbf{F}_{\text{int}}(\mathbf{r}, t) = -\langle \sum_i [\nabla_i u(\mathbf{r}^N)] \delta(\mathbf{r} - \mathbf{r}_i) \rangle$.

As a corollary, for a single particle $N = 1$, $\mathbf{r}^N \equiv \mathbf{r}_1$, $\mathbf{F}_{\text{int}}(\mathbf{r}, t) = 0$, and the resulting equation of motion takes on the following form (leaving away arguments \mathbf{r}, t):

$$m \frac{d\mathbf{J}}{dt} = (-q \dot{\mathbf{A}} - \nabla V_{\text{ext}}) n + q \mathbf{J} \times \mathbf{B} + \nabla \cdot \boldsymbol{\tau}_{\text{id}} + \frac{\hbar^2}{4m} \nabla \nabla^2 n, \quad (135)$$

$$\boldsymbol{\tau}_{\text{id}} = -m \frac{\mathbf{J}\mathbf{J}}{n} - \frac{\hbar^2}{4m} \frac{(\nabla n)(\nabla n)}{n}, \quad (136)$$

which is exact, i.e., equivalent to the Schrödinger equation for a single quantum particle. For $N \geq 2$ internal interactions will be relevant and the one-body description is no longer closed as both $\mathbf{F}_{\text{int}}(\mathbf{r}, t)$ and $\boldsymbol{\tau}(\mathbf{r}, t)$ are unknown. To address this issue, we return to the quantum dynamical case in Sec. IV.B, where we introduce functional generators for these fields, which then allow us to construct a formally closed one-body theory.

The classical and quantum force balance relationships, Eqs. (49) and (133), bear striking similarities to each other; note that the external force field is $\mathbf{f}_{\text{ext}}(\mathbf{r}, t) = -q \dot{\mathbf{A}}(\mathbf{r}, t) + q \mathbf{v}(\mathbf{r}, t) \times \mathbf{B}(\mathbf{r}, t) - \nabla V_{\text{ext}}(\mathbf{r}, t)$. Sometimes the first term on the right-hand side of Eq. (133) is subsumed into a modified kinetic stress tensor $\boldsymbol{\tau}_{\text{QM}}(\mathbf{r}, t) = \boldsymbol{\tau}(\mathbf{r}, t) + \hbar^2 \nabla \nabla n(\mathbf{r}, t) / 4m$, which then renders Eqs. (49) and (133) formally identical.

III. THE ADIABATIC STATE

A. The adiabatic construction

In the following we describe the concept of splitting the internal force field of a nonequilibrium system into an adiabatic and an additional superadiabatic contribution. We restrict ourselves to the case of classical overdamped Brownian many-body dynamics. The adiabatic construction, illustrated in Fig. 2, was explicitly demonstrated on the basis of computer simulation results by Fortini *et al.* (2014) using a one-dimensional hard-core system. A range of subsequent studies were aimed at the Gaussian core model (Bernreuther and Schmidt, 2016; Stuhlmüller *et al.*, 2018), the Lennard-Jones liquid (Schindler and Schmidt, 2016), Weeks-Chandler-Andersen repulsive particles (de las Heras and Schmidt, 2020), and hard disks (de las Heras and Schmidt, 2018a; Jahreis and Schmidt, 2020). An elegant and computationally straightforward implementation in simulation work is via the custom flow method of de las Heras, Renner, and Schmidt (2019), as described in Sec. IV.F.

We start by recalling the BD one-body force field balance (88), where the time-dependent internal force field

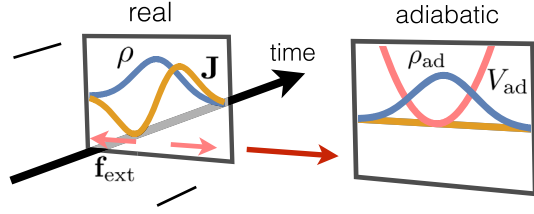


FIG. 2. Illustration of the adiabatic construction. Left panel: the real system evolves in time according to BD. It is characterized by an in general inhomogeneous density distribution $\rho(\mathbf{r}, t)$ and an inhomogeneous one-body current $\mathbf{J}(\mathbf{r}, t) \neq 0$. The adiabatic state is constructed at each fixed time, such that $\rho(\mathbf{r}, t)$ is identical to the density profile $\rho_{\text{ad},t}(\mathbf{r})$ in the adiabatic system at the time considered. Right panel: the adiabatic system is in equilibrium, and hence there is no average current. The inhomogeneous adiabatic density profile is stabilized by the action of an external potential $V_{\text{ad},t}(\mathbf{r})$, which acts solely in the adiabatic system, but not in the real system. In the real system it is the external force field $\mathbf{f}_{\text{ext}}(\mathbf{r}, t)$ that drives the dynamics.

$\mathbf{f}_{\text{int}}(\mathbf{r}, t)$ is defined via the correlator (82) and the ratio (86), i.e.,

$$\mathbf{f}_{\text{int}}(\mathbf{r}, t)\rho(\mathbf{r}, t) = -\left\langle \sum_i [\nabla_i u(\mathbf{r}^N)] \delta(\mathbf{r} - \mathbf{r}_i) \right\rangle. \quad (137)$$

The time-dependent density profile is $\rho(\mathbf{r}, t) = \langle \hat{\rho} \rangle$, where the average is carried out over the nonequilibrium many-body probability distribution $\Psi(\mathbf{r}^N, t)$. We compare Eq. (88) at time t to the force balance relationship in a second system, which is at rest (on average) and in equilibrium. Hence, in this so-called adiabatic system

$$0 = -k_B T \nabla \ln \rho_{\text{ad},t}(\mathbf{r}) + \mathbf{f}_{\text{ad},t}(\mathbf{r}) - \nabla V_{\text{ad},t}(\mathbf{r}), \quad (138)$$

where $\rho_{\text{ad},t}(\mathbf{r})$ is the density profile and $V_{\text{ad},t}(\mathbf{r})$ is the external potential in the adiabatic system; $-\nabla V_{\text{ad},t}(\mathbf{r})$ is the external force field, which is necessarily of a gradient nature as the adiabatic system is in equilibrium. The internal force field $\mathbf{f}_{\text{ad},t}(\mathbf{r})$ in the adiabatic system, expressed as an average, is given via

$$\mathbf{f}_{\text{ad},t}(\mathbf{r})\rho_{\text{ad},t}(\mathbf{r}) = -\left\langle \sum_i [\nabla_i u(\mathbf{r}^N)] \delta(\mathbf{r} - \mathbf{r}_i) \right\rangle_{\text{eq}}, \quad (139)$$

which is similar in form to the nonequilibrium internal force field [Eq. (137)], with the sole distinction (and an important one) being that an equilibrium average is carried out (at fixed N, V, T , i.e., canonically, indicated by the subscript eq). The density profile in the adiabatic system is the equilibrium average $\rho_{\text{ad},t}(\mathbf{r}) = \langle \hat{\rho} \rangle_{\text{eq}}$.

Assume the most general case of a spatially inhomogeneous system that evolves in time, i.e., consider $\rho(\mathbf{r}, t)$ as having nontrivial dependence on both of its arguments. At each time t we choose the adiabatic system in such a way that its density profile coincides with that in the nonequilibrium system. This amounts to the density matching condition

$$\rho_{\text{ad},t}(\mathbf{r}) = \rho(\mathbf{r}, t), \quad (140)$$

where the adiabatic density profile has acquired a parametric dependence on time but is itself stationary as the adiabatic system is in equilibrium at the same temperature T of the nonequilibrium system. (More precisely, were one to evolve the adiabatic system according to its own time evolution, i.e., along a new adiabatic time axis t_{ad} , then with respect to t_{ad} no changes in the adiabatic density profile occur.)

The many-body distributions in the real system and in the adiabatic system will in general differ from each other [$\Psi(\mathbf{r}^N, t) \neq \Psi_{\text{ad},t}(\mathbf{r}^N)$]. However,

$$\int d\mathbf{r}^N \hat{\rho} \Psi_{\text{ad},t}(\mathbf{r}^N) = \int d\mathbf{r}^N \hat{\rho} \Psi(\mathbf{r}^N, t), \quad (141)$$

which is the density matching condition (140) written in explicit average form.

Per construction $\Psi_{\text{ad},t}(\mathbf{r}^N)$ needs necessarily to be of normalized Boltzmann form, as is appropriate for the canonical ensemble at fixed N, V , and T . One might wonder whether such a distribution is guaranteed to exist. Note that we are dealing with a potentially complex situation, as $\rho_{\text{ad},t}(\mathbf{r})$ can have a virtually arbitrary shape (as long as it is one that occurs in a real time evolution of the system). The answer to the question is affirmative, based on a Hamiltonian with an unchanged interparticle interaction potential $u(\mathbf{r}^N)$, i.e., the adiabatic system is composed of, say, Lennard-Jones particles, when the real system under investigation is a time-dependent process in the Lennard-Jones system. The freedom that we need to introduce in the adiabatic system is the presence of an adiabatic external potential, which is, from the standpoint of the real system, of an entirely virtual nature and, in particular, different than the real force field $\mathbf{f}_{\text{ext}}(\mathbf{r}, t)$ that drives the time evolution. Mathematically, for a given $u(\mathbf{r}^N)$, there is a unique map in equilibrium, from the density distribution to the external potential, $\rho_{\text{ad}} \rightarrow V_{\text{ad}}$. This is indeed ensured by the theorem due to Mermin (1965) and Evans (1979).

It is of interest to study the internal force field in the adiabatic reference system. To gain access to $\mathbf{f}_{\text{ad},t}(\mathbf{r})$, there are two obvious routes.

- (i) We can use the correlator expression (139) and carry out the average. The Mermin-Evans theorem ensures that $V_{\text{ad},t}(\mathbf{r})$ is unique. Hence, the Hamiltonian is fully and uniquely specified, as is the canonical equilibrium probability distribution, which is required to carry out the average.
- (ii) The second route takes a shortcut, based directly on the external potential $V_{\text{ad},t}(\mathbf{r})$ (which again is determined in principle from the Mermin-Evans theorem) and a trivial rearranging of the equilibrium force balance relationship (138) into the form

$$\mathbf{f}_{\text{ad},t}(\mathbf{r}) = k_B T \nabla \ln \rho_{\text{ad},t}(\mathbf{r}) + \nabla V_{\text{ad},t}(\mathbf{r}). \quad (142)$$

Both routes are directly accessible in many-body simulation work and they can be equally useful. The density profile in the adiabatic system is known [recall the density matching condition (140)]. Hence, using either method in practice requires one to have an explicit representation of the

Mermin-Evans map $\rho_{\text{ad}} \rightarrow V_{\text{ad}}$. For computer simulation work, custom flow (de las Heras, Renner, and Schmidt, 2019) delivers this task.

An important point concerns higher-order correlation functions, i.e., those beyond the one-body density profile. While the density profile is per construction guaranteed to be the same in the dynamical and in the adiabatic system, higher-body correlation functions in general will differ. This is a straightforward consequence of the differences in underlying many-body distributions; recall the Boltzmann form in the adiabatic system versus the result of the Smoluchowski dynamics in the real system. In practice, the respective two-body density correlation functions are accessible in simulation work; see Fortini *et al.* (2014). Moreover, recent conceptual advances in DFT have demonstrated the relevance of two-body correlations, e.g., in the quest for systematically incorporating interparticle attraction; see the pioneering work by Tschopp *et al.* (2020) and Tschopp and Brader (2021).

As is the case for the higher-correlation functions, there is hence no reason to expect that the internal force density in the adiabatic system will be identical to the counterpart in the real system, and therefore $\mathbf{f}_{\text{int}}(\mathbf{r}, t) \neq \mathbf{f}_{\text{ad},t}(\mathbf{r})$ in general. Note that for the case of pair forces the pair distribution function determines the local force density. Nevertheless, as the interparticle interaction potential is the same in the real and in the adiabatic system, and the one-body density distribution has the same form, we might want $\mathbf{f}_{\text{ad},t}(\mathbf{r})$ to capture some of the properties of $\mathbf{f}_{\text{int}}(\mathbf{r}, t)$. (This is made rigorous in Sec. IV.) As a consequence the difference between the real force density and that of the adiabatic system might be a simpler object than the bare $\mathbf{f}_{\text{int}}(\mathbf{r}, t)$ itself. Hence, we define the superadiabatic force field $\mathbf{f}_{\text{sup}}(\mathbf{r}, t)$ as the difference

$$\mathbf{f}_{\text{sup}}(\mathbf{r}, t) = \mathbf{f}_{\text{int}}(\mathbf{r}, t) - \mathbf{f}_{\text{ad}}(\mathbf{r}, t), \quad (143)$$

where we have changed the notation $\mathbf{f}_{\text{ad},t}(\mathbf{r})$ to $\mathbf{f}_{\text{ad}}(\mathbf{r}, t)$. Here the term superadiabatic refers to the contribution above adiabatic or, more accurately, the contribution that acts in addition to the adiabatic force field. [This implies no simple relationship of the relative sign, the direction, or the magnitude of $\mathbf{f}_{\text{sup}}(\mathbf{r}, t)$ relative to either $\mathbf{f}_{\text{int}}(\mathbf{r}, t)$ or $\mathbf{f}_{\text{ad}}(\mathbf{r}, t)$.] We cover the behavior of these fields in model setups with several simplifying geometries when discussing power functional applications in Sec. IV. Figure 3 shows an illustration.

We insert the adiabatic-superadiabatic internal force splitting (143) into the nonequilibrium force balance relationship (88) and trivially obtain the equation of motion in the form

$$\begin{aligned} \gamma \mathbf{v}(\mathbf{r}, t) = & -k_B T \nabla \ln \rho(\mathbf{r}, t) \\ & + \mathbf{f}_{\text{ad}}(\mathbf{r}, t) + \mathbf{f}_{\text{sup}}(\mathbf{r}, t) + \mathbf{f}_{\text{ext}}(\mathbf{r}, t), \end{aligned} \quad (144)$$

with the adiabatic construction (Fortini *et al.*, 2014) implied [i.e., the density matching condition (140) that uniquely specifies the adiabatic system]. The functional dependencies of $\mathbf{f}_{\text{ad}}(\mathbf{r}, t)$ and $\mathbf{f}_{\text{sup}}(\mathbf{r}, t)$ are fundamentally different from each other. In the adiabatic system, owing to the Mermin-Evans map $\rho_{\text{ad}} \rightarrow V_{\text{ad}}$ and Eq. (142), we have a density-functional dependence

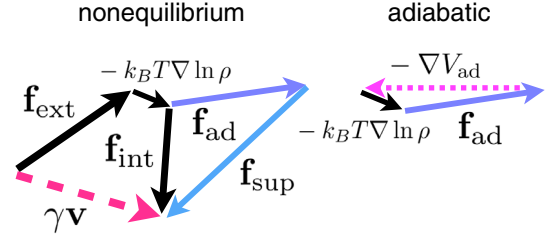


FIG. 3. Force balance in nonequilibrium (left panel) and in the adiabatic system (right panel). In nonequilibrium the sum of the external force field $\mathbf{f}_{\text{ext}}(\mathbf{r}, t)$, the diffusive force field $-k_B T \nabla \ln \rho(\mathbf{r}, t)$, and the internal force field $\mathbf{f}_{\text{int}}(\mathbf{r}, t)$ add up and generate the scaled flow $\gamma \mathbf{v}(\mathbf{r}, t)$. The internal force field $\mathbf{f}_{\text{int}}(\mathbf{r}, t)$ consists of a sum of adiabatic and superadiabatic contributions [$\mathbf{f}_{\text{ad}}(\mathbf{r}, t) + \mathbf{f}_{\text{sup}}(\mathbf{r}, t)$]. In the adiabatic system the sum of the diffusive force field $-k_B T \nabla \ln \rho(\mathbf{r}, t)$, the internal adiabatic force field $\mathbf{f}_{\text{ad}}(\mathbf{r}, t)$, and the adiabatic external force field $-\nabla V_{\text{ad},t}(\mathbf{r})$ vanishes, as there is no flow (average one-body motion) in equilibrium. The superadiabatic force field $\mathbf{f}_{\text{sup}}(\mathbf{r}, t)$ constitutes the genuine nonequilibrium contribution to the real dynamics.

$$\mathbf{f}_{\text{ad}}(\mathbf{r}, t) = \mathbf{f}_{\text{ad}}(\mathbf{r}, t, [\rho]) = \mathbf{f}_{\text{ad},t}(\mathbf{r}, [\rho_{\text{ad}}]), \quad (145)$$

where the adiabatic and dynamic density profiles are identical [see Eq. (140)] by construction. Hence, $\mathbf{f}_{\text{ad}}(\mathbf{r}, t)$ is an instantaneous (Markov-type) density functional with neither memory nor dependence on other kinematic variables. Its complexity lies entirely in the spatially nonlocal dependence on the density distribution. We see in Sec. IV that the superadiabatic force field depends functionally on density and flow as follows:

$$\mathbf{f}_{\text{sup}}(\mathbf{r}, t) = \mathbf{f}_{\text{sup}}(\mathbf{r}, t, [\rho, \mathbf{J}]) = \mathbf{f}_{\text{sup}}(\mathbf{r}, t, [\rho, \mathbf{v}]), \quad (146)$$

i.e., with an additional dependence on the current distribution or, equivalently, on the microscopic velocity field. In general the functional dependence will again be nonlocal in space, but also nonlocal in time [in the form of history dependence, i.e., dependence on $\rho(\mathbf{r}, t')$ and $\mathbf{v}(\mathbf{r}, t')$ at times t' that do not lie in the future, i.e., $t' \leq t$].

In general $\mathbf{f}_{\text{sup}}(\mathbf{r}, t) \neq 0$ only if the system is in motion, i.e., $\mathbf{v}(\mathbf{r}, t') \neq 0$. The superadiabatic force field vanishes [$\mathbf{f}_{\text{sup}}(\mathbf{r}, t) = 0$] if the system is at rest at all prior times [$\mathbf{v}(\mathbf{r}, t') = 0$]. Hence, in a system with no flow the equation of motion (144) reduces to

$$0 = -k_B T \nabla \ln \rho(\mathbf{r}, t) + \mathbf{f}_{\text{ad}}(\mathbf{r}, t) + \mathbf{f}_{\text{ext}}(\mathbf{r}, t), \quad (147)$$

where the density profile and hence the adiabatic force field are both invariant in time. Necessarily the external force field is also invariant in time and of the form $-\nabla V_{\text{ext}}(\mathbf{r})$. We hence recover the exact static equilibrium limit from the time-dependent theory. (This is still a highly nontrivial many-body problem encompassing a broad range of relevant physical phenomena from phase behavior in bulk and at interfaces, structural correlations, etc.) The adiabatic construction hence allows one to systematically split the problem of determining $\mathbf{f}_{\text{int}}(\mathbf{r}, t)$ into the problem of separately determining

(and hence modeling and rationalizing) both the adiabatic and superadiabatic contributions.

As it turns out, the adiabatic-superadiabatic splitting is not merely a formal one. Important and prominent physical effects such as drag against a dense surrounding, both bulk and shear viscosity, and nonequilibrium structural forces that are of genuine nonequilibrium character are solely accounted for by the superadiabatic effects, i.e., they can be understood only if $\mathbf{f}_{\text{sup}}(\mathbf{r}, t)$ is correctly accounted for (Sec. IV presents the corresponding theoretical development as well as concrete applications). In contrast $\mathbf{f}_{\text{ad}}(\mathbf{r}, t)$ is free of any of the previously mentioned effects.

Nevertheless, $\mathbf{f}_{\text{ad}}(\mathbf{r}, t)$ is in general neither a negligible nor a small contribution [although there are special cases where $\mathbf{f}_{\text{ad}}(\mathbf{r}, t) = 0$ or a small number, such as in strong shear flow of a nearly homogeneous system (Jahreis and Schmidt, 2020) or the specifically tailored systems of de las Heras and Schmidt (2020)]. We later demonstrate the functional structure, which involves a superadiabatic current-density functional $P_t^{\text{exc}}[\rho, \mathbf{J}]$, which generates the superadiabatic force field via functional differentiation as follows:

$$\mathbf{f}_{\text{sup}}(\mathbf{r}, t, [\rho, \mathbf{J}]) = -\frac{\delta P_t^{\text{exc}}[\rho, \mathbf{J}]}{\delta \mathbf{J}(\mathbf{r}, t)}. \quad (148)$$

The magnitude and direction of $\mathbf{f}_{\text{ad}}(\mathbf{r}, t)$ and those of $\mathbf{f}_{\text{sup}}(\mathbf{r}, t)$ are in general decoupled from each other. As a rule of thumb, $\mathbf{f}_{\text{ad}}(\mathbf{r}, t)$ is more prominent the more the density profile deviates from a homogeneous profile, and $\mathbf{f}_{\text{sup}}(\mathbf{r}, t)$ grows large with increased driving.

In the following, we first address the adiabatic force profile, then describe the theoretical (equilibrium density-functional) structure that one can associate with it. The Mermin-Evans theorem has the important feature that the adiabatic force field is obtained from a generating (intrinsic excess Helmholtz) free energy functional $F_{\text{exc}}[\rho]$ via

$$\mathbf{f}_{\text{ad}}(\mathbf{r}, t) = -\nabla \left. \frac{\delta F_{\text{exc}}[\rho]}{\delta \rho(\mathbf{r})} \right|_{\rho(\mathbf{r})=\rho(\mathbf{r}, t)}. \quad (149)$$

$F_{\text{exc}}[\rho]$ is an intrinsic object in the sense that it is independent of the external potential, and characteristic for (and dependent on) the internal interaction potential $u(\mathbf{r}^N)$. This might come as a surprise given the coupled nature of the many-body problem behind the equilibrium force balance relationship (138), but this property can be made entirely rigorous. Moreover, a functional minimization principle lies behind this beautiful mathematical structure, and powerful physical theory, which is the density-functional framework, to which we turn in the following and which we lay out in some detail.

As a final remark, it is worthwhile to point out that the concept of integrating out degrees of freedom, or partial noise averaging in the nonequilibrium system in order to arrive at effective internal interactions [which differ in general from the bare $u(\mathbf{r}^N)$] is entirely different in character from the adiabatic construction. See Farage, Krininger, and Brader (2015) for an insightful study of how self-propulsion of active Brownian particles generates an effective attractive tail of the pair potential, which originally was purely repulsive. Turci and

Wilding (2021) recently addressed many-body contributions to the effective attraction.

B. Timeline of density-functional theory

The free gas-liquid interface, as treated by van der Waals (1894) via a square-gradient approximation, can be viewed historically as the first DFT. He concluded correctly that the interface between the coexisting bulk fluid phases has finite width and is hence not a sharp two-dimensional mathematical object. The theory extends the work performed in his Ph.D. thesis of 1873 [see the reissue (van der Waals, 2004)], which itself was dedicated to gas-liquid bulk phase coexistence in bulk.⁶

The theory by Onsager (1949) of the isotropic-nematic phase transition of long and thin hard rods is based on the virial (i.e., low-density) expansion together with a geometrical scaling argument that involves the particle aspect ratio; van Roij (2005) gave a clear account of this. The phase transition is of first order and the treatment is exact in the scaling limit. While neither Onsager nor van der Waals knew of free energy density functionals, each of them was able to deduce a self-consistency equation that in hindsight can be viewed as the Euler-Lagrange equation of an underlying density functional.

The following decades saw much progress in the description of the liquid state. Particular highlights include the formulation of the integral equation closure by Percus and Yevick (1958) and of scaled-particle theory for hard spheres by Reiss, Frisch, and Lebowitz (1959). Percus (1976) presented the exact solution for one-dimensional hard rods (Tonks, 1936) that are exposed to an arbitrary external potential. His solution has the form of an exact and closed self-consistency equation for the density profile, with no higher-order correlators involved. These by then classic approaches [see Hansen and McDonald (2013)] formed the grassroots upon which Rosenfeld (1989) later built his formidable fundamental-measure density-functional theory for hard sphere systems.

The birth of modern DFT is the treatment given by Hohenberg and Kohn (1964) of the ground state properties of the electron gas. Their work established that the ground state energy of a quantum system is a functional of the one-body density distribution $n(\mathbf{r})$, and a unique map exists $n(\mathbf{r}) \rightarrow V_{\text{ext}}(\mathbf{r})$. Only one year later, Mermin (1965) generalized the theory to finite temperatures. At $T > 0$ entropy becomes relevant, and the framework that he developed applies to quantum statistical physics. In the same year, Kohn and Sham reintroduced orbitals into DFT; see Kohn (1999) for an accessible and compact description of the essentials of electronic DFT.

In a far-reaching work, Evans (1979) laid out the structure and the foundation of the present-day use of classical DFT. [Evans *et al.* (2016) discussed prior work.] The paper also contains the first formulation of the DDFT equation of motion. The DDFT approach lay virtually dormant for 20 years, until

⁶Clerk-Maxwell (1874) reviewed that work a year after its publication in the journal *Nature*.

Marconi and Tarazona (1999) put it at the center of a new research activity; see also Archer and Evans (2004).

Three important innovations were put forward in the same year: Levy (1979) formulated the constrained search proof of the Hohenberg-Kohn theorem. Rosenfeld and Ashcroft (1979) formulated the modified hypernetted chain theory, including the hypothesis of universality of the short-range structure in liquids. Ramakrishnan and Yussouff (1979) developed their first-principles order-parameter theory of freezing, which was based on a functional Taylor expansion of the excess free energy functional around the homogeneous bulk liquid.

Tarazona and Evans (1984) used weight functions in classical DFT to smooth the density profile via spatial convolution. They take the weight function to be proportional to the Mayer function $\exp[-\beta\phi(r)] - 1$, where $\phi(r)$ is the pair potential. The method allowed them to incorporate nonlocal interparticle correlations into DFT. Rosenfeld (1988) formulated his scaled-field particle approach, which unifies the hitherto distinct scaled-particle and Percus-Yevick theories. Vanderlick, Davis, and Percus (1989) formulated the exact solution for mixtures of one-dimensional polydisperse hard rods in an arbitrary external potential.

Rosenfeld (1989) constructed fundamental-measure theory (FMT) for hard sphere mixtures. His density-functional approach is geometric in nature and was at that time (and still is) different in theoretical structure than all other existing DFT approximations. Kierlik and Rosinberg (1990) gave an alternative and elegant formulation of FMT based on scalar weight functions. In a noteworthy extension of his hard sphere functional, Rosenfeld (1994) obtained an initial generalization of FMT to nonspherical hard bodies; he identified a relationship to the Gauss-Bonnet theorem of integral geometry and related the Mayer bond to topological properties of the system. This approach was carried further for specific systems such as hard needle-sphere (Schmidt, 2001a) and hard plate-sphere mixtures (Esztermann, Reich, and Schmidt, 2006). More generally shaped bodies were addressed by Hansen-Goos and Mecke (2009) and Wittmann, Marechal, and Mecke (2015).

The hard sphere FMT functional received a boost in popularity through the version by Rosenfeld *et al.* (1997), which is based on respecting the properties of the free energy functional upon dimensional reduction. This version of FMT cured the initial defect of FMT, which yielded the fluid unstable with respect to the crystal. Tarazona (2000) introduced a new tensorial weight function into FMT from considering cavitylike, one-dimensional density distributions. His functional predicted freezing from first principles in excellent quantitative agreement with simulation benchmarks. Remaining inaccuracies are due to the description of the fluid rather than the solid. To go beyond the Percus-Yevick compressibility equation of state that is seemingly inherent to FMT, Roth *et al.* (2002) formulated the White Bear version of FMT, which they based on the Carnahan-Starling equation of state; Hansen-Goos and Roth (2006) generalized this approach to multicomponent mixtures of hard spheres. Davidchack, Laird, and Roth (2016) compared the performance of different versions of FMT against benchmark simulation data. Minimization in three dimensions was performed by Levesque, Vuilleumier, and Borgis (2012). Recently Lutsko (2020) reconsidered the original deficiency

of the functional of Rosenfeld (1989) and obtained a class of what he referred to as explicitly stable functionals.

Progress was made at overcoming the hard sphere paradigm and hence to arrive at a first-principles version of FMT for a wider range of microscopic models. This includes the penetrable step function pair potential (Schmidt, 1999), as an example of a non-hard-core model, used to test the universality of the bridge functional (Rosenfeld *et al.*, 2000). The FMT for the Asakura-Oosawa model colloid-polymer mixture (Schmidt *et al.*, 2000) of hard sphere colloids and ideal effective polymer spheres proved to be a valuable tool for the study of adsorption and confinement phenomena in such systems. See Schmidt (2001b, 2004, 2011a) for work on free energy functionals for more general nonadditive hard sphere mixtures.

On a more conceptual level, classical DFT was generalized to quenched-annealed mixtures (Schmidt, 2002), where the quenched component forms a random matrix and the annealed component represents an equilibrated fluid that is adsorbed in the resulting pore structure. The theory predicts quenched-annealed fluid structure with an accuracy comparable to liquid integral equation theory (Schmidt *et al.*, 2002). de las Heras and Schmidt (2014) demonstrated how to practically obtain canonical information from grand canonical DFT results. This proved to be a crucial step in clarifying the role of ensembles in DDFT (de las Heras *et al.*, 2016). Recently Lin and Oettel (2019) and Lin, Martius, and Oettel (2020) constructed a DFT using nonlocal functional ideas combined with machine learning; see also the approach of Cats *et al.* (2021).

Today there is a broad range of applications of DFT, from fundamental toy situations to applied, relevant problems such as the calculation of solvation free energies of complex molecules, where DFT performs orders of magnitude faster than simulations, as shown by Jeanmairet, Levesque, and Borgis (2013), Jeanmairet *et al.* (2013), and Sergiievskiy *et al.* (2014) on the basis of their classical molecular density-functional model for water. The behavior of patchy colloids has been addressed by using DFT (de las Heras, Tavares, and Telo da Gama, 2011), as well as complex capillary phase behavior in model liquid crystals (de las Heras, Velasco, and Mederos, 2005). DFT is applied to complex problems such as the nucleation of crystals (Lutsko and Lam, 2018) and the hard sphere crystal-fluid interface (Härtel *et al.*, 2012). FMT was formulated for lattice models by Lafuente and Cuesta (2004); see Oettel *et al.* (2016) for an insightful application.

C. Sketch of classical DFT

For an introduction to classical DFT see Evans (1979), Hansen and McDonald (2013), and the reviews by Tarazona, Cuesta, and Martínez-Ratón (2008), Lutsko (2010), and Roth (2010). We consider systems of particles in d space dimensions, where all forces are represented by time-independent gradient fields. The total force that acts on particle i is

$$\mathbf{f}_i(\mathbf{r}^N) = -\nabla_i u(\mathbf{r}^N) - \nabla_i V_{\text{ext}}(\mathbf{r}_i). \quad (150)$$

The total potential energy is $u(\mathbf{r}^N) + \sum_i V_{\text{ext}}(\mathbf{r}_i)$ and the Hamiltonian has no explicit time dependence. We are interested in equilibrium states and typically work in the grand

ensemble at chemical potential μ , absolute temperature T , and system volume V . The grand potential is expressed as

$$\Omega([\rho], \mu, V, T) = F([\rho], V, T) + \int d\mathbf{r} \rho(\mathbf{r}) [V_{\text{ext}}(\mathbf{r}) - \mu], \quad (151)$$

where the square brackets indicate a functional dependence and $F[\rho]$ is the intrinsic Helmholtz free energy density functional, which is independent of $V_{\text{ext}}(\mathbf{r})$. The space integral in the external contribution runs over V . The dependence on V is often disregarded, as it can be subsumed into an appropriate form of $V_{\text{ext}}(\mathbf{r})$ that models system walls.

The minimization principle states that Ω is minimized at fixed values of μ , V , and T by the true equilibrium density distribution $\rho_0(\mathbf{r})$. Hence,

$$\left. \frac{\delta \Omega[\rho]}{\delta \rho(\mathbf{r})} \right|_{\rho=\rho_0} = 0 \quad (\text{min}). \quad (152)$$

The value of the functional at the minimum is the equilibrium value of the grand potential Ω_0 itself,

$$\Omega_0(\mu, V, T) = \Omega([\rho_0], \mu, V, T). \quad (153)$$

The intrinsic free energy functional $F[\rho]$ can be split into ideal and excess (over ideal gas) contributions, according to

$$F[\rho] = F_{\text{id}}[\rho] + F_{\text{exc}}[\rho], \quad (154)$$

where the dependence on the thermodynamic parameters T and V has been suppressed in the notation; no dependence on μ occurs, as this is accounted for solely by the second term in Eq. (151). The ideal gas free energy functional is given by

$$F_{\text{id}}[\rho] = k_B T \int d\mathbf{r} \rho(\mathbf{r}) (\{\ln[\rho(\mathbf{r})\Lambda^d]\} - 1). \quad (155)$$

Recall that $\Lambda = \sqrt{2\pi\beta\hbar^2/m}$ is the thermal de Broglie wavelength, with $\beta = 1/k_B T$. Changing the value of Λ adds only a constant to $F_{\text{id}}[\rho]$, which has no effect on the minimization (152). The excess free energy functional $F_{\text{exc}}[\rho]$ is due to the internal interaction potential $u(\mathbf{r}^N)$, and typically approximations are required to proceed toward application to actual physical problems (freezing, adsorption, etc.).

Inserting the intrinsic-external splitting (151) and the ideal-excess decomposition (154) of the intrinsic free energy into the minimization condition (152) yields

$$0 = \frac{\delta \Omega[\rho]}{\delta \rho(\mathbf{r})} \quad (156)$$

$$= \frac{\delta}{\delta \rho(\mathbf{r})} (F_{\text{id}}[\rho] + F_{\text{exc}}[\rho]) + \frac{\delta}{\delta \rho(\mathbf{r})} \int d\mathbf{r}' \rho(\mathbf{r}') [V_{\text{ext}}(\mathbf{r}') - \mu] \quad (157)$$

$$= k_B T \ln[\rho(\mathbf{r})\Lambda^d] + \frac{\delta F_{\text{exc}}[\rho]}{\delta \rho(\mathbf{r})} + \int d\mathbf{r}' \frac{\delta \rho(\mathbf{r}')}{\delta \rho(\mathbf{r})} [V_{\text{ext}}(\mathbf{r}') - \mu] \quad (158)$$

$$= k_B T \ln[\rho(\mathbf{r})\Lambda^d] + \frac{\delta F_{\text{exc}}[\rho]}{\delta \rho(\mathbf{r})} + V_{\text{ext}}(\mathbf{r}) - \mu, \quad (159)$$

where we have used in the last step the fact that $\delta \rho(\mathbf{r}')/\delta \rho(\mathbf{r}) = \delta(\mathbf{r} - \mathbf{r}')$. Solving for the first term on the right-hand side of Eq. (159) and exponentiating gives

$$\rho(\mathbf{r}) = \Lambda^{-d} \exp\left(-\frac{\delta F_{\text{exc}}[\rho]}{\delta \rho(\mathbf{r})} - \beta V_{\text{ext}}(\mathbf{r}) + \beta \mu\right), \quad (160)$$

which forms a self-consistency equation for the determination of the equilibrium density profile $\rho_0(\mathbf{r})$. [Recall that the minimization Eq. (152) holds at $\rho(\mathbf{r}) = \rho_0(\mathbf{r})$.] In the case of the ideal gas $F_{\text{exc}}[\rho] = 0$ and the Euler-Lagrange equation (160) reduces to the generalized barometric law $\rho(\mathbf{r}) = \Lambda^{-d} \exp[-\beta V_{\text{ext}}(\mathbf{r}) + \beta \mu]$.

We can alternatively rearrange the Euler-Lagrange equation (159) in the following form:

$$V_{\text{ext}}(\mathbf{r}) = \mu - k_B T \ln[\rho(\mathbf{r})\Lambda^d] - \frac{\delta F_{\text{exc}}[\rho]}{\delta \rho(\mathbf{r})}, \quad (161)$$

which makes the functional map $\rho(\mathbf{r}) \rightarrow V_{\text{ext}}(\mathbf{r})$ explicit: the right-hand side of Eq. (161) is independent of $V_{\text{ext}}(\mathbf{r})$, as it depends solely on $\rho(\mathbf{r})$ (and on the form of the functional $F_{\text{exc}}[\rho]$). Hence, knowing the density profile is enough, in principle, to evaluate the right-hand side of Eq. (161) and obtain the corresponding external potential. One hence obtains, formally, a corresponding pair of functions $V_{\text{ext}}(\mathbf{r})$ and $\rho(\mathbf{r})$ that minimize the grand potential functional, i.e., that satisfy Eq. (152). Physically, it is this hence identified external potential that then leads in equilibrium to the prescribed target density profile.

The DFT framework is well suited for addressing phase behavior, where multiple macrostates can coexist. This applies to general situations with nonvanishing $V_{\text{ext}}(\mathbf{r})$, such as in capillaries. At coexistence, we have multiple stable phases, labeled by an index α , with corresponding density profiles $\rho_\alpha(\mathbf{r})$. The map

$$\rho_\alpha(\mathbf{r}) \rightarrow V_{\text{ext}}(\mathbf{r}) \quad (162)$$

is then unique, as it should be. The external potential is the same in the coexisting phases, as is the external force field $-\nabla V_{\text{ext}}(\mathbf{r})$. On the other hand, $V_{\text{ext}}(\mathbf{r}) \rightarrow \rho(\mathbf{r})$ is not unique, due to the multiplicity of the density profile(s). This is a real effect at phase coexistence. Typically, for discontinuous (first-order) phase transitions, the location of the interface between the two coexisting phases constitutes further freedom in the construction of a valid density profile.

D. Statistical mechanics and variations

We work in the grand ensemble (or ‘‘grand canonical’’ ensemble), where the particle number N fluctuates and its mean is controlled by the chemical potential μ , which renders μ , V , and T the macrovariables. The grand partition sum is defined as

$$\Xi(\mu, V, T) = \text{Tr} e^{-\beta(H-\mu N)}, \quad (163)$$

where the Hamiltonian is for $N = \text{const}$ particles, and the classical ‘‘trace’’ is defined as the sum over all particles and the integral over each N -specific phase space as follows:

$$\text{Tr} = \sum_{N=0}^{\infty} \frac{1}{h^{3N} N!} \int d\mathbf{r}^N d\mathbf{p}^N. \quad (164)$$

The corresponding thermodynamic potential is the grand potential, which is given by

$$\Omega(\mu, V, T) = -k_B T \ln \Xi(\mu, V, T). \quad (165)$$

The microstates now encompass all \mathbf{r}^N and \mathbf{p}^N , with $N = 0, 1, 2, \dots$, distributed according to

$$\Psi_{\mu VT}(\mathbf{r}^N, \mathbf{p}^N) = \frac{e^{-\beta(H-\mu N)}}{\Xi}, \quad (166)$$

where μ , V , and T are control parameters; see their occurrence on the right-hand side of Eq. (166). Averages are built according to

$$\langle \cdot \rangle_{\mu VT} = \text{Tr} \cdot \Psi_{\mu VT}. \quad (167)$$

It is then elementary to see that thermodynamic identities are generated as parametric derivatives, such as

$$-\left. \frac{\partial \Omega}{\partial \mu} \right|_{VT} = \langle N \rangle_{\mu VT}. \quad (168)$$

Thus far everything has been general and applicable to arbitrary forms of N -body Hamiltonians. Consider now the specific form

$$H = \sum_i \frac{\mathbf{p}_i^2}{2m} + u(\mathbf{r}^N) + \sum_i V_{\text{ext}}(\mathbf{r}_i), \quad (169)$$

which has no explicit time dependence, splits into internal and external one-body contributions, and generates potential forces only. Trivially, H depends on the function $V_{\text{ext}}(\mathbf{r})$ as a time-independent one-body field. When H is input into Eq. (165) the dependence on $V_{\text{ext}}(\cdot)$ persists and renders Ω a functional of $V_{\text{ext}}(\cdot)$. We spell out the dependence explicitly as follows:

$$\Omega(\mu, V, T, [V_{\text{ext}}]) = -k_B T \ln \text{Tr} \exp \left[-\beta \left(\sum_i \frac{\mathbf{p}_i^2}{2m} + u(\mathbf{r}^N) + \sum_i V_{\text{ext}}(\mathbf{r}_i) - \mu N \right) \right], \quad (170)$$

where the only dependence on the external potential is made explicit in the notation. Hence, any input field $V_{\text{ext}}(\cdot)$ is converted to a number (the value of Ω with units of energy) by carrying out the high-dimensional integrals that constitute the classical trace. In particular the space integrals are coupled via $u(\mathbf{r}^N)$ and there is no hope in general of finding an exact result. Nevertheless, Eq. (170) is important as a meaningful starting point for an exact microscopic formal description as the basis of statistical mechanics in equilibrium. Recognizing the apparently trivial functional dependence on $V_{\text{ext}}(\mathbf{r})$, and the consequences that this has, is an important modern achievement; see the wealth of research carried out on the basis of Evans (1979).

To study and understand the functional relationship better, it is useful to consider functional derivatives of the grand potential with respect to $V_{\text{ext}}(\mathbf{r})$. All the usual reasons for studying derivatives, as a means of studying an object itself, apply here. The parameters μ , V , and T are kept constant upon building the functional derivative and hence

$$\left. \frac{\delta \Omega}{\delta V_{\text{ext}}(\mathbf{r})} \right|_{\mu VT} = -\frac{k_B T}{\Xi} \text{Tr} \frac{\delta}{\delta V_{\text{ext}}(\mathbf{r})} e^{-\beta(H-\mu N)} \quad (171)$$

$$= \Xi^{-1} \text{Tr} e^{-\beta(H-\mu N)} \frac{\delta H}{\delta V_{\text{ext}}(\mathbf{r})} \quad (172)$$

$$= \left\langle \frac{\delta H}{\delta V_{\text{ext}}(\mathbf{r})} \right\rangle_{\mu VT}. \quad (173)$$

In Eqs. (171)–(173) \mathbf{r} is a generic position coordinate (which is in general different from \mathbf{r}_i). The functional derivative commutes with the classical trace operation (164), and hence operates only on the Boltzmann factor in Eq. (171). The functional chain rule then reproduces the exponential and generates the derivative of the Hamiltonian, which is

$$\frac{\delta H}{\delta V_{\text{ext}}(\mathbf{r})} = \frac{\delta}{\delta V_{\text{ext}}(\mathbf{r})} \sum_i V_{\text{ext}}(\mathbf{r}_i) \quad (174)$$

$$= \sum_i \frac{\delta V_{\text{ext}}(\mathbf{r}_i)}{\delta V_{\text{ext}}(\mathbf{r})} \quad (175)$$

$$= \sum_i \delta(\mathbf{r} - \mathbf{r}_i) \equiv \hat{\rho}(\mathbf{r}). \quad (176)$$

Insertion into Eq. (173) yields

$$\left. \frac{\delta \Omega}{\delta V_{\text{ext}}(\mathbf{r})} \right|_{\mu VT} = \rho(\mathbf{r}), \quad (177)$$

where $\rho(\mathbf{r}) = \langle \hat{\rho}(\mathbf{r}) \rangle_{\mu VT}$ is the equilibrium one-body density distribution in the grand ensemble. Equation (177) is a powerful generalization of the much more elementary Eq. (168), which relates only the mean particle number to the negative partial derivative of the grand potential with respect to the chemical potential.

As an aside, sometimes one chooses to define a “local” chemical potential via

$$\mu_{\text{loc}}(\mathbf{r}) = \mu - V_{\text{ext}}(\mathbf{r}), \quad (178)$$

where $\mu = \text{const}$ is the “true” chemical potential.⁷ This allows us to rewrite Eq. (177) in a form that is even more in line with Eq. (168), namely,

⁷The concept of a species-dependent local chemical potential has been exploited in work on sedimentation in binary colloidal mixtures (de las Heras *et al.*, 2012; de las Heras and Schmidt, 2013, 2015).

$$-\left.\frac{\delta\Omega}{\delta\mu_{\text{loc}}(\mathbf{r})}\right|_{VT} = \rho(\mathbf{r}). \quad (179)$$

Several remarks are in order.

- (i) The relationship (177) applies to the elementary concept of the (grand ensemble) grand potential. No further functional needs to be established, apart from recognizing that the (standard) partition sum is already functionally dependent on $V_{\text{ext}}(\mathbf{r})$.
- (ii) The mean density $\rho(\mathbf{r})$ is microscopically sharp (i.e., it can resolve inhomogeneities on small length scales, as determined by the interaction forces). In practice, this involves packing effects on the length scale of the particle size.
- (iii) Although functional calculus has certainly proved to be powerful, at this stage it is not at all obvious how deep the result (177) is, and whether it holds by a mere accident.

Having had a useful outcome of applying functional calculus to the partition sum, it is natural to consider its second functional derivative. Using Eq. (177) this can immediately be rewritten as

$$\left.\frac{\delta^2\Omega}{\delta V_{\text{ext}}(\mathbf{r}')\delta V_{\text{ext}}(\mathbf{r})}\right|_{\mu VT} = \left.\frac{\delta\rho(\mathbf{r})}{\delta V_{\text{ext}}(\mathbf{r}')}\right|_{\mu VT}, \quad (180)$$

which is a surprising result, as it relates an abstract object (left-hand side) to the physical response of the density distribution at space point \mathbf{r} upon changing the external potential at point \mathbf{r}' . Hence, the right-hand side of Eq. (180) constitutes a density-response function. We return to this point for an in-depth study in Sec. III.G of the Ornstein-Zernike relation.

Before doing so we further investigate Eq. (180). At fixed thermodynamic parameters, consider

$$\frac{\delta\rho(\mathbf{r})}{\delta V_{\text{ext}}(\mathbf{r}')} = \frac{\delta}{\delta V_{\text{ext}}(\mathbf{r}')}\frac{1}{\Xi}\text{Tr}e^{-\beta(H-\mu N)}\hat{\rho}(\mathbf{r}) \quad (181)$$

$$= \left(-\frac{1}{\Xi^2}\frac{\delta}{\delta V_{\text{ext}}(\mathbf{r}')}\Xi\right)\text{Tr}e^{-\beta(H-\mu N)}\hat{\rho}(\mathbf{r}) + \frac{1}{\Xi}\text{Tr}\frac{\delta}{\delta V_{\text{ext}}(\mathbf{r}')}\text{Tr}e^{-\beta(H-\mu N)}\hat{\rho}(\mathbf{r}) \quad (182)$$

$$\equiv \text{(i)} + \text{(ii)}. \quad (183)$$

We consider the two contributions separately.

- (i) We rearrange the first term in Eq. (182) as

$$\begin{aligned} & \left(-\frac{1}{\Xi}\frac{\delta}{\delta V_{\text{ext}}(\mathbf{r}')}\Xi\right)\text{Tr}\frac{1}{\Xi}e^{-\beta(H-\mu N)}\hat{\rho}(\mathbf{r}) \\ &= \left(-\frac{1}{\Xi}\text{Tr}e^{-\beta(H-\mu N)}(-\beta)\frac{\delta H}{\delta V_{\text{ext}}(\mathbf{r}')}\right)\rho(\mathbf{r}) \end{aligned} \quad (184)$$

$$= \beta\left(\text{Tr}\frac{1}{\Xi}e^{-\beta(H-\mu N)}\hat{\rho}(\mathbf{r}')\right)\rho(\mathbf{r}) \quad (185)$$

$$= \beta\rho(\mathbf{r}')\rho(\mathbf{r}), \quad (186)$$

where we have used the functional derivative of the Hamiltonian $\delta H/\delta V_{\text{ext}}(\mathbf{r}') = \sum_i \delta(\mathbf{r}' - \mathbf{r}_i) \equiv \hat{\rho}(\mathbf{r}')$.

- (ii) The second term in Eq. (182) can be transformed as

$$\begin{aligned} & \frac{1}{\Xi}\text{Tr}e^{-\beta(H-\mu N)}(-\beta)\frac{\delta H}{\delta V_{\text{ext}}(\mathbf{r}')}\hat{\rho}(\mathbf{r}) \\ &= \frac{-\beta}{\Xi}\text{Tr}e^{-\beta(H-\mu N)}\hat{\rho}(\mathbf{r}')\hat{\rho}(\mathbf{r}) \end{aligned} \quad (187)$$

$$= -\beta\langle\hat{\rho}(\mathbf{r}')\hat{\rho}(\mathbf{r})\rangle. \quad (188)$$

Adding Eqs. (186) and (188) together yields

$$-\frac{\delta\rho(\mathbf{r})}{\delta\beta V_{\text{ext}}(\mathbf{r}')} = \langle\hat{\rho}(\mathbf{r}')\hat{\rho}(\mathbf{r})\rangle - \rho(\mathbf{r})\rho(\mathbf{r}'), \quad (189)$$

which relates a density-response function (left-hand side) with a density-density correlation function, i.e., the covariance of $\hat{\rho}(\mathbf{r})$ and $\hat{\rho}(\mathbf{r}')$ (right-hand side). We return to static two-body correlation functions later, when we summarize their standard definition (Sec. III.F) and derive the static Ornstein-Zernike relation (Sec. III.G). Dynamic correlations functions are described in Sec. IV. We next turn to proving the existence of the free energy density functional.

E. Levy's constrained search

The standard Mermin-Evans derivation of classical DFT (Evans, 1979) was described by Hansen and McDonald (2013); see *Two Theorems in Density Functional Theory* in Appendix B of that work. The first step consists of constructing a many-body variational theory on the level of many-body distribution functions, using the Mermin grand potential functional

$$\Omega_M[\Psi] = \text{Tr}\Psi(H - \mu N + k_B T \ln \Psi) \quad (190)$$

and then, via *reductio ad absurdum*, obtaining the functional dependence on the density profile.

For the quantum case, Levy (1979) developed and used his method as an alternative, and arguably more explicit, derivation of the Hohenberg-Kohn theorem. Dwandaru and Schmidt (2011) applied the method to classical DFT and argued that it has similar advantages over the conventional Mermin-Evans proof.

The starting point of Levy's search is to consider a function space $\{\Psi(\mathbf{r}^N, \mathbf{p}^N)\}$ of normalized many-body distribution functions [$\text{Tr}\Psi(\mathbf{r}^N, \mathbf{p}^N) = 1$], where the grand canonical trace (164) is as previously defined. Each many-body distribution implies a corresponding density profile. Hence, we have a functional map

$$\Psi \rightarrow \rho(\mathbf{r}) = \text{Tr}\Psi\hat{\rho}, \quad (191)$$

which allows us to build subspaces of distribution functions Ψ that generate the same given $\rho(\mathbf{r})$. Hence, within one subspace $\{\Psi_1, \Psi_2, \dots\}$, all $\Psi_1 \rightarrow \rho(\mathbf{r})$, $\Psi_2 \rightarrow \rho(\mathbf{r})$, etc. In a different

(primed) subspace $\{\Psi'_1, \Psi'_2, \dots\}$ all $\Psi'_1 \rightarrow \rho'(\mathbf{r})$, $\Psi'_2 \rightarrow \rho'(\mathbf{r})$, etc., with a unique $\rho'(\mathbf{r})$, but $\rho'(\mathbf{r}) \neq \rho(\mathbf{r})$.

The Mermin-Evans form of the intrinsic many-body Helmholtz free energy functional is given by

$$F[\Psi_0] = \text{Tr} \Psi_0 \left(\sum_i \frac{\mathbf{p}_i^2}{2m} + u(\mathbf{r}^N) + k_B T \ln \Psi_0 \right), \quad (192)$$

which resembles the Mermin functional (190), where the external energy and chemical potential contributions have been split off. The first two terms in the integrand of Eq. (192) represent the internal kinetic and potential energy U_{int} , and the third term involving the logarithm is entropy S multiplied by negative temperature. Hence, overall the structure is indeed that of an intrinsic free energy, $U_{\text{int}} - TS$. In Eq. (192), Ψ_0 is an equilibrium many-body probability distribution function associated with a Mermin external potential $V_M(\mathbf{r})$. In the proof by contradiction one shows that any density distribution $\rho_0(\mathbf{r})$ determines uniquely a corresponding Mermin potential $V_M(\mathbf{r})$, which renders Ψ_0 known. This implies functional dependence $\Psi_0[\rho]$, which leads to the free energy (192) also being functionally dependent on $\rho(\mathbf{r})$.

Here we argue differently and instead operate on the function space of general many-body phase space distribution functions Ψ . The Levy definition of the intrinsic Helmholtz free energy functional (Dwandar and Schmidt, 2011) is

$$F_L[\rho] = \min_{\Psi \rightarrow \rho} \text{Tr} \Psi \left(\sum_i \frac{\mathbf{p}_i^2}{2m} + u(\mathbf{r}^N) + k_B T \ln \Psi \right), \quad (193)$$

where the minimization is performed in the subspace $\{\Psi | \Psi \rightarrow \rho(\mathbf{r})\}$, i.e., it is a search for the minimum under the constraint of a given one-body density, as expressed in Eq. (191). It is this constraint that makes the value of the integral (193) functionally dependent on $\rho(\mathbf{r})$. This works for any normalized, non-negative trial form of Ψ . [The integral in Eq. (191) can be carried out regardless of whether Ψ is a valid equilibrium distribution.]

The Levy version of the *grand potential functional* is defined as

$$\Omega_L[\rho] = F_L[\rho] + \int d\mathbf{r} \rho(\mathbf{r}) [V_{\text{ext}}(\mathbf{r}) - \mu], \quad (194)$$

where $F_L[\rho]$ is given via Eq. (193). The functional $\Omega_L[\rho]$ forms the basis of DFT as follows.

Theorem.—The Levy form (194) of the grand potential functional has the properties

$$\Omega_L[\rho_0] = \Omega_0, \quad (195)$$

$$\Omega_L[\rho] \geq \Omega_0, \quad (196)$$

with the equilibrium density profile $\rho_0(\mathbf{r})$ and any trial density profile $\rho(\mathbf{r})$.

Proof.—The idea for the proof is based on Levy's argument of a double minimization. The first step consists of the constrained (search) minimization. The constraint is then

relaxed and the overall minimum is identified. We show this explicitly in the following.

For completeness we spell out $\rho_0(\mathbf{r}) = \text{Tr} \Psi_0 \hat{\rho}$, where $\Psi_0 = \Xi^{-1} \exp\{-\beta[\sum_i \mathbf{p}_i^2/(2m) + u(\mathbf{r}^N) + \sum_i V_{\text{ext}}(\mathbf{r}_i) - \mu N]\}$, the grand potential is $\Omega_0 = -k_B T \ln \Xi$, and the grand partition sum is $\Xi = \text{Tr} \exp[-\beta(H - \mu N)]$. It is a standard exercise (Hansen and McDonald, 2013) to show via the Gibbs-Bogoliubov inequality that the Mermin functional (190) satisfies $\Omega_M[\Psi_0] = \Omega_0 \leq \Omega_M[\Psi]$. Rephrasing this, we can obtain from Ω_M , as defined in Eq. (190), the following value of the grand potential via minimization in the space of many-body distribution functions:

$$\Omega_0 = \min_{\Psi} \text{Tr} \Psi \left(\sum_i \frac{\mathbf{p}_i^2}{2m} + u(\mathbf{r}^N) + k_B T \ln \Psi + \sum_i V_{\text{ext}}(\mathbf{r}_i) - \mu N \right). \quad (197)$$

We next decompose the overall minimization into two steps,

$$\min_{\Psi}(\cdot) = \min_{\rho} \min_{\Psi \rightarrow \rho}(\cdot), \quad (198)$$

where the inner (right) minimization on the right-hand side is a search under the constraint of prescribed $\rho(\mathbf{r})$ and the outer (left) minimization then finds the minimum upon varying $\rho(\mathbf{r})$.

Applying this general concept to Eq. (197) yields

$$\Omega_0 = \min_{\rho} \min_{\Psi \rightarrow \rho} \text{Tr} \Psi \left(\sum_i \frac{\mathbf{p}_i^2}{2m} + u(\mathbf{r}^N) + k_B T \ln \Psi + \sum_i V_{\text{ext}}(\mathbf{r}_i) - \mu N \right). \quad (199)$$

Inside of the inner minimization $\rho(\mathbf{r})$ is fixed and hence

$$\Omega_0 = \min_{\rho} \min_{\Psi \rightarrow \rho} \text{Tr} \Psi \left(\sum_i \frac{\mathbf{p}_i^2}{2m} + u(\mathbf{r}^N) + k_B T \ln \Psi + \int d\mathbf{r} V_{\text{ext}}(\mathbf{r}) \sum_i \delta(\mathbf{r} - \mathbf{r}_i) - \mu N \right) \quad (200)$$

$$= \min_{\rho} \left[\min_{\Psi \rightarrow \rho} \text{Tr} \Psi \left(\sum_i \frac{\mathbf{p}_i^2}{2m} + u(\mathbf{r}^N) + k_B T \ln \Psi \right) + \int d\mathbf{r} [V_{\text{ext}}(\mathbf{r}) - \mu] \min_{\Psi \rightarrow \rho} \text{Tr} \Psi \sum_i \delta(\mathbf{r} - \mathbf{r}_i) \right] \quad (201)$$

$$= \min_{\rho} \left(F_L[\rho] + \int d\mathbf{r} [V_{\text{ext}}(\mathbf{r}) - \mu] \rho(\mathbf{r}) \right), \quad (202)$$

where the final form is written using Eq. (193) for $F_L[\rho]$. This proves the theorem and identifies the Levy form (193) with the aforementioned intrinsic free energy functional $F[\rho]$ [Eq. (154)].

Levy's constrained search method is flexible. Dwandar and Schmidt (2011) used it to formulate classical DFT in the canonical ensemble. Here the constraint of the fixed particle number is implemented straightforwardly by setting up the previously mentioned reasoning in the canonical ensemble. The canonical intrinsic free energy functional formally

resembles the grand ensemble form (193), but with the trace and many-body probability distribution function expressed canonically; see Dwandaru and Schmidt (2011) for details. Schmidt (2011b) used Levy's method for the construction of an internal-energy functional, which depends both on the density profile and on a microscopically resolved entropy density (both act as constraints). An extended set of closely related fluctuation profiles in inhomogeneous fluids were systematically studied by Eckert *et al.* (2020). The fluctuation profiles include the local compressibility. Based on early work (Stewart and Evans, 2012, 2014), this one-body function was shown to be a highly useful indicator for important phenomena ranging from solvent-mediated interactions (Chacko, Evans, and Archer, 2017), solvophobicity and hydrophobicity (Evans and Stewart, 2015), and drying and wetting (Evans, Stewart, and Wilding, 2016, 2017) to the physical mechanism behind hydrophobicity (Coe, Evans, and Wilding, 2022).

In practice, approximations for canonical functionals are scarce. There are alternative ways to obtain canonical information; see the method by González *et al.* (1997) and the framework of White *et al.* (2000) and White and González (2002). Starting from grand ensemble data requires one, in principle, to carry out an inverse Laplace transform, which is a numerically difficult task. The direct decomposition method of de las Heras and Schmidt (2014) circumvents this problem by instead solving a linear set of equations that is numerically tractable. Obtaining canonical information can be crucial, particularly for small systems, and when comparing to results from experiment or simulation. For ensemble differences to vanish, typically the thermodynamic limit is required. The decomposition method allows one to obtain canonical information from grand canonical results, as are characteristic for numerical DFT applications. de las Heras *et al.* (2016) used this approach to formulate particle-conserving adiabatic dynamics in order to avoid erroneous particle number fluctuations of dynamical density-functional theory; see also Schindler, Wittmann, and Brader (2019) and Wittmann, Löwen, and Brader (2021).

F. Static two-body correlation functions

We recall the fundamental property of the grand potential Ω , as expressed via the grand partition sum and viewed as a functional of the external potential, to generate correlation functions from functional derivatives [Eqs. (177), (180), and (189) in Sec. III.D]. Explicitly,

$$\frac{\delta\Omega[V_{\text{ext}}]}{\delta V_{\text{ext}}(\mathbf{r})} = \rho(\mathbf{r}), \quad (203)$$

$$\frac{\delta^2\Omega[V_{\text{ext}}]}{\delta V_{\text{ext}}(\mathbf{r}')\delta V_{\text{ext}}(\mathbf{r})} = \frac{\delta\rho(\mathbf{r})}{\delta V_{\text{ext}}(\mathbf{r}')} \quad (204)$$

$$= -\beta[\langle\hat{\rho}(\mathbf{r})\hat{\rho}(\mathbf{r}')\rangle - \rho(\mathbf{r})\rho(\mathbf{r}')]. \quad (205)$$

From the interchangeability of the order of the second derivatives in Eq. (204), the symmetry $\delta\rho(\mathbf{r})/\delta V_{\text{ext}}(\mathbf{r}') = \delta\rho(\mathbf{r}')/\delta V_{\text{ext}}(\mathbf{r})$ follows.

We summarize the definitions of several closely related two-body functions (Hansen and McDonald, 2013). The *density-density correlation function* $H_2(\mathbf{r}, \mathbf{r}')$ is defined as

$$H_2(\mathbf{r}, \mathbf{r}') = \langle\hat{\rho}(\mathbf{r})\hat{\rho}(\mathbf{r}')\rangle - \rho(\mathbf{r})\rho(\mathbf{r}'), \quad (206)$$

where the symmetry $H_2(\mathbf{r}, \mathbf{r}') = H_2(\mathbf{r}', \mathbf{r})$ holds. One can alternatively express Eq. (206) as the autocorrelator of density fluctuations around the mean density profile,

$$H_2(\mathbf{r}, \mathbf{r}') = \langle[\hat{\rho}(\mathbf{r}) - \rho(\mathbf{r})][\hat{\rho}(\mathbf{r}') - \rho(\mathbf{r}')]\rangle. \quad (207)$$

To show the equivalence of Eqs. (206) and (207), we omit the position arguments and indicate the dependence on \mathbf{r}' with a prime. Multiplying out Eq. (207) we obtain $\langle\hat{\rho}\hat{\rho}'\rangle - \langle\hat{\rho}\rho'\rangle - \langle\rho\hat{\rho}'\rangle + \langle\rho\rho'\rangle = \langle\hat{\rho}\hat{\rho}'\rangle - \langle\hat{\rho}\rangle\rho' - \rho\langle\hat{\rho}'\rangle + \rho\rho' = \langle\hat{\rho}\hat{\rho}'\rangle - \rho\rho' - \rho\rho' + \rho\rho' = \langle\hat{\rho}\hat{\rho}'\rangle - \rho\rho'$, which is Eq. (206).

The *total correlation function* $h(\mathbf{r}, \mathbf{r}')$ is defined via

$$H_2(\mathbf{r}, \mathbf{r}') = \rho(\mathbf{r})\rho(\mathbf{r}')h(\mathbf{r}, \mathbf{r}') + \rho(\mathbf{r})\delta(\mathbf{r} - \mathbf{r}'), \quad (208)$$

where rearranging gives

$$h(\mathbf{r}, \mathbf{r}') = \frac{H_2(\mathbf{r}, \mathbf{r}')}{\rho(\mathbf{r})\rho(\mathbf{r}')} - \frac{\delta(\mathbf{r} - \mathbf{r}')}{\rho(\mathbf{r})}. \quad (209)$$

The correlation function $h(\mathbf{r}, \mathbf{r}')$ carries no units (the delta function carries units of inverse volume).

The *pair correlation function* $g(\mathbf{r}, \mathbf{r}')$ is defined via

$$g(\mathbf{r}, \mathbf{r}') = 1 + h(\mathbf{r}, \mathbf{r}') \quad (210)$$

$$= \frac{H_2(\mathbf{r}, \mathbf{r}') + \rho(\mathbf{r})\rho(\mathbf{r}')}{\rho(\mathbf{r})\rho(\mathbf{r}')} - \frac{\delta(\mathbf{r} - \mathbf{r}')}{\rho(\mathbf{r})} \quad (211)$$

$$= \frac{\langle\hat{\rho}(\mathbf{r})\hat{\rho}(\mathbf{r}')\rangle}{\rho(\mathbf{r})\rho(\mathbf{r}')} - \frac{\delta(\mathbf{r} - \mathbf{r}')}{\rho(\mathbf{r})}. \quad (212)$$

Alternatively and equivalently, one can express the pair correlation function as

$$g(\mathbf{r}, \mathbf{r}') = \frac{1}{\rho(\mathbf{r})\rho(\mathbf{r}')} \left\langle \sum_i \sum_j' \delta(\mathbf{r} - \mathbf{r}_i) \delta(\mathbf{r}' - \mathbf{r}_j) \right\rangle, \quad (213)$$

where the primed sum indicates that the terms with $i = j$ have been omitted. The equivalence with the prior definition (212) can be seen by considering the product of the two density operators,

$$\hat{\rho}(\mathbf{r})\hat{\rho}(\mathbf{r}') = \sum_i \delta(\mathbf{r} - \mathbf{r}_i) \sum_j \delta(\mathbf{r}' - \mathbf{r}_j) \quad (214)$$

$$= \sum_i \sum_j' \delta(\mathbf{r} - \mathbf{r}_i) \delta(\mathbf{r}' - \mathbf{r}_j) + \delta(\mathbf{r} - \mathbf{r}') \sum_i \delta(\mathbf{r} - \mathbf{r}_i), \quad (215)$$

where the last term is $\delta(\mathbf{r} - \mathbf{r}')\hat{\rho}(\mathbf{r})$. Averaging yields the sum of a distinct part (from different particles) and a self part (considering the same particle twice) according to

$$\langle\hat{\rho}(\mathbf{r})\hat{\rho}(\mathbf{r}')\rangle = \left\langle \sum_i \sum_j' \delta(\mathbf{r} - \mathbf{r}_i) \delta(\mathbf{r}' - \mathbf{r}_j) \right\rangle + \delta(\mathbf{r} - \mathbf{r}') \langle\hat{\rho}(\mathbf{r})\rangle, \quad (216)$$

where $\rho(\mathbf{r}) = \langle \hat{\rho}(\mathbf{r}) \rangle$. Input of the result (216) into Eq. (212) yields Eq. (213).

Finally, the *density-response function* is defined as

$$\chi(\mathbf{r}, \mathbf{r}') = \frac{\delta\rho(\mathbf{r})}{\delta V_{\text{ext}}(\mathbf{r}')}, \quad (217)$$

which is often formulated in the form of a response relationship. Here the density change $\delta\rho(\mathbf{r})$ at position \mathbf{r} in response to a change in external potential $\delta V_{\text{ext}}(\mathbf{r}')$ at position \mathbf{r}' is expressed as

$$\delta\rho(\mathbf{r}) = \int d\mathbf{r}' \chi(\mathbf{r}, \mathbf{r}') \delta V_{\text{ext}}(\mathbf{r}'). \quad (218)$$

A priori the density-response function is different in character than the previously mentioned density-density correlation functions. However, in the present classical context, we can identify these conceptually different objects:

$$\chi(\mathbf{r}, \mathbf{r}') = -\beta H_2(\mathbf{r}, \mathbf{r}'). \quad (219)$$

We have thus far used explicit correlator expressions and functional derivatives of the partition sum (in the form of the grand potential) with respect to the external potential. We next turn to the density-functional structure.

One defines the *one-body direct correlation function* as

$$c_1([\rho], \mathbf{r}; T, V) = -\beta \frac{\delta F_{\text{exc}}[\rho]}{\delta\rho(\mathbf{r})}, \quad (220)$$

where $F_{\text{exc}}[\rho]$ is the excess (over ideal gas) contribution of the Helmholtz excess free energy functional; recall the ideal-excess splitting (154). Strictly speaking, Eq. (220) defines a functional, and the direct correlation function $c_1(\mathbf{r})$ is obtained by evaluating this functional, for given thermodynamic parameters, at the physical equilibrium density profile $\rho_0(\mathbf{r})$, i.e.,

$$c_1(\mathbf{r}) = c_1([\rho_0], \mathbf{r}; T, V). \quad (221)$$

We can build higher than first derivatives of the excess free energy density functional. Going to the second derivative, i.e., one order higher than in Eq. (220), gives the two-body direct correlation “function” $c_2(\mathbf{r}, \mathbf{r}')$, defined as

$$c_2([\rho], \mathbf{r}, \mathbf{r}'; T, V) = -\beta \frac{\delta^2 F_{\text{exc}}[\rho]}{\delta\rho(\mathbf{r})\delta\rho(\mathbf{r}')}, \quad (222)$$

where we have again made the functional dependence on $\rho(\mathbf{r})$ explicit in the notation. Evaluating at the equilibrium density profile $[\rho(\mathbf{r}) = \rho_0(\mathbf{r})]$ gives the two-body direct correlation function, central to liquid integral equation theory (Hansen and McDonald, 2013). In a bulk fluid $c_2(\mathbf{r}, \mathbf{r}') = c_2(|\mathbf{r} - \mathbf{r}'|)$ due to global translational and rotational symmetry; see Hermann and Schmidt (2021, 2022) for the consequences that arise from symmetries according to Noether’s theorem.

G. Static Ornstein-Zernike relation

The Ornstein-Zernike relation connects the two-body direct correlation function with the density-response function (which can be expressed and rewritten in various forms, as described in Sec. III.F). Here we give a derivation that identifies the underlying physical concept and separates this from the more technical points that arise from the use of the different form of correlators and response functions H_2 , h , g , and χ . This type of derivation was used recently in equilibrium by Eckert *et al.* (2020) in their derivation of Ornstein-Zernike relations for fluctuation profiles, and by Tschopp and Brader (2021) in their fundamental-measure theory for inhomogeneous two-body correlation functions. The dynamical generalization formed the basis of the nonequilibrium Ornstein-Zernike relation (Brader and Schmidt, 2013, 2014).

We address the general, inhomogeneous case in the following. Consider the Euler-Lagrange equation (161) of DFT, which we make fully explicit as

$$k_B T \ln[\rho_0(\mathbf{r})\Lambda^d] = - \left. \frac{\delta F_{\text{exc}}[\rho]}{\delta\rho(\mathbf{r})} \right|_{\rho(\mathbf{r})=\rho_0(\mathbf{r})} - V_{\text{ext}}(\mathbf{r}) + \mu, \quad (223)$$

where $\rho_0(\mathbf{r})$ is the equilibrium density profile in the presence of the external potential $V_{\text{ext}}(\mathbf{r})$. Hence, Eq. (223) is valid for any corresponding pair of fields $\rho_0(\mathbf{r})$ and $V_{\text{ext}}(\mathbf{r})$. As Eq. (223) stays true upon changing $V_{\text{ext}}(\mathbf{r})$ and correspondingly changing $\rho_0(\mathbf{r})$, its derivative with respect to the external potential is also true. Introducing a new primed spatial position variable, from Eq. (223) we hence obtain

$$\begin{aligned} & \frac{\delta k_B T \ln[\rho_0(\mathbf{r})\Lambda^d]}{\delta V_{\text{ext}}(\mathbf{r}')} \\ &= - \frac{\delta}{\delta V_{\text{ext}}(\mathbf{r}')} \left. \frac{\delta F_{\text{exc}}}{\delta\rho(\mathbf{r})} \right|_{\rho(\mathbf{r})=\rho_0(\mathbf{r})} - \frac{\delta(V_{\text{ext}}(\mathbf{r}) - \mu)}{\delta V_{\text{ext}}(\mathbf{r}')}. \end{aligned} \quad (224)$$

As the variation is performed at a constant thermodynamic state point, the second term on the right-hand side is simply

$$- \frac{\delta(V_{\text{ext}}(\mathbf{r}) - \mu)}{\delta V_{\text{ext}}(\mathbf{r}')} = - \frac{\delta V_{\text{ext}}(\mathbf{r})}{\delta V_{\text{ext}}(\mathbf{r}')} = -\delta(\mathbf{r} - \mathbf{r}'), \quad (225)$$

as no dependence on the density profile is involved. To calculate the remaining terms, we need (i) the standard rules of functional calculus and (ii) to recognize the relationship with the previously mentioned correlators. The left-hand side of Eq. (224) can be related to Eq. (205), i.e., $H_2(\mathbf{r}, \mathbf{r}') = -k_B T \delta\rho(\mathbf{r})/\delta V_{\text{ext}}(\mathbf{r}')$, by rewriting it as

$$k_B T \frac{\delta \ln[\rho(\mathbf{r})\Lambda^d]}{\delta V_{\text{ext}}(\mathbf{r}')} = \frac{k_B T}{\rho(\mathbf{r})} \frac{\delta\rho(\mathbf{r})}{\delta V_{\text{ext}}(\mathbf{r}')} = - \frac{H_2(\mathbf{r}, \mathbf{r}')}{\rho(\mathbf{r})}, \quad (226)$$

where we have dropped the subscript 0. To obtain the remaining (first) term on the right-hand side of Eq. (224), we carry out the functional derivative by using the functional chain rule and once more the definition (205),

$$\begin{aligned}
 & - \left. \frac{\delta}{\delta V_{\text{ext}}(\mathbf{r}')} \frac{\delta F_{\text{exc}}[\rho]}{\delta \rho(\mathbf{r})} \right|_{\rho=\rho_0} \\
 & = - \int d\mathbf{r}'' \frac{\delta^2 F_{\text{exc}}[\rho]}{\delta \rho(\mathbf{r}'') \delta \rho(\mathbf{r})} \frac{\delta \rho(\mathbf{r}'')}{\delta V_{\text{ext}}(\mathbf{r}')} \quad (227)
 \end{aligned}$$

$$= - \int d\mathbf{r}'' \frac{\delta^2 F_{\text{exc}}[\rho]}{\delta \rho(\mathbf{r}'') \delta \rho(\mathbf{r})} \left(-\frac{1}{k_B T} H_2(\mathbf{r}'', \mathbf{r}') \right) \quad (228)$$

$$= \int d\mathbf{r}'' \frac{\delta^2 \beta F_{\text{exc}}[\rho]}{\delta \rho(\mathbf{r}'') \delta \rho(\mathbf{r})} H_2(\mathbf{r}'', \mathbf{r}') \quad (229)$$

$$= - \int d\mathbf{r}'' c_2(\mathbf{r}'', \mathbf{r}) H_2(\mathbf{r}'', \mathbf{r}') \quad (230)$$

$$= - \int d\mathbf{r}'' c_2(\mathbf{r}, \mathbf{r}'') H_2(\mathbf{r}'', \mathbf{r}'). \quad (231)$$

We can now restore the starting equality (224) by equating Eq. (226) with the sum of Eq. (231) and the delta function (225). The result is

$$H_2(\mathbf{r}, \mathbf{r}') = \rho(\mathbf{r}) \int d\mathbf{r}'' c_2(\mathbf{r}, \mathbf{r}'') H_2(\mathbf{r}'', \mathbf{r}') + \rho(\mathbf{r}) \delta(\mathbf{r} - \mathbf{r}'), \quad (232)$$

where we have multiplied by $-\rho(\mathbf{r})$. Equation (232) can already be viewed as the static Ornstein-Zernike relation. Its standard form is expressed in terms of the total correlation function $h(\mathbf{r}, \mathbf{r}')$, where according to Eq. (209) we have $H_2(\mathbf{r}, \mathbf{r}') = \rho(\mathbf{r})\rho(\mathbf{r}')h(\mathbf{r}, \mathbf{r}') + \rho(\mathbf{r})\delta(\mathbf{r} - \mathbf{r}')$. We insert this identity into the integral in Eq. (232),

$$\int d\mathbf{r}'' c_2(\mathbf{r}, \mathbf{r}'') H_2(\mathbf{r}'', \mathbf{r}') \quad (233)$$

$$\begin{aligned}
 & = \int d\mathbf{r}'' c_2(\mathbf{r}, \mathbf{r}'') [\rho(\mathbf{r}'')\rho(\mathbf{r}')h(\mathbf{r}'', \mathbf{r}') + \rho(\mathbf{r}'')\delta(\mathbf{r}'' - \mathbf{r}')] \\
 & = \int d\mathbf{r}'' c_2(\mathbf{r}, \mathbf{r}'') \rho(\mathbf{r}'') \rho(\mathbf{r}') h(\mathbf{r}'', \mathbf{r}') \\
 & \quad + \int d\mathbf{r}'' c_2(\mathbf{r}, \mathbf{r}'') \rho(\mathbf{r}'') \delta(\mathbf{r}'' - \mathbf{r}') \quad (234)
 \end{aligned}$$

$$= \rho(\mathbf{r}') \left(\int d\mathbf{r}'' c_2(\mathbf{r}, \mathbf{r}'') \rho(\mathbf{r}'') h(\mathbf{r}'', \mathbf{r}') + c_2(\mathbf{r}, \mathbf{r}') \right). \quad (235)$$

We use this result in Eq. (232), divide by $\rho(\mathbf{r}')\rho(\mathbf{r})$, and obtain the standard form of the *inhomogeneous Ornstein-Zernike relation* as

$$h(\mathbf{r}, \mathbf{r}') = c_2(\mathbf{r}, \mathbf{r}') + \int d\mathbf{r}'' c_2(\mathbf{r}, \mathbf{r}'') \rho(\mathbf{r}'') h(\mathbf{r}'', \mathbf{r}'), \quad (236)$$

where the total correlation function $h(\mathbf{r}, \mathbf{r}')$ is a probabilistic object, defined via Eqs. (207) and (209), and $c_2(\mathbf{r}, \mathbf{r}')$ is the total correlation function, defined as the second functional density derivative (222) of the excess free energy functional.

The Ornstein-Zernike relation is a fundamental sum rule, different in character from hierarchies that relate two-body to

three-body (and/or higher) correlation functions. The Ornstein-Zernike relation is closed on the two-body level. (It also involves the one-body density profile.) Three- and higher-body versions exist and can be systematically derived. Alternatively, without the density-functional context, the Ornstein-Zernike relation can be viewed as the definition of the direct correlation function $c_2(\mathbf{r}, \mathbf{r}')$. (This is the original concept by Ornstein and Zernike.) The combination with a “closure” relation, i.e., an approximate additional relation between h and c_2 , forms the basis of liquid state integral equation theory. In a bulk fluid $\rho(\mathbf{r}) = \rho_b = \text{const}$ and the spatial dependence is only on $r_{\alpha\beta} = |\mathbf{r}_\alpha - \mathbf{r}_\beta|$, where $\alpha, \beta = 1, 2, 3$ labels the space points. We then have

$$h(r_{13}) = c_2(r_{13}) + \rho_b \int d\mathbf{r}_2 c_2(r_{12}) h(r_{23}). \quad (237)$$

One can visualize the integrals via diagrammatic notation, which gives deep insights into the mathematical structure and forms a useful calculation device. There are generalizations to mixtures and to anisotropic interparticle interactions. While this is conceptually straightforward, in actual applications the use can be highly challenging. We demonstrate in Sec. IV.D how the power functional permits one to generalize to time-dependent correlation functions.

H. Approximate free energy functionals

In practical applications of DFT an approximation for the nontrivial excess part $F_{\text{exc}}[\rho]$ of the density functional is required. Carrying out such work, an example being to investigate the behavior of a given fluid in the presence of an external potential, requires solving the Euler-Lagrange equation (160), which is typically performed numerically. Owing to decades of fundamental research efforts, a wide range of useful concrete prescriptions for $F_{\text{exc}}[\rho]$ is available. The different functionals vary both in the underlying concepts to perform the approximation and in the resulting mathematical complexity. We refer the interested reader to the pertinent literature⁸ and here describe only several basic concepts that are relevant to the construction of power functional approximations.

Arguably the simplest model form for $F_{\text{exc}}[\rho]$ is the local-density approximation (LDA). This scheme requires as input the bulk fluid equation of state, which determines the excess free energy density per unit volume $\psi_{\text{exc}}(\rho_b)$ as a function of the bulk density ρ_b . The LDA density functional then sums up local contributions from all space points via $F_{\text{exc}}[\rho] = \int d\mathbf{r} \psi_{\text{exc}}(\rho(\mathbf{r}))$, thereby ignoring all spatial correlations that the internal interactions generate. Nevertheless, for slowly varying spatial inhomogeneities (as measured on the length scale of interparticle correlations in the system) the LDA can be a good approximation. [See the studies of colloidal sedimentation by de las Heras *et al.* (2012), Geigenfeind and

⁸Good starting points are Evans (1992), Tarazona, Cuesta, and Martínez-Ratón (2008), Lutsko (2010), Roth (2010), Hansen and McDonald (2013), and Evans *et al.* (2016).

de las Heras (2017), Eckert, Schmidt, and de las Heras (2021).]

Taking simple account of some correlation effects is possible via the following square-gradient approximation:

$$F_{\text{exc}}[\rho] = \int d\mathbf{r} \left(\psi_{\text{exc}}(\rho(\mathbf{r})) + \frac{m}{2} [\nabla\rho(\mathbf{r})]^2 \right), \quad (238)$$

where m determines the strength of the square-gradient contribution. Microscopically, m is related to the second moment of the bulk direct correlation function $m = k_B T \int d\mathbf{r} r^2 c_2(r)/6$ (for $d = 3$), which allows to make a connection with the underlying model fluid.

Building the functional derivative of Eq. (238) with respect to the density profile gives

$$\frac{\delta F_{\text{exc}}[\rho]}{\delta\rho(\mathbf{r})} = \frac{\partial\psi_{\text{exc}}(\rho)}{\partial\rho(\mathbf{r})} - m\nabla^2\rho(\mathbf{r}), \quad (239)$$

which can be directly input into the Euler-Lagrange equation (160). The resulting theory is along the lines of van der Waals's historical treatment of the free gas-liquid interface and is akin to a Landau theory when $\rho(\mathbf{r})$ is identified as the local order parameter. Approximations of the form of Eq. (238) are sometimes referred to as semilocal.

A better accounting of the microscopic correlations that arise from interparticle forces and, in particular, from short-ranged repulsion requires genuine nonlocal approximations. Most nonlocal functionals rely on the introduction of one or several weighted densities that are obtained by convolution of the density profile with suitable weight function(s). Arguably the most successful scheme of this form is Rosenfeld's fundamental-measure theory for hard sphere mixtures (as well as for certain further model fluids). In short, the weighted densities are built according to

$$n_\alpha(\mathbf{r}) = \int d\mathbf{r}' \rho(\mathbf{r}') w_\alpha(\mathbf{r} - \mathbf{r}'), \quad (240)$$

where α is an index that labels the different weight functions. The Rosenfeld (1989) functional has the form

$$F_{\text{exc}}[\rho] = k_B T \int d\mathbf{r} \Phi(\{n_\alpha(\mathbf{r})\}), \quad (241)$$

where the scaled excess free energy density per volume $\Phi(\{n_\alpha(\mathbf{r})\})$ depends on all weighted densities. It is given by the simple rational expression

$$\Phi(\{n_\alpha(\mathbf{r})\}) = -n_0 \ln(1 - n_3) + \frac{n_1 n_2}{1 - n_3} + \frac{n_2^3}{24\pi(1 - n_3)^2} \quad (242)$$

in the form by Kierlik and Rosinberg (1990); we have omitted the position argument of $n_\alpha(\mathbf{r})$ for clarity. For the one-dimensional hard-core system ("hard rods") $\Phi_{1D}(\{n_\alpha\}) = -n_0 \ln(1 - n_1)$ and the fundamental-measure functional is identical to Percus's exact functional. In three dimensions a range of improved FMTs exist: these successfully describe freezing and crossover to reduced dimensionality. The White

Bear version incorporates the quasiexact Carnahan-Starling equation of state; see Roth (2010). We recall Sec. III.B, which gives an overview of further developments in constructing free energy density functionals.

I. Dynamical density-functional theory

The original proposal of Evans (1979) for the dynamical DFT was subsequently reconsidered by Marconi and Tarazona (1999), Archer and Evans (2004), and Español and Löwen (2009). In the following their dynamical theory is described on the basis of the adiabatic construction, which was laid out in Sec. III.A.

We recall the Euler-Lagrange equation (159) of equilibrium DFT as follows:

$$\frac{\delta F[\rho]}{\delta\rho(\mathbf{r})} + V_{\text{ext}}(\mathbf{r}) - \mu = 0, \quad (243)$$

where for compactness of notation we have left out the fact that equality holds for $\rho(\mathbf{r}) = \rho_0(\mathbf{r})$, where $\rho_0(\mathbf{r})$ indicates the equilibrium density profile. Building the negative gradient of Eq. (243) yields

$$-\nabla \frac{\delta F[\rho]}{\delta\rho(\mathbf{r})} - \nabla V_{\text{ext}}(\mathbf{r}) = 0, \quad (244)$$

which has the clear physical interpretation of a force balance relationship of vanishing sum of intrinsic and external forces.

The aim is to formulate a dynamical one-body theory that drives the time evolution in nonequilibrium, based on the equilibrium intrinsic force term in Eq. (244). We recall from Sec. II the one-body continuity equation

$$\dot{\rho}(\mathbf{r}, t) = -\nabla \cdot \mathbf{J}(\mathbf{r}, t), \quad (245)$$

which links changes in the time-dependent density profile to the divergence of the microscopic current distribution $\mathbf{J}(\mathbf{r}, t)$. We have seen that the exact equation of motion (83) for the case of overdamped Brownian motion represents the current as being instantaneously generated by the sum of all force densities that act in the system as follows:

$$\gamma \mathbf{J}(\mathbf{r}, t) = -k_B T \nabla \rho(\mathbf{r}, t) + \mathbf{F}_{\text{int}}(\mathbf{r}, t) + \rho \mathbf{f}_{\text{ext}}(\mathbf{r}, t). \quad (246)$$

As before γ is the friction constant against the static background solvent. In equilibrium, we know that the internal force density and the external force field satisfy, respectively,

$$\mathbf{F}_{\text{int}}(\mathbf{r}) = -\left\langle \sum_i \delta(\mathbf{r} - \mathbf{r}_i) \nabla_i u \right\rangle_{\text{eq}} = -\rho(\mathbf{r}) \nabla \frac{\delta F_{\text{exc}}[\rho]}{\delta\rho(\mathbf{r})}, \quad (247)$$

$$\mathbf{f}_{\text{ext}}(\mathbf{r}) = -\nabla V_{\text{ext}}(\mathbf{r}). \quad (248)$$

To use Eq. (247) in a dynamical context we use the concept of the *adiabatic state*, which as described in Sec. III.A consists of considering, at each time t , a true equilibrium adiabatic system, with its genuine one-body density profile $\rho_{\text{ad},t}(\mathbf{r})$. As the adiabatic system is in equilibrium, its density distribution

is independent of time. However, per construction the nonequilibrium system has at each time t a corresponding adiabatic state. The nonequilibrium system and the adiabatic system share the same internal interaction potential $u(\mathbf{r}^N)$ and they are related by the identification

$$\rho(\mathbf{r}, t) = \rho_{\text{ad},t}(\mathbf{r}), \quad (249)$$

where the dependence on time is real in the nonequilibrium system and parametric only in the adiabatic system (where t instead “selects” the fitting adiabatic state in a sequence of equilibrium systems indexed by t). In the adiabatic system, via the Hohenberg-Kohn-Mermin-Evans map, we can identify a unique external one-body potential $V_{\text{ad},t}(\mathbf{r})$ that stabilizes the given $\rho_{\text{ad},t}(\mathbf{r})$. Again the dependence on time of the adiabatic external potential is merely parametric. The adiabatic system is in equilibrium, and hence its external potential $V_{\text{ad},t}(\mathbf{r})$ is static. (This point is of mere conceptual importance; in practice one treats the adiabatic system using a corresponding equilibrium ensemble that relieves one of a secondary time evolution in the adiabatic system.)

In the adiabatic system the external force field needs to balance the intrinsic force field, $-k_B T \nabla \ln \rho_{\text{ad},t}(\mathbf{r}) + \mathbf{f}_{\text{ad},t}(\mathbf{r}) - \nabla V_{\text{ad},t}(\mathbf{r}) = 0$, where $\mathbf{f}_{\text{ad},t}(\mathbf{r})$ is the one-body force field in the adiabatic system that arises due to internal interactions. Hence, we have a chain of functional relationships

$$\rho(\mathbf{r}, t) \rightarrow \rho_{\text{ad},t}(\mathbf{r}) \rightarrow V_{\text{ad},t}(\mathbf{r}) \rightarrow \mathbf{f}_{\text{ad},t}(\mathbf{r}). \quad (250)$$

Dynamical DFT amounts to approximating the real internal one-body force field by that in the adiabatic system as follows:

$$\mathbf{f}_{\text{int}}(\mathbf{r}, t) \approx \mathbf{f}_{\text{ad},t}(\mathbf{r}). \quad (251)$$

As a result of the approximation all forces are known in the nonequilibrium system [as $\rho(\mathbf{r}, t)$ is known at time t and $\mathbf{f}_{\text{ad},t}(\mathbf{r})$ is a density functional]. As the force balance is known via the approximation (251), the dynamical theory is closed. [The continuity equation (245) forms the supplemental, secondary relation.] Hence, we have the instantaneous relationship

$$\gamma \mathbf{J}(\mathbf{r}, t) = -k_B T \nabla \rho(\mathbf{r}, t) + \rho \mathbf{f}_{\text{ad}}(\mathbf{r}, t) + \rho \mathbf{f}_{\text{ext}}(\mathbf{r}, t), \quad (252)$$

where we have dropped the subscript t and $\mathbf{f}_{\text{ext}}(\mathbf{r}, t)$ needs no longer be restricted to gradient form. Note that in cases where it is restricted the real external potential, which generates the instantaneous external force field via $\mathbf{f}_{\text{ext}}(\mathbf{r}, t) = -\nabla V_{\text{ext}}(\mathbf{r}, t)$, will in general be significantly different than the external potential that acts in the adiabatic system [$V_{\text{ad},t}(\mathbf{r})$]. Hence, $V_{\text{ext}}(\mathbf{r}, t) \neq V_{\text{ad},t}(\mathbf{r})$, possibly strikingly so. To see this, first consider a switching process that changes $V_{\text{ext}}(\mathbf{r}, t)$ abruptly but that had not allowed enough time to pass to generate a noticeable effect on $\rho(\mathbf{r}, t)$, hence leaving $V_{\text{ad},t}(\mathbf{r})$ virtually intact. It is important to appreciate the difference between the two external potentials: $V_{\text{ext}}(\mathbf{r}, t)$ drives the time evolution in the real system, whereas $V_{\text{ad},t}(\mathbf{r})$ instead stops the time evolution in the adiabatic system. When the real system is in equilibrium, both potentials are identical. As a second

illustrative example, consider free expansion of an initially confined density distribution, where at any time the adiabatic potential needs to stabilize the broadening density profile, although after the initial time $V_{\text{ext}}(\mathbf{r}, t) \equiv 0$; see Schmidt and Brader (2013).

Using the approximation (251) in a practical application requires one to have access to the adiabatic map (250), of which the nontrivial part is the following map from the density profile to the external potential in the adiabatic system:

$$\rho_{\text{ad},t}(\mathbf{r}) \rightarrow V_{\text{ad},t}(\mathbf{r}). \quad (253)$$

DFT as an approximative computational scheme is perfectly suited to this task. Consider the following Euler-Lagrange equation in the adiabatic system:

$$k_B T \ln \rho_{\text{ad},t}(\mathbf{r}) + \frac{\delta F_{\text{exc}}[\rho_{\text{ad},t}]}{\delta \rho_{\text{ad},t}(\mathbf{r})} = \mu_{\text{ad}} - V_{\text{ad},t}(\mathbf{r}), \quad (254)$$

where μ_{ad} is the chemical potential that controls the density in the adiabatic system and $F_{\text{exc}}[\rho]$ is the intrinsic excess free energy functional, which arises from $u(\mathbf{r}^N) \neq 0$. Hence, the internal force field in the adiabatic system is available as a density functional as

$$\mathbf{f}_{\text{ad},t}(\mathbf{r}) = -\nabla \left. \frac{\delta F_{\text{exc}}[\rho]}{\delta \rho(\mathbf{r})} \right|_{\rho(\mathbf{r})=\rho_{\text{ad},t}(\mathbf{r})}, \quad (255)$$

which is a directly accessible quantity [recall $\rho(\mathbf{r}, t) = \rho_{\text{ad},t}(\mathbf{r})$] once the excess free energy functional is known (as an approximation, as is typical for equilibrium DFT applications).

In summary, the DDFT equations of motion are

$$\dot{\rho}(\mathbf{r}, t) = -\nabla \cdot \mathbf{J}(\mathbf{r}, t), \quad (256)$$

$$\gamma \mathbf{J}(\mathbf{r}, t) = -k_B T \nabla \rho(\mathbf{r}, t) - \rho(\mathbf{r}, t) \nabla \frac{\delta F_{\text{exc}}[\rho]}{\delta \rho(\mathbf{r}, t)} + \rho(\mathbf{r}, t) \mathbf{f}_{\text{ext}}(\mathbf{r}, t). \quad (257)$$

Eliminating the current (which is a useful object in its own right, as we demonstrate in Sec. IV) yields the following standard form of DDFT:

$$\begin{aligned} \dot{\rho}(\mathbf{r}, t) = & D \nabla^2 \rho(\mathbf{r}, t) + \gamma^{-1} \nabla \cdot \rho(\mathbf{r}, t) \nabla \frac{\delta F_{\text{exc}}[\rho]}{\delta \rho(\mathbf{r}, t)} \\ & - \gamma^{-1} \nabla \cdot \rho(\mathbf{r}, t) \mathbf{f}_{\text{ext}}(\mathbf{r}, t), \end{aligned} \quad (258)$$

where $D = k_B T / \gamma$ is the single-particle diffusion constant and $\nabla^2 = \nabla \cdot \nabla$ is the Laplace operator. For the ideal gas $F_{\text{exc}}[\rho] = 0$, as there are no interparticle interactions [$u(\mathbf{r}^N) \equiv 0$]. Hence, the second term on the right-hand side of Eq. (258) vanishes. The leaves over the sum of the first term (diffusion) and the third term (drift), which then constitutes the correct drift-diffusion equation for the ideal gas.

The contribution due to the internal interactions in the system [the second term on the right-hand side of Eq. (258)] will in general have spatially nonlocal dependence on the density distribution. Recall that $F_{\text{exc}}[\rho]$ describes in

equilibrium all correlation effects, from the particle scale to macroscopic scales (say, near a gas-liquid critical point or in complete wetting situations). The temporal dependence of the equation of motion (258) remains simplistic though, and it is virtually unchanged over the ideal drift-diffusion equation: The time dependence is local (i.e., Markovian) and hence memory effects are absent. A further, and related, problem is the value of γ (and hence of the diffusion constant $D = k_B T / \gamma$). If γ has the value of the free single-particle motion, how can slowing down, as is typical at high densities, occur? The theory seems to lack a corresponding mechanism. Several ways to remedy this seeming absence of essential physics have been proposed (some are described later) and are primarily based on an empirical footing. As a recent representative investigation of the differences of intrinsic time-scales obtained from dynamical DFT as compared to BD simulation work, we mention the studies of the van Hove pair correlation function in liquids by Treffenstädt and Schmidt (2021) and Treffenstädt, Schindler, and Schmidt (2022). We give an overview of the dynamical test-particle limit, which underlies their treatment, in Sec. IV.E.

Nevertheless, per construction the equilibrium limit of the interacting many-body system with arbitrary spatial inhomogeneity is incorporated in an, in principle, exact fashion. This is typically not the case in approaches that are developed genuinely in nonequilibrium (where the assumption of a homogeneous bulk fluid is often made). It is difficult to conceive how an entirely different dynamical approach would be able to reduce naturally to DFT when applied to time evolution in equilibrium.

We later show that power functional theory delivers this feat, and that the internal force density field exactly splits into $\mathbf{f}_{\text{int}}(\mathbf{r}, t) = \mathbf{f}_{\text{ad}}(\mathbf{r}, t) + \mathbf{f}_{\text{sup}}(\mathbf{r}, t)$, where the adiabatic force field $\mathbf{f}_{\text{ad}}(\mathbf{r}, t)$ is identical to that in DDFT, and the superadiabatic force field is generated from a kinematic excess free power functional $P_t^{\text{exc}}[\rho, \mathbf{J}]$ via functional differentiation, $\mathbf{f}_{\text{sup}}(\mathbf{r}, t) = -\delta P_t^{\text{exc}} / \delta \mathbf{J}(\mathbf{r}, t)$. Power functional theory elevates the microscopic current distribution $\mathbf{J}(\mathbf{r}, t)$ from the status of a mere bookkeeping device to that of a genuine degree of freedom (an order parameter) of the physical system.

Our presentation of the DDFT based on Eq. (251) is as *ad hoc* as the original proposal of the theory (Evans, 1979). There has been much refined reasoning, based on the Langevin picture and Dean's equation (Marconi and Tarazona, 1999), on the Smoluchowski equation (Archer and Evans, 2004), and on the projection-operator formalism (Español and Löwen, 2009). While these studies shed some light on deep connections with the many-body dynamics and each of the derivations has also gained widespread recognition, they have thus far not provided a systematic basis for assessing the fundamental approximation that is involved. This step remained *ad hoc*, in the sense that no systematic way for improvement is implied. In contrast, we later see that the adiabatic state arises naturally in the power functional framework, as a formally exact one-body treatment of the dynamics, which allows one to formalize and build concrete approximations for the superadiabatic force contributions.

Applications of the DDFT framework are numerous; an exhaustive list was given by te Vrugt, Löwen, and Wittkowski (2020). Here we mention selected insightful DDFT studies.

Royall *et al.* (2007) presented an investigation of sedimentation of model hard-sphere-like colloidal dispersions confined in horizontal capillaries based on the use of laser scanning confocal microscopy, Brownian dynamics computer simulations, and DDFT [additional details were given by Schmidt *et al.* (2008)]. The researchers could obtain quantitative agreement of the results from the respective approaches for the time evolution of the one-body density distribution and the osmotic pressure on the walls. To match the theoretical results to the experimental data, a density-dependent mobility γ^{-1} was empirically introduced.

Dzubiella and Likos (2003) formulated the DDFT concept based on the mean-field (quadratic in density) free energy functional. DDFT has been used to describe protein adsorption on polymer-coated nanoparticles (Angioletti-Uberti, Ballauff, and Dzubiella, 2014, 2018) and the uptake kinetics of molecular cargo into hollow hydrogels (Moncho-Jordá *et al.*, 2019). DDFT has been applied to lane formation in oppositely driven binary mixtures (Chakrabarti, Dzubiella, and Löwen, 2003, 2004). DDFT has been used for lattice models for problems such as growth of hard-rod monolayers via deposition (Klopotek *et al.*, 2017). Bleibel, Domínguez, and Oettel (2016) derived a DDFT including two-body hydrodynamic interactions. Menzel *et al.* (2016) established a DDFT for active microswimmer suspensions. A DDFT for translational Brownian dynamics that includes hydrodynamic interactions was described by Rex and Löwen (2009). Scacchi and Brader (2018) investigated the formation of a cavitation bubble as a local phase transition.

Goddard *et al.* (2012) derived a DFT for colloidal fluids including inertia and hydrodynamic interactions. Wittkowski, Löwen, and Brand (2012) formulated an extended DDFT for colloidal mixtures with temperature gradients. Using DDFT Scacchi, Archer, and Brader (2017) investigated the laning instability of a sheared colloidal suspension. Wächtler, Kogler, and Klapp (2016) performed a stability analysis based on DDFT in order to investigate nonequilibrium lane formation in a two-dimensional Lennard-Jones fluid composed of two particle species driven in opposite directions. Anero, Español, and Tarazona (2013) constructed an approach that they call functional thermodynamics, which represents a generalization of dynamic density-functional theory to nonisothermal situations. DDFT has also been used to describe polymeric systems (Qi and Schmid, 2017). Archer and Rauscher (2004) aimed to clarify confusion in the literature as to whether dynamical density-functional theories for the one-body density of a classical Brownian fluid should contain a stochastic noise term.

IV. POWER FUNCTIONAL THEORY

A. Dynamic minimization principle

Power functional theory is based on a formally exact minimization principle on the one-body level of dynamic correlation functions. The theory was formulated originally for Brownian dynamics by Schmidt and Brader (2013), and subsequently generalized to nonrelativistic quantum dynamics (Schmidt, 2015), and classical Hamiltonian dynamics (Schmidt, 2018). Here we provide an overview of the central concepts. Key ideas of the microscopic foundation are

described in Sec. IV.B. For the full treatment, see the original papers.

The kinematic fields, i.e., the density $\rho(\mathbf{r}, t)$ [referred to as $n(\mathbf{r}, t)$ in the quantum case], the current $\mathbf{J}(\mathbf{r}, t)$, and in the case of inertial dynamics also the time derivative of the current $\dot{\mathbf{J}}(\mathbf{r}, t)$, are the relevant functional variables. Two continuity equations interrelate these fields. The variational principle is instantaneous in time, involving minimization with respect to the highest relevant time derivative, i.e., with respect to $\mathbf{J}(\mathbf{r}, t)$ in the overdamped Brownian case, and with respect to $\dot{\mathbf{J}}(\mathbf{r}, t)$ in both the classical and quantum inertial cases. Integration in time then determines the current (in the inertial cases) as well as the density according to

$$\mathbf{J}(\mathbf{r}, t) = \mathbf{J}(\mathbf{r}, 0) + \int_0^t dt' \dot{\mathbf{J}}(\mathbf{r}, t'), \quad (259)$$

$$\rho(\mathbf{r}, t) = \rho(\mathbf{r}, 0) - \int_0^t dt' \nabla \cdot \mathbf{J}(\mathbf{r}, t'). \quad (260)$$

In practice, one proceeds in discrete time steps such that minimization at time t allows one to proceed in time by one step, then update according to Eqs. (259) and (260), and proceed to the next time step; see [Treffenstädt and Schmidt \(2020\)](#).

We first collect from Sec. II the one-body equations of motion for the three different types of dynamics. For overdamped Brownian dynamics the relationship of the current and the force densities (83) is

$$\gamma \mathbf{J}(\mathbf{r}, t) = -k_B T \nabla \rho(\mathbf{r}, t) + \mathbf{F}_{\text{int}}(\mathbf{r}, t) + \rho(\mathbf{r}, t) \mathbf{f}_{\text{ext}}(\mathbf{r}, t), \quad (261)$$

where the internal force density distribution is $\mathbf{F}_{\text{int}}(\mathbf{r}, t) = -\langle \sum_i \delta(\mathbf{r} - \mathbf{r}_i) \nabla_i u(\mathbf{r}^N) \rangle$, with the average being taken over the instantaneous configuration space probability distribution.

In molecular dynamics the equations of motion (49) and (52) are

$$m \dot{\mathbf{J}}(\mathbf{r}, t) = \nabla \cdot \boldsymbol{\tau}(\mathbf{r}, t) + \mathbf{F}_{\text{int}}(\mathbf{r}, t) + \rho(\mathbf{r}, t) \mathbf{f}_{\text{ext}}(\mathbf{r}, t), \quad (262)$$

$$\boldsymbol{\tau}(\mathbf{r}, t) = -\frac{1}{m} \left\langle \sum_i \delta(\mathbf{r} - \mathbf{r}_i) \mathbf{p}_i \mathbf{p}_i \right\rangle, \quad (263)$$

where the kinetic stress distribution $\boldsymbol{\tau}(\mathbf{r}, t)$ captures transport effects. The averages here in $\mathbf{F}_{\text{int}}(\mathbf{r}, t)$ and $\boldsymbol{\tau}(\mathbf{r}, t)$ are over the many-body phase space distribution function.

The quantum dynamics in Eqs. (133) and (134) are similar to the classical inertial case but incorporate additional wave-like, genuine quantum effects as follows:

$$m \dot{\mathbf{J}}(\mathbf{r}, t) = \nabla \cdot \boldsymbol{\tau}(\mathbf{r}, t) + \mathbf{F}_{\text{int}}(\mathbf{r}, t) + \frac{\hbar^2}{4m} \nabla \nabla^2 n(\mathbf{r}, t) + n(\mathbf{r}, t) \mathbf{f}_{\text{ext}}(\mathbf{r}, t), \quad (264)$$

$$\boldsymbol{\tau}(\mathbf{r}, t) = -\frac{1}{2m} \left\langle \sum_i [\hat{\mathbf{p}}_i \delta_i \hat{\mathbf{p}}_i + \hat{\mathbf{p}}_i \delta_i \hat{\mathbf{p}}_i^T] \right\rangle, \quad (265)$$

where $\delta_i = \delta(\mathbf{r} - \mathbf{r}_i)$ and all averages are bra-kets using the instantaneous wave function. The continuity equations (259)

and (260) apply (with the symbol ρ replaced by n in the notation).

The central object of power functional theory is the free power functional $R_t[\rho, \mathbf{J}]$ (BD) or free power *rate functional* $G_t[\rho, \mathbf{J}, \dot{\mathbf{J}}]$ (MD) and $G_t[n, \mathbf{J}, \dot{\mathbf{J}}]$ [quantum mechanical (QM)]. Staying with BD, the exact minimization principle states that at each time t

$$\left. \frac{\delta R_t[\rho, \mathbf{J}]}{\delta \mathbf{J}(\mathbf{r}, t)} \right|_{\rho, \mathbf{J}=\mathbf{J}_0} = 0 \quad (\text{min}), \quad (266)$$

where $\mathbf{J}_0(\mathbf{r}, t)$ is the real, physically realized current distribution of the physical dynamics. Hence, $\mathbf{J}_0(\mathbf{r}, t) = \langle \sum_i \mathbf{v}_i \delta_i \rangle$, averaged over the actual many-body phase space distribution function at time t .

The derivative in Eq. (266) is performed as a spatial variation, instantaneously at a fixed time t ; the same time argument occurs in both $R_t[\rho, \mathbf{J}]$ and $\mathbf{J}(\mathbf{r}, t)$. This constitutes a “time-slice” variation where the spatial argument can be chosen freely but time is prescribed; see Fig. 4 for a graphical illustration of the concept and Appendix A.2 for background. The dependence of $R_t[\rho, \mathbf{J}]$ on its functional arguments is in general nonlocal in space, but it is causal in time, such that the value of the density and the current contribute only at times $\leq t$ (i.e., there is no unphysical dependence on future times $> t$). The physical units of $R_t[\rho, \mathbf{J}]$ are those of energy per time, i.e., power, $[R_t] = \text{J/s} = \text{W}$. The density distribution $\rho(\mathbf{r}, t)$ is kept fixed under the variation (266). Hence, the variation can be viewed as a partial functional derivative with respect to the current, with the density distribution kept constant. This is not an uncommon situation in functional calculus; see Hamilton’s principle (Appendix A.1).

For MD and QM the power functional minimization principle is

$$\left. \frac{\delta G_t[\rho, \mathbf{J}, \dot{\mathbf{J}}]}{\delta \dot{\mathbf{J}}(\mathbf{r}, t)} \right|_{\rho, \mathbf{J}=\mathbf{J}_0} = 0 \quad (\text{min}), \quad (267)$$

where the subscript 0 again indicates the physically realized dynamics $\dot{\mathbf{J}}_0(\mathbf{r}, t) = \langle d\dot{\mathbf{J}}/dt \rangle$, with the average taken over the state of the system at time t . The derivative (267) is taken in a time slice, and the density and the current distributions are held constant under the variation. The functional dependence on time is again causal, i.e., on the value of the argument fields at times $\leq t$. Together with the continuity equations (259)

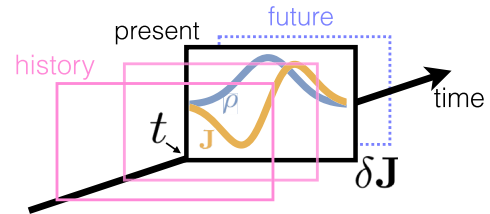


FIG. 4. Time-slice variational principle for overdamped BD. The position-resolved current variation $\delta \mathbf{J}(\mathbf{r}, t)$ is performed at a fixed time t . The values at times $< t$ (history) and $> t$ (future) are unaffected by the purely spatial variation in a time slice at the present time t .

and (260), one has formally exact equations of motion that are closed on the one-body level. The many-body problem is entirely encapsulated in the functional dependence of $G_t[\rho, \mathbf{J}, \dot{\mathbf{J}}]$ on its arguments.

As with the splitting of the grand potential density functional in equilibrium, in the dynamical case a splitting of the functional into intrinsic and external contributions holds. We return to BD, where the total power functional splits according to

$$R_t[\rho, \mathbf{J}] = P_t[\rho, \mathbf{J}] + \dot{F}[\rho] - X_t[\rho, \mathbf{J}]. \quad (268)$$

In Eq. (268) the superadiabatic free power $P_t[\rho, \mathbf{J}]$ consists of ideal and excess contributions, $P_t[\rho, \mathbf{J}] = P_t^{\text{id}}[\rho, \mathbf{J}] + P_t^{\text{exc}}[\rho, \mathbf{J}]$, with $P_t^{\text{id}}[\rho, \mathbf{J}]$ the exact dissipation functional of the ideal gas and $P_t^{\text{exc}}[\rho, \mathbf{J}]$ accounting for the excess superadiabatic effects (above excess free energy changes). Free energy changes emerge via the time derivative $\dot{F}[\rho] \equiv dF[\rho]/dt$ of the Helmholtz excess free energy functional $F[\rho]$ of an equilibrium system with the unchanged interparticle interaction potential $u(\mathbf{r}^N)$. The remaining term $-X_t[\rho, \mathbf{J}]$ in Eq. (268) is the negative external power. The total power functional $R_t[\rho, \mathbf{J}]$ constitutes free power in the sense that not only energetic but also entropic effects are accounted for, analogously to the free energy in equilibrium.

The intrinsic contribution to the total free power is the sum $W_t[\rho, \mathbf{J}] \equiv P_t[\rho, \mathbf{J}] + \dot{F}[\rho]$, which depends on the internal interactions but is independent of the external forces (which in general are of time-dependent one-body form). A splitting into ideal and excess (above ideal) parts holds according to

$$W_t[\rho, \mathbf{J}] = W_t^{\text{id}}[\rho, \mathbf{J}] + W_t^{\text{exc}}[\rho, \mathbf{J}], \quad (269)$$

where $W_t^{\text{id}}[\rho, \mathbf{J}]$ is due to the diffusive motion and $W_t^{\text{exc}}[\rho, \mathbf{J}]$ arises from the interparticle interactions. Both terms consist of a sum of adiabatic and superadiabatic contributions

$$W_t^{\text{id}}[\rho, \mathbf{J}] = \dot{F}_{\text{id}}[\rho] + P_t^{\text{id}}[\rho, \mathbf{J}], \quad (270)$$

$$W_t^{\text{exc}}[\rho, \mathbf{J}] = \dot{F}_{\text{exc}}[\rho] + P_t^{\text{exc}}[\rho, \mathbf{J}]. \quad (271)$$

As one might expect for the noninteracting system, the two ideal terms (270) are temporally local (as later given explicitly). The excess part (271) consists of an instantaneous contribution, which one can identify with the time derivative $\dot{F}_{\text{exc}}[\rho]$ (also given explicitly later), and a temporally nonlocal, i.e., memory-dependent, superadiabatic term $P_t^{\text{exc}}[\rho, \mathbf{J}]$. The latter in general is also spatially nonlocal, as is $\dot{F}_{\text{exc}}[\rho]$, due to the coupling via the interparticle interaction potential. We recall the total time derivative of the equilibrium free energy functional as

$$\dot{F}[\rho] = \frac{d}{dt} F[\rho] = \int d\mathbf{r} \left(\nabla \frac{\delta F[\rho]}{\delta \rho(\mathbf{r}, t)} \right) \cdot \mathbf{J}(\mathbf{r}, t), \quad (272)$$

which follows from the functional chain rule of differentiation, the continuity equation, and integration by parts; see Eqs. (25)–(27). In Eq. (272) the functional derivative of $F[\rho]$ with respect to the time-dependent density is defined via the adiabatic construction (Sec. III.A) as

$$\frac{\delta F[\rho]}{\delta \rho(\mathbf{r}, t)} = \left. \frac{\delta F[\rho_{\text{ad},t}]}{\delta \rho_{\text{ad},t}(\mathbf{r})} \right|_{\rho_{\text{ad},t}(\mathbf{r})=\rho(\mathbf{r},t)}, \quad (273)$$

where $\rho_{\text{ad},t}(\mathbf{r})$ is a trial density distribution in the adiabatic system.

The ideal contribution to the time derivative (272) can be made more explicit as

$$\dot{F}_{\text{id}}[\rho] = \int d\mathbf{r} \left(\nabla \frac{\delta F_{\text{id}}[\rho]}{\delta \rho(\mathbf{r}, t)} \right) \cdot \mathbf{J}(\mathbf{r}, t) \quad (274)$$

$$= k_B T \int d\mathbf{r} [\nabla \ln \rho(\mathbf{r}, t)] \cdot \mathbf{J}(\mathbf{r}, t), \quad (275)$$

where we recall that the ideal gas free energy functional is $F_{\text{id}}[\rho] = k_B T \int d\mathbf{r} \rho(\mathbf{r}) \{ \ln[\rho(\mathbf{r}) \Lambda^d] - 1 \}$.

The external power is the instantaneous expression

$$X_t[\rho, \mathbf{J}] = \int d\mathbf{r} [\mathbf{J}(\mathbf{r}, t) \cdot \mathbf{f}_{\text{ext}}(\mathbf{r}, t) - \rho(\mathbf{r}, t) \dot{V}_{\text{ext}}(\mathbf{r}, t)], \quad (276)$$

where the first contribution in the integral is the mechanical power due to motion along the external force field. The second contribution is static with respect to the particle coordinates and describes a ‘‘charging’’ effect due to temporal changes in the external potential landscape at fixed particle positions.

The ideal dissipation functional is

$$P_t^{\text{id}}[\rho, \mathbf{J}] = \frac{\gamma}{2} \int d\mathbf{r} \frac{[\mathbf{J}(\mathbf{r}, t)]^2}{\rho(\mathbf{r}, t)}, \quad (277)$$

where, as previously, γ is the friction constant and the expression is spatially local and temporally Markovian, as one might expect for ideal diffusive motion.

Inserting the splitting (268) into the minimization principle (266) yields

$$0 = \frac{\delta P_t^{\text{id}}[\rho, \mathbf{J}]}{\delta \mathbf{J}(\mathbf{r}, t)} + \frac{\delta P_t^{\text{exc}}[\rho, \mathbf{J}]}{\delta \mathbf{J}(\mathbf{r}, t)} + \frac{\delta \dot{F}_{\text{id}}[\rho]}{\delta \mathbf{J}(\mathbf{r}, t)} + \frac{\delta \dot{F}_{\text{exc}}[\rho]}{\delta \mathbf{J}(\mathbf{r}, t)} - \frac{\delta X_t[\rho, \mathbf{J}]}{\delta \mathbf{J}(\mathbf{r}, t)}. \quad (278)$$

Three of the individual contributions can be obtained explicitly, using Eqs. (275), (276), and (277), which give

$$\frac{\delta P_t^{\text{id}}}{\delta \mathbf{J}} = \frac{\gamma \mathbf{J}}{\rho}, \quad \frac{\delta \dot{F}_{\text{id}}}{\delta \mathbf{J}} = k_B T \nabla \ln \rho, \quad \frac{\delta X_t}{\delta \mathbf{J}} = \mathbf{f}_{\text{ext}}. \quad (279)$$

where arguments have been omitted for brevity. Use of the microscopic velocity field $\mathbf{v}(\mathbf{r}, t) = \mathbf{J}(\mathbf{r}, t)/\rho(\mathbf{r}, t)$ then gives upon rearrangement of Eq. (278) a force balance relationship

$$\gamma \mathbf{v}(\mathbf{r}, t) = -k_B T \nabla \ln \rho(\mathbf{r}, t) - \nabla \frac{\delta F_{\text{exc}}[\rho]}{\delta \rho(\mathbf{r}, t)} - \frac{\delta P_t^{\text{exc}}[\rho, \mathbf{J}]}{\delta \mathbf{J}(\mathbf{r}, t)} + \mathbf{f}_{\text{ext}}(\mathbf{r}, t), \quad (280)$$

where the negative friction force (left-hand side) equals the sum of all driving forces (right-hand side). From averaging

over the microscopic dynamics (Sec. II.C) we also know the equation of motion [Eq. (261)],

$$\gamma \mathbf{v}(\mathbf{r}, t) = -k_B T \nabla \ln \rho(\mathbf{r}, t) + \mathbf{f}_{\text{int}}(\mathbf{r}, t) + \mathbf{f}_{\text{ext}}(\mathbf{r}, t), \quad (281)$$

which is divided here by $\rho(\mathbf{r}, t)$; recall that the internal force field and the internal force density are related via $\mathbf{f}_{\text{int}}(\mathbf{r}, t) = \mathbf{F}_{\text{int}}(\mathbf{r}, t)/\rho(\mathbf{r}, t)$. When comparing Eqs. (280) and (281), we can hence identify the internal one-body force field as

$$\mathbf{f}_{\text{int}}(\mathbf{r}, t) = -\nabla \frac{\delta F_{\text{exc}}[\rho]}{\delta \rho(\mathbf{r}, t)} - \frac{\delta P_t^{\text{exc}}[\rho, \mathbf{J}]}{\delta \mathbf{J}(\mathbf{r}, t)}. \quad (282)$$

The right-hand side of Eq. (282) depends functionally on $\rho(\mathbf{r}, t)$ and $\mathbf{J}(\mathbf{r}, t)$, as both $F_{\text{exc}}[\rho]$ and $P_t^{\text{exc}}[\rho, \mathbf{J}]$ inherit their functional dependence from $R_t[\rho, \mathbf{J}]$. Hence, the left-hand side of Eq. (282) is also a functional of these fields, i.e.,

$$\mathbf{f}_{\text{int}}(\mathbf{r}, t) = \mathbf{f}_{\text{int}}(\mathbf{r}, t, [\rho, \mathbf{v}]), \quad (283)$$

where the pairs $\rho(\mathbf{r}, t), \mathbf{v}(\mathbf{r}, t)$ and $\rho(\mathbf{r}, t), \mathbf{J}(\mathbf{r}, t)$ are two alternative sets of functional arguments (de las Heras and Schmidt, 2018a). We split the internal force field into adiabatic and superadiabatic parts $\mathbf{f}_{\text{int}}(\mathbf{r}, t) = \mathbf{f}_{\text{ad}}(\mathbf{r}, t) + \mathbf{f}_{\text{sup}}(\mathbf{r}, t)$, where the two contributions are

$$\mathbf{f}_{\text{ad}}(\mathbf{r}, t) = -\nabla \frac{\delta F_{\text{exc}}[\rho]}{\delta \rho(\mathbf{r}, t)}, \quad \mathbf{f}_{\text{sup}}(\mathbf{r}, t) = -\frac{\delta P_t^{\text{exc}}[\rho, \mathbf{J}]}{\delta \mathbf{J}(\mathbf{r}, t)}. \quad (284)$$

The adiabatic force field $\mathbf{f}_{\text{ad}}(\mathbf{r}, t, [\rho])$ is an instantaneous density functional. The superadiabatic force field $\mathbf{f}_{\text{sup}}(\mathbf{r}, t, [\rho, \mathbf{v}])$ depends on both the density and the velocity field (or, equivalently, on the current distribution); we refer to such an object as a *kinematic functional*.

Hence, the total internal force field is

$$\mathbf{f}_{\text{int}}(\mathbf{r}, t, [\rho, \mathbf{v}]) = \mathbf{f}_{\text{ad}}(\mathbf{r}, t, [\rho]) + \mathbf{f}_{\text{sup}}(\mathbf{r}, t, [\rho, \mathbf{v}]), \quad (285)$$

where the adiabatic force field depends instantaneously, at time t , on the density distribution. The superadiabatic force field also depends on the microscopic velocity field, and it does so via causal dependence on time, i.e., the values of density and velocity at all times $\leq t$ contribute, and they determine the internal force field at time t . The internal one-body force density field $\mathbf{f}_{\text{int}}(\mathbf{r}, t)$ plays a crucial role in the power functional formulation of the dynamics, as it explicitly contains the interparticle coupling that generates the many-body effects.

We can express the adiabatic force field in correlator form (139) as

$$\mathbf{f}_{\text{ad}}(\mathbf{r}, t, [\rho]) = \frac{-1}{\rho(\mathbf{r}, t)} \left\langle \sum_i \delta(\mathbf{r} - \mathbf{r}_i) \nabla_i u(\mathbf{r}^N) \right\rangle_{\text{eq}}, \quad (286)$$

where the average is performed in an equilibrium system with density profile $\rho_{\text{ad},t}(\mathbf{r}) = \rho(\mathbf{r}, t)$. This density is generated via an appropriate external Mermin potential $V_{\text{ad},t}(\mathbf{r})$, which acts only in the adiabatic system, not in the real dynamical system;

see Sec. III.A. If a real external potential $V_{\text{ext}}(\mathbf{r}, t)$ is present, then in general $V_{\text{ext}}(\mathbf{r}, t) \neq V_{\text{ad},t}(\mathbf{r}, t)$.

Recall that within classical DFT we have

$$\mathbf{f}_{\text{ad}}(\mathbf{r}, t, [\rho]) = -\nabla \frac{\delta F_{\text{exc}}[\rho_{\text{ad}}]}{\delta \rho_{\text{ad},t}(\mathbf{r})} \Big|_{\rho_{\text{ad},t}(\mathbf{r})=\rho(\mathbf{r},t)}. \quad (287)$$

Considering the force balance (281), we can conclude that the external force field only appears explicitly; the internal force field is independent thereof via the kinematic functional dependence. It is hence instructive to rearrange Eq. (281) as

$$\mathbf{f}_{\text{ext}}(\mathbf{r}, t) = \gamma \mathbf{v}(\mathbf{r}, t) + k_B T \nabla \ln \rho(\mathbf{r}, t) - \mathbf{f}_{\text{int}}(\mathbf{r}, t, [\rho, \mathbf{v}]), \quad (288)$$

which in this form constitutes a balance relationship of external forces (left-hand side) with friction due to the flow, ideal diffusive forces, and internal forces (three contributions on the right-hand side). Notably, the right-hand side of Eq. (288) is independent of $\mathbf{f}_{\text{ext}}(\mathbf{r}, t)$. Hence, if the kinematics, i.e., the history of $\rho(\mathbf{r}, t)$ and $\mathbf{v}(\mathbf{r}, t)$, are known, then one can determine the external force field $\mathbf{f}_{\text{ext}}(\mathbf{r}, t)$ that generates the dynamics. This implies the following functional map:

$$\text{kinematics} \rightarrow \text{external force field}, \quad (289)$$

$$\{\rho(\mathbf{r}, t), \mathbf{v}(\mathbf{r}, t)\} \rightarrow \mathbf{f}_{\text{ext}}(\mathbf{r}, t). \quad (290)$$

This nonequilibrium map can be viewed as a generalization of the following equilibrium Hohenberg-Kohn-Mermin-Evans map:

$$\rho(\mathbf{r}) \rightarrow V_{\text{ext}}(\mathbf{r}). \quad (291)$$

Given an initial equilibrium state at $t = 0$, one can prescribe target kinematic fields $\rho(\mathbf{r}, t > 0)$ and $\mathbf{v}(\mathbf{r}, t > 0)$ (which satisfy physical constraints such as the continuity equation) and determine the external force field $\mathbf{f}_{\text{ext}}(\mathbf{r}, t)$ that generates the prescribed dynamics. This requires access to the kinematic functional dependence of the internal force field, as realized in the custom flow method by de las Heras, Renner, and Schmidt (2019), which is described in Sec. IV.F.

Two simple special cases are worth spelling out.

(i) For ideal motion $P_t^{\text{exc}}[\rho, \mathbf{J}] = \dot{F}_{\text{exc}}[\rho] = 0$, and hence

$$\dot{\rho}(\mathbf{r}, t) = \nabla \cdot \gamma^{-1} \rho(\mathbf{r}, t) [k_B T \nabla \ln \rho(\mathbf{r}, t) - \mathbf{f}_{\text{ext}}(\mathbf{r}, t)] \quad (292)$$

$$= D \nabla^2 \rho(\mathbf{r}, t) - \gamma^{-1} \nabla \cdot \rho(\mathbf{r}, t) \mathbf{f}_{\text{ext}}(\mathbf{r}, t), \quad (293)$$

which is the free drift-diffusion equation with diffusion constant $D = k_B T / \gamma$.

(ii) Neglecting only the superadiabatic excess contribution $P_t^{\text{exc}}[\rho, \mathbf{J}] = 0$ leads to

$$\gamma \mathbf{v}(\mathbf{r}, t) = -k_B T \nabla \ln \rho(\mathbf{r}, t) - \nabla \frac{\delta F_{\text{exc}}[\rho]}{\delta \rho(\mathbf{r}, t)} + \mathbf{f}_{\text{ext}}(\mathbf{r}, t), \quad (294)$$

which is the equation of motion (257) according to DDFT by Evans (1979) and Marconi and Tarazona (1999).

We return to the description of the general framework and address molecular dynamics next. The kinematic fields are $\rho(\mathbf{r}, t)$, $\mathbf{J}(\mathbf{r}, t)$, and $\dot{\mathbf{J}}(\mathbf{r}, t)$.⁹ Consider Hamiltonians that contain an internal interaction potential $u(\mathbf{r}^N)$ and an external potential $V_{\text{ext}}(\mathbf{r}, t)$ and the contributions from a magnetic field $\mathbf{B}(\mathbf{r}, t) = \nabla \times \mathbf{A}(\mathbf{r}, t)$. The power rate functional satisfies the minimization principle

$$\left. \frac{\delta G_t[\rho, \mathbf{J}, \dot{\mathbf{J}}]}{\delta \dot{\mathbf{J}}(\mathbf{r}, t)} \right|_{\rho, \mathbf{J}, \dot{\mathbf{J}} = \dot{\mathbf{J}}_0} = 0 \quad (\text{min}). \quad (295)$$

The minimum is attained at the physically realized form of the acceleration density $\dot{\mathbf{J}}_0(\mathbf{r}, t)$.

The total power rate (with units $\text{J/s}^2 = \text{W/s}$) splits into the following intrinsic and external contributions:

$$G_t[\rho, \mathbf{J}, \dot{\mathbf{J}}] = G_t^{\text{int}}[\rho, \mathbf{J}, \dot{\mathbf{J}}] - \int d\mathbf{r} \dot{\mathbf{J}}(\mathbf{r}, t) \cdot [q\mathbf{v}(\mathbf{r}, t) \times \mathbf{B}(\mathbf{r}, t) - q\dot{\mathbf{A}}(\mathbf{r}, t) - \nabla V_{\text{ext}}(\mathbf{r}, t)], \quad (296)$$

where the intrinsic contribution $G_t^{\text{int}}[\rho, \mathbf{J}, \dot{\mathbf{J}}]$ depends solely on the interparticle interaction potential. An insertion into the minimization principle (295) gives an Euler-Lagrange equation of the form

$$\frac{\delta G_t^{\text{int}}[\rho, \mathbf{J}, \dot{\mathbf{J}}]}{\delta \dot{\mathbf{J}}(\mathbf{r}, t)} = q\mathbf{v}(\mathbf{r}, t) \times \mathbf{B}(\mathbf{r}, t) - q\dot{\mathbf{A}}(\mathbf{r}, t) - \nabla V_{\text{ext}}(\mathbf{r}, t). \quad (297)$$

We split the intrinsic contribution into an approximate ideal and an excess contribution

$$G_t^{\text{int}}[\rho, \mathbf{J}, \dot{\mathbf{J}}] = G_t^{\text{id}}[\rho, \mathbf{J}, \dot{\mathbf{J}}] + G_t^{\text{exc}}[\rho, \mathbf{J}, \dot{\mathbf{J}}], \quad (298)$$

where the approximate ideal contribution is given by

$$G_t^{\text{id}}[\rho, \mathbf{J}, \dot{\mathbf{J}}] = \int d\mathbf{r} \frac{\dot{\mathbf{J}}(\mathbf{r}, t)}{\rho(\mathbf{r}, t)} \cdot \left(\frac{m\dot{\mathbf{J}}(\mathbf{r}, t)}{2} - \nabla \cdot \boldsymbol{\tau}^{\text{id}}(\mathbf{r}, t) \right), \quad (299)$$

$$\boldsymbol{\tau}^{\text{id}}(\mathbf{r}, t) = -m \frac{\mathbf{J}(\mathbf{r}, t)\dot{\mathbf{J}}(\mathbf{r}, t)}{\rho(\mathbf{r}, t)}, \quad (300)$$

⁹An alternative and equivalent set of kinematic fields is $\rho(\mathbf{r}, t)$, $\mathbf{v}(\mathbf{r}, t)$, and $\mathbf{a}(\mathbf{r}, t)$, where $\mathbf{a}(\mathbf{r}, t)$ is the local acceleration field. Rather than the bare microscopic acceleration $\mathbf{a}(\mathbf{r}, t) = \dot{\mathbf{J}}(\mathbf{r}, t)/\rho(\mathbf{r}, t)$ Renner, Schmidt, and de las Heras (2022) recently argued that for constructing approximations it is advantageous to remove transport effects and instead use $\mathbf{a}(\mathbf{r}, t) = \partial \mathbf{v}(\mathbf{r}, t)/\partial t = \dot{\mathbf{J}}(\mathbf{r}, t)/\rho(\mathbf{r}, t) + \mathbf{v}(\mathbf{r}, t)[\nabla \cdot \mathbf{J}(\mathbf{r}, t)]/\rho(\mathbf{r}, t)$.

with $\boldsymbol{\tau}^{\text{id}}(\mathbf{r}, t)$ a factorized form of the kinetic stress tensor. Calculating the derivative

$$\frac{\delta G_t^{\text{id}}[\rho, \mathbf{J}, \dot{\mathbf{J}}]}{\delta \dot{\mathbf{J}}(\mathbf{r}, t)} = m \frac{\dot{\mathbf{J}}(\mathbf{r}, t)}{\rho(\mathbf{r}, t)} - \frac{\nabla \cdot \boldsymbol{\tau}^{\text{id}}(\mathbf{r}, t)}{\rho(\mathbf{r}, t)} \quad (301)$$

and inserting Eq. (298) into the Euler-Lagrange equation (297) yield upon rearranging the force balance relationship

$$\frac{m\dot{\mathbf{J}}(\mathbf{r}, t)}{\rho(\mathbf{r}, t)} = \frac{\nabla \cdot \boldsymbol{\tau}^{\text{id}}(\mathbf{r}, t)}{\rho(\mathbf{r}, t)} - \frac{\delta G_t^{\text{exc}}[\rho, \mathbf{J}, \dot{\mathbf{J}}]}{\delta \dot{\mathbf{J}}(\mathbf{r}, t)} - \nabla V_{\text{ext}}(\mathbf{r}, t), \quad (302)$$

where we have omitted the external magnetic contributions for simplicity.

We also know the exact force balance directly from the many-body dynamics (262) as

$$\frac{m\dot{\mathbf{J}}(\mathbf{r}, t)}{\rho(\mathbf{r}, t)} = \frac{\nabla \cdot \boldsymbol{\tau}(\mathbf{r}, t)}{\rho(\mathbf{r}, t)} + \mathbf{f}_{\text{int}}(\mathbf{r}, t) - \nabla V_{\text{ext}}(\mathbf{r}, t), \quad (303)$$

where the internal force field is the phase space average

$$\mathbf{f}_{\text{int}}(\mathbf{r}, t) = - \left\langle \sum_i \delta(\mathbf{r} - \mathbf{r}_i) \nabla_i u(\mathbf{r}^N) \right\rangle / \rho(\mathbf{r}, t). \quad (304)$$

The kinetic stress is given by

$$\boldsymbol{\tau}(\mathbf{r}, t) = - \frac{1}{m} \left\langle \sum_i \delta(\mathbf{r} - \mathbf{r}_i) \mathbf{p}_i \mathbf{p}_i \right\rangle. \quad (305)$$

By comparing Eqs. (302) and (303) we can identify

$$- \frac{\delta G_t^{\text{exc}}[\rho, \mathbf{J}, \dot{\mathbf{J}}]}{\delta \dot{\mathbf{J}}(\mathbf{r}, t)} = \mathbf{f}_{\text{int}}(\mathbf{r}, t) + \frac{\nabla \cdot [\boldsymbol{\tau}(\mathbf{r}, t) - \boldsymbol{\tau}^{\text{id}}(\mathbf{r}, t)]}{\rho(\mathbf{r}, t)}. \quad (306)$$

Hence, $G_t^{\text{exc}}[\rho, \mathbf{J}, \dot{\mathbf{J}}]$ is a functional generator of the nontrivial part of the transport plus the internal force field. [Here the functional derivative is also taken while $\rho(\mathbf{r}, t)$ and $\mathbf{J}(\mathbf{r}, t)$ are kept fixed, and the physical field values need to be inserted after the derivative has been taken.]

Together with the continuity equations, the Euler-Lagrange equation forms a closed set of equations on the one-body level. The quantum version is similar in structure but contains important additional wave contributions, as described at the end of Sec. IV.B.

B. Microscopic foundation

1. Power functional for molecular dynamics

We return to classical Hamiltonian dynamics and describe the key concepts of the many-body functional description that underpins the power functional. For the full presentation, see Schmidt (2018).

The microscopic many-body power rate functional is defined as

$$\mathcal{G}_t = \int d\mathbf{r}^N d\boldsymbol{\pi}^N \sum_i \frac{(\mathbf{f}_i - m\mathbf{a}_i)^2}{2m} \Psi(\mathbf{r}^N, \boldsymbol{\pi}^N, t) - \int d\mathbf{r} \frac{m}{2\langle \hat{\rho} \rangle} \left\langle \frac{d\dot{\mathbf{J}}}{dt} \right\rangle^2. \quad (307)$$

In Eq. (307) the particle-labeled acceleration fields $\mathbf{a}_i(\mathbf{r}^N, \boldsymbol{\pi}^N, t)$ are trial variational fields on phase space; we use the notation $\mathbf{a}^N = \mathbf{a}_1, \dots, \mathbf{a}_N$ in the following. At the physical dynamics $m\mathbf{a}_i = \mathbf{f}_i$, where \mathbf{f}_i is the force on particle i . Furthermore, \mathcal{G}_t is an instantaneous functional at time t (time-slice derivatives need to be taken). The units of \mathcal{G}_t are power per time, i.e., ‘‘power rate,’’ which can be seen by observing that $[\int d\mathbf{r}^N d\boldsymbol{\pi}^N \Psi] = 1$ and $[\mathbf{f}_i^2/2m] = [\mathbf{f} \cdot \mathbf{a}_i] = \text{Nm/s}^2 = \text{J/s}^2 = \text{W/s}$. The second term in Eq. (307) is independent of the \mathbf{a}_i .

Minimizing \mathcal{G}_t at a fixed time with respect to the \mathbf{a}^N implies that

$$\frac{\delta \mathcal{G}_t}{\delta \mathbf{a}_i(\mathbf{r}^N, \boldsymbol{\pi}^N, t)} = 0 \quad (\text{min}). \quad (308)$$

Explicitly carrying out the derivative yields

$$\frac{\delta \mathcal{G}_t}{\delta \mathbf{a}_i(\mathbf{r}^N, \boldsymbol{\pi}^N, t)} = [-\mathbf{f}_i(\mathbf{r}^N, \boldsymbol{\pi}^N, t) + m\mathbf{a}_i(\mathbf{r}^N, \boldsymbol{\pi}^N, t)]\Psi. \quad (309)$$

Hence, \mathcal{G}_t acts like a Gibbs-Appell-Gauss function (see Appendix A.3) in that it uniquely determines the physical dynamics by minimization. However, beyond this role it is also a generator of dynamical correlators via

$$\frac{\delta \mathcal{G}_t}{\delta q \dot{\mathbf{A}}(\mathbf{r}', t)} = \dot{\mathbf{J}}(\mathbf{r}', t), \quad (310)$$

where the derivative acts on both the explicit appearance of \mathbf{f}_i and the ‘‘hidden’’ appearance in $d\dot{\mathbf{J}}/dt$ in Eq. (307).

To connect the many-body variational principle with the one-body level, the following constrained search is performed:

$$G_t[\rho, \mathbf{J}, \dot{\mathbf{J}}] = \min_{\mathbf{a}^N \rightarrow \rho, \mathbf{J}, \dot{\mathbf{J}}} \mathcal{G}_t. \quad (311)$$

Hence, $G_t[\rho, \mathbf{J}, \dot{\mathbf{J}}]$ is a one-body functional that is minimized by $\dot{\mathbf{J}}(\mathbf{r}, t)$ at the physical dynamics; see Eq. (295). We recall the Levy method’s use in the classical equilibrium density functional (Sec. III.E) and refer the interested reader to Schmidt (2018) for the details of the present dynamical treatment.

2. Power functional for Brownian dynamics

We return to overdamped Brownian many-body dynamics, as described in Sec. II.C, and present the key ideas of Schmidt and Brader (2013). They introduce trial velocity fields $\tilde{\mathbf{v}}_i(\mathbf{r}^N, t)$, $i = 1, \dots, N$, on configuration space and define the free power as an operator (phase space function) as

$$\hat{\mathcal{R}}_t = \sum_i \left(\frac{\gamma}{2} \tilde{\mathbf{v}}_i(\mathbf{r}^N, t) - \mathbf{f}_i^{\text{tot}}(\mathbf{r}^N, t) \right) \cdot \tilde{\mathbf{v}}_i(\mathbf{r}^N, t) + \sum_i \dot{V}_{\text{ext}}(\mathbf{r}_i, t). \quad (312)$$

For Brownian motion the total force on particle i consists of deterministic and diffusive contributions and is given by

$$\mathbf{f}_i^{\text{tot}} = -\nabla_i u(\mathbf{r}^N) - \nabla_i V_{\text{ext}}(\mathbf{r}_i, t) + \mathbf{f}_{\text{nc}}(\mathbf{r}_i, t) - k_B T \nabla_i \ln \Psi, \quad (313)$$

where $\mathbf{f}_{\text{nc}}(\mathbf{r}, t)$ is a nonconservative external force field. Averaging over configuration space creates the following functional dependence on the trial velocities:

$$\mathcal{R}_t = \int d\mathbf{r}^N \Psi(\mathbf{r}^N, t) \hat{\mathcal{R}}_t(\mathbf{r}^N, \tilde{\mathbf{v}}^N, t). \quad (314)$$

Owing to its quadratic structure, \mathcal{R}_t is minimized by the true velocity

$$\frac{\delta \mathcal{R}_t}{\delta \tilde{\mathbf{v}}_i(\mathbf{r}^N, t)} = 0 \quad (\text{min}), \quad (315)$$

and hence at the minimum $\tilde{\mathbf{v}}_i = \mathbf{v}_i \equiv \gamma^{-1} \mathbf{f}_i^{\text{tot}}$; i.e., the true dynamics is recovered. This can be seen by calculating the functional (time-slice) derivative as follows:

$$\frac{\delta \mathcal{R}_t}{\delta \tilde{\mathbf{v}}_i} = (\gamma \tilde{\mathbf{v}}_i - \mathbf{f}_i^{\text{tot}})\Psi, \quad (316)$$

where arguments \mathbf{r}^N, t have been omitted for clarity. As $\Psi(\mathbf{r}^N, t) \neq 0$ in general, the proposition follows.

A constrained search for the minimum yields the one-body power functional

$$R_t[\rho, \mathbf{J}] = \min_{\tilde{\mathbf{v}}^N \rightarrow \rho, \mathbf{J}} \mathcal{R}_t. \quad (317)$$

See Schmidt and Brader (2013) for the full treatment, as well as the relationship to the time derivative of the many-body Mermin functional; see also Chan and Finken (2005) and Lutsko and Oettel (2021). We describe in Sec. IV.C progress in formulating concrete approximations for the power functional.

3. Quantum power functional theory

The quantum case is somewhat similar in mathematical structure to the previously described classical Hamiltonian power functional treatment. The additional quantum effects both arise in explicit, \hbar -dependent terms and affect the structure of the nontrivial parts of the functional generator. We follow Schmidt (2015).

We introduce complex-valued trial acceleration fields $\mathbf{a}^N \equiv \mathbf{a}_1(\mathbf{r}^N, t), \dots, \mathbf{a}_N(\mathbf{r}^N, t)$ and define a many-body power rate functional

$$\mathcal{G}_t = \int d\mathbf{r}^N \sum_i \frac{|(\hat{\mathbf{f}}_i - m\mathbf{a}_i)\Psi|^2}{2m} - \int d\mathbf{r} \frac{m}{2\langle \hat{n} \rangle} \left\langle \frac{d\dot{\mathbf{J}}}{dt} \right\rangle^2, \quad (318)$$

where in the second term the trial fields \mathbf{a}^N do not enter. Because of the quadratic structure of \mathcal{G}_t , at the minimum the modulus squared expression vanishes, and hence

$$m\mathbf{a}_i(\mathbf{r}^N, t)\Psi(\mathbf{r}^N, t) = \hat{\mathbf{f}}_i(\mathbf{r}^N, t)\Psi(\mathbf{r}^N, t) \quad (319)$$

for the specific set \mathbf{a}^N at the minimum. (This fixes the dynamics if Eq. (319) is known at all times.) Hence, the time-slice derivative satisfies

$$\frac{\delta \mathcal{G}_t}{\delta \mathbf{a}_i(\mathbf{r}^N, t)} = 0 \quad (\text{min}). \quad (320)$$

Furthermore, \mathcal{G}_t is a one-body generator via

$$\frac{\delta \mathcal{G}_t}{\delta q \dot{\mathbf{A}}(\mathbf{r}, t)} = \dot{\mathbf{J}}(\mathbf{r}, t). \quad (321)$$

We introduce a one-body constraint

$$\dot{\mathbf{J}}(\mathbf{r}, t) = \left\langle \sum_i \left(\frac{\mathbf{a}_i + \mathbf{a}_i^*}{2} \delta_i + \frac{\nabla \cdot \hat{\boldsymbol{\tau}}_i}{m} + \frac{\hbar^2}{4m^2} \nabla \nabla^2 \hat{n}_i \right) \right\rangle, \quad (322)$$

where the left-hand side constitutes a prescribed target and \mathbf{a}^N are trial fields in position representation. The constrained search is

$$G_t[n, \mathbf{J}, \dot{\mathbf{J}}] = \min_{\mathbf{a}^N \rightarrow n, \mathbf{J}, \dot{\mathbf{J}}} \mathcal{G}_t. \quad (323)$$

The true time evolution is still at the global minimum, and hence

$$\left. \frac{\delta G_t[n, \mathbf{J}, \dot{\mathbf{J}}]}{\delta \dot{\mathbf{J}}(\mathbf{r}, t)} \right|_{n, \mathbf{J}} = 0 \quad (\text{min}), \quad (324)$$

where the derivative is functional in position and at fixed time (time slice). We split the total power rate functional into intrinsic and external contributions according to

$$G_t[n, \mathbf{J}, \dot{\mathbf{J}}] = G_t^{\text{int}}[n, \mathbf{J}, \dot{\mathbf{J}}] - \int d\mathbf{r} \dot{\mathbf{J}} \cdot \left(\frac{q \mathbf{J} \times \mathbf{B}}{n} - q \dot{\mathbf{A}} - \nabla V_{\text{ext}} \right), \quad (325)$$

where the intrinsic contribution $G_t^{\text{int}}[n, \mathbf{J}, \dot{\mathbf{J}}]$ is independent of the external forces; we have omitted the arguments \mathbf{r} and t for compactness of notation. From the minimization condition (324) one obtains

$$\frac{\delta G_t^{\text{int}}[n, \mathbf{J}, \dot{\mathbf{J}}]}{\delta \dot{\mathbf{J}}} = \frac{q \mathbf{J} \times \mathbf{B}}{n} - q \dot{\mathbf{A}} - \nabla V_{\text{ext}}, \quad (326)$$

where the left-hand side is intrinsic and the right-hand side constitutes the external force field. We split further into ideal and excess contributions according to

$$G_t^{\text{int}}[n, \mathbf{J}, \dot{\mathbf{J}}] = G_t^{\text{id}}[n, \mathbf{J}, \dot{\mathbf{J}}] + G_t^{\text{exc}}[n, \mathbf{J}, \dot{\mathbf{J}}], \quad (327)$$

where the ideal contribution (Brütting *et al.*, 2019) is

$$G_t^{\text{id}}[n, \mathbf{J}, \dot{\mathbf{J}}] = \int d\mathbf{r} \frac{\dot{\mathbf{J}}}{n} \cdot \left(\frac{m \dot{\mathbf{J}}}{2} - \nabla \cdot \boldsymbol{\tau}_{\text{id}} - \frac{\hbar^2}{4m} \nabla \nabla^2 n \right), \quad (328)$$

with the factorized dyadic form

$$\boldsymbol{\tau}_{\text{id}} = -m \frac{\mathbf{J} \mathbf{J}}{n} - \frac{\hbar^2}{4m} \frac{(\nabla n)(\nabla n)}{n}. \quad (329)$$

The term $G_t^{\text{exc}}[n, \mathbf{J}, \dot{\mathbf{J}}]$ in Eq. (327) contains effects due to internal interactions and possibly further transport terms. The derivative of the ideal term is

$$\left. \frac{\delta G_t^{\text{id}}[n, \mathbf{J}, \dot{\mathbf{J}}]}{\delta \dot{\mathbf{J}}} \right|_{n, \mathbf{J}} = m \frac{\dot{\mathbf{J}}}{n} - \frac{1}{n} \nabla \cdot \boldsymbol{\tau}_{\text{id}} - \frac{1}{n} \frac{\hbar^2}{4m} \nabla \nabla^2 n, \quad (330)$$

which we insert into the force balance equation (326). This gives the final equation of motion

$$m \dot{\mathbf{J}} = -n \frac{\delta G_t^{\text{exc}}[n, \mathbf{J}, \dot{\mathbf{J}}]}{\delta \dot{\mathbf{J}}} + \nabla \cdot \boldsymbol{\tau}_{\text{id}} + \frac{\hbar^2}{4m} \nabla \nabla^2 n + q \mathbf{J} \times \mathbf{B} - n(q \dot{\mathbf{A}} + \nabla V_{\text{ext}}). \quad (331)$$

Together with the continuity equation, Eq. (331) forms a closed dynamical theory on the one-body level. This is a formal (yet important) result, as G_t^{exc} is unknown in practice, as this would require solution of the coupled many-body dynamics under the action of arbitrary external fields $V_{\text{ext}}(\mathbf{r}, t)$ and $\mathbf{A}(\mathbf{r}, t)$. However, (i) approximations can be found (searched for) and (ii) the functional relationship $-(\delta G_t^{\text{exc}}/\delta \dot{\mathbf{J}})[n, \mathbf{J}, \dot{\mathbf{J}}]$ is established.

The connection to time-dependent DFT is via the ground state energy functional

$$E[n] = \min_{\Psi \rightarrow n} \langle \Psi | \hat{H} | \Psi \rangle - \int d\mathbf{r} n(\mathbf{r}, t) V_{\text{ext}}(\mathbf{r}, t). \quad (332)$$

In Eq. (332) $E[n]$ is the intrinsic (kinetic and internal interaction) contribution; often the interaction part is split further into Hartree, exchange, and correlation terms. The first and second time derivatives are

$$\frac{d}{dt} E[n] = \int d\mathbf{r} \dot{\mathbf{J}} \cdot \nabla \frac{\delta E[n]}{\delta n}, \quad (333)$$

$$\frac{d^2}{dt^2} E[n] = \int d\mathbf{r} \dot{\mathbf{J}} \cdot \nabla \frac{\delta E[n]}{\delta n} + \int d\mathbf{r} d\mathbf{r}' \dot{\mathbf{J}} \mathbf{J}' : \nabla \nabla' \frac{\delta^2 E[n]}{\delta n \delta n'}, \quad (334)$$

where $n' = n(\mathbf{r}', t)$ and $\mathbf{J}' = \mathbf{J}(\mathbf{r}', t)$. The corresponding force field is alternatively obtained via

$$-\left. \frac{\delta \dot{E}[n]}{\delta \dot{\mathbf{J}}(\mathbf{r}, t)} \right|_{n, \mathbf{J}} = -\left. \frac{\delta \dot{E}[n]}{\delta \mathbf{J}(\mathbf{r}, t)} \right|_n = -\nabla \frac{\delta E[n]}{\delta n(\mathbf{r}, t)}. \quad (335)$$

Splitting $G_t^{\text{exc}}[n, \mathbf{J}, \dot{\mathbf{J}}] = \dot{E}[n] + G_t^{\text{sup}}[n, \mathbf{J}, \dot{\mathbf{J}}]$ and insertion into the equation of motion yield

$$m \dot{\mathbf{J}} = -n \frac{\delta G_t^{\text{sup}}[n, \mathbf{J}, \dot{\mathbf{J}}]}{\delta \dot{\mathbf{J}}} - n \nabla \frac{\delta E[n]}{\delta n} + \nabla \cdot \boldsymbol{\tau}_{\text{id}} + \frac{\hbar^2}{4m} \nabla \nabla^2 n + q \mathbf{J} \times \mathbf{B} - n(q \dot{\mathbf{A}} + \nabla V_{\text{ext}}), \quad (336)$$

where $G_t^{\text{sup}}[n, \mathbf{J}, \dot{\mathbf{J}}]$ describes nonequilibrium effects beyond the adiabatic ground state; see Brütting *et al.* (2019) for an explicit model calculation.

C. Superadiabatic free power approximations

Recall that the one-body equation of motion (280) for overdamped BD, as formulated by Schmidt and Brader (2013), taken together with the continuity equation, provides a formally exact description of the dynamics provided that the internal interaction contributions $F_{\text{exc}}[\rho]$ and $P_t^{\text{exc}}[\rho, \mathbf{J}]$ are known. The equation of motion is closed; i.e., no further higher-order correlators are required. The adiabatic force field stems from the equilibrium excess free energy density functional $F_{\text{exc}}[\rho]$; the superadiabatic force field is generated from the superadiabatic free power functional $P_t^{\text{exc}}[\rho, \mathbf{J}]$. Both functionals depend only on the internal interaction potential $u(\mathbf{r}^N)$, and they are unknown in practice. $F_{\text{exc}}[\rho]$ is, however, a well-studied object (although many mysteries remain).

What can we say about $P_t^{\text{exc}}[\rho, \mathbf{J}]$? It certainly needs to provide mechanisms to slow down the dynamics in typical situations, as DDFT (where $P_t^{\text{exc}}[\rho, \mathbf{J}] \equiv 0$) is often too fast. The superadiabatic free power functional hence should both describe the dissipative, irreversible effects and provide a genuine structure-forming mechanism that occurs in non-equilibrium. Reversible effects are already accounted for by the adiabatic contribution (via the total time derivative $\dot{F}[\rho]$).

A series of studies have demonstrated that the superadiabatic free power functional $P_t^{\text{exc}}[\rho, \mathbf{J}]$ is indeed amenable to analytical approximations (de las Heras and Schmidt, 2018a, 2020; Stuhlmüller *et al.*, 2018; Treffenstädt and Schmidt, 2020, 2021). de las Heras and Schmidt (2018a) showed that it is possible to use the local velocity gradient instead of the current distribution as the relevant kinematic variable; their central ideas are presented later. By considering higher than quadratic contributions to the power functional, the velocity gradient concept was shown by Stuhlmüller *et al.* (2018) to also describe structural nonequilibrium forces, i.e., nonequilibrium force contributions that sustain density gradients. This approach was fully developed by de las Heras and Schmidt (2020) in their splitting of the force balance into flow and structural components. Treffenstädt and Schmidt (2020) demonstrated how to describe the spatially and temporally nonlocal nature of viscous forces. Treffenstädt and Schmidt (2021) applied this approach to the dynamical two-body structure of the bulk hard sphere fluid, i.e., its van Hove function.

Microscopic stress tensor.—Let $\sigma(\mathbf{r}, t)$ be the total interaction stress (we do not need to consider the kinetic stress in overdamped BD). We then have

$$\gamma \mathbf{J}(\mathbf{r}, t) = \nabla \cdot \sigma(\mathbf{r}, t). \quad (337)$$

To be fully explicit, the right-hand side of Eq. (337) expresses the divergence of a tensor field with components $(\nabla \cdot \sigma)_\beta = \sum_{\alpha=1}^d \partial \sigma_{\alpha\beta} / \partial r_\alpha$, where $\alpha, \beta = 1, \dots, d$ labels the Cartesian components and r_α is the α th component of \mathbf{r} . Note that the interaction stress differs from the kinetic stress $\tau(\mathbf{r}, t)$ described in Sec. II.B in the context of molecular dynamics. Rather than the transport mechanism that $\tau(\mathbf{r}, t)$ provides, the interaction stress $\sigma(\mathbf{r}, t)$ arises from the forces that act in the system; for detailed background information, see the accounts of Balucani and Zoppi (1994) and (in a polymer context) Bird, Armstrong, and Hassager (1987).

Strongly influenced by the formulation of mode-coupling theory on the level of the stress tensor and the strain rate tensor [see the review by Brader (2010)], de las Heras and Schmidt (2018a) showed that

$$\frac{\delta \mathcal{R}_t}{\delta \nabla \mathbf{v}_{\text{sol}}(\mathbf{r}, t)} = \sigma(\mathbf{r}, t), \quad (338)$$

where $\gamma \mathbf{v}_{\text{sol}}(\mathbf{r}, t)$ is the external force field that is induced by solvent flow. Hence, building the divergence yields

$$\nabla \cdot \frac{\delta \mathcal{R}_t}{\delta \nabla \mathbf{v}_{\text{sol}}(\mathbf{r}, t)} = \nabla \cdot \sigma(\mathbf{r}, t) = \gamma \mathbf{J}(\mathbf{r}, t), \quad (339)$$

where we have used Eq. (337). We choose an inverse operator to ∇ of “electrostatic form” defined as operating on some test function $f(\mathbf{r})$ via the convolution

$$\nabla^{-1} f(\mathbf{r}) = \int d\mathbf{r}' \frac{\mathbf{r} - \mathbf{r}'}{4\pi|\mathbf{r} - \mathbf{r}'|^3} f(\mathbf{r}'). \quad (340)$$

The convolution kernel is a radial, inverse square distance vector field (equivalent to the electric field of a point charge). The application of ∇^{-1} creates a vectorial dependence via the distance vector $\mathbf{r} - \mathbf{r}'$ on the right-hand side of Eq. (340). Note that $\nabla \cdot \nabla^{-1} f(\mathbf{r}) = f(\mathbf{r})$, which can readily be seen by observing that $\delta(\mathbf{r}) = \nabla \cdot \mathbf{r} / 4\pi|\mathbf{r}|^3$.

A well-known alternative to Eq. (340) is the Irving-Kirkwood form of the stress tensor as it applies to pairwise forces (Irving and Kirkwood, 1950). It is important to realize that the stress tensor is a nonunique quantity (Schofield and Henderson, 1982), as only the corresponding force density, i.e., the divergence of the stress tensor, is an observable quantity; see Eq. (337). The presence of the derivative allows significant freedom in the particular choice of definition of the stress tensor.

Using the electrostatic form, we obtain the specific expression

$$\sigma(\mathbf{r}, t) = \int d\mathbf{r}^N \Psi(\mathbf{r}^N, t) \sum_i \frac{(\mathbf{r} - \mathbf{r}_i) \mathbf{f}_i^{\text{tot}}(\mathbf{r}^N, t)}{4\pi|\mathbf{r} - \mathbf{r}_i|^3}, \quad (341)$$

where the numerator is a dyadic product of relative distance and the force on particle i . Further significance for the form (341) comes from considering the integrated stress as follows:

$$\Sigma(t) = \int d\mathbf{r} \sigma(\mathbf{r}, t) \quad (342)$$

$$= -\frac{1}{3} \int d\mathbf{r}^N \Psi(\mathbf{r}^N, t) \sum_i \mathbf{r}_i \mathbf{f}_i^{\text{tot}}(\mathbf{r}^N, t). \quad (343)$$

Hence, the averaged Clausius virial is then simply $-\text{tr} \Sigma(t)$.

One-body level.—We start by using the splitting of the power functional into ideal dissipative, superadiabatic, reversible, and external contributions, $R_t = P_t^{\text{id}} + P_t^{\text{exc}} + \dot{F} - X_t$. Here the external power is

$$X_t = \int d\mathbf{r}[\mathbf{J}(\mathbf{r}, t) \cdot \mathbf{f}_{\text{ext}}(\mathbf{r}, t) - \rho(\mathbf{r}, t)\dot{V}_{\text{ext}}(\mathbf{r}, t)] \quad (344)$$

$$= - \int d\mathbf{r}[\boldsymbol{\sigma}_{\text{ext}}(\mathbf{r}, t) : \nabla \mathbf{v}(\mathbf{r}, t) + \rho(\mathbf{r}, t)\dot{V}_{\text{ext}}(\mathbf{r}, t)], \quad (345)$$

where we have introduced the external stress tensor field

$$\boldsymbol{\sigma}_{\text{ext}}(\mathbf{r}, t) = \nabla^{-1} \rho(\mathbf{r}, t) \mathbf{f}_{\text{ext}}(\mathbf{r}, t). \quad (346)$$

The colon in Eq. (345) indicates a double tensor contraction; for two matrices \mathbf{A} and \mathbf{B} this is defined as $\mathbf{A}:\mathbf{B} = \sum_{ij} A_{ij}B_{ji} = \text{tr} \mathbf{A} \cdot \mathbf{B}$.

Hence, we can generate the velocity gradient tensor field via

$$\frac{\delta R_t}{\delta \boldsymbol{\sigma}_{\text{ext}}(\mathbf{r}, t)} = \nabla \mathbf{v}(\mathbf{r}, t). \quad (347)$$

We can express the ideal dissipation and the adiabatic power contributions via

$$P_t^{\text{id}}[\rho, \mathbf{v}] = -\frac{1}{2} \int d\mathbf{r} \boldsymbol{\sigma}(\mathbf{r}, t) : \nabla \mathbf{v}(\mathbf{r}, t), \quad (348)$$

$$\dot{F}[\rho] = \int d\mathbf{r} \boldsymbol{\sigma}_{\text{ad}}(\mathbf{r}, t) : \nabla \mathbf{v}(\mathbf{r}, t), \quad (349)$$

where $\boldsymbol{\sigma}(\mathbf{r}, t)$, as before, is the total stress distribution; see Eq. (337). The adiabatic stress distribution is

$$\boldsymbol{\sigma}_{\text{ad}}(\mathbf{r}, t) = -\nabla^{-1} \rho(\mathbf{r}, t) \nabla \frac{\delta F[\rho]}{\delta \rho(\mathbf{r}, t)}. \quad (350)$$

We can now reformulate the variational principle $\delta R_t / \delta \mathbf{J} = 0$ in tensor form as follows:

$$\nabla \cdot \frac{\delta R_t}{\delta \nabla \mathbf{v}(\mathbf{r}, t)} \Big|_{\rho} = 0 \quad (\text{min}) \quad (351)$$

at the physical dynamics. An equivalent form is obtained by integration as follows:

$$\frac{\delta R_t}{\delta \nabla \mathbf{v}(\mathbf{r}, t)} \Big|_{\rho} = \boldsymbol{\sigma}_{\text{stat}}(\mathbf{r}, t), \quad (352)$$

where $\boldsymbol{\sigma}_{\text{stat}}(\mathbf{r}, t)$ is a static (artificial) stress with vanishing divergence, $\nabla \cdot \boldsymbol{\sigma}_{\text{stat}} = 0$.

To make this framework more explicit, first consider

$$\frac{\delta P_t^{\text{id}}}{\delta \nabla \mathbf{v}(\mathbf{r}, t)} = -\boldsymbol{\sigma}(\mathbf{r}, t). \quad (353)$$

We can now collect all stress tensor contributions $\boldsymbol{\sigma} = \boldsymbol{\sigma}_{\text{ad}} + \boldsymbol{\sigma}_{\text{sup}} + \boldsymbol{\sigma}_{\text{ext}} + \boldsymbol{\sigma}_{\text{stat}}$, where the superadiabatic stress tensor distribution is

$$\boldsymbol{\sigma}_{\text{sup}}(\mathbf{r}, t) = \nabla^{-1} \mathbf{F}_{\text{sup}}(\mathbf{r}, t) \quad (354)$$

$$= -\nabla^{-1} \rho(\mathbf{r}, t) \frac{\delta P_t^{\text{exc}}}{\delta \mathbf{J}(\mathbf{r}, t)} \Big|_{\rho} \quad (355)$$

$$\equiv \frac{\delta P_t^{\text{exc}}}{\delta \nabla \mathbf{v}(\mathbf{r}, t)} \Big|_{\rho}. \quad (356)$$

Hence, we have alternative forms of dependence on $\rho(\mathbf{r}, t)$ and on $\mathbf{J}(\mathbf{r}, t)$, $\mathbf{v}(\mathbf{r}, t)$, or $\nabla \mathbf{v}(\mathbf{r}, t)$, and hence $P_t^{\text{exc}}[\rho, \mathbf{J}] \equiv P_t^{\text{exc}}[\rho, \mathbf{v}] \equiv P_t^{\text{exc}}[\rho, \nabla \mathbf{v}]$. In particular, the velocity gradient form is useful as a starting point for introducing approximations, as this ensures consistency with spatial translational invariance according to Noether's theorem; see [Hermann and Schmidt \(2021\)](#).

The most general bilinear form (assuming the existence of a power series) is

$$P_t^{\text{exc}}[\rho, \mathbf{v}] = k_B T \int d\mathbf{r} \int d\mathbf{r}' \int_0^t dt' \rho(\mathbf{r}, t) \nabla \mathbf{v}(\mathbf{r}, t) : \mathbf{M}(\mathbf{r} - \mathbf{r}', t - t') : \nabla \mathbf{v}(\mathbf{r}', t') \rho(\mathbf{r}', t'). \quad (357)$$

Note that terms linear in $\nabla \mathbf{v}(\mathbf{r}, t)$ are already accounted for in the adiabatic term, and also that local contributions are contained in the ideal dissipation functional. The kernel $\mathbf{M}(\mathbf{r} - \mathbf{r}', t - t')$ is a dimensionless fourth-rank tensor that depends on the internal interaction potential $u(\mathbf{r}^N)$. We can approximate further using a spatially local and Markovian form. Owing to rotational symmetry, this is

$$P_t^{\text{exc}}[\rho, \mathbf{v}] = \frac{1}{2} \int d\mathbf{r} \rho [n_{\text{rot}} (\nabla \times \mathbf{v})^2 + n_{\text{div}} (\nabla \cdot \mathbf{v})^2], \quad (358)$$

where the constants n_{rot} and n_{div} possess units of energy \times time. The dynamic shear viscosity is $\eta = \rho n_{\text{rot}}$ and the bulk (or volume) viscosity is $\zeta = \rho n_{\text{div}}$. For cases where $\rho = \text{const}$ the resulting superadiabatic force density is

$$\mathbf{F}_{\text{sup}}(\mathbf{r}, t) = -\frac{\delta P_t^{\text{exc}}[\rho, \mathbf{v}]}{\delta \mathbf{v}(\mathbf{r}, t)} \quad (359)$$

$$= \eta [\nabla^2 \mathbf{v}(\mathbf{r}, t) - \nabla \nabla \cdot \mathbf{v}(\mathbf{r}, t)] + \zeta \nabla \nabla \cdot \mathbf{v}(\mathbf{r}, t), \quad (360)$$

which is identical to the Stokes form of hydrodynamic friction.

Higher-order terms.—Consider only rotational shear components and a spatially local form ([Stuhlmüller et al., 2018](#))

$$P_t^{\text{exc}}[\rho, \mathbf{v}] = \int d\mathbf{r} \left[\int_0^t dt' n_{t't'} (\nabla \times \mathbf{v}) \cdot (\nabla \times \mathbf{v}') - \int_0^t dt' \int_0^t dt'' m_{t't''} (\nabla \cdot \mathbf{v}) (\nabla \times \mathbf{v}') \cdot (\nabla \times \mathbf{v}'') \right], \quad (361)$$

where further terms involving $\nabla \cdot \mathbf{v}$ have been omitted. The temporal convolution kernels $n_{t't'}$ and $m_{t't''}$ depend only on the time differences $t - t'$ and $t - t''$ (and hence $t' - t''$). The resulting superadiabatic force density is

$$\mathbf{F}_{\text{sup}}(\mathbf{r}, t) = \int_0^t dt' \nabla \cdot n_{t't'} \nabla \mathbf{v}' - \int_0^t dt' \int_0^t dt'' \nabla m_{t't''} (\nabla \times \mathbf{v}') \cdot (\nabla \times \mathbf{v}'') \quad (362)$$

$$= \eta \nabla^2 \mathbf{v} - \chi \nabla (\nabla \times \mathbf{v})^2, \quad (363)$$

where the form of Eq. (363) holds in steady state, with coefficients given by

$$\eta = \lim_{t \rightarrow \infty} \int_0^t dt' n_{t'}, \quad (364)$$

$$\chi = \lim_{t \rightarrow \infty} \int_0^t dt' \int_0^{t'} dt'' m_{t't''}. \quad (365)$$

In Eqs. (364) and (365) η is the coefficient of shear viscosity and χ is the coefficient of the migration force, which is a structural (nondissipative) force field that can sustain and generate density gradients in nonequilibrium, both in steady state and in time-dependent situations. See [Stuhlmüller *et al.* \(2018\)](#) for explicit numerical results for a fluid under inhomogeneous shear flow. That novel types of transport coefficients, such as the migration coefficient χ , arise is natural and follows inherently from the kinematic point of view. Obtaining a quantitative and systematic understanding of how χ depends on density, temperature, etc., would be an interesting topic for future work. We return to the physics under shear flow in Sec. IV.G.

D. Nonequilibrium Ornstein-Zernike relation

We give an abridged version of the dynamical Ornstein-Zernike theory of [Brader and Schmidt \(2013\)](#). The derivation of the full tensorial version of the nonequilibrium Ornstein-Zernike equation was given by [Brader and Schmidt \(2014\)](#). We recall the static Ornstein-Zernike theory (Sec. III.G) as a template for relating probabilistic and direct correlation function hierarchies to each other. The power functional concept provides a time-dependent analog.

In nonequilibrium it is natural to go from the pair correlation function $g(\mathbf{r}, \mathbf{r}')$ to the van Hove function $G_{\text{vH}}(\mathbf{r}_1, t_1, \mathbf{r}_2, t_2) \equiv G_{\text{vH}}(1, 2)$, where we have used compact notation for spacetime points $1 \equiv \mathbf{r}_1, t_1$ and $2 \equiv \mathbf{r}_2, t_2$. The van Hove function measures the probability of finding a particle at point 2 given that a particle is at point 1. Even in a bulk fluid at equilibrium the van Hove function is nontrivial due to the time lag between the two events; see [Treffenstädt and Schmidt \(2021\)](#) and [Treffenstädt, Schindler, and Schmidt \(2022\)](#) for recent work. The requirements for a nonequilibrium Ornstein-Zernike relation are as follows.

- (i) It should determine $G_{\text{vH}}(1, 2)$.
- (ii) It is not a hierarchy involving higher (three-body, etc.) correlators.
- (iii) An analog of the direct correlation function $c_2(\mathbf{r}, \mathbf{r}')$ should occur.

We resort to the microscopic dynamics as specified via the Smoluchowski equation. Averages are built according to $O(t) = \langle \hat{O}(\mathbf{r}^N, t) \rangle = \int d\mathbf{r}^N \hat{O}(\mathbf{r}^N, t) \Psi(\mathbf{r}^N, t)$. Examples include $\rho(\mathbf{r}, t) = \langle \hat{\rho} \rangle$ and $\mathbf{J}(\mathbf{r}, t) = \langle \hat{\mathbf{J}} \rangle$, with $\dot{\rho}(\mathbf{r}, t) = -\nabla \cdot \mathbf{J}(\mathbf{r}, t)$. The van Hove function is defined as

$$G_{\text{vH}}(1, 2) = \rho(1)^{-1} \langle \hat{\rho}(1) \hat{\rho}(2) \rangle, \quad (366)$$

where we take the two times to be ordered ($t_1 \geq t_2$). The two-time average is taken over the distribution at the earlier time t_2 , with the conditional probability of finding the state at the later

time t_1 . For a quiescent bulk fluid, Eq. (366) reduces to the standard form [see [Hansen and McDonald \(2013\)](#)] such that the dependence is only on the moduli $|t_1 - t_2|$ and $|\mathbf{r}_1 - \mathbf{r}_2|$. Besides introducing the inhomogeneous general form (366), [Brader and Schmidt \(2013\)](#) also considered the *front van Hove current* defined as

$$\mathbf{J}_{\text{vH}}^f(1, 2) = \langle \hat{\mathbf{J}}(1) \hat{\rho}(2) \rangle, \quad (367)$$

where the first, ‘‘front,’’ factor in the correlator is the current operator. [Brader and Schmidt \(2014\)](#) also considered a corresponding van Hove current-current correlator $\langle \hat{\mathbf{J}}(1) \hat{\mathbf{J}}(2) \rangle$.

The two-body continuity equation relates the two-body correlators according to

$$\frac{\partial}{\partial t_1} \rho(1) G_{\text{vH}}(1, 2) = -\nabla_1 \cdot \mathbf{J}_{\text{vH}}^f(1, 2), \quad (368)$$

where ∇_1 indicates the derivative with respect to \mathbf{r}_1 . In formal analogy to the static case, here we consider dynamical functional derivatives. We rewrite the Smoluchowski equation as

$$\frac{\partial}{\partial t} \Psi = \hat{\Omega}(t) \Psi, \quad (369)$$

with the Smoluchowski time evolution operator [Eq. (63)]

$$\hat{\Omega}(t) = -\sum_i \nabla_i \cdot \hat{\mathbf{v}}_i, \quad (370)$$

where both ∇_i and $\hat{\mathbf{v}}_i$ act via differentiation and the velocity operator is $\gamma \hat{\mathbf{v}}_i = -(\nabla_i u) - k_B T \nabla_i - (\nabla_i V_{\text{ext},i}) + \mathbf{f}_{\text{nc},i}$. The formal solution of Eq. (369) is

$$\Psi(\mathbf{r}^N, t) = e_+ \int_{t_0}^t ds \hat{\Omega}(s) \Psi(\mathbf{r}^N, t_0), \quad (371)$$

where t_0 is an initial time and the time-ordered exponential is defined via its power series

$$\begin{aligned} e_+ \int_{t_0}^t ds \hat{\Omega}(s) &= 1 + \int_{t_0}^t ds \hat{\Omega}(s) + \int_{t_0}^t ds_1 \int_{t_0}^{s_1} ds_2 \hat{\Omega}(s_1) \hat{\Omega}(s_2) \\ &+ \int_{t_0}^t ds_1 \int_{t_0}^{s_1} ds_2 \int_{t_0}^{s_2} ds_3 \hat{\Omega}(s_1) \hat{\Omega}(s_2) \hat{\Omega}(s_3) + \dots \end{aligned} \quad (372)$$

Hence, the time arguments build a succession t_0, s_3, s_2, s_1, t along increasing time. This order of labels allows one to write the nested time integrals in a natural way; note that times with increasing subscripts s_1, s_2, \dots can be naturally ordered according to increasing temporal distance into the past, viewed from the time t at present. An excellent, accessible account of the calculus of time-ordered exponentials was given by [Brader, Cates, and Fuchs \(2012\)](#).

We use the following three ingredients.

- (i) Time-dependent functional derivatives satisfy $\delta \tilde{u}(\mathbf{r}, t) / \delta \tilde{u}(\mathbf{r}', t') = \delta(\mathbf{r} - \mathbf{r}') \delta(t - t')$, where $\tilde{u}(\mathbf{r}, t)$ is a test function; see also Appendix A.2.

(ii) The chain rule is

$$\begin{aligned} \frac{\delta}{\delta \hat{u}(\mathbf{r}, t)} e_+^{\int_{t_1}^{t_2} ds \hat{\Omega}(s)} \\ = \int_{t_1}^{t_2} ds e_+^{\int_s^{t_2} ds' \hat{\Omega}(s')} \frac{\delta \hat{\Omega}(s)}{\delta \hat{u}(\mathbf{r}, t)} e_+^{\int_{t_1}^s ds' \hat{\Omega}(s')}. \end{aligned} \quad (373)$$

(iii) The general definition of the two-time correlator between operators $\hat{a}(1)$ and $\hat{b}(2)$ is

$$\begin{aligned} \langle \hat{a}(1) \hat{b}(2) \rangle \\ = \int d\mathbf{r}^N \hat{a}(1) e_+^{\int_{t_2}^{t_1} ds \hat{\Omega}(s)} \hat{b}(2) e_+^{\int_{t_0}^{t_2} ds \hat{\Omega}(s)} \Psi(\mathbf{r}^N, t_0). \end{aligned} \quad (374)$$

Using (i)–(iii) one can show the following relations, for which we define the field

$$\mathcal{V}(2) = \int_{t_0}^{t_2} dt'_2 D \nabla_2^2 V_{\text{ext}}(2'), \quad (375)$$

where $2' \equiv \mathbf{r}_2, t'_2$, the free diffusion constant is $D = k_B T / \gamma$, and $\mathcal{V}(2)$ has units of energy. The relationships are

$$\frac{\delta \mathbf{J}(1)}{\delta \beta \mathcal{V}(2)} = I(1, 2) + \frac{\partial}{\partial t_2} \mathbf{J}_{\text{vH}}^f(1, 2), \quad (376)$$

$$\frac{\delta \rho(1)}{\delta \beta \mathcal{V}(2)} = \rho(1) \frac{\partial}{\partial t_2} G_{\text{vH}}(1, 2). \quad (377)$$

The instantaneous contribution is

$$I(1, 2) = -\gamma^{-1} \rho(1) \frac{\delta \nabla V_{\text{ext}}(1)}{\delta \beta \mathcal{V}(2)}. \quad (378)$$

The consistency with the equilibrium result from DFT can be seen by integrating Eq. (377) in time and assuming that decorrelation happens at long times,

$$\int_{-\infty}^{t_2} dt'_2 \frac{\delta \rho(1)}{\delta \beta \mathcal{V}(2')} = \int_{-\infty}^{t_2} dt'_2 \rho(1) \frac{\partial}{\partial t'_2} G_{\text{vH}}(1, 2') \quad (379)$$

$$= \langle \hat{\rho}(\mathbf{r}_1) \hat{\rho}(\mathbf{r}_2) \rangle - \rho(\mathbf{r}_1) \rho(\mathbf{r}_2) \quad (380)$$

$$= \left. \frac{\delta \rho(\mathbf{r}_1)}{\delta \beta V_{\text{ext}}(\mathbf{r}_2)} \right|_{\text{eq}}. \quad (381)$$

Note that the equilibrium result here is obtained via a dynamical mechanism that differs from the standard static route; see Sec. III.G.

To proceed, we first consider the adiabatic contribution to the current (DDFT approximation), which is

$$\mathbf{J}_{\text{DDFT}}(1) = \frac{\rho(1)}{\gamma} \left(-\nabla \frac{\delta F[\rho]}{\delta \rho(1)} - \nabla V_{\text{ext}}(1) + \mathbf{f}_{\text{nc}}(1) \right). \quad (382)$$

We calculate the derivative $\delta \mathbf{J}(1) / \delta \beta \mathcal{V}(3)$ and use Eqs. (376) and (377) to obtain

$$\begin{aligned} \mathbf{J}_{\text{vH}}^{\text{f,DDFT}}(1, 3) = \mathbf{J}(1) G_{\text{vH}}(1, 3) - D \rho(1) \nabla_1 \left[G_{\text{vH}}(1, 3) \right. \\ \left. - \int d\mathbf{r}_2 c_2(1, 2_1) \rho(2_1) [G_{\text{vH}}(2_1, 3) - \rho(3_{-\infty})] \right], \end{aligned} \quad (383)$$

where the notation is $\rho(3_{-\infty}) = \rho(\mathbf{r}_3, -\infty)$ and $2_1 \equiv \mathbf{r}_2, t_1$. Hence, $c_2(1, 2_1) = c_2(\mathbf{r}_1, \mathbf{r}_2, t_1)$ is an equal-time object (as is appropriate for adiabatic correlations). We then have

$$c_2(\mathbf{r}_1, \mathbf{r}_2, t_1) = -\beta \left. \frac{\delta^2 F_{\text{exc}}[\rho]}{\delta \rho(\mathbf{r}_1) \delta \rho(\mathbf{r}_2)} \right|_{\rho=\rho(\mathbf{r}, t_1)}. \quad (384)$$

Equilibrium is obtained as a special limit $\mathbf{J}(1) = 0 \forall t$ and the equal-time limit $t_1 = t_3$. Using the condition that at equal times $G_{\text{vH}}(1, 3_1) = \rho(3_1) [h(1, 3_1) + 1] + \rho(1) \delta(\mathbf{r}_1 - \mathbf{r}_3)$, we obtain

$$\begin{aligned} \mathbf{J}_{\text{vH}}^{\text{f,DDFT}}(1, 3) = -D \rho(1) \nabla_1 \left[\delta(\mathbf{r}_1 - \mathbf{r}_3) \right. \\ \left. + \rho(3_1) \left(h(1, 3_1) - c_2(1, 3_1) \right) \right. \\ \left. - \int d\mathbf{r}_2 c_2(1, 2_1) \rho(2_1) h(2_1, 3_1) \right]. \end{aligned} \quad (385)$$

For short times, the first term in the square brackets alone already gives the exact result for the decay. Hence, the term in parentheses needs to vanish, which proves the equilibrium OZ relation (236). This dynamical method hence provides an alternative way to derive the static identity.

Considering next the superadiabatic contribution, we split the total front van Hove current according to

$$\mathbf{J}_{\text{vH}}^f(1, 3) = \mathbf{J}_{\text{vH}}^{\text{f,DDFT}}(1, 3) + \mathbf{J}_{\text{vH}}^{\text{f,sup}}(1, 3). \quad (386)$$

The superadiabatic contribution satisfies

$$\begin{aligned} \mathbf{J}_{\text{vH}}^{\text{f,sup}}(1, 3) = \mathbf{J}_{\text{vH}}^{\text{f,sup}}(1, 3_{-\infty}) - \rho(1) \int_{-\infty}^{t_3} dt'_3 \nabla_3 \cdot \mathbf{M}(1, 3') \rho(3') \\ + \rho(1) \int d2 \{ \mathbf{M}(1, 2) \cdot [\mathbf{J}_{\text{vH}}^f(2, 3) - \mathbf{J}(2) \rho(3_{-\infty})] \\ + \mathbf{m}(1, 2) \rho(2) [G_{\text{vH}}(2, 3) - \rho(3_{-\infty})] \}, \end{aligned} \quad (387)$$

with $\mathbf{m}(1, 2)$ the vectorial time direct correlation function and $\mathbf{M}(1, 3)$ the tensorial time direct correlation function.

From the general equation of motion

$$\mathbf{J}(1) = \mathbf{J}_{\text{DDFT}}(1) - \frac{\rho(1)}{\gamma} \frac{\delta P_{t_1}^{\text{exc}}[\rho, \mathbf{J}]}{\delta \mathbf{J}(1)}, \quad (388)$$

one can identify

$$\mathbf{m}(1, 2) = -\gamma^{-1} \frac{\delta}{\delta\rho(2)} \frac{\delta P_{t_1}^{\text{exc}}[\rho, \mathbf{J}]}{\delta\mathbf{J}(1)}, \quad (389)$$

$$\mathbf{M}(1, 2)^\top = -\gamma^{-1} \frac{\delta}{\delta\mathbf{J}(2)} \frac{\delta P_{t_1}^{\text{exc}}[\rho, \mathbf{J}]}{\delta\mathbf{J}(1)}. \quad (390)$$

This forms a connection from the dynamic pair structure to the superadiabatic power functional. A more general relationship can be obtained by considering sourced dynamics, as introduced by [Brader and Schmidt \(2014\)](#). Furthermore, functional line integration ([Brader and Schmidt, 2015b](#)) provides a systematic means to obtain nonequilibrium identities and, in particular, formulate dynamical versions of common liquid state perturbation techniques. [Hermann and Schmidt \(2021, 2022\)](#) formulated exact sum rules for forces and correlations on the basis of Noether's theorem, which allows one to exploit symmetries in variational calculus. These Noether sum rules involve time direct correlation functions, and they express their interdependence with and relationship to averaged dynamical correlators.

E. Dynamical test-particle limit and mixtures

The dynamical test-particle limit provides a formally exact route to the time-dependent pair structure. It hence constitutes an alternative to the nonequilibrium Ornstein-Zernike route; see Sec. [IV.D](#). The concept relies on identifying the van Hove function with a correspondingly constructed one-body density profile and suitable initial conditions. The van Hove current is related to a nonequilibrium one-body current. The dynamical test-particle limit generalizes the static test particle of [Percus \(1962\)](#) to both equilibrium pair dynamics (say, in a homogeneous fluid) and the time-dependent nonequilibrium pair structure.

The dynamical test-particle concept was first introduced by [Archer, Hopkins, and Schmidt \(2007\)](#) on the basis of dynamical density-functional theory and exemplified in a system of Gaussian core particles; this model has become central to the study of interpenetrable soft matter ([Archer and Evans, 2001](#); [Archer, Evans, and Roth, 2002](#)). [Hopkins *et al.* \(2010\)](#) carried out a thorough test-particle study for the hard sphere fluid. [Brader and Schmidt \(2015a\)](#) overcame the DDFT limitations by providing the formally exact closed equations of motion for the van Hove function based on power functional theory ([Schmidt and Brader, 2013](#)). [Schindler and Schmidt \(2016\)](#) showed, by analyzing BD computer simulation results, that the superadiabatic contributions that determine the dynamics of the van Hove function are comparable in magnitude to the adiabatic contributions (i.e., those that are in principle accounted for in dynamical DFT).

For the hard sphere fluid, [Treffenstädt and Schmidt \(2021\)](#) recently specified the superadiabatic forces that drive the equilibrium van Hove function as consisting of drag, viscous, and structural contributions. These force types are relevant in active Brownian particles, liquids under shear, and lane-forming mixtures, respectively. The explicit power functional approximation reproduces these universal force fields in quantitative agreement with Brownian dynamics simulation results. [Treffenstädt and Schmidt \(2021\)](#) and [Treffenstädt, Schindler, and Schmidt \(2022\)](#) argued that these findings

demonstrate the existence of close interrelationships between equilibrium and nonequilibrium hard sphere properties, as expected from the general power functional point of view. We give an outline of the dynamical test-particle theory in the following.

We use the following splitting into so-called self and distinct parts:

$$G_{\text{vH}}(1, 2) = G_{\text{vH}}^{\text{s}}(1, 2) + G_{\text{vH}}^{\text{d}}(1, 2), \quad (391)$$

$$\mathbf{J}_{\text{vH}}(1, 2) = \mathbf{J}_{\text{vH}}^{\text{s}}(1, 2) + \mathbf{J}_{\text{vH}}^{\text{d}}(1, 2), \quad (392)$$

where the self part (superscript s) refers to the autocorrelation of particle $i = j$ and the distinct part (superscript d) refers to pairs of different particles ($i \neq j$). Hence,

$$G_{\text{vH}}^{\text{s}}(1, 2) = \rho(1)^{-1} \sum_i \langle \hat{\rho}_i(1) \hat{\rho}_i(2) \rangle, \quad (393)$$

$$G_{\text{vH}}^{\text{d}}(1, 2) = \rho(1)^{-1} \sum'_{ij} \langle \hat{\rho}_i(1) \hat{\rho}_j(2) \rangle, \quad (394)$$

where spacetime points are indicated as $1 \equiv \mathbf{r}, t$ and $2 \equiv \mathbf{r}', t'$, the particle-labeled density operator is $\hat{\rho}_i(1) = \delta(\mathbf{r} - \mathbf{r}_i)$, and the primed sum indicates that the case $i = j$ has been omitted.

The dynamical test-particle method applies to general nonequilibrium; here we limit ourselves to the description of the equilibrium dynamics of a bulk fluid of density ρ_{b} . We introduce two time-dependent one-body density distributions $\rho_{\text{s}}(\mathbf{r}, t)$ and $\rho_{\text{d}}(\mathbf{r}, t)$ that represent the self and the distinct part of the van Hove function, respectively. Here we reuse the symbols \mathbf{r} and t to indicate the difference between the bare variables $\mathbf{r} - \mathbf{r}' \rightarrow \mathbf{r}$ and $t - t' \rightarrow t$, as is appropriate for a bulk fluid. Consider the initial state ($t = 0$) to be such that

$$\rho_{\text{s}}(\mathbf{r}, 0) = \delta(\mathbf{r}), \quad (395)$$

$$\rho_{\text{d}}(\mathbf{r}, 0) = \rho_{\text{b}} g(r), \quad (396)$$

where $g(r)$ is the static pair correlation function; see Sec. [III.G](#). The self initial condition (395) describes the “tagged” particle as being located at the origin at the initial time (or, equivalently, the origin of the coordinate system as being moved to the position of the tagged particle at time $t = 0$). The distinct initial condition (396) is the density profile of all other particles in the fluid according to the static test-particle limit ([Percus, 1962](#)); see [Rosenfeld \(1993\)](#) for details on enforcing self-consistency with the Ornstein-Zernike route and [Thorneywork *et al.* \(2014\)](#) for a comparison to experimental results.

In the dynamical test-particle limit, we identify the time evolution of the self and distinct one-body fields with that of the self and distinct part of the van Hove function as follows:

$$G_{\text{vH}}^{\text{s}}(\mathbf{r}, t) = \rho_{\text{s}}(\mathbf{r}, t), \quad (397)$$

$$G_{\text{vH}}^{\text{d}}(\mathbf{r}, t) = \rho_{\text{d}}(\mathbf{r}, t), \quad (398)$$

where calculating the right-hand sides constitutes a dynamical one-body problem.

To perform this task, we need to generalize power functional theory to mixtures. We sketch in the following the presentation by [Brader and Schmidt \(2015a\)](#). The generalization to orientational degrees of freedom by [Krinninger, Schmidt, and Brader \(2016\)](#) is closely related; [Krinninger and Schmidt \(2019\)](#) gave a comprehensive account. Applications of the rotational version were presented by [Hermann, de las Heras, and Schmidt \(2019\)](#), [Hermann *et al.* \(2019\)](#), and [Landgraf, Schmidt, and de las Heras \(2022\)](#).

The many-body Smoluchowski dynamics for general mixtures is obtained by keeping the continuity equation (13) $\dot{\Psi} = -\sum_i \nabla_i \cdot \mathbf{v}_i \Psi$ but introducing γ_i as the friction constant of particle i and relating the configurational velocity of particle i to the forces via

$$\gamma_i \mathbf{v}_i = -k_B T \nabla_i \ln \Psi - \nabla_i u(\mathbf{r}^N) + \mathbf{f}_{\text{ext},i}(\mathbf{r}_i, t), \quad (399)$$

where $\mathbf{f}_{\text{ext},i}(\mathbf{r}, t)$ is the external field that acts individually on particle i . We recover the one-component version [Eq. (14)] when we set $\gamma_i = \gamma$ and $\mathbf{f}_{\text{ext},i}(\mathbf{r}, t) = \mathbf{f}_{\text{ext}}(\mathbf{r}, t) \forall i$. In the one-component system, we have the further requirement that $u(\mathbf{r}^N)$ is invariant under permutations of the particle indices, which is not necessarily implied in Eq. (399).

From this most general dynamics of having N particles with distinct properties, we specialize to mixtures by introducing sets \mathcal{N}_α of particle labels i that contain identical particles of the same species α . We can then obtain the species-resolved density and current operators, respectively, by restricting the particle summation to those particles of the same species as follows:

$$\hat{\rho}_\alpha = \sum_{i \in \mathcal{N}_\alpha} \delta(\mathbf{r} - \mathbf{r}_i), \quad \hat{\mathbf{J}}_\alpha = \sum_{i \in \mathcal{N}_\alpha} \delta(\mathbf{r} - \mathbf{r}_i) \mathbf{v}_i. \quad (400)$$

The species-resolved density and the current profile are obtained by the standard averages $\rho_\alpha(\mathbf{r}, t) = \langle \hat{\rho}_\alpha \rangle$ and $\mathbf{J}_\alpha(\mathbf{r}, t) = \langle \hat{\mathbf{J}}_\alpha \rangle$. And as the particle identities are fixed in the course of time, the continuity equation is $\dot{\rho}_\alpha(\mathbf{r}, t) = -\nabla \cdot \mathbf{J}_\alpha(\mathbf{r}, t)$. We also bin the friction constants such that there is a unique friction constant γ_α for each species; formally one can express this as $\gamma_i = \gamma_\alpha \forall i \in \mathcal{N}_\alpha$. Similarly, for the external potential $\mathbf{f}_{\text{ext},i}(\mathbf{r}, t) = \mathbf{f}_{\text{ext}}^\alpha(\mathbf{r}, t) \forall i \in \mathcal{N}_\alpha$, where $\mathbf{f}_{\text{ext}}^\alpha(\mathbf{r}, t)$ is the external force field acting on species α , with conservative contribution $-\nabla V_{\text{ext}}^\alpha(\mathbf{r}, t)$.

The power functional framework generalizes the generating functional R_t to remain a single object ([Brader and Schmidt, 2015a](#); [Krinninger and Schmidt, 2019](#)), but one that depends on the set of all species-resolved profiles $\{\rho_{\alpha'}(\mathbf{r}, t), \mathbf{J}_{\alpha'}(\mathbf{r}, t)\}$, where α' labels the species of the set. The extremal principle is

$$\frac{\delta R_t[\{\rho_{\alpha'}, \mathbf{J}_{\alpha'}\}]}{\delta \mathbf{J}_\alpha(\mathbf{r}, t)} = 0 \quad (\text{min}) \quad \forall \alpha. \quad (401)$$

The power functional for a mixture splits into intrinsic and external contributions according to

$$R_t[\{\rho_{\alpha'}, \mathbf{J}_{\alpha'}\}] = \sum_\alpha (\dot{F}_{\text{id}}[\rho_\alpha] + P_t^{\text{id}}[\rho_\alpha, \mathbf{J}_\alpha] - X_t[\rho_\alpha, \mathbf{J}_\alpha]) + \dot{F}_{\text{exc}}[\{\rho_{\alpha'}\}] + P_t^{\text{exc}}[\{\rho_{\alpha'}, \mathbf{J}_{\alpha'}\}], \quad (402)$$

where the ideal adiabatic, ideal dissipative, and external contributions are given, respectively, by

$$\dot{F}_{\text{id}}[\rho_\alpha] = k_B T \int d\mathbf{r} \mathbf{J}_\alpha(\mathbf{r}, t) \cdot \nabla \ln \rho_\alpha(\mathbf{r}, t), \quad (403)$$

$$P_t^{\text{id}}[\rho_\alpha, \mathbf{J}_\alpha] = \frac{\gamma_\alpha}{2} \int d\mathbf{r} \frac{\mathbf{J}_\alpha^2(\mathbf{r}, t)}{\rho_\alpha(\mathbf{r}, t)}, \quad (404)$$

$$X_t[\rho_\alpha, \mathbf{J}_\alpha] = \int d\mathbf{r} [\mathbf{J}_\alpha(\mathbf{r}, t) \cdot \mathbf{f}_{\text{ext}}^\alpha(\mathbf{r}, t) - \dot{V}_{\text{ext}}^\alpha(\mathbf{r}, t) \rho_\alpha(\mathbf{r}, t)]. \quad (405)$$

Inserting these forms into the free power decomposition (402) and using the minimization principle (401) yield the equations of motion

$$\gamma_\alpha \mathbf{v}_\alpha(\mathbf{r}, t) = -k_B T \nabla \ln \rho_\alpha(\mathbf{r}, t) + \mathbf{f}_{\text{ad}}^\alpha(\mathbf{r}, t) + \mathbf{f}_{\text{sup}}^\alpha(\mathbf{r}, t) + \mathbf{f}_{\text{ext}}^\alpha(\mathbf{r}, t), \quad (406)$$

where the microscopic velocity profile of species α is $\mathbf{v}_\alpha(\mathbf{r}, t) = \mathbf{J}_\alpha(\mathbf{r}, t) / \rho_\alpha(\mathbf{r}, t)$ and the adiabatic and superadiabatic force fields acting on species α are given, respectively, by

$$\mathbf{f}_{\text{ad}}^\alpha(\mathbf{r}, t) = -\nabla \frac{\delta F_{\text{exc}}[\{\rho_{\alpha'}\}]}{\delta \rho_\alpha(\mathbf{r}, t)}, \quad (407)$$

$$\mathbf{f}_{\text{sup}}^\alpha(\mathbf{r}, t) = -\frac{\delta P_t^{\text{exc}}[\{\rho_{\alpha'}, \mathbf{J}_{\alpha'}\}]}{\delta \mathbf{J}_\alpha(\mathbf{r}, t)}. \quad (408)$$

We return to the physics of mixtures in Sec. IV.I when we consider differential and total motion.

Applying this general framework to the dynamics of the van Hove function in its test-particle representation gives the following two-body equation of motion:

$$\frac{\partial}{\partial t} G_{\text{vH}}^\alpha(\mathbf{r}, t) = D \nabla^2 G_{\text{vH}}^\alpha(\mathbf{r}, t) - \gamma^{-1} \nabla \cdot G_{\text{vH}}^\alpha(\mathbf{r}, t) [\mathbf{f}_{\text{ad}}^\alpha(\mathbf{r}, t) + \mathbf{f}_{\text{sup}}^\alpha(\mathbf{r}, t)], \quad (409)$$

where the species index $\alpha = s, d$ labels the self and distinct parts and $D = k_B T / \gamma$ is the diffusion constant, with an identical friction constant for the self and distinct particles ($\gamma \equiv \gamma_s = \gamma_d$).

Results obtained from the adiabatic approximation $\mathbf{f}_{\text{sup}}^\alpha(\mathbf{r}, t) = 0$, i.e., from DDFT, for the repulsive Gaussian core model fluid ([Archer, Hopkins, and Schmidt, 2007](#)) indicate that, for the chosen state point, the DDFT gives a good account of the simulation data. This is not true in general, as was shown on the basis of BD simulation results for the van Hove current for the dense Lennard-Jones bulk liquid of [Schindler and Schmidt \(2016\)](#). They split the total van Hove current by explicitly constructing the adiabatic state in simulations into adiabatic and superadiabatic contributions.

The results indicate that both contributions are of comparable magnitude and that they are distinctly different in form, i.e., in the variation with distance. Recently a comparison of DDFT results with experimental data, obtained in a quasi-two-dimensional hard sphere dispersion using video microscopy, was performed by [Stopper *et al.* \(2018\)](#). They modified the “bare” DDFT and obtained results that were in good agreement with the experimental data.

The test-particle concept was applied to investigate self-diffusion in a model system of rodlike particles in the smectic (or lamellar) phase by [Grelet *et al.* \(2008\)](#). A corresponding experimental system was a colloidal suspension of filamentous *fd* virus particles, which allowed the direct visualization at the scale of the single particle of mass transport between the smectic layers. [Grelet *et al.* \(2008\)](#) found that self-diffusion takes place preferentially in the direction normal to the smectic layers and occurs in steps of one rod length, which is reminiscent of a hopping type of transport. The probability density function was obtained experimentally at different times and found to be in qualitative agreement with theoretical predictions based on a dynamical density-functional theory. Closely related DDFT work was carried out by [Bier and van Roij \(2007, 2008\)](#) and [Bier *et al.* \(2008\)](#).

Most of the previously mentioned empirical corrections to the DDFT dynamics in effect replace the bare diffusion constant D (and γ accordingly) with a reduced value, which is an input to the theory. In their recent investigation for the hard sphere van Hove dynamics, [Treffenstädt and Schmidt \(2021\)](#) proceeded differently. They instead showed that the superadiabatic force contributions generate the slowdown of the dynamics. Their quantitative power functional description of the superadiabatic force contributions yields results that are in good agreement with the BD simulation data. By considering the total and also the differential motion of the van Hove function, i.e., the difference of self and distinct parts, they were able to uniquely identify force contributions that also arise in nonequilibrium; see also [Treffenstädt, Schindler, and Schmidt \(2022\)](#).

F. Custom flow algorithm

The custom flow algorithm constitutes a method to create a desired spatiotemporal pattern of density and velocity by constructing (iteratively) the necessary external force field that creates this prescribed motion. As a causal relationship, one would view the external forces as being at the origin of the motion [$\mathbf{f}_{\text{ext}}(\mathbf{r}, t) \rightarrow \{\rho(\mathbf{r}, t), \mathbf{J}(\mathbf{r}, t)\}$]. However, from power functional theory ([Schmidt and Brader, 2013](#)) the functional map is

$$\{\rho(\mathbf{r}, t), \mathbf{J}(\mathbf{r}, t)\} \rightarrow \mathbf{f}_{\text{int}}(\mathbf{r}, t). \quad (410)$$

In the force balance relation the flow is given by

$$\gamma \mathbf{v}(\mathbf{r}, t) = -k_B T \nabla \ln \rho(\mathbf{r}, t) + \mathbf{f}_{\text{int}}(\mathbf{r}, t) + \mathbf{f}_{\text{ext}}(\mathbf{r}, t), \quad (411)$$

where the external force field in general consists of conservative and nonconservative contributions [$\mathbf{f}_{\text{ext}}(\mathbf{r}, t) = -\nabla V_{\text{ext}}(\mathbf{r}, t) + \mathbf{f}_{\text{nc}}(\mathbf{r}, t)$]. As $\mathbf{f}_{\text{int}}(\mathbf{r}, t) = \mathbf{f}_{\text{int}}(\mathbf{r}, t, [\rho, \mathbf{J}])$, the force balance implies

$$\{\rho(\mathbf{r}, t), \mathbf{J}(\mathbf{r}, t)\} \rightarrow \mathbf{f}_{\text{ext}}(\mathbf{r}, t), \quad (412)$$

which constitutes a reversal of the causal relationship. One might wonder whether this has consequences and whether it can be exploited, say, on the level of BD simulations. To investigate this point, we reorder the equation of motion trivially as

$$\mathbf{f}_{\text{ext}}(\mathbf{r}, t) = k_B T \nabla \ln \rho(\mathbf{r}, t) - \mathbf{f}_{\text{int}}(\mathbf{r}, t) + \gamma \mathbf{v}(\mathbf{r}, t), \quad (413)$$

where the microscopic velocity field is $\mathbf{v}(\mathbf{r}, t) = \mathbf{J}(\mathbf{r}, t) / \rho(\mathbf{r}, t)$.

We first consider steady states, where there is no explicit time dependence in the one-body fields. Hence,

$$\mathbf{f}_{\text{ext}}(\mathbf{r}) = k_B T \nabla \ln \rho(\mathbf{r}) - \mathbf{f}_{\text{int}}(\mathbf{r}) + \gamma \mathbf{v}(\mathbf{r}). \quad (414)$$

In Eq. (414) we know from power functional theory that the right-hand side depends only on the density profile and current, not directly on the external force field. In a BD scheme, however, one needs to implement this relationship in a computational way. This can be performed using the custom flow iteration scheme of [de las Heras, Renner, and Schmidt \(2019\)](#) to solve for $\mathbf{f}_{\text{ext}}(\mathbf{r})$. Consider $\rho(\mathbf{r})$ and $\mathbf{J}(\mathbf{r})$ to be fixed target fields and search for the form of $\mathbf{f}_{\text{ext}}(\mathbf{r})$ that generates, in BD simulations, these targets in steady state. The targets need to be physical, including the condition $\nabla \cdot \rho(\mathbf{r}) \mathbf{v}(\mathbf{r}) = 0$ for a steady state. The iteration step is

$$\mathbf{f}_{\text{ext}}^{(k)}(\mathbf{r}) = k_B T \nabla \ln \rho(\mathbf{r}) - \mathbf{f}_{\text{int}}^{(k-1)}(\mathbf{r}) + \gamma \mathbf{v}(\mathbf{r}), \quad (415)$$

where k labels the steps and $\rho(\mathbf{r})$ and $\mathbf{v}(\mathbf{r})$ are the known targets. The internal force field is sampled as

$$\mathbf{f}_{\text{int}}^{(k-1)}(\mathbf{r}) = -\frac{1}{\rho(\mathbf{r})} \left\langle \sum_i \delta(\mathbf{r} - \mathbf{r}_i) \nabla_i u(\mathbf{r}^N) \right\rangle, \quad (416)$$

where the system is exposed to the action of the external force field $\mathbf{f}_{\text{ext}}^{(k-1)}(\mathbf{r})$. The iteration can be started with the ideal gas ansatz as follows:

$$\mathbf{f}_{\text{ext}}^{(0)}(\mathbf{r}) = k_B T \nabla \ln \rho(\mathbf{r}) + \gamma \mathbf{v}(\mathbf{r}). \quad (417)$$

[de las Heras, Renner, and Schmidt \(2019\)](#) formulated convergence criteria and showed that in practice convergence is fast and reliable and to a unique solution. This demonstrates that for steady states Eq. (414) performs the functional inversion from $\mathbf{f}_{\text{ext}}(\mathbf{r}) \rightarrow \{\rho(\mathbf{r}), \mathbf{v}(\mathbf{r})\}$ to $\{\rho(\mathbf{r}), \mathbf{v}(\mathbf{r})\} \rightarrow \mathbf{f}_{\text{ext}}(\mathbf{r})$. Note that the splitting of the internal force field into adiabatic and superadiabatic contributions, $\mathbf{f}_{\text{int}}(\mathbf{r}) = \mathbf{f}_{\text{ad}}(\mathbf{r}) + \mathbf{f}_{\text{sup}}(\mathbf{r})$, has not been used here. [As a striking example of the method, one can keep $\rho(\mathbf{r})$ fixed and vary $\mathbf{v}(\mathbf{r})$ only; see [de las Heras, Renner, and Schmidt \(2019\)](#).]

As a special case, for inverting in equilibrium, where $\mathbf{v}(\mathbf{r}) = 0$, the force balance (414) simplifies to

$$\mathbf{f}_{\text{ext}}(\mathbf{r}) = k_B T \nabla \ln \rho(\mathbf{r}) - \mathbf{f}_{\text{int}}(\mathbf{r}). \quad (418)$$

In Eq. (418) the iteration step is

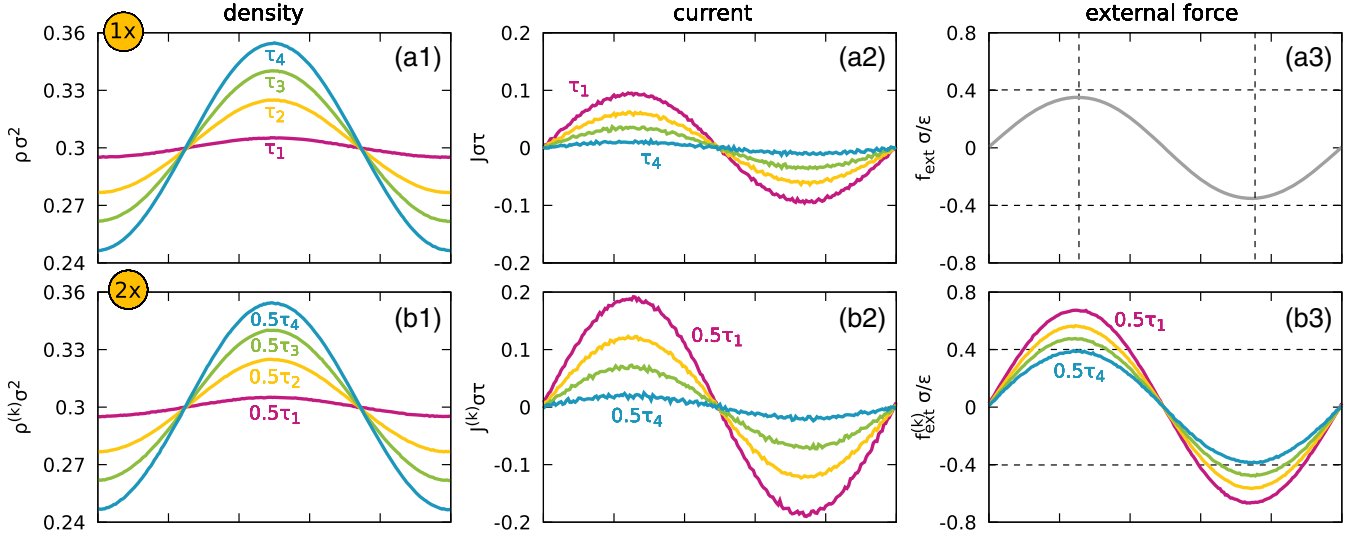


FIG. 5. Custom flow method applied to a fluid of steeply repulsive particles of size σ and strength of repulsion ϵ . Shown are the density profile (left column), the local current (middle column), and the external force field (right column) at four consecutive times $0 < \tau_1 < \tau_2 < \tau_3 < \tau_4$. The system is initially in a homogeneous bulk fluid state (constant density and vanishing external force). In the original system, at times $t \geq 0$ a density inhomogeneity (a1) and corresponding flow (a2) develop due to the action of a sinusoidal external force (a3) that is instantaneously switched on at $t = 0$. Eventually the system practically reaches a new equilibrium at $t = \tau_4$ with almost zero current. In the fast-forward system (second row) the density and the current are prescribed to evolve twice as fast as in the original system. The resulting sequence of density profiles (b1) is identical to that in the original system (a1) when the time label is rescaled by 0.5 (as indicated). Correspondingly, the amplitude of the current (b2) is twice as large as in the original system, but it is otherwise unchanged. The superscript (k) indicates the iteration step. The custom flow method finds the external force field (b3) that generates the prescribed slow time evolution. The resulting external force (b3) varies in the course of time, in contrast to the behavior in the original system (a3). Adapted from [de las Heras, Renner, and Schmidt, 2019](#).

$$\mathbf{f}_{\text{ext}}^{(k)}(\mathbf{r}) = k_B T \nabla \ln \rho(\mathbf{r}) - \mathbf{f}_{\text{int}}^{(k-1)}(\mathbf{r}), \quad (419)$$

with the iteration start at the ideal gas solution $\mathbf{f}_{\text{ext}}^{(0)}(\mathbf{r}) = k_B T \nabla \ln \rho(\mathbf{r})$. The sampling provides $\mathbf{f}_{\text{int}}^{(k-1)}(\mathbf{r})$ from carrying out Eq. (416) under the action of $\mathbf{f}_{\text{ext}}^{(k-1)}(\mathbf{r})$. This provides a powerful method to perform the adiabatic construction in practice (Sec. III.A). If the sampling is performed as a Monte Carlo calculation, then one needs the external potential that, in effective one-dimensional situations of planar geometry (space coordinate x), can be obtained from integration as follows:

$$V_{\text{ext}}^{(k)}(x) = -k_B T \ln[\rho(x)\Lambda^d] + \int dx f_{\text{int},x}^{(k-1)}(x). \quad (420)$$

In more general situations, one needs to use an inverse ∇^{-1} operator to perform the integration; see [Borgis et al. \(2013\)](#) and [de las Heras and Schmidt \(2018b\)](#).

From the DFT context (Sec. III.C), we know that the internal force field can be expressed as

$$\mathbf{f}_{\text{int}}(\mathbf{r}) = -\nabla \frac{\delta F_{\text{exc}}[\rho]}{\delta \rho(\mathbf{r})}. \quad (421)$$

Hence, the force balance is

$$\mathbf{f}_{\text{ext}}(\mathbf{r}) = k_B T \nabla \ln \rho(\mathbf{r}) + \nabla \frac{\delta F_{\text{exc}}[\rho]}{\delta \rho(\mathbf{r})}, \quad (422)$$

where the right-hand side is a density functional. Hence, the Mermin-Evans map $\rho(\mathbf{r}) \rightarrow \mathbf{f}_{\text{ext}}(\mathbf{r})$, with $\mathbf{f}_{\text{ext}}(\mathbf{r}) = -\nabla V_{\text{ext}}(\mathbf{r})$. The method of [Fortini et al. \(2014\)](#) can be derived from the present scheme, as shown by [de las Heras, Renner, and Schmidt \(2019\)](#). They also summarized three different methods to sample the current distribution in BD simulations. This includes (i) using the force density balance; (ii) the method of the centered finite time difference, where the velocity of particle i is given as $\mathbf{v}_i(t) = [\mathbf{r}_i(t + \Delta t) + \mathbf{r}_i(t - \Delta t)] / (2\Delta t)$, with Δt the time step in the BD algorithm; and (iii) using the continuity equation. These methods can be implemented separately, and hence provide valuable consistency checks.

Having restricted ourselves to steady states in the previous description of custom flow, the method is amenable to time-dependent problems; see [de las Heras, Renner, and Schmidt \(2019\)](#). Here a coarse-graining time step is introduced and the previously described steady state strategy is performed in each step. Figure 5 shows corresponding illustrative results of a density peak that grows in time (top row) and that is then sped up to proceed at twice its original speed (bottom row).¹⁰ Recently [Renner, Schmidt, and de las Heras \(2021\)](#) considered the problem of prescribed flow in the context of molecular dynamics. They proposed a generic formulation of iterative custom flow methods and demonstrated that a particularly simple variant indeed allows one to generate tailor-made flow.

¹⁰The Supplemental Material for [de las Heras, Renner, and Schmidt \(2019\)](#) contains a video that is sped up by a factor of 3, as also reflected in the accompanying shred guitar soundtrack.

G. Viscous and structural forces

The rheology of colloidal systems is a rich and diverse subject; see the excellent account given by Brader (2010). In his seminal treatment Dhont (1996) provided detailed background information. Here we consider inhomogeneous shear flow that is spatially oscillatory; see Fig. 6 for an illustration. The external force field that generates the flow is assumed to have the form

$$\mathbf{f}_{\text{ext}}(y) = f_0 \sin(2\pi y/L) \mathbf{e}_x, \quad (423)$$

where $f_0 = \text{const}$ controls the strength of the driving, y is the coordinate perpendicular to the driving, L is the system size in the y direction, and \mathbf{e}_x is the unit vector in the x direction. Note that the field acts along the x direction but varies its strength in the orthogonal y direction, which constitutes a generic shear situation, where no unique flow potential exists.

The steady state force balance relation is

$$\gamma \mathbf{v}(\mathbf{r}) = -k_B T \nabla \ln \rho(\mathbf{r}) + \mathbf{f}_{\text{ad}}(\mathbf{r}) + \mathbf{f}_{\text{sup}}(\mathbf{r}) + \mathbf{f}_{\text{ext}}(\mathbf{r}). \quad (424)$$

The induced flow in steady state will also be along the x direction and the system will be homogeneous in x . We can hence split Eq. (424) into its vector components in the flow (\mathbf{e}_x) and gradient (\mathbf{e}_y) directions, respectively, given by

$$\gamma \mathbf{v}(\mathbf{r}) = \mathbf{f}_{\text{visc}}(\mathbf{r}) + \mathbf{f}_{\text{ext}}(\mathbf{r}), \quad (425)$$

$$0 = -k_B T \nabla \ln \rho(\mathbf{r}) + \mathbf{f}_{\text{ad}}(\mathbf{r}) + \mathbf{f}_{\text{struc}}(\mathbf{r}). \quad (426)$$

In Eqs. (425) and (426) we have split the superadiabatic force field into two mutually orthogonal contributions according to $\mathbf{f}_{\text{sup}}(\mathbf{r}) = \mathbf{f}_{\text{visc}}(\mathbf{r}) + \mathbf{f}_{\text{struc}}(\mathbf{r})$, where the viscous contribution is parallel to the flow [$\mathbf{f}_{\text{visc}}(\mathbf{r}) \parallel \mathbf{e}_x$] and the ‘‘structural’’ force contribution is perpendicular to the flow [$\mathbf{f}_{\text{struc}}(\mathbf{r}) \parallel \mathbf{e}_y$].

We assume that the superadiabatic free power functional consists of two parts that correspond to viscous and structural effects,

$$P_t^{\text{exc}}[\rho, \mathbf{v}] = P_t^{\text{visc}}[\rho, \mathbf{v}] + P_t^{\text{struc}}[\rho, \mathbf{v}]. \quad (427)$$

The viscous contribution (358) is given by

$$P_t^{\text{visc}}[\rho, \mathbf{v}] = \frac{1}{2} \int d\mathbf{r} [\eta (\nabla \times \mathbf{v})^2 + \zeta (\nabla \cdot \mathbf{v})^2], \quad (428)$$

where η and ζ are related to the shear viscosity and volume (or ‘‘bulk’’) viscosity, respectively. The present geometry has no compressional flow component, i.e., $\nabla \cdot \mathbf{v} = 0$, and hence only the shear contribution contributes. Hence, the functional derivative with respect to the velocity field $-\rho^{-1} \delta P_t^{\text{visc}} / \delta \mathbf{v}$ gives a viscous superadiabatic force field corresponding to that in Stokes flow,

$$\mathbf{f}_{\text{visc}}(y) = \eta \nabla^2 \mathbf{v}(y) \approx \frac{\partial^2}{\partial y^2} \frac{\eta f_0}{\gamma} \sin(ky) \mathbf{e}_x \quad (429)$$

$$= -\frac{\eta f_0 k^2}{\gamma} \sin(ky) \mathbf{e}_x = -\frac{\eta k^2}{\gamma} \mathbf{f}_{\text{ext}}(y), \quad (430)$$

where we have made the approximation $\mathbf{v}(\mathbf{r}) = \mathbf{f}_{\text{ext}}(\mathbf{r})/\gamma$ in Eq. (429) and have introduced the wave number $k = 2\pi/L$ that characterizes the oscillatory shear field.

In the gradient direction, as described in Eq. (426), we neglect the adiabatic interparticle interaction contribution over the ideal diffusive part, as is appropriate at low densities. Hence, $\mathbf{f}_{\text{ad}}(\mathbf{r}) \approx 0$ and we obtain

$$k_B T \nabla \ln \rho(\mathbf{r}) = \mathbf{f}_{\text{struc}}(\mathbf{r}), \quad (431)$$

where the structural force field is necessarily a kinematic functional, i.e., in general $\mathbf{f}_{\text{struc}}(\mathbf{r}, t, [\rho, \mathbf{v}])$.

We next assume the following form [Eq. (361)] of the structural contribution to the superadiabatic functional:

$$\begin{aligned} P_t^{\text{struc}}[\rho, \mathbf{v}] &= - \int d\mathbf{r} \int_0^t dt' \int_0^t dt'' m_{tt''}(\nabla \cdot \mathbf{v})(\nabla \times \mathbf{v}') \cdot (\nabla \times \mathbf{v}''), \end{aligned} \quad (432)$$

where the primed (double primed) velocity depends on t' (t'') and the position argument \mathbf{r} has been omitted for clarity. We obtain the structural force density distribution $\mathbf{F}_{\text{struc}}(\mathbf{r}, t) = \rho(\mathbf{r}, t) \mathbf{f}_{\text{struc}}(\mathbf{r}, t)$ via differentiation as follows:

$$\mathbf{F}_{\text{struc}}(\mathbf{r}, t) = -\frac{\delta P_t^{\text{struc}}[\rho, \mathbf{v}]}{\delta \mathbf{v}(\mathbf{r}, t)} \quad (433)$$

$$= - \int_0^t dt' \int_0^t dt'' \nabla m_{tt''}(\nabla \times \mathbf{v}') \cdot (\nabla \times \mathbf{v}'') \quad (434)$$

$$= -\chi \nabla [\nabla \times \mathbf{v}(\mathbf{r})]^2, \quad (435)$$

where in the last step we have assumed that $\rho \approx \rho_b = \text{const}$ and that the system is in steady state. The amplitude of the structural force is given by the moment

$$\chi = \lim_{t \rightarrow \infty} \int_0^t dt' \int_0^t dt'' m_{tt''}. \quad (436)$$

We next apply Eq. (435) to the form of the velocity field $\mathbf{v} \approx \mathbf{f}_{\text{ext}}/\gamma = f_0 \sin(ky) \mathbf{e}_x/\gamma$, which is straightforward to do as follows:

$$-\chi \nabla [\nabla \times \mathbf{v}(\mathbf{r})]^2 = -\chi \frac{\partial}{\partial y} \left(\frac{\partial f_0}{\partial y} \frac{1}{\gamma} \sin(ky) \right)^2 \mathbf{e}_y \quad (437)$$

$$= -\frac{\chi f_0^2 k^2}{\gamma^2} \frac{\partial}{\partial y} \cos^2(ky) \mathbf{e}_y \quad (438)$$

$$= \frac{\chi f_0^2 k^3}{\gamma^2} \sin(2ky) \mathbf{e}_y. \quad (439)$$

The result for the structural (‘‘migration’’) force displays a striking period doubling effect; the force tends to push particles into the two regions of low shear rate. We can obtain the steady state density profile from Eq. (431), again

under the assumption of the density profile having only small deviations from its bulk value, as follows:

$$\rho(y) = \rho_b - \frac{\chi f_0^2 k^2}{2\gamma^2 k_B T} \cos(2ky). \quad (440)$$

The shape of the density profile [Eq. (440)] agrees well with results both from Brownian dynamics computer simulations and with low-density results from an exact numerical solution of the Smoluchowski equation (Stuhlmüller *et al.*, 2018). From fitting the amplitude to the simulation data, one can obtain the value of the migration force amplitude χ . Note that the structural force field causes no dissipation, as $\mathbf{v} \cdot \mathbf{f}_{\text{struc}} = 0$, i.e., the force field is orthogonal to the flow direction.

de las Heras and Schmidt (2020) went further in systematically splitting the force balance relationship into flow and structural parts, given, respectively, by

$$\gamma \mathbf{v}(\mathbf{r}, t) = \mathbf{f}_{\text{flow}}(\mathbf{r}, t) + \mathbf{f}_{\text{ext},f}(\mathbf{r}, t), \quad (441)$$

$$0 = \mathbf{f}_{\text{id}}(\mathbf{r}, t) + \mathbf{f}_{\text{ad}}(\mathbf{r}, t) + \mathbf{f}_{\text{struc}}(\mathbf{r}, t) + \mathbf{f}_{\text{ext},s}(\mathbf{r}, t), \quad (442)$$

where $\mathbf{f}_{\text{id}}(\mathbf{r}, t) = -k_B T \nabla \ln \rho(\mathbf{r}, t)$. Here both the superadiabatic and the external force field are split into flow and structural contributions: $\mathbf{f}_{\text{sup}}(\mathbf{r}, t) = \mathbf{f}_{\text{flow}}(\mathbf{r}, t) + \mathbf{f}_{\text{struc}}(\mathbf{r}, t)$ and $\mathbf{f}_{\text{ext}}(\mathbf{r}, t) = \mathbf{f}_{\text{ext},f}(\mathbf{r}, t) + \mathbf{f}_{\text{ext},s}(\mathbf{r}, t)$. The different contributions are characterized by their symmetry properties under motion reversal, which then also determines the corresponding analytical form of the power functional approximation. Furthermore, a vectorial decomposition yields force components parallel and perpendicular to the flow field, which then can be rationalized separately; see de las Heras and Schmidt (2020) for details.

H. Viscoelasticity and memory

In light of significant recent interest in the study of memory kernels as fundamental objects for collective dynamics (Jung and Schmid, 2016; Lesnicki *et al.*, 2016; Jung, Hanke, and Schmid, 2017), Treffenstädt and Schmidt (2020) considered the hard sphere fluid exposed to transient switching phenomena under shear. Both the spatial variation of the shear field and its time dependence were highly idealized and chosen to trigger a strong response of the system. The results were obtained with event-driven BD simulations (Scala, Voigtmann, and De Michele, 2007), and the output from simulation was rationalized on the basis of an approximative form of the superadiabatic free power functional. As both the flow profile and the force profile are available from the simulations, this strategy allows for an unambiguous test of the theory. The shear protocol is specified by an external force that varies as a step function in space, i.e., with an infinite gradient at the shear plane(s) perpendicular to the flow direction. This shear force field is first instantaneously switched on, starting from a quiescent fluid, and then instantaneously switched off after the system has reached a steady shear state. Both transient processes, that after switching on and that after switching off, were analyzed on the basis

of the same viscoelastic power functional approximation. (Recall that the sole input to any superadiabatic force is the history of the kinematic fields, which are known in this case.) Figures 1(b) and 1(c) show data from BD compared to the results from the power functional approximation.

Different types of model forms for the memory kernel were considered. The following first form constitutes a simple reference, and it is local in space and has a purely exponential temporal decay: $K_L(\Delta \mathbf{r}, \Delta t) = \delta(\Delta \mathbf{r}) \tau_M^{-1} \exp(-\Delta t / \tau_M) \Theta(\Delta t)$, with τ_M indicating the memory time and $\Theta(\cdot)$ denoting the Heaviside step function. Here $\Delta \mathbf{r}$ is the spatial difference between the two coupled spacetime points and Δt is their temporal difference. The second version is spatially nonlocal and hence can account for spatial correlation effects. This memory kernel is assumed to have a diffusing form,

$$K_D(\Delta \mathbf{r}, \Delta t) = \frac{e^{-\Delta r^2 / (4D_M \Delta t) - \Delta t / \tau_M}}{(4\pi D_M \Delta t)^{3/2} \tau_M} \Theta(\Delta t), \quad (443)$$

with memory diffusion coefficient D_M . The memory time τ_M again sets the timescale for the decay. In principle, the parameters τ_M and D_M are determined by the underlying interparticle interactions. Adjusting these parameters to match the simulation data leads to good agreement with the BD results; see Figs. 1(b) and 1(c). In particular, the global motion reversal after switching off the shear force field is captured correctly. The theory hence provides an explanation for the effect. The superadiabatic forces that oppose the externally driven current arise due to memory after switching off. The behavior is of a genuinely viscoelastic nature: in the sheared steady state, viscous forces oppose the current, but they elastically generate an opposing current after switch off. See Treffenstädt and Schmidt (2020) for details on the theoretical treatment and for further results and comparisons. The concepts were also used by Treffenstädt and Schmidt (2021) to investigate the dynamics of the van Hove dynamical pair correlation function, where again memory was found to play an important role. Furthermore, the self and distinct splitting was complemented by splitting into total and differential motion, as laid out in the following in a different context.

I. Superdemixing and laning

The formation of lanes is a prominent effect that occurs generically once two or more different species are driven against each other. Such situations arise in a binary colloidal mixture under sedimentation, where light particles cream up and heavy particles settle down, or when oppositely charged particles are exposed to a uniform electric field. Dzubiella, Hoffmann, and Löwen (2002) presented an early pioneering study of the effect. Experimental systems of magnetic colloids that are placed above suitably patterned substrates offer highly sophisticated control of driving protocols (Loehr *et al.*, 2016, 2018). Geigenfeind, de las Heras, and Schmidt (2020) analyzed the forces that occur in the Brownian dynamics of a generic two-dimensional binary repulsive sphere model. They recast the internal force density for binary mixtures (as laid out in Sec. IV.E) as

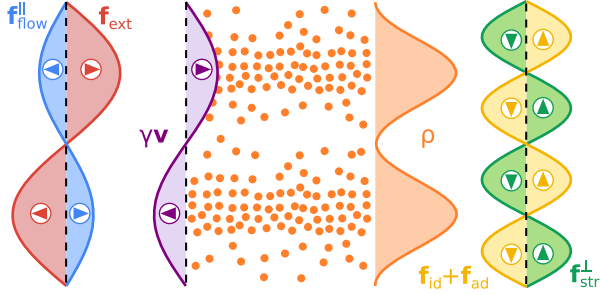


FIG. 6. Prototypical inhomogeneous flow situation in which both viscous (blue) and structural nonequilibrium forces (green) occur in a fluid of repulsive particles (orange dots) that undergo Brownian dynamics. The system is in steady state that results from the action of an external force field \mathbf{f}_{ext} (red) that is parallel to \mathbf{e}_x (horizontal) and varies its magnitude sinusoidally in \mathbf{e}_y (vertical). The induced flow (violet) is directed in the horizontal \mathbf{e}_x direction. Because of the structural forces, the density profile (orange) becomes inhomogeneous. The inhomogeneous density induces ideal and adiabatic forces (yellow) that tend to homogenize the system but are counteracted by the structural nonequilibrium force $\mathbf{f}_{\text{struc}}$ (green). For each vector field its magnitude (curves) and direction (arrows) are indicated. See also [Stuhlmüller *et al.* \(2018\)](#) and [Jahreis and Schmidt \(2020\)](#). From [de las Heras and Schmidt, 2020](#).

$$\mathbf{F}_{\text{int}}^{(\alpha)}(\mathbf{r}, t) = \rho_{\alpha}(\mathbf{r}, t)\mathbf{f}_{\text{int}}(\mathbf{r}, t) \pm \mathbf{G}_{\text{int}}(\mathbf{r}, t), \quad (444)$$

where the two cases \pm refer to species $\alpha = 1, 2$ and the force field \mathbf{f}_{int} acts on the total density $\rho_1 + \rho_2$ and the differential

force density \mathbf{G}_{int} acts on the density difference $\rho_2 - \rho_1$. If the internal interactions are independent of α (ideal mixture), then the species-resolved superadiabatic force field is shown to have the structure

$$\begin{aligned} \mathbf{f}_{\text{sup}}^{(\alpha)}(\mathbf{r}, t) = & \mathbf{f}_{\text{visc}}(\mathbf{r}, t) \pm \frac{\mathbf{G}_{\text{drag}}(\mathbf{r}, t)}{\rho_{\alpha}(\mathbf{r}, t)} \\ & + \mathbf{f}_{\text{struc}}(\mathbf{r}, t) \pm \frac{\mathbf{G}_{\text{struc}}(\mathbf{r}, t)}{\rho_{\alpha}(\mathbf{r}, t)}, \end{aligned} \quad (445)$$

where the viscous force field $\mathbf{f}_{\text{visc}}(\mathbf{r}, t)$ and the differential drag force density $\mathbf{G}_{\text{drag}}(\mathbf{r}, t)$ both act parallel to the flow direction. The total structural force field $\mathbf{f}_{\text{struc}}(\mathbf{r}, t)$ and the differential structural force density $\mathbf{G}_{\text{struc}}(\mathbf{r}, t)$ act perpendicularly to the flow. All four superadiabatic terms were modeled by explicit kinematic functionals, which were shown to reproduce the bare simulation data well. The force splitting concept allows one to uniquely identify the physical mechanism that generates the lane formation. It is the superadiabatic demixing force density $\mathbf{G}_{\text{struc}}(\mathbf{r}, t)$ that drives the two species apart and stabilizes the lanes. Figure 7 gives an illustration of this effect, as well as of the action of all further forces in the driven system. For details on the analytical treatment of the problem, together with the explicit power functional approximation, see [Geigenfeind, de las Heras, and Schmidt \(2020\)](#).

J. Active Brownian particles

Active Brownian particles have become a prototypical model for the study of collective nonequilibrium phenomena.

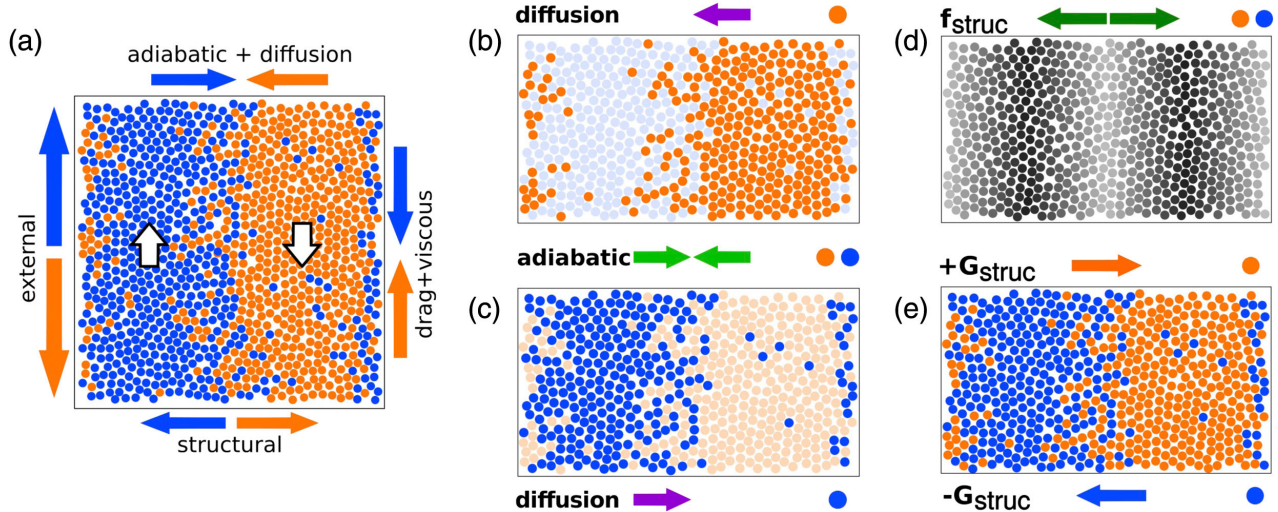


FIG. 7. Lane formation in a counterdriven binary mixture of purely repulsive particles. The blue (red) particles are driven in the upward (downward) direction by a constant external force. (a) As a result two lanes that move against each other (white arrows) form spontaneously. The blue (red) arrows indicate forces that act on the blue (red) species; green arrows indicate forces that act irrespective of the particle color. Each species experiences drag and viscous forces that tend to be directed against the species' local direction of motion. The adiabatic and diffusive forces tend to mix the system (top arrows). The nonequilibrium structural forces (bottom arrows) generate a superdemixing effect that stabilizes the laned state. (b) The diffusive force that acts on the red species tends to expand the red lane. (c) The corresponding effect for the blue particles acts in the opposite direction. Both species are pushed toward the interface by a small adiabatic force field (green arrows). (d) A structural nonequilibrium force $\mathbf{f}_{\text{struc}}$ acts on both species and sustains a density depletion zone at the interface (light gray). (e) The differential superadiabatic force density $\mathbf{G}_{\text{struc}}$ keeps each species inside of its lane and hence stabilizes the inhomogeneous steady state. Adapted from [Geigenfeind, de las Heras, and Schmidt, 2020](#).

The power functional framework is inherently set up to describe such driven systems once the generalization to the angular degrees of freedom (which describe the direction of the active swimming) is performed. We detail the theoretical layout in the following.

We first follow [Krininger, Schmidt, and Brader \(2016\)](#) and [Krininger and Schmidt \(2019\)](#), who considered the drag effect in active Brownian particles. Here the i th particle is described by position \mathbf{r}_i and unit vector orientation $\boldsymbol{\omega}_i$. We consider two-dimensional systems in a volume V ; the orientation $\boldsymbol{\omega}$ is parametrized by $\boldsymbol{\omega} = (\cos \varphi, \sin \varphi)$, where φ is the angle of the particle orientation against the x axis. The set of orientations $\boldsymbol{\omega}_1, \dots, \boldsymbol{\omega}_N \equiv \boldsymbol{\omega}^N$ constitutes internal degrees of freedom. The interparticle interaction potential $u(\mathbf{r}^N)$ is that of spherical particles, independent of $\boldsymbol{\omega}^N$. The particles are self-propelled with a body force field

$$\mathbf{f}_{\text{swim}}(\mathbf{r}, \boldsymbol{\omega}, t) = \gamma s \boldsymbol{\omega}, \quad (446)$$

which is formally an addition to the external one-body force field. The force (446) propels the particles into their forward direction with strength γs ; the propulsion is homogeneous in space and time. The parameter s has the interpretation of the speed of free swimming (i.e., without the effects of collisions with other particles). The one-body fields depend also on orientation $\boldsymbol{\omega}$; hence, we have the density distribution $\rho(\mathbf{r}, \boldsymbol{\omega}, t)$, the translational current distribution $\mathbf{J}(\mathbf{r}, \boldsymbol{\omega}, t)$, and the orientational current distribution $\mathbf{J}^\omega(\mathbf{r}, \boldsymbol{\omega}, t)$. As there are no explicit torques acting in the system, the orientational motion is purely diffusive,

$$\mathbf{J}^\omega(1) = -\frac{k_B T}{\gamma^\omega} \nabla^\omega \rho(1), \quad (447)$$

where $1 \equiv \mathbf{r}, \boldsymbol{\omega}, t$ is a shorthand, γ^ω is the friction constant for the overdamped rotational motion, and ∇^ω is the orientational derivative, which in two spatial dimensions is simply $\nabla^\omega \rightarrow \partial/\partial\varphi$. The rotational current features in the continuity equation, which has the form

$$\dot{\rho}(1) = -\nabla \cdot \mathbf{J}(1) - \nabla^\omega \cdot \mathbf{J}^\omega(1). \quad (448)$$

We consider steady states, and hence $\dot{\rho}(1) = 0$. Furthermore, for isotropic, homogeneous fluid steady states $\rho(\mathbf{r}, \boldsymbol{\omega}, t) = \rho_b = \text{const}$ and the current distribution is $\mathbf{J}(\mathbf{r}, \boldsymbol{\omega}, t) = J_b \boldsymbol{\omega}$, where ρ_b is the bulk fluid density and J_b is the strength of the “forward” current (of the swimming motion in the $\boldsymbol{\omega}$ direction). For constant density, the rotational current (447) clearly vanishes [$\mathbf{J}^\omega(1) = 0$], and hence the continuity equation (448) is satisfied.

The task is to find a relationship $J_b(\rho_b)$ that would act like a dynamical equation of state and determine the average current given the fluid density of the system. We assume that the superadiabatic free power contains the following dissipative contribution:

$$P_i^{\text{exc}}[\rho, \mathbf{J}] = \frac{\gamma}{2} \int d1 \int d2 \rho(1) \rho(2) [\mathbf{v}(1) - \mathbf{v}(2)]^2 M(1, 2), \quad (449)$$

where $1 \equiv \mathbf{r}, \boldsymbol{\omega}$ and $2 \equiv \mathbf{r}', \boldsymbol{\omega}'$ are again shorthand notations and $M(1, 2)$ is a density-dependent correlation kernel that couples the two configurational points to each other and the microscopic velocity field \mathbf{v} is defined as usual [$\mathbf{v}(1) = \mathbf{J}(1)/\rho(1)$]. Note that the squared velocity difference in Eq. (449) is a scalar measure of the crossflow that occurs in the system. (Particles with different orientations tend to collide, given a suitable spatial setup.) The squared velocity difference is in Eq. (449) multiplied by the density distribution at both points in order to give a statistical weight to the actual occurrence of such collisions. Hence, besides the fact that Eq. (449) constitutes a simple low-order power series term, we can find a clear physical interpretation of an interflow dissipation measure.

[Hermann *et al.* \(2019\)](#) showed that motility-induced phase separation into active gas and liquid phases is described when taking into account further superadiabatic force contributions besides drag, as previously considered. Primarily, these consist of pressure and “quiet life” chemical potential terms. [Hermann, de las Heras, and Schmidt \(2021\)](#) gave considerable further background on the theory and, in particular, of the angular Fourier decomposition methods, as also used for the exact solution of ideal active sedimentation in two dimensions ([Hermann and Schmidt, 2018](#)). The theory yields the interfacial tension in a natural way, as demonstrated by [Hermann, de las Heras, and Schmidt \(2019\)](#) in a nonequilibrium generalization of the classical square-gradient interfacial theory ([Rowlinson and Widom, 2002](#)). Four different types of superadiabatic force contributions are shown to be relevant [$\mathbf{F}_{\text{sup}}(\mathbf{r}, \boldsymbol{\omega}) = \sum_{\alpha=0}^3 \mathbf{F}_{\text{sup},\alpha}(\mathbf{r}, \boldsymbol{\omega})$] in a full position- and orientation-resolved description.

Both $\mathbf{F}_{\text{sup},0}$ and $\mathbf{F}_{\text{sup},1}$ describe drag, with the isotropic component $\mathbf{F}_{\text{sup},0}$ leading to the reduction of the mean swim speed in bulk. The anisotropic drag force density $\mathbf{F}_{\text{sup},1}$ occurs in inhomogeneous situations and is smaller in magnitude than $\mathbf{F}_{\text{sup},0}$. The force density $\mathbf{F}_{\text{sup},2} = -\nabla \Pi_2$ is naturally expressed as the gradient of a spherical superadiabatic pressure Π_2 . This intrinsic term balances the swim pressure P_{swim} , with corresponding force density $-\nabla P_{\text{swim}}$, that occurs due to the self-propulsion force. The intrinsic quiet life force density $\mathbf{F}_{\text{sup},3} = -\rho \nabla \nu_3$ originates naturally from a nonequilibrium chemical potential ν_3 , and it is this term that balances the strong adiabatic repulsion that primarily occurs in the liquid phase. Ultimately, ν_3 drives the motility-induced phase separation into dilute and dense steady states.

Figures 8 summarizes these results, including an illustration of the nonequilibrium phase coexistence and direction of the relevant forces [Fig. 8(a)], the theoretical bulk phase diagram [Fig. 8(b)] as compared to simulation data, and the behavior of the interfacial tension γ_{gl} [Fig. 8(c)] of the free interface between the phase separated bulk phases. The theory yields $\gamma_{\text{gl}} \geq 0$, in contrast to the findings by [Bialké *et al.* \(2015\)](#); see also [Speck \(2020\)](#) and [de las Heras, Hermann, and Schmidt \(2022\)](#). [Hermann and Schmidt \(2020\)](#) derived an exact sum rule that links the total interface polarization M_{tot} (i.e., the overall degree of orientational order that particles near the interface exhibit) to the value of the swim current in the adjacent bulk phases, $M_{\text{tot}}/L = (J_g - J_l)/(2D_{\text{rot}})$, where L is the length of the interface, J_g (J_l) is the current in the

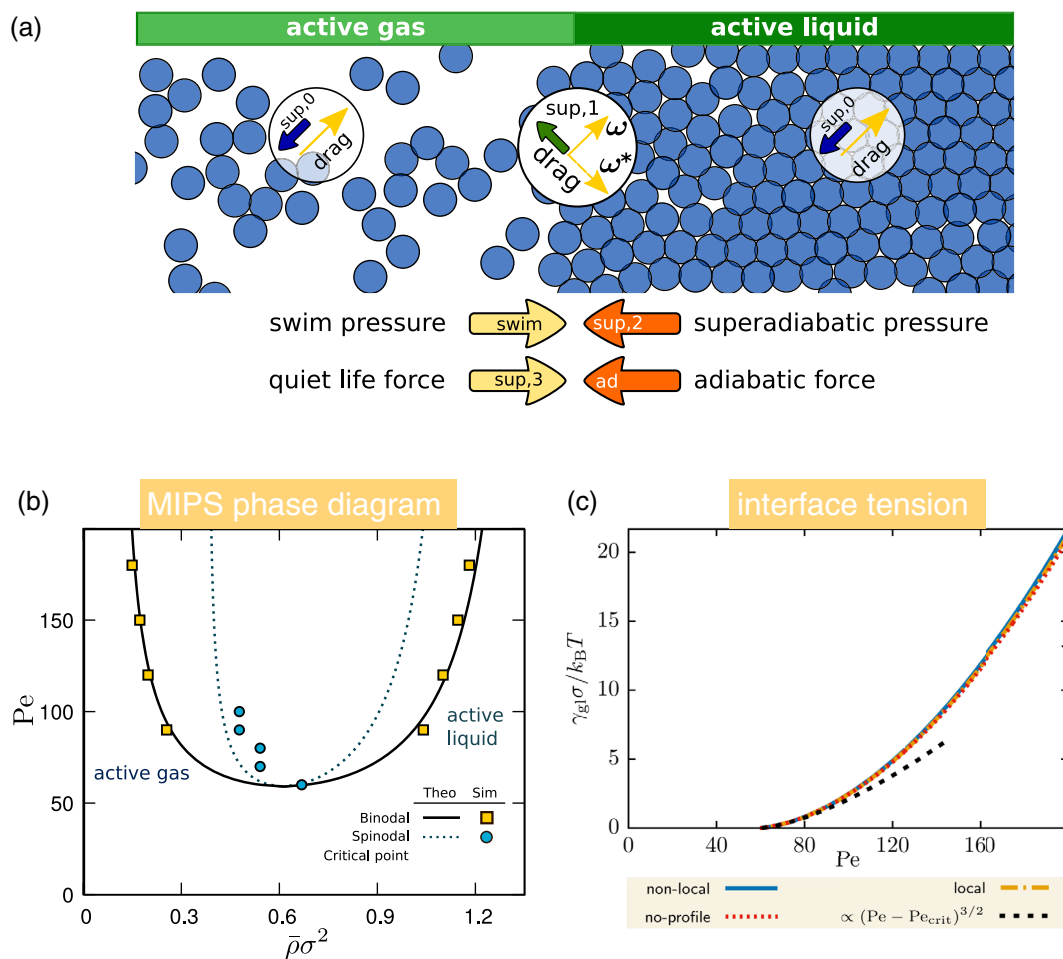


FIG. 8. Motility-induced phase separation of active Brownian particles. (a) Repulsive spheres that swim along an intrinsic orientation ω phase separate spontaneously into a dilute (active gas) and a dense (active liquid) phase. Drag forces hinder the swimming and slow down the motion (white circles). Thick arrows indicate different types of forces: The swim pressure arises from the interface polarization and it is balanced by the intrinsic superadiabatic pressure Π_2 . The quiet life force compresses the liquid and balances the adiabatic force. The interparticle interactions are of a purely repulsive Lennard-Jones type, with length scale σ and energy scale ϵ . (b) Phase diagram as a function of the scaled density $\bar{\rho}\sigma^2$ and Pelet number Pe . Shown are the theoretical results for the binodal and the spinodal compared against simulation data (symbols) for the binodal (Paliwal *et al.*, 2018) and the spinodal (Stenhammar *et al.*, 2013). (a),(b) Adapted from Hermann *et al.*, 2019. (c) Interface tension γ_{gl} as a function of Pelet number Pe , as obtained from the nonequilibrium square-gradient power functional treatment of the problem. Here $\gamma_{gl} \geq 0$, in contrast to the findings of Bialké *et al.* (2015). Three methods (nonlocal, no profile, local) give a unique result: the scaling with mean-field exponent $3/2$ is shown near the critical point. Adapted from Hermann, de las Heras, and Schmidt, 2019.

active gas (liquid), and D_{rot} is the rotational diffusion constant. Hence, Hermann and Schmidt (2020) concluded that the interface polarization is a state function; the power functional approximation respects this exact property. The sum rule itself was verified with a light-controlled Janus-type swimmer in the vicinity of an abrupt activity step, both in an experimental setup and using numerical solution of the underlying Smoluchowski equation (Auschra *et al.*, 2020; Söker *et al.*, 2020). On the basis of Noether's theorem Hermann and Schmidt (2021, 2022) clarified the role of interfacial forces in motility-induced phase separation.

V. CONCLUSIONS AND OUTLOOK

In conclusion, I have described how to approach the dynamics of coupled many-body systems in a functional setting. The functional point of view allows for systematic

coarse graining, or synonymously integrating out degrees of freedom, while retaining a microscopically sharp description both in space and in time. The fundamental variational variables are one-body fields that depend on time and on a single space coordinate. The existence of a generating functional ensures that the description is complete, i.e., that two- and higher-body correlation functions, again microscopically resolved in space and time, are contained in the treatment. The benefits of this variational setup are the relative ease of carrying out practical calculations, as well as the direct access to physical effects, because the one-body fields corresponding to local density, velocity, and acceleration both are manageable in terms of numerical representability and also admit direct physical intuition to be exploited. The kinematic fields represent the dynamical behavior of the system directly. No coarse graining in a hydrodynamical sense of smoothing is implied. Rather, correlations on the particle scale are

accessible. Concretely, for the case of two-body correlation functions, both the dynamical test-particle limit and the nonequilibrium OZ relations allow access.

While the existence of a generating functional guarantees and defines the overarching theoretical structure, the approach is not merely a formal one. This is, in particular, due to the description of the dynamics as stemming from both adiabatic and superadiabatic contributions, where the former are treated within the well-established and powerful framework of density-functional theory. The latter, superadiabatic effects are generated from a unique and increasingly well-characterized object, the free power functional. For the dynamical system the free power plays a role similar to that of the free energy in equilibrium.

While the power functional variational principle may appear to be formal at first glance, it has deep roots in the Gibbs-Appell-Gauss formulation of classical mechanics. The Euler-Lagrange equation that results from the free power minimization principle has the direct physical interpretation of a force balance relationship (or Newton's second law). This situation renders the task of constructing approximations physically intuitive, as I have shown for a number of nonequilibrium phenomena. Moreover, the concept allows straightforward access to the physics via particle-based simulation work. Here I have covered techniques such as custom flow that allow one to access relevant information for the genuine structure and inner working of theory, i.e., for the challenging task of finding approximations for the superadiabatic free power functional.

I have described the essentials of density-functional theory as an appropriate technique to describe the adiabatic state, which is a reference concept that allows one to uniquely define those contributions to the dynamics that can be understood on the basis of an equilibrium free energy. This possibility might seem surprising to some readers, given that the system is genuinely driven out of equilibrium and no near-equilibrium, linear response, or similar restriction applies. But within the functional setting the adiabatic contribution is uniquely identified as that part of the free power that is an instantaneous density functional. The superadiabatic contributions to the dynamics are of a genuine nonequilibrium character, as the corresponding functional generator depends on the motion of the system, as characterized by the flow, acceleration, and time-dependent density profile. The functional dependence is nonlocal in space and time, whereas the latter dependence is causal and, as described in dynamical test-particle and transient shear settings, the dependence can be modeled by memory kernel techniques.

The custom flow concept and simulation algorithm, for both BD and MD, allows one to implement directly the functional point of view of many-body dynamics. Here the reversed map from the motion of the system to the corresponding external driving force field is readily explicitly constructed. The technique solves the inherent inverse problem in an algorithmically straightforward and computationally efficient way. It allows both for scrutiny of the functional concepts and for giving a powerful means for testing and developing concrete power functional approximations. I have described a range of such concrete power functional approximations for dynamical phenomena, ranging from the van Hove function that characterizes the equilibrium dynamics of a quiescent bulk liquid to

viscoelastic, structural, and memory effects of sheared fluids, as well as to nonequilibrium structure formation, such as laning in counterdriven mixtures and motility-induced phase separation of active Brownian particles.

The underlying power functional approximations are based on the unifying concept of kinematic dependence on the flow. Local, semilocal (i.e., those via gradients), and also genuine spatiotemporal nonlocal functional dependencies are relevant. As shown in the description of the adiabatic state, these mathematical tools are formally akin to those used in classical DFT, but with the important physical distinction of representing kinematic functionals that operate on the motion of the system rather than merely being functionally dependent on the density profile. The kinematic dependence is grounded in the many-body foundation of the theory, where the central minimization principle is akin to the Gibbs-Appell-Gaussian formulation of classical mechanics. Levy's search method then facilitates the construction of the reduced one-body description. The theory requires a modest amount of functional calculus; Appendixes A.1 and A.2 give the necessary background for readers who want to increase their knowledge on the topic.

Much of the concrete power functional work has been carried out to date for the case of overdamped Brownian dynamics and tightly interwoven with simulation methodology. These model dynamics are simple and they represent, in a simple fashion, the motion of colloids. The generality of the power functional approach is apparent through the quantum and classical inertial dynamics, as represented by the Schrödinger and Liouville equations, respectively. I have presented significant background for readers who want to access the original publications. The presented power functional approximations both validate the variational concept and demonstrate that the functional point of view allows one to gain insight into the genuine physics at play. The involved objects carry profound physical meaning well beyond the functional nature. Examples thereof include the flow-structure splitting of forces in Brownian dynamics (de las Heras and Schmidt, 2020) and the total-differential decomposition of forces in mixtures (Geigenfeind, de las Heras, and Schmidt, 2020). Furthermore, the memory structure is such that specific combinations of the kinematic fields occur in the memory integral (Treffenstädt and Schmidt, 2021).

The functional point of view both offers insight into the deep structure of nonequilibrium dynamics and represents an excellent candidate for providing a computational framework for the systematic and comprehensive description and classification of many-body dynamics out of equilibrium, performing a role similar to the one that DFT plays as the gold standard for the behavior in equilibrium. As no universal consensus on the description of nonequilibrium dynamics has been reached, the material covered in this review puts forward power functional theory as a competitive contender. Significant potential exists for elucidating the mechanisms that govern the crossover regimes between the considered types of dynamics, i.e., from quantum to classical, and from inertial to overdamped dynamics. There is much potential for cross fertilization between these regimes. Furthermore, it is highly relevant to address from a general point of view open problems such as nonequilibrium phase transitions [see Lips, Ryabov, and Maass (2018) for a striking recent case] and the

foundations of nonequilibrium thermodynamics. On a practical level, it is easier to construct approximations for scalars (P_t^{exc}) than for force fields. Having a reliable theoretical scheme also allows numerical results to be obtained faster than is possible with simulation methods.

Significant work lies ahead, both in conceptual terms, of a practical nature, and for concrete systems and physical phenomena. We describe several potentially fruitful directions in the following. It would be interesting to relate power functional theory to the concept of quasiuniversality of simple fluids, as pioneered by Dyre and co-workers [see Dyre (2016) for a review], as well as to the Rosenfeld (1977) entropy scaling; see Mittal, Errington, and Truskett (2006) and Mittal *et al.* (2008) for applications and Dyre (2018) for a recent review. It would be worthwhile to investigate superadiabatic effects in processes such as spinodal decomposition (Evans, 1979; Archer and Evans, 2004) and in “gravitational” collapse of colloidal monolayers (Bleibel *et al.*, 2014). Exploring possible connections to generalized Langevin equations [see Amati, Meyer, and Schilling (2019) for recent work] and to the use of rate equations [see Dixit, Schilling, and Oettel (2018) for recent work] would be valuable. It would be interesting to see how power functional theory could be useful in going beyond classical nucleation theory (Lutsko, 2018), investigating the “dynamical barrier” in many-body correlations in hard spheres (Robinson *et al.*, 2019), making connections to stochastic thermodynamics (Seifert and Speck, 2010; Seifert, 2012; Leonard *et al.*, 2013), and, in particular, to the concept of the entropy production rate; see the insightful work by Speck (2016).

Furthermore, investigating nonisothermal conditions, where recent work addressed the effects of fluctuating hydrodynamics on Brownian motion (Falasco and Kroy, 2016), would be worthwhile. Relating to the behavior of memory kernels in molecular dynamics (Jung and Schmid, 2016; Lesnicki *et al.*, 2016; Jung, Hanke, and Schmid, 2017) is worthwhile. Identifying the superadiabatic force contributions in driven mixtures of spheres and spherocylinders could be revealing for the observed ordering phenomena in this system (Lüders, Siems, and Nielaba, 2019). Applying power functional theory to the task of classifying new states of active matter (Menzel, 2016) lends an exciting perspective. Even simple types of external fields such as gravity can induce complex phenomena. Obtaining a predictive quantitative framework for the sedimentation dynamics of colloidal mixtures (de las Heras *et al.*, 2012; de las Heras and Schmidt, 2013, 2015; Hermann and Schmidt, 2018; Eckert, Schmidt, and de las Heras, 2021) would be valuable.

It would be highly interesting to explore the consequences of the nonequilibrium Ornstein-Zernike relation (Brader and Schmidt, 2013, 2014) and, in particular, to apply it to concrete problems. Given the central role of the equilibrium Ornstein-Zernike equation for liquid state theory, one would expect its nonequilibrium version to play a similarly crucial future role in the description of dynamical phenomena in complex liquids. When it is flanked by the dynamical test-particle limit (Archer, Hopkins, and Schmidt, 2007; Hopkins *et al.*, 2010; Brader and Schmidt, 2015a), one appears to be well equipped for a fresh view on the dynamical two-body structure of complex systems and to explore fundamental

links to, say, mode-coupling theory [see Janssen (2018) for a recent review] in order to investigate transient dynamics of colloidal liquids (Zausch *et al.*, 2008). The relationship to recent progress beyond the usual hydrodynamic description obtained in the Zwanzig-Mori projection-operator formalism (Vogel and Fuchs, 2020) is also worth exploring. Furthermore, the dynamical sum rules that follow from Noether’s theorem (Hermann and Schmidt, 2021) provide valuable resources.

Finally, and arguably most importantly and also implicit in all of the previously mentioned items, we point out the importance of future developments of first-principles microscopically based approximations to the excess power functional. This task surely is highly challenging but has significant potential for an ultimately high reward.

ACKNOWLEDGMENTS

I thank Joseph Brader, Daniel de las Heras, and Sophie Hermann for their input and great scientific contributions. Daniel and Sophie are acknowledged for careful proofreading and significant feedback on the article, for which I also thank the referees and the editors. All remaining errors are mine. I thank Elias Bernreuther, Moritz Brütting, Brams Dwandaru, Tobias Eckert, Andrea Fortini, Thomas Geigenfeind, Paul Hopkins, Nikolai Jahreis, Philip Krinninger, Jonas Landgraf, Johannes Renner, Florian Sarmüller, Thomas Schindler, Nico Stuhlmüller, Lucas Treffenstädt, and Thomas Trepl, for their numerous and significant scientific contributions. I am grateful for my stimulating and useful exchange with Bob Evans, Thomas Fischer, and Roland Roth. This work is supported by the German Research Foundation (DFG) via Project No. 436306241.

APPENDIX: FUNCTIONAL CALCULUS

1. Variations and Hamilton’s principle

Consider a classical mechanical system with M degrees of freedom represented by the generalized coordinates $q_1, \dots, q_M \equiv \mathbf{q}$ and by the corresponding generalized velocities $\dot{q}_1, \dots, \dot{q}_M \equiv \dot{\mathbf{q}}$. The Lagrangian $L(\mathbf{q}, \dot{\mathbf{q}}, t)$ specifies the system via the difference between total kinetic and potential energy.

The action integral is then defined as

$$S = \int_{t_1}^{t_2} dt L(\mathbf{q}(t), \dot{\mathbf{q}}(t), t) \quad (\text{A1})$$

for given starting and ending configurations $\mathbf{q}_1 = \mathbf{q}(t_1)$ and $\mathbf{q}_2 = \mathbf{q}(t_2)$, i.e., as specified by all values of the generalized coordinates at an initial time t_1 and a final time t_2 .

There are several equivalent ways to carry out the variation of the action integral. Often one introduces an auxiliary function $\epsilon(t)$ that “perturbs” the path via $\mathbf{q}(t) \rightarrow \mathbf{q}(t) + \epsilon(t)$ and the corresponding change in velocity. Taylor expanding in the perturbation to first order then gives the desired result.

The method via functional differentiation is more formal. To calculate functional derivatives $\delta/\delta f(x)$ with respect to a function $f(x)$, one often needs in practice two rules: First, the rules of differentiation in several variables apply (upon replacing sums over indices of variables by integrals over the argument x). Second, $\delta f(x)/\delta f(x') = \delta(x - x') = \delta(x' - x)$, where $\delta(\cdot)$ is the

Dirac distribution (which is even). The method of functional differentiation might seem less intuitive at first glance, but as it is entirely algebraic it is powerful in practice. Our account is fully explicit in spelling out all function arguments. In practice, this can be advantageous over commonly used, more compact notation; see [Hansen and McDonald \(2013\)](#).

As a demonstration of functional differentiation, we apply the functional derivative to the action integral as follows:

$$\frac{\delta S}{\delta \mathbf{q}(t')} = \frac{\delta}{\delta \mathbf{q}(t')} \int_{t_1}^{t_2} dt L(\mathbf{q}(t), \dot{\mathbf{q}}(t), t) \quad (\text{A2})$$

$$= \int_{t_1}^{t_2} dt \frac{\delta}{\delta \mathbf{q}(t')} L(\mathbf{q}(t), \dot{\mathbf{q}}(t), t) \quad (\text{A3})$$

$$= \int_{t_1}^{t_2} dt \left(\frac{\partial L}{\partial \mathbf{q}(t)} \cdot \frac{\delta \mathbf{q}(t)}{\delta \mathbf{q}(t')} + \frac{\partial L}{\partial \dot{\mathbf{q}}(t)} \cdot \frac{\partial \dot{\mathbf{q}}(t)}{\partial \mathbf{q}(t')} \right) \quad (\text{A4})$$

$$= \int_{t_1}^{t_2} dt \left(\frac{\partial L}{\partial \mathbf{q}(t)} \cdot \mathbf{1} \delta(t-t') + \frac{\partial L}{\partial \dot{\mathbf{q}}(t)} \cdot \frac{d}{dt} \frac{\delta \mathbf{q}(t)}{\delta \mathbf{q}(t')} \right) \quad (\text{A5})$$

$$= \int_{t_1}^{t_2} dt \left[\frac{\partial L}{\partial \mathbf{q}(t)} \delta(t-t') - \left(\frac{d}{dt} \frac{\partial L}{\partial \dot{\mathbf{q}}(t)} \right) \cdot \mathbf{1} \delta(t-t') \right] + \frac{\partial L}{\partial \dot{\mathbf{q}}} \delta(t-t') \Big|_{t_1}^{t_2} \quad (\text{A6})$$

$$= \frac{\partial L}{\partial \mathbf{q}(t')} - \frac{d}{dt} \frac{\partial L}{\partial \dot{\mathbf{q}}} \Big|_{t=t'}, \quad (\text{A7})$$

where $\mathbf{1}$ is the $M \times M$ unit matrix. The boundary term in Eq. (A6) vanishes for $t_1 < t' < t_2$. Multiplication by $\mathbf{1}$ yields the vector to its left in Eq. (A6). Renaming the time variable t' as t and requesting stationarity, i.e., a vanishing derivative, leads to the following Lagrange equations of motion:

$$\frac{d}{dt} \frac{\partial L}{\partial \dot{\mathbf{q}}} - \frac{\partial L}{\partial \mathbf{q}} = 0. \quad (\text{A8})$$

To illustrate the method further, we also derive Hamilton's equations of motion. Rewrite the action integral (A1) as

$$S = \int_{t_1}^{t_2} dt \left(\sum_i \dot{q}_i p_i - H(\mathbf{q}, \mathbf{p}, t) \right), \quad (\text{A9})$$

where $H(\mathbf{q}, \mathbf{p}, t)$ is the Hamiltonian and $p_1, \dots, p_M \equiv \mathbf{p}$ are the generalized momenta corresponding to \mathbf{q} . We vary the action both in momentum and in coordinates independently of each other (using, as before and as is common, "partial" functional derivatives). We start as follows with the variation in the j th generalized momentum:

$$\frac{\delta S}{\delta p_j(t')} = \int_{t_1}^{t_2} dt \frac{\delta}{\delta p_j(t')} \left(\sum_i \dot{q}_i p_i - H(\mathbf{q}, \mathbf{p}, t) \right) \quad (\text{A10})$$

$$= \int_{t_1}^{t_2} dt \left(\sum_i \dot{q}_i(t) \frac{\delta p_i(t)}{\delta p_j(t')} - \frac{\delta H(\mathbf{q}, \mathbf{p}, t)}{\delta p_j(t')} \right) \quad (\text{A11})$$

$$= \int_{t_1}^{t_2} dt \sum_i \left(\dot{q}_i(t) \delta_{ij} \delta(t-t') - \frac{\partial H}{\partial p_i(t)} \frac{\delta p_i(t)}{\delta p_j(t')} \right) \quad (\text{A12})$$

$$= \dot{q}_j(t') - \frac{\partial H}{\partial p_j} \Big|_{t'}, \quad (\text{A13})$$

where we have used $\delta p_i(t)/\delta p_j(t') = \delta(t-t')\delta_{ij}$, with δ_{ij} the Kronecker symbol. We rename t' as t , and by requesting $\delta S/\delta \mathbf{p}(t) = 0$ we obtain

$$\dot{\mathbf{q}} = \frac{\partial H}{\partial \mathbf{p}}, \quad (\text{A14})$$

which is one part of Hamilton's equations of motion.

We next vary the coordinates as follows:

$$\frac{\delta S}{\delta q_j(t')} = \int_{t_1}^{t_2} dt \frac{\delta}{\delta q_j(t')} \left(\sum_i \dot{q}_i p_i - H(\mathbf{q}, \mathbf{p}, t) \right) \quad (\text{A15})$$

$$= \int_{t_1}^{t_2} dt \left(-\frac{\delta}{\delta q_j(t')} \sum_i q_i \dot{p}_i - \frac{\partial H}{\partial q_j(t')} \delta(t-t') \right) + \frac{\delta}{\delta q_j(t')} \sum_i q_i p_i \Big|_{t_1}^{t_2} \quad (\text{A16})$$

$$= -\frac{\partial H}{\partial q_j} \Big|_{t'} - \dot{p}_j(t') + p_j \delta(t-t') \Big|_{t_1}^{t_2}, \quad (\text{A17})$$

where the boundary term¹¹ vanishes for $t_1 < t' < t_2$. After imposing the requirement that $\delta S/\delta \mathbf{q}(t) = 0$, we conclude that

$$\dot{\mathbf{p}} = -\frac{\partial H}{\partial \mathbf{q}}, \quad (\text{A18})$$

which together with Eq. (A14) forms the complete set of Hamilton's equations of motion.

2. Spatiotemporal and time-slice functional derivatives

Functional dependencies can be on functions of a single argument, such as on time, as described in Appendix A.1 for the action integral. The more general case involves functions of several variables, and we describe the generalization, which is straightforward, in the following. We take the position $\mathbf{r} = (x, y, z)$ as an example, where x , y , and z are the Cartesian components. Consider a generic functional $A[f]$, where $f(\mathbf{r})$ is its argument function. The rules of functional differentiation laid out in Appendix A.1 then continue to hold, including the functional chain rule, etc. When building the functional derivative of $f(\mathbf{r})$ with respect to itself $f(\mathbf{r}')$, one has to take account of the increased dimensionality of the arguments \mathbf{r} and \mathbf{r}' . The result is $\delta f(\mathbf{r})/\delta f(\mathbf{r}') = \delta(\mathbf{r}-\mathbf{r}')$, where $\delta(\cdot)$ indicates the Dirac distribution in three dimensions. The dimensionality is implicit in the notation, as the argument $\mathbf{r}-\mathbf{r}'$ is a three-dimensional vector. [More explicit notation is $\delta^{(3)}(\mathbf{r}) \equiv \delta^{(1)}(x)\delta^{(1)}(y)\delta^{(1)}(z)$, where the superscript indicates the dimension.]

Spatiotemporal functional derivatives with respect to a function $f(\mathbf{r}, t)$ follow the same scheme, with $\delta f(\mathbf{r}, t)/\delta f(\mathbf{r}', t') = \delta(\mathbf{r}-\mathbf{r}')\delta(t-t')$, where the spatial part of the

¹¹For modern work on the status of the boundary values in Hamilton's principle, see [Galley \(2013\)](#).

result is again a three-dimensional Dirac distribution (multiplied by a one-dimensional Dirac distribution in time). Note that two distinct positions \mathbf{r} and \mathbf{r}' , as well as two distinct times t and t' , are involved. Physically speaking, given some functional $A[f]$ of $f(\mathbf{r}, t)$, functionally differentiating $[\delta A[f]/\delta f(\mathbf{r}, t)]$ monitors the response of $A[f]$ to a change in argument function at the spacetime point \mathbf{r}, t .

An important special case involves only a single time argument. Consider again the situation of a time-dependent function $f(\mathbf{r}, t)$, but disregard the temporal dependence and allow only position changes. A simple example is an instantaneous position integral $A_t[f] = \int d\mathbf{r} f(\mathbf{r}, t)$, where t is fixed and hence treated as a constant. The time-slice functional derivative then yields $\delta A_t[f]/\delta f(\mathbf{r}, t) = \int d\mathbf{r}' \delta f(\mathbf{r}, t)/\delta f(\mathbf{r}', t) = \int d\mathbf{r}' \delta(\mathbf{r} - \mathbf{r}') = 1$ for an appropriate integration domain. Hence, the fundamental rule for the time-slice derivative is $\delta f(\mathbf{r}, t)/\delta f(\mathbf{r}', t) = \delta(\mathbf{r} - \mathbf{r}')$, with no time dependence on the right-hand side. Here the time-slice derivative is notated by the same time argument (t) that appears twice on the left-hand side.

3. Gibbs-Appell-Gaussian classical mechanics

We describe the Gibbs-Appell-Gaussian formulation of classical mechanics following the presentation by [Evans and Morriss \(2013\)](#); an excellent pedagogical account was given by [Desloge \(1988\)](#). Consider Newton's second law while using Cartesian coordinates in a system with no constraints,

$$m_i \ddot{\mathbf{r}}_i(t) = \mathbf{f}_i(t), \quad (\text{A19})$$

where \mathbf{f}_i is the total force acting on particle i . Introduce the acceleration

$$\mathbf{a}_i(t) = \ddot{\mathbf{r}}_i(t) \quad (\text{A20})$$

at time t . The task is to determine $\mathbf{a}_i(t)$. To do so, keep all positions $\mathbf{r}_i(t)$ and all velocities $\mathbf{v}_i(t) = \dot{\mathbf{r}}_i(t)$ fixed at time t . There are then two alternatives.

- (i) Determine the acceleration from Newton's second law according to

$$\mathbf{a}_i(t) = \frac{\mathbf{f}_i(t)}{m_i}, \quad (\text{A21})$$

where the right-hand side is (and must be) known. This fixes the dynamics and constitutes Newton's version of classical mechanics.

- (ii) The alternative is to construct a scalar cost function $G_t(\mathbf{r}^N, \mathbf{v}^N, \mathbf{a}^N, t)$ such that, at the minimum with respect to all $\mathbf{a}_i(t)$, Newton's second law holds. Here the accelerations $\mathbf{a}_i(t)$ are considered to be trial functions. (Conceptually, this is a significant step in addition to the thinking behind Hamilton's principle.) Define the Gibbs-Appell Gaussian as

$$G_t = \sum_i \left(\frac{m_i}{2} \mathbf{a}_i^2(t) - \mathbf{f}_i(t) \cdot \mathbf{a}_i(t) \right). \quad (\text{A22})$$

At the minimum

$$\frac{\partial G_t}{\partial \mathbf{a}_i(t)} = 0 \quad (\text{min}), \quad (\text{A23})$$

from which we conclude that

$$m_i \mathbf{a}_i(t) - \mathbf{f}_i(t) = 0, \quad (\text{A24})$$

as desired, i.e., Eq. (A21). Hence, the result is analogous to that of method (i). In contrast to method (i), here the accelerations have the status of trial variables, i.e., they do not have to possess the correct physical values at the stage of Eq. (A22).

When one puts things into context, classical mechanics features three alternative variational principles, attributable to d'Alembert: $\sum_i (m_i \ddot{\mathbf{r}}_i - \mathbf{f}_i) \cdot \delta \mathbf{r}_i = 0$, Jourdain: $\sum_i (m_i \ddot{\mathbf{r}}_i - \mathbf{f}_i) \cdot \delta \dot{\mathbf{r}}_i = 0$, and Gibbs, Appell, and Gauss: $\sum_i (m_i \ddot{\mathbf{r}}_i - \mathbf{f}_i) \cdot \delta \ddot{\mathbf{r}}_i = 0$. Here the variations are performed, respectively, in position $\delta \mathbf{r}_i$, velocity $\delta \dot{\mathbf{r}}_i$, or acceleration $\delta \ddot{\mathbf{r}}_i$. See [Evans and Morriss \(2013\)](#) for a thorough account, including the treatment of constraints.

REFERENCES

- Amati, G., H. Meyer, and T. Schilling, 2019, "Memory effects in the Fermi-Pasta-Ulam model," *J. Stat. Phys.* **174**, 219.
- Anero, J. G., P. Español, and P. Tarazona, 2013, "Functional thermodynamics: A generalization of dynamic density functional theory to non-isothermal situations," *J. Chem. Phys.* **139**, 034106.
- Angioletti-Uberti, S., M. Ballauff, and J. Dzubiella, 2014, "Dynamic density functional theory of protein adsorption on polymer-coated nanoparticles," *Soft Matter* **10**, 7932.
- Angioletti-Uberti, S., M. Ballauff, and J. Dzubiella, 2018, "Competitive adsorption of multiple proteins to nanoparticles: The Vroman effect revisited," *Mol. Phys.* **116**, 3154.
- Archer, A. J., and R. Evans, 2001, "Binary Gaussian core model: Fluid-fluid phase separation, and interfacial properties," *Phys. Rev. E* **64**, 041501.
- Archer, A. J., and R. Evans, 2004, "Dynamical density functional theory and its application to spinodal decomposition," *J. Chem. Phys.* **121**, 4246.
- Archer, A. J., R. Evans, and R. Roth, 2002, "Microscopic theory of solvent-mediated long-range forces: Influence of wetting," *Europhys. Lett.* **59**, 526.
- Archer, A. J., P. Hopkins, and M. Schmidt, 2007, "Dynamics in inhomogeneous liquids and glasses via the test particle limit," *Phys. Rev. E* **75**, 040501(R).
- Archer, A. J., and M. Rauscher, 2004, "Dynamical density functional theory for interacting Brownian particles: Stochastic or deterministic?," *J. Phys. A* **37**, 9325.
- Auschra, S., V. Holubec, N. A. Söker, F. Cichos, and K. Kroy, 2020, "Polarization-density patterns of active particles in motility gradients," [arXiv:2010.16234](#).
- Balucani, U., and M. Zoppi, 1994, *Dynamics of the Liquid State* (Clarendon Press, Oxford).
- Bechinger, C., R. Di Leonardo, H. Löwen, C. Reichhardt, G. Volpe, and G. Volpe, 2016, "Active particles in complex and crowded environments," *Rev. Mod. Phys.* **88**, 045006.

- Berner, J., B. Müller, J. Ruben Gomez-Solano, M. Krüger, and C. Bechinger, 2018, “Oscillating modes of driven colloids in overdamped systems,” *Nat. Commun.* **9**, 999.
- Bernreuther, E., and M. Schmidt, 2016, “Superadiabatic forces in the dynamics of the one-dimensional Gaussian core model,” *Phys. Rev. E* **94**, 022105.
- Bialké, J., J. T. Siebert, H. Löwen, and T. Speck, 2015, “Negative Interfacial Tension in Phase-Separated Active Brownian Particles,” *Phys. Rev. Lett.* **115**, 098301.
- Bier, M., and R. van Roij, 2007, “Relaxation dynamics in fluids of platelike colloidal particles,” *Phys. Rev. E* **76**, 021405.
- Bier, M., and R. van Roij, 2008, “Nonequilibrium steady states in fluids of platelike colloidal particles,” *Phys. Rev. E* **77**, 021401.
- Bier, M., R. van Roij, M. Dijkstra, and P. van der Schoot, 2008, “Self-Diffusion of Particles in Complex Fluids: Temporary Cages and Permanent Barriers,” *Phys. Rev. Lett.* **101**, 215901.
- Bird, R. B., R. C. Armstrong, and O. Hassager, 1987 *Dynamics of Polymeric Liquid, Vol. 1: Fluid Mechanics*, 2nd ed. (John Wiley, New York).
- Bleibel, J., A. Domínguez, and M. Oettel, 2016, “A dynamic DFT approach to generalized diffusion equations in a system with long-ranged and hydrodynamic interactions,” *J. Phys. Condens. Matter* **28**, 244021.
- Bleibel, J., A. Domínguez, M. Oettel, and S. Dietrich, 2014, “Capillary attraction induced collapse of colloidal monolayers at fluid interfaces,” *Soft Matter* **10**, 4091.
- Borgis, D., R. Assaraf, B. Rotenberg, and R. Vuilleumier, 2013, “Computation of pair distribution functions and three-dimensional densities with a reduced variance principle,” *Mol. Phys.* **111**, 3486.
- Brader, J. M., 2010, “Nonlinear rheology of colloidal dispersions,” *J. Phys. Condens. Matter* **22**, 363101.
- Brader, J. M., M. E. Cates, and M. Fuchs, 2012, “First-principles constitutive equation for suspension rheology,” *Phys. Rev. E* **86**, 021403.
- Brader, J. M., and M. Krüger, 2011, “Density profiles of a colloidal liquid at a wall under shear flow,” *Mol. Phys.* **109**, 1029.
- Brader, J. M., and M. Schmidt, 2013, “Nonequilibrium Ornstein-Zernike relation for Brownian many-body dynamics,” *J. Chem. Phys.* **139**, 104108.
- Brader, J. M., and M. Schmidt, 2014, “Dynamic correlations in Brownian many-body systems,” *J. Chem. Phys.* **140**, 034104.
- Brader, J. M., and M. Schmidt, 2015a, “Power functional theory for the dynamic test particle limit,” *J. Phys. Condens. Matter* **27**, 194106.
- Brader, J. M., and M. Schmidt, 2015b, “Free power dissipation from functional line integration,” *Mol. Phys.* **113**, 2873.
- Brütting, M., T. Trepl, D. de las Heras, and M. Schmidt, 2019, “Superadiabatic forces via the acceleration gradient in quantum many-body dynamics,” *Molecules* **24**, 3660.
- Cats, P., S. Kuipers, S. de Wind, R. van Damme, G. M. Coli, M. Dijkstra, and R. van Roij, 2021, “Machine-learning free-energy functionals using density profiles from simulations,” *APL Mater.* **9**, 031109.
- Chacko, B., R. Evans, and A. J. Archer, 2017, “Solvent fluctuations around solvophobic, solvophilic, and patchy nanostructures and the accompanying solvent mediated interactions,” *J. Chem. Phys.* **146**, 124703.
- Chakrabarti, J., J. Dzubiella, and H. Löwen, 2003, “Dynamical instability in driven colloids,” *Europhys. Lett.* **61**, 415.
- Chakrabarti, J., J. Dzubiella, and H. Löwen, 2004, “Reentrance effect in the lane formation of driven colloids,” *Phys. Rev. E* **70**, 012401.
- Chan, G. K.-L., and R. Finken, 2005, “Time-Dependent Density Functional Theory of Classical Fluids,” *Phys. Rev. Lett.* **94**, 183001.
- Clerk-Maxwell, J., 1874, “van der Waals on the continuity of the gaseous and liquid states,” *Nature (London)* **10**, 477.
- Coe, M. K., R. Evans, and N. B. Wilding, 2022, “Density Depletion and Enhanced Fluctuations in Water near Hydrophobic Solutes: Identifying the Underlying Physics,” *Phys. Rev. Lett.* **128**, 045501.
- Davidchack, R. L., B. B. Laird, and R. Roth, 2016, “Hard spheres at a planar hard wall: Simulations and density functional theory,” *Condens. Matter Phys.* **19**, 23001.
- de las Heras, D., J. M. Brader, A. Fortini, and M. Schmidt, 2016, “Particle conservation in dynamical density functional theory,” *J. Phys. Condens. Matter* **28**, 244024.
- de las Heras, D., N. Doshi, T. Cosgrove, J. Phipps, D. I. Gittins, J. S. van Duijneveldt, and M. Schmidt, 2012, “Floating nematic phase in colloidal platelet-sphere mixtures,” *Sci. Rep.* **2**, 789.
- de las Heras, D., S. Hermann, and M. Schmidt, 2022, “Interfacial tension in motility-induced phase separation” (to be published).
- de las Heras, D., J. Renner, and M. Schmidt, 2019, “Custom flow in overdamped Brownian dynamics,” *Phys. Rev. E* **99**, 023306.
- de las Heras, D., and M. Schmidt, 2013, “Phase stacking diagram of colloidal mixtures under gravity,” *Soft Matter* **9**, 8636.
- de las Heras, D., and M. Schmidt, 2014, “Full Canonical Information from Grand Potential Density Functional Theory,” *Phys. Rev. Lett.* **113**, 238304.
- de las Heras, D., and M. Schmidt, 2015, “Sedimentation stacking diagram of binary colloidal mixtures and bulk phases in the plane of chemical potentials,” *J. Phys. Condens. Matter* **27**, 194115.
- de las Heras, D., and M. Schmidt, 2018a, “Velocity Gradient Power Functional for Brownian Dynamics,” *Phys. Rev. Lett.* **120**, 028001.
- de las Heras, D., and M. Schmidt, 2018b, “Better than Counting: Density Profiles from Force Sampling,” *Phys. Rev. Lett.* **120**, 218001.
- de las Heras, D., and M. Schmidt, 2020, “Flow and Structure in Nonequilibrium Brownian Many-Body Systems,” *Phys. Rev. Lett.* **125**, 018001.
- de las Heras, D., J. M. Tavares, and M. M. Telo da Gama, 2011, “Phase diagrams of binary mixtures of patchy colloids with distinct numbers of patches: The network fluid regime,” *Soft Matter* **7**, 5615.
- de las Heras, D., E. Velasco, and L. Mederos, 2005, “Capillary Smectization and Layering in a Confined Liquid Crystal,” *Phys. Rev. Lett.* **94**, 017801.
- Desloge, E. A., 1988, “The Gibbs-Appell equation of motion,” *Am. J. Phys.* **56**, 841.
- Dhont, J. K. G., 1996, *An Introduction to the Dynamics of Colloids* (Elsevier, Amsterdam).
- Dixit, M., T. Schilling, and M. Oettel, 2018, “Growth of films with anisotropic particles: Simulations and rate equations,” *J. Chem. Phys.* **149**, 064903.
- Dufty, J., R. Evans, J. Lutsko, and S. Trickey (CECAM), 2019, “Fundamentals of density functional theory for $T > 0$: Quantum meets classical,” https://members.cecama.org/storage/files_workshops/file_4385.pdf.
- Dwandar, W. S. B., and M. Schmidt, 2011, “Variational principle of classical density-functional theory via Levy’s constrained search method,” *Phys. Rev. E* **83**, 061133.
- Dyre, J. C., 2006, “Colloquium: The glass transition and elastic models of glass-forming liquids,” *Rev. Mod. Phys.* **78**, 953.
- Dyre, J. C., 2016, “Simple liquids’ quasiuniversality and the hard-sphere paradigm,” *J. Phys. Condens. Matter* **28**, 323001.
- Dyre, J. C., 2018, “Perspective: Excess-entropy scaling,” *J. Chem. Phys.* **149**, 210901.

- Dzubiella, J., G. P. Hoffmann, and H. Löwen, 2002, “Lane formation in colloidal mixtures driven by an external field,” *Phys. Rev. E* **65**, 021402.
- Dzubiella, J., and C. N. Likos, 2003, “Mean-field dynamical density functional theory,” *J. Phys. Condens. Matter* **15**, L147.
- Eckert, T., M. Schmidt, and D. de las Heras, 2021, “Gravity-induced phase phenomena in plate-rod colloidal mixtures,” *Commun. Phys.* **4**, 202.
- Eckert, T., N. C. X. Stuhlmüller, F. Sammüller, and M. Schmidt, 2020, “Fluctuation Profiles in Inhomogeneous Fluids,” *Phys. Rev. Lett.* **125**, 268004.
- Español, P., and H. Löwen, 2009, “Derivation of dynamical density functional theory using the projection operator technique,” *J. Chem. Phys.* **131**, 244101.
- Esztermann, A., H. Reich, and M. Schmidt, 2006, “Density functional theory for colloidal mixtures of hard platelets, rods, and spheres,” *Phys. Rev. E* **73**, 011409.
- Evans, D. J., and G. P. Morriss, 2013, *Statistical Mechanics of Nonequilibrium Liquids*, 2nd ed. (Cambridge University Press, Cambridge, England).
- Evans, R., 1979, “The nature of the liquid-vapour interface and other topics in the statistical mechanics of non-uniform, classical fluids,” *Adv. Phys.* **28**, 143.
- Evans, R., 1992, “Density functionals in the theory of non-uniform fluids,” in *Fundamentals of Inhomogeneous Fluids*, edited by D. Henderson (Dekker, New York).
- Evans, R., D. Frenkel, and M. Dijkstra, 2019, “From simple liquids to colloids and soft matter,” *Phys. Today* **72**, No. 2, 38.
- Evans, R., M. Oettel, R. Roth, and G. Kahl, 2016, “New developments in classical density functional theory,” *J. Phys. Condens. Matter* **28**, 240401.
- Evans, R., and M. C. Stewart, 2015, “The local compressibility of liquids near non-adsorbing substrates: A useful measure of solvophobicity and hydrophobicity?” *J. Phys. Condens. Matter* **27**, 194111.
- Evans, R., M. C. Stewart, and N. B. Wilding, 2016, “Critical Drying of Liquids,” *Phys. Rev. Lett.* **117**, 176102.
- Evans, R., M. C. Stewart, and N. B. Wilding, 2017, “Drying and wetting transitions of a Lennard-Jones fluid: Simulations and density functional theory,” *J. Chem. Phys.* **147**, 044701.
- Evans, R., M. C. Stewart, and N. B. Wilding, 2019, “A unified description of hydrophilic and superhydrophobic surfaces in terms of the wetting and drying transitions of liquids,” *Proc. Natl. Acad. Sci. U.S.A.* **116**, 23901.
- Evans, R., and N. B. Wilding, 2015, “Quantifying Density Fluctuations in Water at a Hydrophobic Surface: Evidence for Critical Drying,” *Phys. Rev. Lett.* **115**, 016103.
- Falasco, G., and K. Kroy, 2016, “Nonisothermal fluctuating hydrodynamics and Brownian motion,” *Phys. Rev. E* **93**, 032150.
- Farage, T. F. F., P. Krinninger, and J. M. Brader, 2015, “Effective interactions in active Brownian suspensions,” *Phys. Rev. E* **91**, 042310.
- Fortini, A., D. de las Heras, J. M. Brader, and M. Schmidt, 2014, “Superadiabatic Forces in Brownian Many-Body Dynamics,” *Phys. Rev. Lett.* **113**, 167801.
- Galley, C. R., 2013, Classical Mechanics of Nonconservative Systems,” *Phys. Rev. Lett.* **110**, 174301.
- Geigenfeind, T., and D. de las Heras, 2017, “The role of sample height in the stacking diagram of colloidal mixtures under gravity” *J. Phys. Condens. Matter* **29**, 064006.
- Geigenfeind, T., D. de las Heras, and M. Schmidt, 2020, “Superadiabatic demixing in nonequilibrium colloids,” *Commun. Phys.* **3**, 23.
- Giacomello, A., L. Schimmele, S. Dietrich, and M. Tasinkevych, 2016, “Perpetual superhydrophobicity,” *Soft Matter* **12**, 8927.
- Giacomello, A., L. Schimmele, S. Dietrich, and M. Tasinkevych, 2019, “Recovering superhydrophobicity in nanoscale and macroscale surface textures,” *Soft Matter* **15**, 7462.
- Goddard, B. D., A. Nold, N. Savva, G. A. Pavliotis, and S. Kalliadasis, 2012, “General Dynamical Density Functional Theory for Classical Fluids,” *Phys. Rev. Lett.* **109**, 120603.
- González, A., J. A. White, F. L. Román, S. Velasco, and R. Evans, 1997, “Density Functional Theory for Small Systems: Hard Spheres in a Closed Spherical Cavity,” *Phys. Rev. Lett.* **79**, 2466.
- Götze, W., 2008, *Complex Dynamics of Glass Forming Liquids* (Oxford University Press, Oxford).
- Grelet, E., M. P. Lettinga, M. Bier, R. van Roij, and P. van der Schoot, 2008, “Dynamical and structural insights into the smectic phase of rod-like particles,” *J. Phys. Condens. Matter* **20**, 494213.
- Härtel, A., M. Oettel, R. E. Rozas, S. U. Egelhaaf, J. Horbach, and H. Löwen, 2012, “Tension and Stiffness of the Hard Sphere Crystal-Fluid Interface,” *Phys. Rev. Lett.* **108**, 226101.
- Hansen, J. P., and I. R. McDonald, 2013, *Theory of Simple Liquids*, 4th ed. (Academic Press, London).
- Hansen-Goos, H., and K. Mecke, 2009, “Fundamental Measure Theory for Inhomogeneous Fluids of Nonspherical Hard Particles,” *Phys. Rev. Lett.* **102**, 018302.
- Hansen-Goos, H., and R. Roth, 2006, “Density functional theory for hard-sphere mixtures: The White Bear version mark II,” *J. Phys. Condens. Matter* **18**, 8413.
- Hermann, S., D. de las Heras, and M. Schmidt, 2019, “Non-negative Interfacial Tension in Phase-Separated Active Brownian Particles,” *Phys. Rev. Lett.* **123**, 268002.
- Hermann, S., D. de las Heras, and M. Schmidt, 2021, “Phase separation of active Brownian particles in two dimensions: Anything for a quiet life,” *Mol. Phys.* **119**, e1902585.
- Hermann, S., P. Krinninger, D. de las Heras, and M. Schmidt, 2019, “Phase coexistence of active Brownian particles,” *Phys. Rev. E* **100**, 052604.
- Hermann, S., and M. Schmidt, 2018, “Active ideal sedimentation: Exact two-dimensional steady states,” *Soft Matter* **14**, 1614.
- Hermann, S., and M. Schmidt, 2020, “Active interface polarization as a state function,” *Phys. Rev. Research* **2**, 022003(R).
- Hermann, S., and M. Schmidt, 2021, “Noether’s theorem in statistical mechanics,” *Commun. Phys.* **4**, 176.
- Hermann, S., and M. Schmidt, 2022, “Why Noether’s theorem applies to statistical mechanics,” *J. Phys. Condens. Matter* (in press), 10.1088/1361-648X/ac5b47.
- Hernández-Muñoz, J., E. Chacón, and P. Tarazona, 2019, “Density functional analysis of atomic force microscopy in a dense fluid,” *J. Chem. Phys.* **151**, 034701.
- Hohenberg, P., and W. Kohn, 1964, “Inhomogeneous electron gas,” *Phys. Rev.* **136**, B864.
- Hopkins, P., A. Fortini, A. J. Archer, and M. Schmidt, 2010, “The van Hove distribution function for Brownian hard spheres: Dynamical test particle theory and computer simulations for bulk dynamics,” *J. Chem. Phys.* **133**, 224505.
- Irving, J. H., and J. G. Kirkwood, 1950, “The statistical mechanical theory of transport processes. IV. The equations of hydrodynamics,” *J. Chem. Phys.* **18**, 817.
- Jahreis, N., and M. Schmidt, 2020, “Shear-induced deconfinement of hard disks,” *Colloid Polym. Sci.* **298**, 895.
- Janssen, L. M. C., 2018, Mode-coupling theory of the glass transition: A primer,” *Front. Phys.* **6**, 97.
- Jeanmairet, G., M. Levesque, and D. Borgis, 2013, “Molecular density functional theory of water describing hydro-

- phobicity at short and long length scales,” *J. Chem. Phys.* **139**, 154101.
- Jeanmairet, G., M. Levesque, R. Vuilleumier, and D. Borgis, 2013, “Molecular density functional theory of water,” *J. Phys. Chem. Lett.* **4**, 619.
- Jeanmairet, G., B. Rotenberg, D. Borgis, and M. Salanne, 2019, “Study of a water-graphene capacitor with molecular density functional theory,” *J. Chem. Phys.* **151**, 124111.
- Jones, R. O., 2015, “Density functional theory: Its origins, rise to prominence, and future,” *Rev. Mod. Phys.* **87**, 897.
- Jones, R. O., and O. Gunnarsson, 1989, “The density functional formalism, its applications and prospects,” *Rev. Mod. Phys.* **61**, 689.
- Jung, G., M. Hanke, and F. Schmid, 2017, “Iterative reconstruction of memory kernels,” *J. Chem. Theory Comput.* **13**, 2481.
- Jung, G., and F. Schmid, 2016, “Computing bulk and shear viscosities from simulations of fluids with dissipative and stochastic interactions,” *J. Chem. Phys.* **144**, 204104.
- Kierlik, E., and M. L. Rosinberg, 1990, “Free-energy density functional for the inhomogeneous hard-sphere fluid: Application to interfacial adsorption,” *Phys. Rev. A* **42**, 3382.
- Klopotek, M., H. Hansen-Goos, M. Dixit, T. Schilling, F. Schreiber, and M. Oettel, 2017, “Monolayers of hard rods on planar substrates. II. Growth,” *J. Chem. Phys.* **146**, 084903.
- Kohn, W., 1999, “Nobel Lecture: Electronic structure of matter—Wave functions and density functionals,” *Rev. Mod. Phys.* **71**, 1253.
- Krinninger, P., and M. Schmidt, 2019, “Power functional theory for active Brownian particles: General formulation and power sum rules,” *J. Chem. Phys.* **150**, 074112.
- Krinninger, P., M. Schmidt, and J. M. Brader, 2016, “Nonequilibrium Phase Behavior from Minimization of Free Power Dissipation,” *Phys. Rev. Lett.* **117**, 208003; **119**, 029902(E) (2017).
- Lafuente, L., and J. A. Cuesta, 2004, “Density Functional Theory for General Hard-Core Lattice Gases,” *Phys. Rev. Lett.* **93**, 130603.
- Landgraf, J., M. Schmidt, and D. de las Heras, 2022, “Superadiabatic torques in anisotropic colloidal particles” (to be published).
- Leonard, T., B. Lander, U. Seifert, and T. Speck, 2013, “Stochastic thermodynamics of fluctuating density fields: Non-equilibrium free energy differences under coarse-graining,” *J. Chem. Phys.* **139**, 204109.
- Lesnicki, D., R. Vuilleumier, A. Carof, and B. Rotenberg, 2016, “Molecular Hydrodynamics from Memory Kernels,” *Phys. Rev. Lett.* **116**, 147804.
- Levesque, M., R. Vuilleumier, and D. Borgis, 2012, “Scalar fundamental measure theory for hard spheres in three dimensions: Application to hydrophobic solvation,” *J. Chem. Phys.* **137**, 034115.
- Levy, M., 1979, “Universal variational functionals of electron densities, first-order density matrices, and natural spin-orbitals, and solution of the v -representability problem,” *Proc. Natl. Acad. Sci. U.S.A.* **76**, 6062.
- Lin, S.-C., G. Martius, and M. Oettel, 2020, “Analytical classical density functionals from an equation learning network,” *J. Chem. Phys.* **152**, 021102.
- Lin, S.-C., and M. Oettel, 2019, “A classical density functional from machine learning and a convolutional neural network,” *SciPost Phys.* **6**, 25.
- Lips, D., A. Ryabov, and P. Maass, 2018, “Brownian Asymmetric Simple Exclusion Process,” *Phys. Rev. Lett.* **121**, 160601.
- Loehr, J., M. Loenne, A. Ernst, D. de las Heras, and T. M. Fischer, 2016, “Topological protection of multiparticle dissipative transport,” *Nat. Commun.* **7**, 11745.
- Loehr, J., *et al.*, 2018, “Colloidal topological insulators,” *Commun. Phys.* **1**, 4.
- Lüders, A., U. Siems, and P. Nielaba, 2019, “Dynamic ordering of driven spherocylinders in a nonequilibrium suspension of small colloidal spheres,” *Phys. Rev. E* **99**, 022601.
- Lutsko, J. F., 2010, “Recent developments in classical density functional theory,” in *Advances in Chemical Physics*, Vol. 144, edited by S. A. Rice (John Wiley & Sons, New York), p. 1.
- Lutsko, J. F., 2018, “Systematically extending classical nucleation theory,” *New J. Phys.* **20**, 103015.
- Lutsko, J. F., 2020, “Explicitly stable fundamental-measure-theory models for classical density functional theory,” *Phys. Rev. E* **102**, 062137.
- Lutsko, J. F., and J. Lam, 2018, “Classical density functional theory, unconstrained crystallization, and polymorphic behavior,” *Phys. Rev. E* **98**, 012604.
- Lutsko, J. F., and M. Oettel, 2021, “Reconsidering power functional theory,” *J. Chem. Phys.* **155**, 094901.
- Maes, C., 2020, “Fluctuating Motion in an Active Environment,” *Phys. Rev. Lett.* **125**, 208001.
- Marchetti, M. C., J. F. Joanny, S. Ramaswamy, T. B. Liverpool, J. Prost, M. Rao, and R. A. Simha, 2013, “Hydrodynamics of soft active matter,” *Rev. Mod. Phys.* **85**, 1143.
- Marconi, U. M. B., and P. Tarazona, 1999, “Dynamic density functional theory of fluids,” *J. Chem. Phys.* **110**, 8032.
- Martin-Jimenez, D., E. Chacón, P. Tarazona, and R. Garcia, 2016, “Atomically resolved three-dimensional structures of electrolyte aqueous solutions near a solid surface,” *Nat. Commun.* **7**, 12164.
- Menzel, A. M., 2016, “On the way of classifying new states of active matter,” *New J. Phys.* **18**, 071001.
- Menzel, A. M., A. Saha, C. Hoell, and H. Löwen, 2016, “Dynamical density functional theory for microswimmers,” *J. Chem. Phys.* **144**, 024115.
- Mermin, N. D., 1965, “Thermal properties of the inhomogeneous electron gas,” *Phys. Rev.* **137**, A1441.
- Mittal, J., J. R. Errington, and T. M. Truskett, 2006, “Thermodynamics Predicts How Confinement Modifies the Dynamics of the Equilibrium Hard-Sphere Fluid,” *Phys. Rev. Lett.* **96**, 177804.
- Mittal, J., T. M. Truskett, J. R. Errington, and G. Hummer, 2008, “Layering and Position-Dependent Diffusive Dynamics of Confined Fluids,” *Phys. Rev. Lett.* **100**, 145901.
- Moncho-Jordá, A., A. Germán-Bellod, S. Angioletti-Uberti, I. Adroher-Benítez, and J. Dzubiella, 2019, “Nonequilibrium uptake kinetics of molecular cargo into hollow hydrogels tuned by electrosteric interactions,” *ACS Nano* **13**, 1603.
- Nagel, S. R., 2017, “Experimental soft-matter science,” *Rev. Mod. Phys.* **89**, 025002.
- Nakatsukasa, T., K. Matsuyanagi, M. Matsuo, and Y. Yabana, 2016, “Time-dependent density-functional description of nuclear dynamics,” *Rev. Mod. Phys.* **88**, 045004.
- Oettel, M., M. Klopotek, M. Dixit, E. Empting, T. Schilling, and H. Hansen-Goos, 2016, “Monolayers of hard rods on planar substrates. I. Equilibrium,” *J. Chem. Phys.* **145**, 074902 2016.
- Onida, G., L. Reining, and A. Rubio, 2002, “Electronic excitations: Density-functional versus many-body Green’s-function approaches,” *Rev. Mod. Phys.* **74**, 601.
- Onsager, L., 1949, “The effects of shape on the interaction of colloidal particles,” *Ann. N.Y. Acad. Sci.* **51**, 627.

- Paliwal, S., J. Rodenburg, R. van Roij, and M. Dijkstra, 2018, "Chemical potential in active systems: Predicting phase equilibrium from bulk equations of state?," *New J. Phys.* **20**, 015003.
- Percus, J. K., 1962, "Approximation Methods in Classical Statistical Mechanics," *Phys. Rev. Lett.* **8**, 462.
- Percus, J. K., 1976, "Equilibrium state of a classical fluid of hard rods in an external-field," *J. Stat. Phys.* **15**, 505.
- Percus, J. K., and G. J. Yevick, 1958, "Analysis of classical statistical mechanics by means of collective coordinates," *Phys. Rev.* **110**, 1.
- Qi, S., and F. Schmid, 2017, "Hybrid particle-continuum simulations coupling Brownian dynamics and local dynamic density functional theory," *Soft Matter* **13**, 7938.
- Ramakrishnan, T. V., and M. Yussouff, 1979, "First-principles order-parameter theory of freezing," *Phys. Rev. B* **19**, 2775.
- Reiss, H., H. L. Frisch, and J. L. Lebowitz, 1959, "Statistical mechanics of rigid spheres," *J. Chem. Phys.* **31**, 369.
- Remsing, R. C., 2019, "Commentary: Playing the long game wins the cohesion-adhesion rivalry," *Proc. Natl. Acad. Sci. U.S.A.* **116**, 23874.
- Renner, J., M. Schmidt, and D. de las Heras, 2021, "Custom flow in molecular dynamics," *Phys. Rev. Research* **3**, 013281.
- Renner, J., M. Schmidt, and D. de las Heras, 2022, "Shear and Bulk Acceleration Viscosities in Simple Fluids," *Phys. Rev. Lett.* **128**, 094502.
- Rex, M., and H. Löwen, 2009, "Dynamical density functional theory for colloidal dispersions including hydrodynamic interactions," *Eur. Phys. J. E* **28**, 139.
- Robinson, J. F., F. Turci, R. Roth, and C. P. Royall, 2019, "Morphometric Approach to Many-Body Correlations in Hard Spheres," *Phys. Rev. Lett.* **122**, 068004.
- Robledo, A., and C. Varea, "On the relationship between the density functional formalism and the potential distribution theory for nonuniform fluids," *J. Stat. Phys.* **26**, 513 1981.
- Rosenfeld, Y., 1977, "Relation between the transport coefficients and the internal entropy of simple systems," *Phys. Rev. A* **15**, 2545.
- Rosenfeld, Y., 1988, "Scaled field particle theory of the structure and the thermodynamics of isotropic hard particle fluids," *J. Chem. Phys.* **89**, 4272.
- Rosenfeld, Y., 1989, "Free-Energy Model for the Inhomogeneous Hard-Sphere Fluid Mixture and Density-Functional Theory of Freezing," *Phys. Rev. Lett.* **63**, 980.
- Rosenfeld, Y., 1993, "Free-energy model for inhomogeneous fluid mixtures: Yukawa-charged hard-spheres, general interactions, and plasmas," *J. Chem. Phys.* **98**, 8126.
- Rosenfeld, Y., 1994, "Density functional theory of molecular fluids: Free-energy model for the inhomogeneous hard-body fluid," *Phys. Rev. E* **50**, R3318(R).
- Rosenfeld, Y., and N. W. Ashcroft, 1979, "Theory of simple classical fluids: Universality in the short-range structure," *Phys. Rev. A* **20**, 1208.
- Rosenfeld, Y., M. Schmidt, H. Löwen, and P. Tarazona, 1997, "Fundamental-measure free energy density functional for hard spheres: Dimensional crossover and freezing," *Phys. Rev. E* **55**, 4245.
- Rosenfeld, Y., M. Schmidt, M. Watzlawek, and H. Löwen, 2000, "Fluid of penetrable spheres: Testing the universality of the bridge functional," *Phys. Rev. E* **62**, 5006.
- Rotenberg, B., 2020, "Use the force! Reduced variance estimators for densities, radial distribution functions, and local mobilities in molecular simulations," *J. Chem. Phys.* **153**, 150902.
- Roth, R., 2010, "Fundamental measure theory for hard-sphere mixtures: A review," *J. Phys. Condens. Matter* **22**, 063102.
- Roth, R., R. Evans, A. Lang, and G. Kahl, 2002, "Fundamental measure theory for hard-sphere mixtures revisited: The White Bear version," *J. Phys. Condens. Matter* **14**, 12063.
- Rowlinson, J. S., and B. Widom, 2002, *Molecular Theory of Capillarity* (Dover, New York).
- Royall, C. P., J. Dzubiella, M. Schmidt, and A. van Blaaderen, 2007, "Nonequilibrium Sedimentation of Colloids on the Particle Scale," *Phys. Rev. Lett.* **98**, 188304.
- Runge, E., and E. K. U. Gross, 1984, "Density-Functional Theory for Time-Dependent Systems," *Phys. Rev. Lett.* **52**, 997.
- Sammüller, F., and M. Schmidt, 2021, "Adaptive Brownian dynamics," *J. Chem. Phys.* **155**, 134107 2021.
- Scacchi, A., A. J. Archer, and J. M. Brader, 2017, "Dynamical density functional theory analysis of the laning instability in sheared soft matter," *Phys. Rev. E* **96**, 062616.
- Scacchi, A., and J. M. Brader, 2018, "Local phase transitions in driven colloidal suspensions," *Mol. Phys.* **116**, 378.
- Scala, A., T. Voigtmann, and C. De Michele, 2007, "Event-driven Brownian dynamics for hard spheres," *J. Chem. Phys.* **126**, 134109.
- Schilling, T., 2021, Coarse-grained modelling out of equilibrium," *arXiv:2107.09972*.
- Schindler, T., and M. Schmidt, 2016, "Dynamic pair correlations and superadiabatic forces in a dense Brownian liquid," *J. Chem. Phys.* **145**, 064506.
- Schindler, T., R. Wittmann, and J. M. Brader, 2019, "Particle-conserving dynamics on the single-particle level," *Phys. Rev. E* **99**, 012605.
- Schmidt, M., 1999, "An *ab initio* density functional for penetrable spheres," *J. Phys. Condens. Matter* **11**, 10163.
- Schmidt, M., 2001a, "Density functional theory for colloidal rod-sphere mixtures," *Phys. Rev. E* **63**, 050201(R).
- Schmidt, M., 2001b, "Density functional for the Widom-Rowlinson model," *Phys. Rev. E* **63**, 010101(R).
- Schmidt, M., 2002, "Density functional theory for fluids in porous media," *Phys. Rev. E* **66**, 041108.
- Schmidt, M., 2004, "Rosenfeld functional for non-additive hard spheres," *J. Phys. Condens. Matter* **16**, L351.
- Schmidt, M., 2011a, "Density functional for ternary non-additive hard sphere mixtures," *J. Phys. Condens. Matter* **23**, 415101.
- Schmidt, M., 2011b, "Statics and dynamics of inhomogeneous liquids via the internal-energy functional," *Phys. Rev. E* **84**, 051203.
- Schmidt, M., 2015, "Quantum power functional theory for many-body dynamics," *J. Chem. Phys.* **143**, 174108.
- Schmidt, M., 2018, "Power functional theory for Newtonian many-body dynamics," *J. Chem. Phys.* **148**, 044502.
- Schmidt, M., and J. M. Brader, 2013, "Power functional theory for Brownian dynamics," *J. Chem. Phys.* **138**, 214101.
- Schmidt, M., H. Löwen, J. M. Brader, and R. Evans, 2000, "Density Functional for a Model Colloid-Polymer Mixture," *Phys. Rev. Lett.* **85**, 1934.
- Schmidt, M., C. P. Royall, A. van Blaaderen, and J. Dzubiella, 2008, "Non-equilibrium sedimentation of colloids: Confocal microscopy and Brownian dynamics simulations," *J. Phys. Condens. Matter* **20**, 494222.
- Schmidt, M., E. Schöll-Paschinger, J. Köfinger, and G. Kahl, 2002, "Model colloid-polymer mixtures in porous matrices: Density functional versus integral equations," *J. Phys. Condens. Matter* **14**, 12099.
- Schofield, P., and J. R. Henderson, 1982, "Statistical mechanics of inhomogeneous fluids," *Proc. R. Soc. A* **379**, 231.
- Seifert, U., 2012, "Stochastic thermodynamics, fluctuation theorems and molecular machines," *Rep. Prog. Phys.* **75**, 126001.

- Seifert, U., and T. Speck, 2010, “Fluctuation-dissipation theorem in nonequilibrium steady states,” *Europhys. Lett.* **89**, 10007.
- Sergievskiy, V. P., G. Jeanmairet, M. Levesque, and D. Borgis, 2014, “Fast computation of solvation free energies with molecular density functional theory: Thermodynamic-ensemble partial molar volume corrections,” *J. Phys. Chem. Lett.* **5**, 1935.
- Söker, N. A., S. Auschra, V. Holubec, K. Kroy, and F. Cichos, 2020, “Active-particle polarization without alignment forces,” *arXiv:2010.15106*.
- Speck, T., 2016, “Thermodynamic formalism and linear response theory for nonequilibrium steady states,” *Phys. Rev. E* **94**, 022131.
- Speck, T., 2020, “Collective forces in scalar active matter,” *Soft Matter* **16**, 2652.
- Squires, T. M., and S. R. Quake, 2005, “Microfluidics: Fluid physics at the nanoliter scale,” *Rev. Mod. Phys.* **77**, 977.
- Stenhammar, J., A. Tiribocchi, R. J. Allen, D. Marenduzzo, and M. E. Cates, 2013, “Continuum Theory of Phase Separation Kinetics for Active Brownian Particles,” *Phys. Rev. Lett.* **111**, 145702.
- Stewart, M. C., and R. Evans, 2012, “Phase behavior and structure of a fluid confined between competing (solvophobic and solvophilic) walls,” *Phys. Rev. E* **86**, 031601.
- Stewart, M. C., and R. Evans, 2014, “Layering transitions and solvation forces in an asymmetrically confined fluid,” *J. Chem. Phys.* **140**, 134704.
- Stopper, D., A. L. Thorneywork, R. P. A. Dullens, and R. Roth, 2018, “Bulk dynamics of Brownian hard disks: Dynamical density functional theory versus experiments on two-dimensional colloidal hard spheres,” *J. Chem. Phys.* **148**, 104501.
- Stuhlmüller, N. C. X., T. Eckert, D. de las Heras, and M. Schmidt, 2018, “Structural Nonequilibrium Forces in Driven Colloidal Systems,” *Phys. Rev. Lett.* **121**, 098002.
- Tarantino, W., and C. A. Ullrich, 2021, “A reformulation of time-dependent Kohn-Sham theory in terms of the second time derivative of the density,” *J. Chem. Phys.* **154**, 204112.
- Tarazona, P., 2000, “Density Functional for Hard Sphere Crystals: A Fundamental Measure Approach,” *Phys. Rev. Lett.* **84**, 694.
- Tarazona, P., J. A. Cuesta, and Y. Martínez-Ratón, 2008, “Density functional theories of hard particle systems,” *Lect. Notes Phys.* **753**, 247.
- Tarazona, P., and R. Evans, 1984, “A simple density functional theory for inhomogeneous liquids: Wetting by gas at a solid-liquid interface,” *Mol. Phys.* **52**, 847.
- Tchenkoué, M. M., M. Penz, I. Theophilou, M. Ruggenthaler, and A. Rubio, 2019, “Force balance approach for advanced approximations in density functional theories,” *J. Chem. Phys.* **151**, 154107.
- te Vrugt, M., H. Löwen, and R. Wittkowski, 2020, “Classical dynamical density functional theory: From fundamentals to applications,” *Adv. Phys.* **69**, 121.
- Thorneywork, A. L., R. Roth, D. G. A. L. Aarts, and R. P. A. Dullens, 2014, “Communication: Radial distribution functions in a two-dimensional binary colloidal hard sphere system,” *J. Chem. Phys.* **140**, 161106.
- Tonks, L., 1936, “The complete equation of state of one, two and three-dimensional gases of hard elastic spheres,” *Phys. Rev.* **50**, 955.
- Treffenstädt, L. L., T. Schindler, and M. Schmidt, 2022, “Dynamic decay and superadiabatic forces in the van Hove dynamics of bulk hard sphere fluids,” *arXiv:2201.06099*.
- Treffenstädt, L. L., and M. Schmidt, 2020, “Memory-induced motion reversal in Brownian liquids,” *Soft Matter* **16**, 1518.
- Treffenstädt, L. L., and M. Schmidt, 2021, “Universality in Driven and Equilibrium Hard Sphere Liquid Dynamics,” *Phys. Rev. Lett.* **126**, 058002.
- Tschopp, S. M., and J. M. Brader, 2021, “Fundamental measure theory of inhomogeneous two-body correlation functions,” *Phys. Rev. E* **103**, 042103.
- Tschopp, S. M., H. D. Vuijk, A. Sharma, and J. M. Brader, 2020, “Mean-field theory of inhomogeneous fluids,” *Phys. Rev. E* **102**, 042140.
- Turci, F., and N. B. Wilding, 2021, “Phase Separation and Multibody Effects in Three-Dimensional Active Brownian Particles,” *Phys. Rev. Lett.* **126**, 038002.
- Vanderlick, T. K., H. T. Davis, and J. K. Percus, 1989, “The statistical mechanics of inhomogeneous hard rod mixtures,” *J. Chem. Phys.* **91**, 7136.
- van der Waals, J. D., 1894, “The thermodynamic theory of capillarity under the hypothesis of a continuous variation of density,” *Z. Phys. Chem.* **13U**, 657; English translation, J. S. Rowlinson, *J. Stat. Phys.* **20**, 197 (1979).
- van der Waals, J. D., 2004, in *On the Continuity of the Gaseous and Liquid States*, edited by J. S. Rowlinson (Dover, New York).
- van Roij, R., 2005, “The isotropic and nematic liquid crystal phase of colloidal rods,” *Eur. J. Phys.* **26**, S57.
- Vogel, F., and M. Fuchs, 2020, “Stress correlation function and linear response of Brownian particles,” *Eur. Phys. J. E* **43**, 70.
- Wächtler, C. W., F. Kogler, and S. H. L. Klapp, 2016, “Lane formation in a driven attractive fluid,” *Phys. Rev. E* **94**, 052603.
- White, J. A., and A. González, “The extended variable space approach to density functional theory in the canonical ensemble,” 2002, *J. Phys. Condens. Matter* **14**, 11907.
- White, J. A., A. González, F. L. Román, and S. Velsasco, “Density-Functional Theory of Inhomogeneous Fluids in the Canonical Ensemble,” 2000, *Phys. Rev. Lett.* **84**, 1220.
- Wittkowski, R., H. Löwen, and H. R. Brand, 2012, “Extended dynamical density functional theory for colloidal mixtures with temperature gradients,” *J. Chem. Phys.* **137**, 224904.
- Wittmann, R., H. Löwen, and J. M. Brader, 2021, “Order-preserving dynamics in one dimension—Single-file diffusion and caging from the perspective of dynamical density functional theory,” *Mol. Phys.* **119**, e1867250.
- Wittmann, R., M. Marechal, and K. Mecke, 2015, “Fundamental mixed measure theory for non-spherical colloids,” *Europhys. Lett.* **109**, 26003.
- Zausch, J., J. Horbach, M. Laurati, S. U. Egelhaaf, J. M. Brader, T. Voigtmann, and M. Fuchs, 2008, “From equilibrium to steady state: The transient dynamics of colloidal liquids under shear,” *J. Phys. Condens. Matter* **20**, 404210.
- Zwanzig, R., 2001, *Nonequilibrium Statistical Mechanics* (Oxford University Press, Oxford).